UNIVERSITY OF CALIFORNIA SANTA CRUZ

Transitions in eukaryotic algae distributions and physiology from subtropical to tropical environments

A dissertation submitted in partial satisfaction of the requirements
for the degree Doctor of Philosophy

in

Ocean Sciences

by

Charlotte A. Eckmann

June 2023

The dissertation of Charlotte A. Eckmann is approved:

_____
Professor Alexandra Z. Worden

_____
Professor Raphael M. Kudela

_____
Professor Marilou Sison-Mangus

_____
Professor Ute Hentschel Humeida

_____
Peter Biehl
Vice Provost and Dean, Graduate Studies

TABLE OF CONTENTS

List of Figures and Tables

Chapter 1

CHAPTER 2

CHAPTER 3

ABSTRACT

Transitions in eukaryotic algae distributions and physiology from subtropical to tropical environments

Charlotte A. Eckmann

The seasonal and geographical dynamics of phytoplankton have important implications for primary production, carbon sequestration, and predicting future ocean change. The distribution of phytoplankton is influenced by their environmental needs and preferences and can be examined at various levels, from strain or species to size class or broad taxonomic grouping. The first two chapters of this thesis focus on phytoplankton distribution by taxonomic group as determined by 16S and 18S rRNA gene amplicon sequencing. In chapter one, a time-series study of the seasonally oligotrophic northwestern Sargasso Sea underscores the importance of prasinophytes, a polyphyletic group of green algae. Prasinophytes (mostly Class II Mamiellophyceae) comprised approximately half the eukaryotic phytoplankton amplicons during the time of year where deep mixing brings nutrients to the surface. At the end of the deep mixing, the mixed layer shoaled quickly, which could lead to carbon export when the algae were trapped at depth. The focus of the second chapter is expanded to include other phytoplankton groups in addition to prasinophytes. This chapter explores the eukaryotic phytoplankton communities of various tropical habitats, from the green-algae-dominated salt ponds to the mangroves, reefs, and offshore habitats where stramenopiles become more relatively abundant. The Stramenopile group dictyochophytes were examined at high taxonomic resolution

previously not reported for this region, with much of that group found to be comprised of uncultured environmental clades. The third chapter moves from the field to the laboratory, measuring the cell quotas of cultured representatives of Mamiellophyceae under nutrient replete, limiting, and starved conditions. Together, these chapters seek to increase the knowledge of prasinophytes across geographic areas and environmental parameters.

Not

fanned by the

winds of a summer

parterre, Whose gales

are but sighs of an evening

air, Our delicate, fragile and

exquisite forms, Were nursed

by the billows, and rocked

by the storms.

~ Mary Swift Lamson, from *Ocean Mosses* (1872), as cited by Evenson (2016)

ACKNOWLEDGEMENTS

I started this journey on the shores of central California, relocated to Germany's Baltic coast, and traveled to many places in between. I appreciate the opportunities I've had to expand my scientific and geographic horizons, and I am grateful to those who helped me along the way.

The call to adventure came when Alex Worden reached out about a potential position in her lab. Since that first phone call, she has been a source of knowledge, guidance, and passion. Her commitment to science communication is inspiring; hearing her wax poetic about *Micromonas* is enough to get anyone interested in our work. Thank you, Alex!

My committee has also been unfailingly helpful and supportive (not to mention patient) throughout the oft tumultuous timeline, such as when I passed my qualifying exam from an empty house on the edge of a wildfire evacuation zone. Thank you, Raphe Kudela, Marilou Sison-Mangus, and Ute Hentschel Humeida!

Moving to another continent halfway through my studies was a logistical challenge, and I appreciate those who helped me navigate the transition. From the University of California Santa Cruz (UCSC) side, I thank Chris Edwards, Phoebe Lam, Rondi Robison, Sarah Cupps, and Melissa Miller. Thanks also to Kristin Voss, Jan Muschiol, and Kerstin Petersen from the GEOMAR Helmholtz Centre for Ocean Research (GEOMAR).

Another incredible source of support has been my labmates and coworkers from the Monterey Bay Aquarium Research Institute (MBARI) and GEOMAR. At

last count that was over forty people, so while space precludes me from listing everyone, I hope they all know how thankful I am for the knowledge, kindness, and camaraderie they shared with me. Shoutout to my MBARI Building B buddies—I miss our chats on everything from politics to poster placement. I also want to acknowledge my GEOMAR officemates (and honorary officemates) who among many other great qualities could be reliably counted on for a quick pommes break! I also thank those who traveled with me for cruises, conferences, and holidays, from the "DB buddies" to the "coolest kids in the lab."

I must thank Sebastian Sudek for showing me the ropes and troubleshooting the roadblocks I encountered. I would also like to thank Maria Hamilton, Magda Gutowska, Kenny Hoadley, and Lisa Sudek for their guidance as I learned the fine art of algal culturing. Maria and Rachel Harbeitner Clark helped me navigate the ups and downs of being a graduate student off-campus (and later off-continent). I owe a lot to Charles Bachy, who has much love for and knowledge of the marine unicellular eukaryotes of the world, as well as an incredible sense of humor. Thanks also to Valeria Jimenez and Kriste Makareviciute-Fichtner for sharing expertise, particularly regarding prasinophytes and diatoms, and to Jan Strauss, Jonathan Grone, and Rachele Spezzano, who did the same for multivariate statistics. I was guided deeper into the world of bioinformatics by Fabian Wittmers, who is always eager to use his skills to help others. Chang Jae Choi laid the foundations for much of the research in this dissertation. I also owe gratitude to Jessica Eberle and Kristin Bergauer, who possess a wealth of knowledge on the microbial side of Curaçao.

I have been fortunate to work with many wonderful collaborators during my various projects. Thanks to those affiliated with the Bermuda Institute of Ocean Sciences – Simons Collaboration on Ocean Processes and Ecology (BIOS-SCOPE) for welcoming me into the wonderful world of the Bermuda Atlantic Ocean Time-Series, and those at the Caribbean Research and Management of Biodiversity Institute for facilitating our research on Curaçao. I also want to acknowledge the captains and crewmembers of the R/Vs *Western Flyer*, *Rachel Carson*, *Meteor*, *Atlantic Explorer,* and *Endeavor* who were instrumental in the data I collected and/or processed over the course of my graduate studies.

I did manage to have a bit of a life outside the lab. My participation in science outreach through Scientific Slug and Team OCEAN taught me new skills and helped me see how science, when clearly and engagingly presented, can engage communities in conservation. Thank you to everyone involved in these wonderful organizations!

My friends, those I met in grad school and those who go way back, helped keep me grounded and encouraged me to take breaks and have fun. We had some great times together from beginner backpacking to shooting an award-winning short film. Special thanks to Liz, Nicole, Andrea, Becca, Ian, and Nick for sticking with me over the years.

I would be remiss not to thank my longest supporters, my parents Lynne and David, grandparents Barbara and Don, human siblings Charlie, Bliss, and Eliza, and non-human siblings Caddie, May, Crosley, Luna, and Willy. Their level of involvement in my academic career ranges from “you do something with the ocean,

right?" to providing me detailed information on grants to apply to with deadlines and requirements clearly summarized, but I appreciate it all.

Life goes on during a PhD, with all the beauty and loss it brings. Thank you to Maggie, Bumble, Toby, and my Grandma, Joan, for the years of love and support; I wish I could have shared even more with you. This one is for you all, too.

~

For the work presented in Chapter 1, I acknowledge the following contributions: Field work coordination and site selection (CAC, SJG), sample collection (CC, RJP, SJG), collection and organization of metadata (RJP, KV), DNA extraction (RJP, KV), 16S rRNA amplicon plate prep and initial processing (KV), mentorship on prasinophyte ASV analysis and phylogenetics (CB), pipeline run and iterations with me on ephemeral to persistence analyses (FW), editing (VJ, LB-B), discussion on statistics (JS), research guidance and editing (AZW). Abbreviations as follows: Charles Bachy (CB), Fabian Wittmers (FW), Valeria Jimenez (VJ), Jan Strauss (JS), Leocadio Blanco-Bercial (LB-B), Kevin L. Vergin (KLV), Rachel J. Parsons (RJP), Stephen J. Giovannoni (SJG), Craig A. Carlson (CAC), Alexandra Z. Worden (AZW). I will be the lead author of this research as formulated and have performed all analyses of amplicons and ASVs after initial processing, all statistical analyses, and I drafted and refined the manuscript and prepared the figures.

Chapter 2 has been accepted for publication in the journal *Frontiers in Marine Science* (Eckmann et al., 2023). I acknowledge the following contributions: Field work coordination and site selection (MJV, AZW), sample collection (JSE, FW, SW,

CP, AZW), flow cytometer instrument runs (CP), some DNA extraction (CP, KB, JSE), some 16S amplicon plate prep (KB, JSE), initial organization of metadata (JSE), nutrient analysis (MB), editing (KM, KB, VJ, MJV), mentorship on prasinophyte ASV analysis and phylogenetics (CB), generation of ASV feature table and pipeline run (FW), sampling design, guidance, and editing (AZW). Abbreviations as follows: Charles Bachy (CB), Fabian Wittmers (FW), Marguerite Blum (MB), Mark J. A. Vermeij (MJV), Valeria Jimenez (VJ), Kristin Bergauer (KB), Kriste Makareviciute-Fichtner (KM), Camille Poirier (CP), Jessica Eberle (JSE), Susanne Wilken (SW), Alexandra Z. Worden (AZW). I am the lead author of this research paper. I performed all analyses of amplicons and ASVs after initial processing. I performed all statistical analyses. I drafted and refined the manuscript and prepared the figures.

Chapter 3 draws comparisons from several experiments, and I acknowledge the following contributions: Conceptualization (AEZ and AZW) and implementation (AEZ) of the phosphate starvation semi-continuous batch culture experiment, conceptualization (JG, AZW, ENR, VJ) and implementation (JG, ENR, VJ, LS, VAE) of the phosphate limitation photo-bioreactor experiment, conceptualization (KH, AZW, MH, and LS) and implementation (KH, LS, MH) of the nitrate-limited photo-bioreactor experiments, conceptualization (KH, EH) and implementation (EH) of the *Micromonas polaris* light curves experiment. Abbreviations as follows: Amy E. Zimmerman (AEZ), Alexandra Z. Worden (AZW), Jian Guo (JG), Emily Nahas Reistetter (ENR), Valeria Jimenez (VJ), Lisa Sudek (LS), Virginia A. Elrod (VAE),

Kenneth Hoadley (KH), Maria Hamilton (MH), Eleanor Handler (EH). I will be lead author of a research paper incorporating data collected from these and my own cell culturing experiments. I analyzed cell quota data collected for the experiments listed above, as well as from semi-continuous batch culture experiments I performed on my own. I performed calculations and statistical analyses, drafted the thesis chapter, and prepared the figures.

The research included in this dissertation was financially supported by the UCSC Eugene Cota-Robles fellowship, National Science Foundation, Gordon and Betty Moore Foundation, BIOS-SCOPE, Radcliffe Institute for Advanced Research at Harvard University, and the Hanse-Wissenschaftskolleg for Marine and Climate Science.

INTRODUCTION

Despite making up less than 1% of the global photosynthetic biomass, phytoplankton produce roughly half of the global net primary production (Field, 1998). While this often-quoted figure underlines their importance, there is still much to be learned about the distribution and environmental importance of the organisms responsible for every other breath we take. Phytoplankton have distinct biogeographical patterns shaped by their unique nutrient, light, and temperature tolerances. Broader groups of phytoplankton can share traits and therefore share ecological niches and geographic distribution, but traits can vary within the same phytoplankton group at the species or strain level (Demory et al., 2019; Johnson et al., 2006). To reach a more accurate picture of the complexity and ecological impact of phytoplankton dynamics, it is important to consider both variations in individual strains and species as well as large-scale changes in broader phytoplankton groups.

What constitutes a phytoplankton grouping can vary; for instance, phytoplankton can be classified by cell size— which affects food web placement (Sherr & Sherr, 1988), nutrient uptake kinetics (Munk & Riley, 1952), and sinking rates (Eppley et al., 1967) — or by taxonomy, which can imply shared conserved traits within a monophyletic group. Cell size has long been measured through microscopy (Brock, 1978), coulter counter analysis (C. M. Boyd & Johnson, 1995; Sheldon & Parsons, 1967), and more recently it has been estimated through scatter signals from flow cytometry (Cunningham & Buonnacorsi, 1992). Phytoplankton are sorted into size classes with generally agreed-upon cut-offs, such as picoplankton

(0.2- 2 μm), nanoplankton (2- 20 μm), and microplankton (20- 200 μm) (Fogg, 1986; Sieburth et al., 1978); however, sometimes these groups are operationally more loosely described (e.g., picoplankton have been defined as measuring up to 3 μm due to size fractionation using a 3 μm pore size filter during field sampling (Vaulot et al., 2008)). Modern sequencing approaches have allowed a more robust classification of phytoplankton groups based on molecular phylogeny. Eukaryotic phytoplankton are an incredibly diverse group of organisms (Rengefors et al., 2017; Vargas et al., 2015) with several independent lineages that descended from different heterotrophic ancestors.

There are several eukaryotic "supergroups" of undefined taxonomic rank which are frequently refined and modified as research into their phylogenetic origins and morphological characteristics progresses (Burki et al., 2020). The supergroup Archaeplastida comprises three groups (red algae, glaucophyte algae, and green algae and land plants) all arising from primary endosymbiosis in which a eukaryotic cell engulfed a cyanobacterium and harnessed its photosynthetic ability, relegating the captured bacterium to endosymbiotic existence as an organelle called a plastid (Adl et al., 2012; Burki et al., 2020). Phytoplankton found in other eukaryotic supergroups are formed by various secondary or tertiary endosymbiosis events, in which a photosynthetic alga is taken in by a heterotrophic eukaryote (Archibald, 2012). One such supergroup is known by the acronym TSAR for its four members— telonemids, stramenopiles, alveolates, and rhizarians—which contain photosynthetic representatives arising from secondary or tertiary endosymbiosis. Another supergroup

is the Discoba, which contains the euglenids, some of which are photosynthetic via secondary endosymbiosis of a green alga (Bachy, Hehenberger, et al., 2022; Zakryś et al., 2017). There is also Haptista, which includes haptophytes such as the coccolithophores, and Cryptista, which includes the cryptophytes of red algal endosymbiotic origin (Bachy, Hehenberger, et al., 2022).

Environmental sequencing studies often make use of ribosomal RNA (rRNA) genes, which are useful in determining phylogenetic relationships in both eukaryotes and prokaryotes due to their highly conserved regions flanking hypervariable regions (G. E. Fox et al., 1977). The 18S rRNA gene is found in the genomes of eukaryotes, while the 16S rRNA gene is found in prokaryotes and in organellar DNA, i.e., the DNA of fixed endosymbionts in eukaryotes such as plastids. Due to the diversity of eukaryotic phytoplankton, there are still many undescribed species (Choi et al., 2017; E. Kim et al., 2011), and there is much to learn even about the more well-known species (Burki et al., 2021; Worden et al., 2015).

Both size and phylogeny are important considerations when seeking to understand the distribution of phytoplankton groups in the world ocean (Acevedo-Trejos et al., 2018). Subtropical ocean gyres make up over half of the world ocean surface area, and generally have low surface nutrient concentrations (Neuer et al., 2002). There is evidence from modelling studies that oligotrophic areas of the ocean will expand with projected fossil fuel emission scenarios (Bopp et al., 2013; Polovina et al., 2008). Decreased nutrients in surface waters related to anthropogenic climate forcing could favor certain phytoplankton over others (Agawin et al., 2000; W. K. W.

Li et al., 2009), although a baseline analysis of current phytoplankton is lacking for much of these regions. A modelling study suggested changes in the diversity of a particular phytoplankton group (the genus *Micromonas* from the green algal group prasinophytes) could serve as a proxy for changes in overall phytoplankton diversity with climate change (Demory et al., 2019). There exists much genetic diversity within *Micromonas* that affords its sentinel status, and within the wider prasinophyte group.

Prasinophytes are a widely distributed, polyphyletic group of green algae comprising at least seven Classes (Bachy, Sudek, et al., 2022; Demory et al., 2019; Tragin et al., 2016; Worden et al., 2009). While traditionally considered members of the singular class Prasinophyceae (Moestrup & Throndsen, 1988), this designation was contested due to a lack of common ancestor and unifying morphological or biochemical characteristic (Guillou et al., 2004). Therefore, the more conservative and generic term "prasinophytes" has been adopted for the overall group and will be used in the following chapters to refer to what are traditionally called prasinophytes but now form parts of the Chlorophyceae and Prasinodermophyceae at a phylum-level (Bachy, Wittmers, et al., 2022; Guillou et al., 2004; Tragin et al., 2016), with the Streptophyceae (that comprises land plants) being a sister group. Due to the considerable overlap in cell pigments and morphology across the prasinophyte classes, phylogenetic approaches are often needed to distinguish between them (Clayton et al., 2017). Prasinophyte classes I-IV were designated based on nuclear-encoded small subunit rRNA (Nakayama et al., 1998), and classes V-VII later added based on 18S rRNA gene sequences (Fawley et al., 2000; Guillou et al., 2004).

Prasinophytes share characteristics with the putative common ancestor of green algae and streptophytes (Nakayama et al., 1998; Turmel et al., 2009). Due to their wide geographic distribution, the prasinophyte lineage is also ecologically important (Worden et al., 2004). While previous research has mainly focused on the prasinophytes in the picoplankton size class due to their wide geographic range and cell abundance, the geographical distribution both in and between the extant prasinophytes classes is highly variable, thus this dissertation focuses on both the picoplanktonic and the larger prasinophytes.

Prasinophyte class II, the Mamiellophyceae, contains the most well-studied prasinophytes— *Micromonas*, *Bathycoccus*, and *Ostreococcus*—picoplankton which are found in both coastal and oligotrophic regions from the equator to the Arctic (Lovejoy et al., 2007; Moestrup et al., 2003; Monier et al., 2016; Not et al., 2005). Despite their similarity in size, morphology varies between these groups. *Micromonas* cells are motile, with a single flagellum, which *Bathycoccus* and *Ostreococcus* lack, while *Bathycoccus* are covered in body scales, which *Micromonas* and *Ostreococcus* lack (Chrétiennot-Dinet et al., 1995; Eikrem, 1990; Simon et al., 2017). The Mamiellophyceae also includes the larger, less well-studied groups *Dolichomastix* and *Crustomastix*, which range from 1.5-6 μm in length with flagella that are 10-30 μm long, and cells that are round or bean shaped. *Dolichomastix* cells have scales on the cell body and flagella, while *Crustomastix* cells have no body or flagellar scales (Marin & Melkonian, 2010). A survey of green algal diversity in the Mediterranean found that while *Micromonas* and *Ostreococcus* were predominantly found in

mesotrophic areas, *Crustomastix* clades A and B and *Dolichomastix* clades A and B appeared to favour warm, oligotrophic surface waters (Viprey et al., 2008).

Prasinophyte class I, the Pyramimonadales, is made up of nanoplankton and microplankton (Guillou et al., 2004). These flagellates can have up to sixteen flagella (Moestrup et al., 1987) and are known for their metabolically active cyst stage (Moestrup et al., 2003). Representatives of class I have been found in the Baltic (Moestrup et al., 1987), Mediterranean (Viprey et al., 2008), Pacific (Griffin & Aken, 1990), Atlantic (Griffin & Aken, 1990), and Arctic (Bell & Laybourn-Parry, 2003). There is evidence that members of this group are mixotrophic (here defined as capable of phagocytosis) based on studies of grazing using fluorescently labelled bacteria (Bell & Laybourn-Parry, 2003; Bock et al., 2021).

Prasinophyte class III, the Nephroselmidophyceae, fall within the nanoplankton size range, have two flagella of unequal lengths, and are covered in scales (Lubiana et al., 2017; Nakayama et al., 2007). Representatives of this class are found worldwide, particularly in temperate and tropical areas (Lubiana et al., 2017; Yamaguchi et al., 2011). Some species have been observed to form cysts (Suda et al., 2004), reproduce sexually (Suda et al., 2004), and can be found in both the water column (Lubiana et al., 2017) and sediment (Yamaguchi et al., 2011).

Class IV, also known as the order Chlorodendrophyceae or Chlorodendrales, contains scaly quadri-flagellates in the nanoplankton size class (Massjuk & Lilitska, 2006). It includes the genera *Tetraselmis* and *Scherffelia* (Guillou et al., 2004). *Tetraselmis* has been used widely in aquaculture due to ease of culturing and high

nutrient content (Lu et al., 2017; Pusceddu & Fabiano, 1996). While this group has long been considered part of the prasinophytes, recent studies have demonstrated it to be more closely related to "core" green algae than to other prasinophyte classes (Fučíková et al., 2014; Leliaert et al., 2012).

The Pycnococcaceae, class V, consists of scale-less, non-flagellated coccoid cells 1.5–4.0 μm in diameter based on the type *Pycnococcus provasolii* (Nakayama et al., 1998), as well as *Pseudoscourfieldia marina*, a scaly biflagellate (Fawley, 1992). The almost identical 18S rRNA genes of *P. procasolii* and *P. marina* have led to speculation they are different life stages of the same species (Fawley et al., 1999).

Class VI includes the genera *Prasinococcus* and *Prasinoderma,* scale-less coccoid cells in the pico- to nanoplankton size range recently raised to phylum level (Bachy, Wittmers, et al., 2022; Guillou et al., 2004; Leliaert et al., 2012).

Class VII, the Chloropicophyceae, consists of scale-less coccoid cells with diameters ranging from 2 to 5 μm (Lopes dos Santos, Pollina, et al., 2017; Potter et al., 1997). This class is paraphyletic, with some clades grouping together based on 18S rRNA gene trees but separately based on other marker genes. Analysis of the V9 hypervariable region of the 18S rRNA gene from samples collected on the Tara Oceans expedition demonstrated that in some open ocean locations, class VII prasinophytes made up the greatest portion of photosynthetic eukaryote sequences (Lopes dos Santos, Gourvil, et al., 2017). Representatives of class VII were found in oligotrophic regions in the Indian, Atlantic, and Pacific oceans and were most abundant at lower latitudes (Lopes dos Santos et al., 2017).

In this thesis I seek to contribute to knowledge on prasinophytes and other green algae in warm oceans. To this end I hope to provide both deeper understanding of their seasonal and habitat transitions, as well as a baseline against which future change can be assessed. The first two chapters of this thesis focus on the distribution of phytoplankton by taxonomic group as determined by 16S and 18S rRNA gene sequencing. Chapter 1 is a time-series study of the northwestern Sargasso Sea, a seasonally oligotrophic subtropical region. Environmental conditions such as temperature, salinity, and nutrient availability vary seasonally in the surface waters, and these changes are associated with transitions in the phytoplankton community (Giovannoni & Vergin, 2012). This chapter is primarily concerned with the seasonal dynamics of prasinophytes. Systematic time resolved repeat sampling of the same environment has still rarely been performed for these taxa – and hence some of this seeming high variability may simply be just a reflection of results that would come from one-time survey sampling with relatively little contextualization. For these reasons, this chapter focuses on both the picoplanktonic and the larger prasinophytes from approximately monthly DNA sampling across three years, with accompanying oceanographic context in the form of temperature, salinity, and concentrations of chlorophyll *a*, nutrients, and particulate organic matter.

Chapter 2 is a yearly time-series study of the environments on and around the tropical island of Curaçao. These encompass high-salinity, high-nutrient salt ponds to the lower nutrient open Caribbean Sea. This chapter initially set out to advance our understanding of the environmental dynamics of prasinophytes in the tropics. In order

to accomplish this, I contextualized all green algal lineages within the broader information we generated on other eukaryotic algal groups, and, briefly, cyanobacteria. This was important because unlike BATS where there have been many studies on eukaryotic algae, I found very little in the literature for Curaçao or other similar tropical islands. In this process I also noted that there was considerable representation of dictyochophytes in my data. The dictyochophytes are members of the stramenopiles, but unlike diatoms, there is little information on their distribution in warm water settings. Dictyochophytes have been reported in diverse environments (Choi et al., 2020; Coelho et al., 2013; Shi et al., 2011; van de Poll et al., 2018), yet still little is known about their diversity and ecology (Choi et al., 2020). For this reason, these algae are also examined in high taxonomic resolution alongside prasinophytes, so that I could advance knowledge of both groups, which clearly were important – but about which little is known in tropical environments. Finally, while most prasinophyte/green algal classes have multiple cultured representatives, many phylogenetically resolved dictyochophyte clades remain uncultured (Choi et al., 2020). This chapter provides novel insights into green algae and dictyochophyte diversity in tropical coastal habitats, which are understudied in relation to these groups.

The third chapter focuses on the picoplanktonic portion of prasinophytes with experiments on the cultured representatives of Class II Mamiellophyceae. This Class was an obvious candidate to focus on due to their ecological importance, underscored in both chapters 2 and 3, in which their abundance and importance in subtropical and

tropical environments was highlighted. Ideally, field observations would be tested in a laboratory setting to control for the many environmental variables to determine the mechanistic underpinnings of niche specialization. This chapter uses both photo-bioreactor and semi-continuous batch culture methods to manipulate light levels, nutrient concentrations, and partial pressure of CO_2 and measure the associated changes in cellular elemental and macromolecular content.

Within these three chapters, I will use both field and laboratory methods to study the transitions in eukaryotic algae distribution and physiology. The main objectives of my research are:

1. Determine seasonal and geographic patterns in phytoplankton distributions, with attention to phylogenetic relationships
2. Identify environmental parameters such as temperature, nutrient concentrations, or biotic communities that influence the distribution of phytoplankton in distinct environments
3. Determine the effects of variations in light, nutrient concentration, and pCO_2 on the cell quotas of cultured picoprasinophytes from the class Mamiellophyceae

CHAPTER 1:
Seasonal transitions in green algae in the Sargasso Sea near Bermuda expose niche and strategy differentiation

ABSTRACT

Seasonal dynamics of phytoplankton have important implications for primary productivity, export, and understanding future transitions in phytoplankton communities. Here, we studied algal dynamics at the Bermuda Atlantic Time-series Study (BATS), located in the North Atlantic Subtropical Gyre. We used plastid-derived 16S rRNA V1-V2 amplicons from ~monthly photic zone profiles and phylogenetic methods to evaluate prasinophyte green algae, for which prior limited data indicated bloom-time importance at BATS. Prasinophytes comprised ~half (46±24%) the eukaryotic phytoplankton amplicons during deep convective mixing. They were dominated by picoplanktonic Class II members, specifically *Micromonas commoda*, uncultivated *Micromonas* candidate species 1, *Ostreococcus* Clade OII, and *Bathycoccus calidus*. As seasonal stratification set in populations of the dominant sub-species variants tracked the nutricline, forming a deep chlorophyll maximum. Other sub-species variants were also detected. Persistence of the relocated dominants indicated they were poised to increase population numbers upon winter convective mixing, likely underpinning their importance during the spring bloom. In contrast to Class II's omnipresence, Class VII was rarely observed. Additionally, Class I, III, and VI had moderate amplicon percentages when detected, peaking in summer surface waters when eukaryotic phytoplankton were at a minimum, alongside a more prominent, divergent uncultivated prasinophyte. Our studies point to Class II prasinophyte relocation as a mechanism for jump starting high winter and spring abundances, the major period of primary production at BATS. Moreover, we reveal

aspects of niche partitioning, presence of a potentially critical reservoir of warm-period sub-species variants, and provide an unprecedented window into the vertical structure of picoeukaryotes communities in the subtropics.

INTRODUCTION

Despite generally low nutrient concentrations, the ocean's subtropical gyres are important contributors to primary production (PP) and carbon export due to their areal expansiveness (Behrenfeld et al., 2006; Chavez et al., 2011). At the Bermuda Atlantic Time-series Study (BATS) in the North Atlantic Subtropical Gyre, phytoplankton distributional patterns have been characterized at the level of major phytoplankton groupings (Campbell et al., 1997; DuRand et al., 2001; Lomas et al., 2010; Steinberg et al., 2001). A prominent feature at BATS is strong seasonality that shapes water column structure, extent of oligotrophy, phytoplankton successional patterns, productivity, and export (Carlson et al., 2009; Karl et al., 2001; Lomas et al., 2009, 2013). Phytoplankton dynamics at BATS have been explored in the context of biogeochemistry, chlorophyll concentrations, and PP over multiple decades (Lomas et al., 2013; Steinberg et al., 2001). It is well known that the annual deep convective mixing event (DM) between January and April results in entrainment of nutrients from the mesopelagic zone into the photic zone. Subsequent warming and stratification cause low macro-nutrient concentrations in the surface waters during summer (Steinberg et al., 2001). This seasonal stratification is considered analogous to current concepts of future "desertification" and expansion of oligotrophic regions of the ocean (Behrenfeld et al., 2006; Giovannoni & Vergin, 2012; Vergin, Done, et al., 2013).

With respect to uptake of atmospheric CO_2 by phytoplankton, the North Atlantic Subtropic Gyre is currently considered a net CO_2 sink, with an observed

summertime efflux of CO_2 from the ocean to the atmosphere that is more than offset by CO_2 uptake during the DM-associated winter/spring bloom (Bates, 2007). Historically, the highest PP at BATS took place during the winter/spring bloom period, with the greatest fluxes of particulate carbon generally observed around this time (Cruz et al., 2021; Helmke et al., 2010; Lomas & Bates, 2004; Steinberg et al., 2001). In general, the phytoplankton responsible for the bulk of PP in subtropical regions are picoplanktonic (plankton with ≤2 μm cell diameter); their small size results in greater surface area to volume ratio than for larger cells and is advantageous when competing for scarce nutrients (Ohtsuka et al., 2015). However, given nutrient entrainment occurs during the winter/spring periods, periods that are difficult to sample due to weather conditions, it has remained unclear which phytoplankton are key during these periods of high productivity. At the broadest level, the phytoplankton community during the DM and bloom period is dominated by eukaryotic phytoplankton, while the summer stratified and early autumn periods are dominated by cyanobacteria, particularly at the surface (Berube et al., 2016; Choi et al., 2020; DuRand et al., 2001; Giovannoni & Vergin, 2012; Malmstrom et al., 2010). Cyanobacterial abundances increase relative to eukaryotic cell abundances as the water column becomes thermally stratified, such that the latter are low in abundance at the surface during summer and are primarily seen at the more nutrient-rich deep chlorophyll maximum (DCM) (DuRand et al., 2001; Giovannoni & Vergin, 2012). Some of the general eukaryotic groups persisting in the summer DCM have been hypothesized to be the same taxa that form the winter/spring bloom at BATS, but

unfortunately data at the population structure level has so far been lacking (Treusch et al., 2012).

Among eukaryotic phytoplankton reported at BATS are the prasinophytes, unicellular green algae that are ubiquitous in amplicon survey studies (Bachy, Sudek, et al., 2022; Bachy, Wittmers, et al., 2022; Choi et al., 2020; Lopes dos Santos, Gourvil, et al., 2017; Tragin et al., 2016). They have been demonstrated to form a major fraction of the western North Atlantic bloom (north of 40°N), which had classically been attributed to diatoms (Bolaños et al., 2020; Omand et al., 2015). At BATS, the Class II prasinophytes (i.e., Mamiellophyceae) *Micromonas* and *Ostreococcus* were first reported via clone libraries constructed from DCM samples (Cuvelier et al., 2010) QPCR from three profiles indicated that these two picoplanktonic genera, and a third *Bathycoccus,* had higher abundance during deep convective mixing compared to thermally stratified periods (Treusch et al., 2012). At Station ALOHA where convective mixing is weaker these three species are predominantly seen at the DCM (Limardo et al., 2017). However, classifications even at the level of genera and species likely connect only loosely to ecological differences, as they do not encapsulate population biology or some aspects of cellular structure (Simon et al., 2017) and genomic variation (Simmons et al., 2015). For example, genome sequencing shows that ~20% of protein-encoding genes are not shared between two *Micromonas* species, connecting to differences in nutrient transport, storage, regulation, and other features (van Baren et al., 2016). This

diversity likely underlies population structure and niche differentiation (Foulon et al., 2008; van Baren et al., 2016).

To date there is little data that resolves surface communities separately from the vertical strata that exist in open ocean water columns, or that resolves the overall or individual contributions of prasinophytes in a seasonal context. Indeed, the prasinophyte collective has not been studied in a temporal context in the open ocean. Here, we investigate prasinophytes over the seasons at BATS to characterize niche and seasonal transitions of different taxa and their overall importance among phytoplankton communities of the open ocean. More precisely, rather than seasons, we work with different water column stability periods (hereafter stability periods), which are the annual deep convective mixing event (DM), Spring Transition (ST), Stratified Summer (SS), and Autumn Transition (AT). We investigated whether there is a consistent prasinophyte signal associated with the DM and, if so, which taxa contribute to the bloom period, and which prasinophytes are represented across the rest of seasonal cycle – i.e., stability periods – and how they are structured vertically. The specific hypotheses tested were 1) that prasinophytes form an important portion of the annual spring phytoplankton community, 2) that the taxa found during the spring bloom relocate to the DCM during stratified periods (due to closer proximity to available macronutrients at those depths), and 3) that Class VII prasinophytes (i.e., Chloropicophyceae) are abundant open ocean prasinophytes, as implicated in 18S rRNA amplicon based studies using normalization to overall prasinophyte amplicons (Lopes dos Santos, Gourvil, et al., 2017; Tragin et al., 2016). Finally, we sought to

qualitatively consider the extent to which small eukaryotic phytoplankton may contribute to export (Nguyen et al., 2022; Richardson, 2019).

To address these hypotheses and patterns in diversity, we use approximately monthly 16S rRNA gene V1-V2 region amplicon sequencing of vertical profiles extending through the photic zone and synoptic sampling of environmental parameters over three years. Amplicon sequence variants (ASVs) from phytoplankton were assigned to taxonomic groups using phylogenetic methods and analyzed within the framework of stability periods. Prasinophytes were resolved on a newly developed plastid-derived 16S rRNA gene phylogenetic reconstruction, and examined using 18S rRNA from a subset of samples to improve connection between studies utilizing 18S rRNA gene analysis, and available information from 16S rRNA gene environmental sequences. We find that prasinophytes, particularly representatives of the genera *Micromonas*, *Ostreococcus*, *and Bathycoccus*, form about half the eukaryote phytoplankton amplicons during DM. These groups were also detected in high relative abundance at the DCM, with differences detected at the ASV level. Some taxa rank as persistent (present in all stability periods), others are ephemeral, detected during one stability period only, and yet others range between these, suggesting distinctive evolutionary strategies or mortality factors. Several sub-species variants were present either across multiple or all stability periods, particularly within *Ostreococcus* OII, *Micromonas commoda*, and *Bathycoccus calidus*. However, the most expansive sub-species diversity occurred during the SS stability period – which is considered representative of potential future desertification scenarios. Importantly,

we also observed that DM/ST primary producer communities could be exported to the mesopelagic, adding to the evidence for export of picoprasinophytes – mechanisms that presumably are relevant for export of all picoplanktonic cells during transitions between stability periods.

MATERIALS AND METHODS

Oceanographic sampling

Seawater samples were collected from 12 L Niskin bottles affixed to a conductivity-temperature-depth (CTD) profiling rosette at 8 depths from 1 m to 300 m in the vicinity of the BATS site (31°40' N, 64°10' W) from July 2016 to December 2019 for a total of 75 vertical profiles using the R/V *Atlantic Explorer* and R/V *Endeavor*. Most profiles were within 5 km of the BATS station (56 profiles) and the remaining 23 where within 6 to 109 km. DNA samples were collected by filtering 4 L of seawater through a 0.22 μm Sterivex^{TM} (Millipore) filters. Sampling was conducted approximately monthly, although dedicated BIOS-SCOPE process cruises in September 2016, April 2017, July 2018, and July 2019 provided higher sampling effort, e.g. daily profiles, for a concentrated period; additionally, not all sample types were taken for all casts, and March of 2017 was not sampled (Table S1). Concentrations of Chlorophyll *a* (Chl *a*), nitrate+nitrite, phosphate, and particulate organic carbon (POC) were determined at 12-13 depths per profile and measured according to previously reported methods (Lomas et al., 2013). The limit of detection

for nitrate+nitrite and phosphate was 0.05 μmol and 0.03 μmol, respectively, and below this they are reported as zero.

DNA extraction and amplicon sequencing

DNA was extracted from the Sterivex™ filters using the phenol chloroform protocol described in (Giovannoni et al., 1990). The V1-V2 region of the 16S ribosomal RNA (rRNA) gene was amplified via PCR using the primers 27F and 338R with 'general' Illumina overhang adapters (Daims et al., 1999; Vergin, Beszteri, et al., 2013). Amplicon libraries were pooled in equimolar concentrations prior to sequencing. Samples were sequenced using one 2 × 250 paired-end lane with a MiSeq Reagent Kit v2 at the Center for Genome Research and Biocomputing (Oregon State University), Corvallis, Oregon. On average 60,130 ± 26,784 V1-V2 amplicons were sequenced per sample. Sequence data were trimmed [--p-trunc-len-f 180 --p-trunc-len-r 150], dereplicated, checked for chimeras, and assigned to amplicon sequence variants (ASVs) using the DADA2 R package v1.14.0 (Callahan et al., 2016).

Phylogenetic analyses

Quality controlled V1-V2 16S rRNA gene ASVs were classified using best node placement in a rewritten Python3 version of the phylogenetic amplicon placement method PhyloAssigner (Vergin, Beszteri, et al., 2013), which relies on maximum likelihood approaches and a series of consecutive 16S rRNA gene reference trees. All

reference trees/alignments used below as well as the source code of the tool is available as open source on github https://github.com/BIOS-SCOPE/PhyloAssigner_python_UCSB.

ASVs were first placed on a global 16S rRNA gene reference tree as originally published in (Vergin, Beszteri, et al., 2013). Those assigned to plastid or cyanobacterial nodes with best-node placements were subsequently placed on a more resolved plastid and cyanobacteria reference tree (Choi et al., 2017). Amplicons assigned to the Viridiplantae in this second classification step were subset and placed again on a Viridiplantae reference tree (described below) to assign the final taxonomy of these amplicons.

For 16S rRNA phylogeny reconstructions, we collected prasinophyte sequences (>1,200 bp) from GenBank nr representing all classes (including prasinodermophytes to allow comparison with studies using the prior classification) and other prasinophyte and chlorophyte 16S rRNA gene sequences generated from the Marine Microbial Eukaryote Transcriptome Sequencing Project (Keeling et al., 2014). Notably, the plastids from Chlorarachniophytes, Euglenids, and Dinophytes originate from secondary endosymbiosis events wherein a green algal plastid was ultimately acquired (Sibbald & Archibald, 2020). As the plastid evolutionary histories from these eukaryotic lineages and the green lineage are closely related, representative sequences from these groups were also incorporated in our reference dataset. Nine streptophyte sequences were used as outgroups.

Sequences were aligned using MAFFT (Katoh & Standley, 2013). The

Viridiplantae alignment contained 149 sequences. Regions of unambiguous alignment were identified using MUST (Katoh & Standley, 2013; Philippe, 1993), and all gap-containing positions were removed, consisting of a final alignment of 1080 characters. A best-fit model of nucleotide evolution for the alignment was determined using the likelihood ratio test implemented with jModeltest (Posada, 2008) and resulted to GTR+Γ+I. The Maximum Likelihood phylogenetic analysis was calculated using PhyML (Guindon et al., 2010). Bootstrap values were calculated using 1,000 replicates. Prasinophyte and Mamiellophyceae clades were labelled following (Tragin et al., 2016) and (Tragin & Vaulot, 2019), respectively. Within the cluster grouping the genera *Micromonas*, *Mamiella*, and *Mantoniella*, the near full-length 16S is not able to discriminate among *Micromonas* clades A, B, and C but could discriminate between A-C versus D and E *sensu* (Šlapeta et al., 2006). It is a similar case when considering the genus *Bathycoccus* and the distinction between the species *B. prasinos* and *B. calidus* (Bachy et al., 2021). Therefore, sequences assigned to these groups were manually interrogated to provide greater resolution.

Placement accuracy for V1-V2 16S amplicons was tested by building a Maximum Likelihood reconstruction using the same Viridiplantae reference alignment but trimmed to the size of our amplicons. Without masking positions, the tree was then inferred using the same method as described above, which discriminated the same clades as in the near-full-length 16S phylogenetic analysis. Some *Micromonas* ASVs could not be placed at the clade level using the 16S rRNA tree (see above). For these we performed additional comparisons of the 16S rRNA

ASVs to 18S rRNA ASVs assigned taxonomy using the PR^2 database from a prior study that had a subset of the same samples (Blanco-Bercial et al., 2022), and constructed trees using V1-V2 16S amplicons of *Micromonas* (and 3 *Mantoniella* as outgroup) and V4 18S amplicons to connect *Micromonas* clade information between 16S and 18S rRNA gene data (see also Statistical analyses). Other prasinophyte V1-V2 16S ASVs with an LCA best node mismatch, and low nucleotide % identity to the group they were assigned to, were used as queries against NCBI nr, and iterative searches were performed with returned NCBI sequences and PR2 (Guillou et al., 2013). These ASVs were also compared with 18S rRNA ASVs with assigned PR2 taxonomy from a prior study (Blanco-Bercial et al., 2022) to check assignment accuracy.

Water column analyses

The surface mixed layer depth (MLD) was defined as the depth where density was ≥ surface sigma-t plus 0.125 kg m^{-3}. DCM determinations were made using CTD fluorometer measurements, and to provide a consistent means of definition, a two-step categorization was used. Specifically, we first determined the region where measured fluorescence spanned ±35% of the maximum fluorescence (so inclusive on the maximum and spanning depths on either side). This region was termed the DCM for the periods where the MLD was shallower than the DCM region. The water column stability periods at BATS were then defined relative to the DCM and MLD (Blanco-Bercial et al., 2022), with the DM defined as when the MLD is greater than

the photic zone depth (the base of the latter defined as 0.1% of surface light), the spring transition (ST) period beginning when the MLD shoals to ~100 m, the summer stratified (SS) period beginning when the MLD shoals above the DCM and remaining that way until the first entrainment of the DCM into the mixed layer (ML) marks the beginning of the autumn transition (AT) period.

Statistical analyses

Temperature, CTD-derived fluorescence, and salinity data from continuous CTD measurements and Chl *a*, nitrate+nitrite, and phosphate concentrations were plotted using the mba package for Multilevel B-Spline Approximation in R, and averages by stability period and depth were calculated (Finley et al., 2017). The normality of the metadata distributions by depth and water column stability period was tested using the Shapiro test using the R stats package, and, because not all data were normally distributed, the means between groups were compared using the Kruskal-Wallis and Dunn tests using the R stats and rstatix packages (Kassambara, 2019).

Rarefaction curves generated for all samples down to 300 m using vegan and the rareslope function characterized the level of sequence saturation (Dixon, 2003; Oksanen et al., 2015). The final slope of the rarefaction curves was plotted against depth and number of plastid amplicons. Final slopes of above 0.1 are not considered to have reached saturation. Ultimately 435 samples with ≥50 plastid amplicons and with final rarefaction curve slopes indicating saturation were used for further analysis: 75 samples came from the surface (~1-5 m), 98 samples from the DCM, and

the 262 remaining samples were collected from range of depths of 20 m to 300 m (Table S1). Samples were normalized in several ways: relative to total amplicon abundance per sample, relative to plastid amplicons per sample, and relative to prasinophyte (again with Class VI included) amplicons per sample. Averages and standard deviations of prasinophyte groups were computed by depth and by stability period. The means of the percent contributions by depth and stability period was tested for normality and compared as described previously for the metadata comparisons.

The Spearman correlation was used to compare POC to the CTD-derived Chl fluorescence signal (n=556 for all depths, as data was questionable for the CTD profile taken in February 2017) and Chl *a* (n=499) since the data was not normally distributed. Spearman correlations were also used to compare prasinophyte contribution to plastid-derived amplicons to the CTD-derived Chl fluorescence signal (n=435 for all depths), Chl *a* (n=416 for depths 250 m and above, as some samples did not have closely corresponding Chl *a* measurements). Chl *a* versus percent prasinophytes out of plastid amplicons was plotted to demonstrate the relationship between Chl *a* and prasinophyte contributions to the eukaryotic phytoplankton community, with the plot divided into quadrants by Chl *a* values (above and below 0.182 μg kg^{-1}, the 75^{th} percentile Chl *a* value at BATS in the surface 140 m from June 2016 to December 2019) and by the 75^{th} percentile of prasinophyte amplicons out of plastid amplicons.

To visualize changes in the prasinophyte community over time, heatmaps of prasinophyte group abundances relative to prasinophyte sequences at the surface and DCM were generated using the heatmap.2 function in the gplots package in R for those with >0.1% total relative abundance (Warnes, Gregory et al., 2013). Relative abundance of major ASVs out of total 16S rRNA amplicons was plotted across depths from 1 m to 300 m using the mba package for Multilevel B-Spline Approximation in R (Finley et al., 2017).

To determine assignments not resolved using 16S rRNA ASV phylogenetic placement, the V1-V2 16S rRNA and V4 18S rRNA ASVs from a subset of samples also sequenced in a prior 18S study that used PR2 to classify sequences (Blanco-Bercial et al., 2022) were compared using the Spearman correlation with the cor.test function in R. The first analysis was on 16S rRNA ASV81 and ASV1156 and/or 18S rRNA ASVs assigned to *Micromonas* candidate species 1, first reported in the North Pacific (Worden, 2006) and *Micromonas* candidate species 2 (Simon et al., 2017), which were compared at the level of percent contributions and with consideration of other *Micromonas* present. Only samples where these ASVs were detected in at least one of the two marker gene databases were compared (43 in total for the *Micromonas* comparisons), and the comparison input was relative abundances out of all Archaeplastida in each sample. Additionally, V1-V2 16S rRNA grouped as a putative Class IX were compared using the above correlation approach to V4 18S rRNA ASVs for sequences in the prior study identified in PR2 as prasinophyte Clade 9 (Blanco-Bercial et al., 2022) (140 samples from each marker gene).

Multivariate analysis was conducted on a subset of samples with sufficient associated metadata (n=437). To investigate potential differences in the overall prasinophyte community with respect to stability period and environmental conditions, a partial canonical correspondence analysis (pCCA) was performed on Hellinger-transformed abundance data of prasinophytes at the ASV level using the vegan package in R with stability period as the constraining variable to control for effects of water column stability on the environmental variables temperature, salinity, nitrate + nitrite, and phosphate (Dixon, 2003; Oksanen et al., 2015). The pCCA was plotted using the ggplot2 package in R (Wickham, 2011). The significance of the association of environmental factors with prasinophyte ASV distribution was determined using the vegan ANOVA-like permutation test for pCCA, anova.cca. Additionally, analysis of similarity (ANOSIM) tests were performed to compare the prasinophyte communities in different years, depths, and stability periods. The prasinophyte community in the mixed layer during the DM across all study years (n=70) was compared across depths to determine if there was a uniform prasinophyte community throughout the mixed layer. This mixed layer DM prasinophyte community was also compared to that of the stratified surface (n=48) and DCM samples (n=80) across years.

Distribution of ASVs was also visualized using the ggplot2, tidyverse, readxl, lubridate, and patchwork packages in R (Grolemund & Wickham, 2011; Wickham, 2011; Wickham et al., 2019). UpSet plots were plotted using UpsetR package (Conway et al., 2017).

RESULTS

The BATS photic zone showed differences in water column stability affiliated with strong seasonality. The highest surface Chl *a* concentrations over the study (2016-2019) were recorded during the DM/ST and the signal extended throughout the photic zone (Figure 1). The deepest mixing was observed in early April 2017 with the maximal mixed layer extending to 300 m, a depth that may be commonly reached and observed herein due to cruise timing that intersected the event (Figure 1b-d). While salinity in the photic zone did not manifest strong seasonal patterns (Figure S1a, Table S2), thermal stratification was observed and exhibited low nutrient concentrations at the surface, often below high sensitivity detection limits (Figure 1b and S1c-d). Over the course of our study, surface temperatures ranged from 20.92±0.71°C (DM) to 21.30±0.70°C (ST) and reached a high of 26.37±2.25°C (SS) then decreased to 23.96±1.21°C (AT) (Figure 1b).

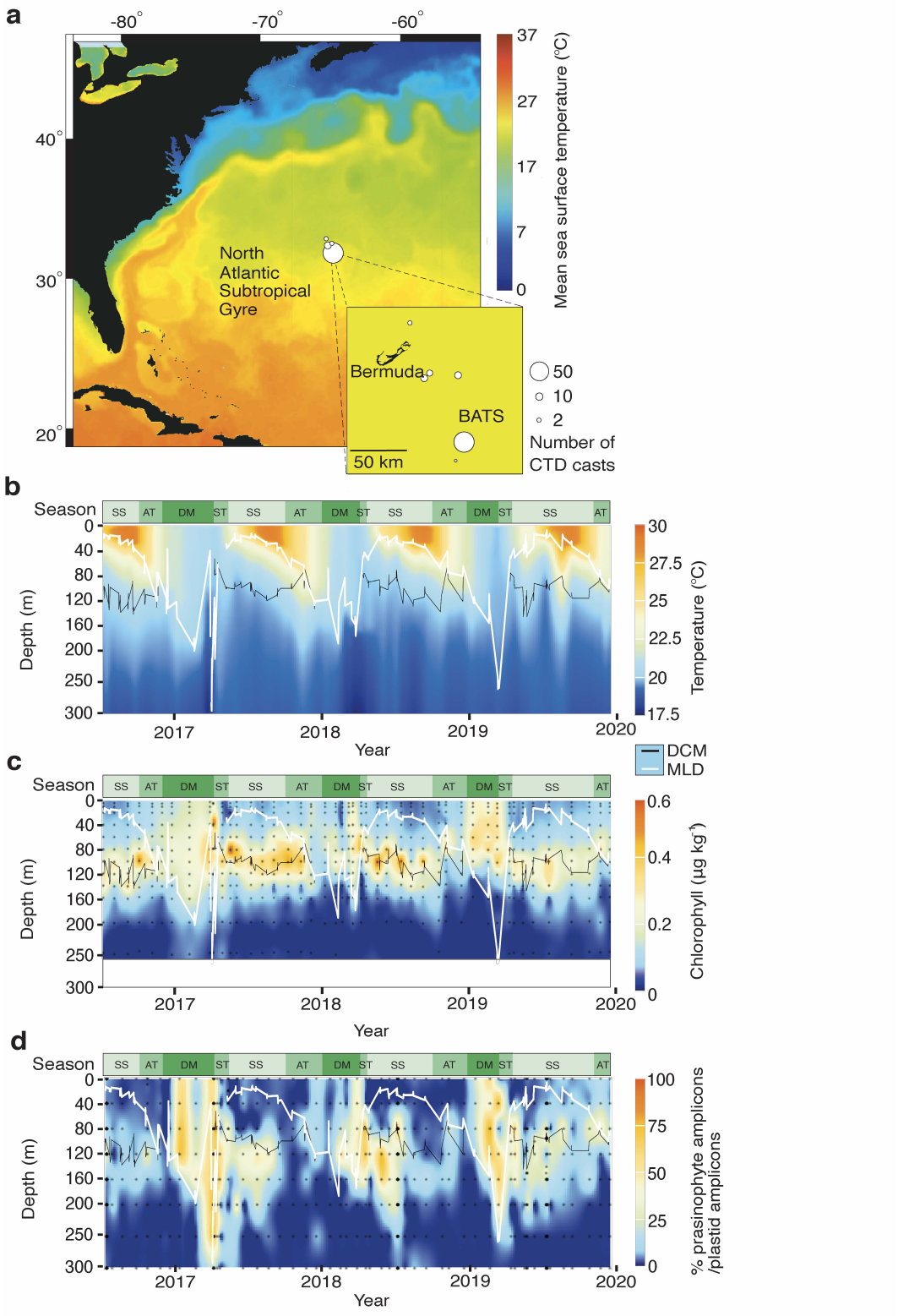

Figure 1. Sampling and oceanographic conditions at the BATS site from 2016 to 2020. (a) Locations of sampling in the proximity of the BATS site superimposed over blended 5 km resolution night sea surface temperature data (shown for December

2019; National Oceanic and Atmospheric Administration CoastWatch). The number of CTD profiles for DNA samples taken at a location is indicated (bubble size), with the inset showing a zoom of the BATS region. (b) Temperature (°C), (c) Chl *a* concentration (μg kg^{-1}) from 12 depths from the surface to 250 m and (d) percentage of amplicons assigned to the prasinophytes out of all plastid-derived amplicons (16S V1-V2) over the course of the study, based on interpolation from discrete data points (black dots corresponding to 8 depths per profile for (c) and (d), and interpolation on the horizontal between continuous measurements over depth for (b)). Superimposed over (b-d) are lines indicating the deep chlorophyll maximum (DCM) in black and mixed layer depth (MLD) in white. Water column stability (SS= stratified summer, AT= autumn transition, DM= deep mixing, and ST= spring transition) are indicated by the green bar.

A systematic method was used to identify the DCM to facilitate interannual comparisons and distinguish analogous regions of the water column in the vertical during the DM period (when no DCM was present). During stratified conditions, a DCM was present, ranging from ~80 m to 120 m, with an average temperature of 20.38±0.78 °C (Figure 1b-c). We compared communities at the ~1% light level (during DM) to those in the identified DCM and to surface communities. The average temperature of the DM mixed layer was 21.05±1.12 °C (Figure 1b). The standing stocks of nitrate+nitrite as well as phosphate were often below detection limits in surface waters, with an average of 0.004±0.015 μmol kg^{-1} and 0.002±0.010 μmol kg^{-1}, respectively, across the years and water column stability periods (Figure S1c-d, Table S1). At the DCM and 1% light level depths, the average was 0.276±0.290 μmol kg^{-1} for nitrate+nitrite and 0.004±0.014 μmol kg^{-1} for phosphate (Figure S1c-d).

At the surface, Chl *a* averaged 0.159±0.092 μg kg^{-1} (DM), 0.129±0.130 μg kg^{-1} (ST), 0.038±0.015 μg kg^{-1} (SS), and 0.066±0.021 μg kg^{-1} (AT). Surface Chl *a* was significantly higher at the DM than SS (Kruskal-Wallis and Dunn test statistic= -

4.506, p<0.001) (Figure S1c). Significant differences in Chl *a* were not detected between the DCM (0.323±0.133 μg kg^{-1}) and outside the stratified period at ~1% light level depths (0.306±0.115 μg kg^{-1}; Kruskal-Wallis and Dunn test statistic= 0.694, p=0.487; Figure S1c). The DM *in vivo* Chl *a* signal extended to ~250 to 300 m when we were on station during a DM event in 2017, while in the other years its detection was extinguished around ~160 m. Chl *a* concentrations were positively correlated with POC concentrations (Spearman ρ= 0.296, p<0.001).

Analysis of the molecular diversity of algal communities using plastid-derived V1-V2 16S rRNA amplicons from 75 profiles (8 depths from the surface to 300 m) revealed trends of prasinophytes at BATS over the annual cycle. First, rarefaction analysis was used to characterize saturation, which occurred for all samples except some samples from 250 m and below that did not meet the plastid count or saturation criteria (Figure S3). Amplicon analyses indicated that periods of prasinophyte highest relative abundances (among eukaryotic phytoplankton) corresponded with overall patterns in Chl *a* (Figure 1c,d). During DM prasinophytes averaged 46.3±24.2% of plastid amplicons in the mixed layer (Figure S2), while prymnesiophytes averaged 18.3±8.2% of plastid amplicons, stramenopiles made up 31.5±21.2%, and the remaining 3.0±2.7% was from other phytoplankton groups. At the surface (~1-5 m), prasinophyte contributions to plastid amplicons ranged from 33.1±24.6% (DM), to 8.8±14.4% (ST), to 4.1±3.4% (SS), and 5.5±6.8% (AT), with significant differences between the DM and the SS (Kruskal-Wallis and Dunn test statistic= -3.708, p= 0.001) (Table S2). Prasinophytes at the DCM averaged 24.5±20.3% out of plastid

amplicons, with prymnesiophytes making up 20.3±8.2%, stramenopiles 52.9±16.1%, and the remaining 1.1±2.3% from other groups. The percentage of prasinophytes out of plastid amplicons was positively correlated ($p<0.001$) to Chl fluorescence (Spearman $\rho= 0.454$) and Chl *a* (Spearman $\rho= 0.244$) (Supplementary Table 4). Thus, overall, the entire DM mixed layer and the DCM had the highest relative prasinophyte contributions out of the identified stability periods and water column zones.

Seasonal delineation of prasinophyte groups within varying depth zones

We compared prasinophyte communities in the surface (~1-5 m) to those of the DCM and of the ~1% light level (during mixing periods). First, we developed a phylogenetic reconstruction of prasinophyte taxa that could be used for placement of amplicons. The reconstruction comprised full-length 16S rRNA gene sequences and resolved most classes as well as delineating several genera to the species-level contingent on the availability of appropriate reference sequences (Figure S4). Several *Micromonas* ASVs required comparison with 18S rRNA ASVs from previous work (Blanco-Bercial et al., 2022) to refine taxonomy as species designation has largely used 18S rRNA gene phylogenies (Simmons et al., 2015; Simon et al., 2017; Tragin et al., 2016). We also compared patterns of unassigned *Micromonas* 16S rRNA ASV81 to 18S rRNA ASVs from a prior study (Blanco-Bercial et al., 2022) of a subset of the same samples, in which we identified uncultivated Clade B._.4 (now *Micromonas* candidate species 1) among other *Micromonas*, and found these ASVs to

be correlated (Spearman test, $\rho=0.61$, $p<0.001$) (Figure S5c). From this analysis ASV81 was identified as being the *Micromonas* candidate species 1 (Simon et al., 2017; Worden, 2006). Likewise, *Micromonas* 16S rRNA ASV1156 correlated with candidate species 2 18S rRNA ASVs in samples with >10 *Micromonas* amplicons (Spearman test, $\rho=0.80$, $p<0.001$) (Figure S5c), and therefore designated *Micromonas* candidate species 2.

Ninety-two ASVs with mismatched LCA and best node assignments in the prasinophyte phylogeny were also investigated. Through blast, 14 were found that had 90-99% identity to environmental clones KX938212 and KX938210 from the North Pacific (Choi, Bachy et al. 2017), 6 with >98% nt to these clones. The complete 16S rRNA gene clone sequences were then used as queries themselves, recovering DQ438491 (98% nt identity) to from the East China Sea. This latter 16S rRNA gene sequence (DQ438491) is linked in PR2 to uncultivated prasinophyte Class IX 18S rRNA sequences. Here, a significant statistical relationship was not recovered between these putative Class IX ASVs in 16S ASVs and Class IX 18S rRNA ASVs (as per PR2) from the 140 samples for which both were compared. After these refinements, our phylogenetic approach indicated all prasinophyte classes (including the Prasinodermophyta) are present at BATS.

The analyses revealed annual cycles in the relative abundance of different prasinophyte genera and classes in the surface waters (~1-5 m) (Figure 2a). During the DM and ST, when Chl *a* concentrations were highest at the surface, Class II, specifically *Bathycoccus*, *Micromonas,* and *Ostreococcus*, had the greatest

prasinophyte contributions, with the latter two having highest relative abundances. Apart from *Micromonas* during 2019, these genera were low or undetected in amplicon data from the surface during SS (Figure 2b). Chl *a* concentrations during SS were extremely low in surface waters and the green algae with highest relative abundances belonged to the Class I Pyramimonadales and unclassified prasinophytes, putatively identified as Class IX (Figure 2a).

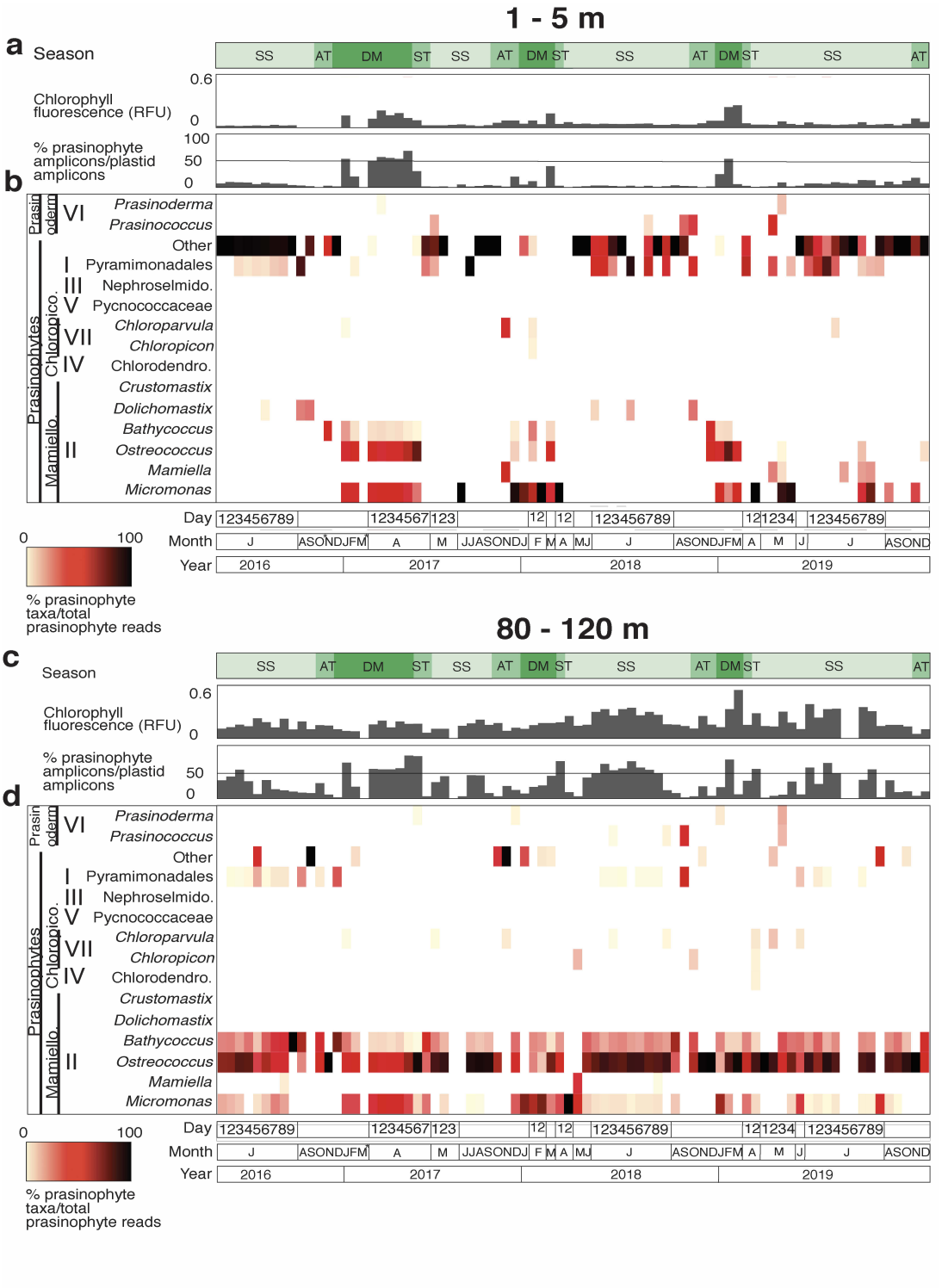

Figure 2. Prasinophyte distributions in the surface 5m and between 80 – 120 m across time and varying states of thermal stability. Data is shown from July 2016 to December 2019. Above each major panel the top bar plot shows *in vivo* Chl *a* fluorescence (RFU). The plot below shows percentage of prasinophyte amplicons out

of plastid amplicons with a line indicating the 50% contribution level. These parameters are plotted for (a) the surface 5 m and (c) between 80-120 m, the proximity of the DCM during stratified periods. The heatmaps show relative abundance of different prasinophyte taxa in relation to the number of prasinophyte sequences in the sample for (b) the surface and (d) the DCM and ~1% light level during mixing periods. Note the X-axis represents sampling dates and is not scaled linearly according to time, due to heavier sampling during highly dynamic periods. Months with an asteria indicate where sampling did not take place at those depths. Water column stability l (SS= stratified summer, AT= autumn transition, DM= deep mixing, and ST= spring transition) are indicated by the green bar.

The distributions of green algal genera in the DCM, or at the ~1% light level during mixing periods, contrasted with those seen in the top 5 m, particular the SS surface. Class II *Bathycoccus* and *Ostreococcus* were detected throughout the year at these lower depths, with *Ostreococcus* generally having the highest relative abundances (Figure 2b). The Class II genus *Micromonas* had elevated relative contributions during DM periods at the 1% light level and were frequently detected at the DCM. Class VI (Prasinodermophyta), Class I Pyramimonadales, Class VII *Chloropicon* and *Chloroparvula*, and prasinophytes putatively belonging to Class IX were detected sporadically at the DCM (Figure 2b).

Class II prasinophytes exhibit highest contributions in association with highest Chlorophyll a concentrations

Qualitatively, higher Chl *a* and prasinophyte relative contributions were observed in the mixed layer during DM and in the DCM during stratified periods (Figs. 1, 2). We next expanded our phylogenetic analyses of samples from the surface and DCM, or 1% light level, to all samples from the upper 140 m (the base of the photic zone) and contextualized findings with Chl *a* patterns (as quantified by extraction and Turner

fluorometry). This was examined in quadrants defined by 75th percentile quartiles for each of these measurements (Figure 3). Chl *a* was significantly different between quadrants except Q2 (>75th percentile Chl *a*, <75th percentile prasinophyte) and Q4 (>75th percentile Chl *a*, >75th percentile prasinophyte). The percent prasinophytes between each quadrant was significantly different except between Q3 (<75th percentile Chl *a*, >75th percentile prasinophyte) and Q4 (>75th percentile Chl *a*, >75th percentile prasinophyte). The quadrant that differed most compositionally was Q1 (<75th percentile Chl *a*, <75th percentile prasinophyte) wherein the high relative abundances of Class II members were displaced by entry of Classes I, III, and putitive Class IX prasinophytes. In contrast, Q2, Q3, and Q4 mostly comprised *Bathycoccus calidus*, *Ostreococcus* Clade OII, *Micromonas* Clade A (*M. commoda sensu stricto*), and *Micromonas* candidate species 1 (Figure 3b).

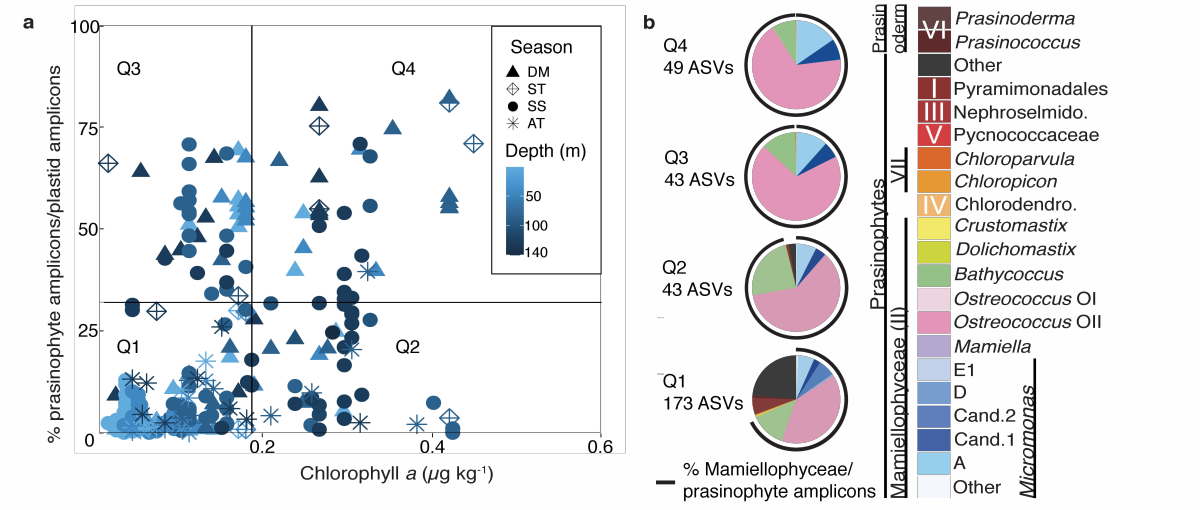

Figure 3. Relationship between Chl *a* and green algal contributions to the eukaryotic phytoplankton community. (a) Chlorophyll *a* (μg kg^{-1}) versus percent prasinophytes out of plastid amplicons. Symbol shape corresponds to stability period and color corresponds to depth. The plot is divided into quadrants by Chl *a* values (above and below 0.182 μg kg^{-1}, the 75th percentile Chl *a* value at BATS in the

surface 140 m from June 2016 to December 2019) and by the 75th percentile of prasinophyte amplicons out of plastid amplicons. (b) Prasinophyte community composition for each quadrant. The number of ASVs per quadrant is indicated, and the black semi-circle around the pie charts indicate the contribution of Class II to prasinophyte ASVs.

Niche partitioning of Class II prasinophyte sub-species variants

Bathycoccus, *Micromonas*, and *Ostreococcus* accounted for up to 85.5% of plastid-derived amplicons and 46.1±24.4% on average in the mixed layer during DM (Figure 1, 2, Supplementary table 1). To examine patterns across the vertical dimension, we undertook normalization to the total number of amplicons (including all bacteria) to diminish the signal from samples with very few phytoplankton, which otherwise (when normalized to e.g. prasinophyte amplicons) appear equally important as at other depths where phytoplankton were more numerous. During DM *Bathycoccus*, *Micromonas*, and *Ostreococcus* formed up to 17.4% of all 16S amplicons (i.e., amplicons from all heterotrophic bacteria and cyanobacteria as well as plastids), and on average 2.8±3.1% of total 16S amplicons. Fleeting contributions were seen from Clade OI *Ostreococcus lucimarinus*, with two ASVs averaging <0.91% of plastid amplicons in the 9 (out of 435) samples in which it was detected (Supplementary table S1). Likewise, *Bathycoccus prasinos* was observed at <0.77% of plastid amplicons in the 4 (out of 435) samples where it was detected (Supplementary table S1). The majority of *Bathycoccus*, *Micromonas*, and *Ostreococcus* relative abundances were formed by a few sub-species variants. For example, together the relative abundances of *Ostreococcus* OII ASV6 and ASV77 accounted for 96.5% of all *Ostreococcus* amplicons across all samples. Likewise, *B. calidus* ASV177

accounted for nearly 100% of *B. calidus* amplicons and 98% of all *Bathycoccus* amplicons.

The dominant sub-species variants exhibited patterns associated with water column stability periods and vertical stratification zones. *Ostreococcus* Clade OII ASV6 was well-represented in the DM and DCM (Figure 4a), and ASV77 had lower relative abundances than ASV6, but had higher relative abundances at the DCM particularly in the AT period (Figure 4b). *B. calidus* ASV177 had broadly similar patterns to *Ostreococcus* Clade OII dominants transitioning from the DM ML into the DCM once the system stratified (Figure 4c). However, while well-represented in the photic zone during the DM period of 2017, it had low relative abundances in 2019.

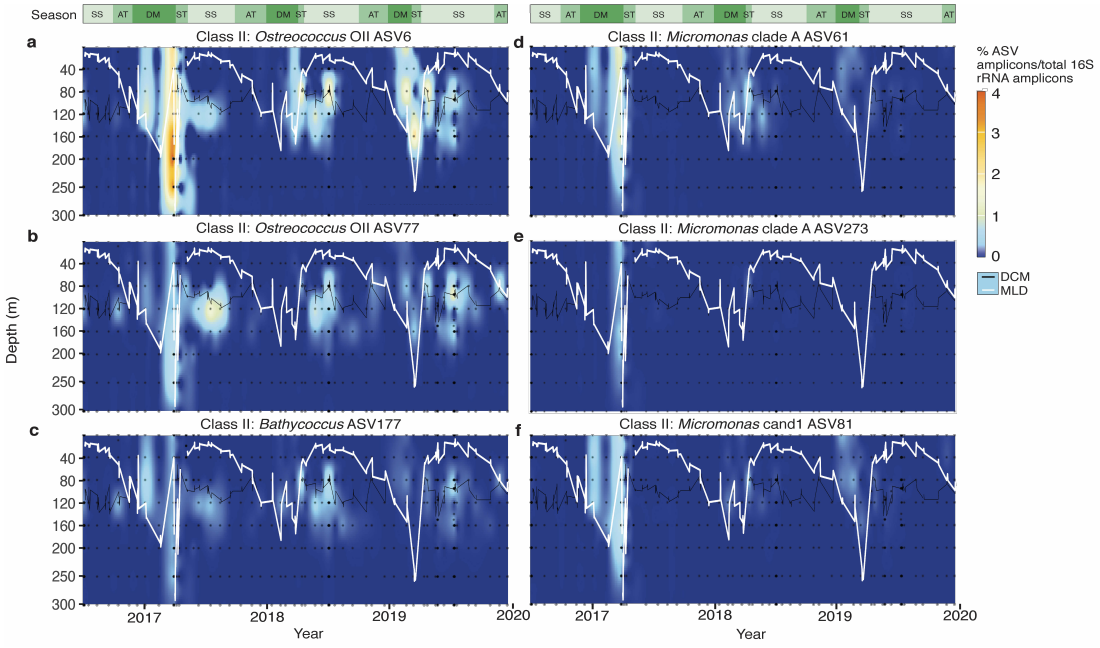

Figure 4. Distribution of highly abundant prasinophyte Class II ASVs. Relative abundance of (a-b) *Ostreococcus* OII (ASV6 and 77), (c) *Bathycoccus* (ASV177), (d-e) *Micromonas* Clade A (ASV61 and ASV273), and (f) *Micromonas* candidate species 1 ASV81 is shown out of total amplicons (including all bacteria and plastids) in the upper 300 m of the water column from July 2016 to December 2019. Data

presentation is interpolated from discrete data points (black dots corresponding to 8 depths per profile). Water column stability periods are as in prior figures. Superimposed are lines indicating the DCM (black) and MLD (white).

The dominant *Micromonas* species at BATS was *Micromonas commoda sensu stricto,* i.e., *Micromonas* Clade A *sensu* that includes the type species strain RCC299, but not *Micromonas* Clades B and C *sensu* [51] (*M. commoda s.s.* hereafter). *M. candidate species* 1 also exhibited high relative abundances (Figure 3). One ASV belonging to *Micromonas* clade E1 was detected, found from 10- 80 m across all years in either summer or autumn (Table S1). Two *Micromonas* clade D (*Micromonas pusilla*) ASVs were detected, at 250 m during the 2017 DM and 120 m during the 2019 SS (Table S1). ASV61, a sub-species variant of *M. commoda s.s.*, and *M.* candidate species 1 ASV81 together contributed up to 81% of all *Micromonas* amplicons. While similar in reaching highest relative abundances during DM, ASV81 exhibited diminished importance during the 2018 DM (Figure 4f). We also compared contributions of another sub-variant of *M. commoda s.s.*, ASV273, to that of ASV61 which highlighted the interannual differences in sub-variant patterns, with ASV273 having a strong presence in the 2017 DM, but not the DM periods of 2018 and 2019 (Figure 4d-e). Moreover, patterns for *Micromonas* candidate species 2 ASV1156 displayed a different seasonal pattern from the more abundant Class II ASVs, reaching its maximum abundance within the upper 120 m ML during the 2017 AT. It was also detected at various depths during the DM periods of 2017, 2018, and 2019 and in the SS surface in 2019 (Figure S6b and 6a).

ASV distributions reveal persistent and ephemeral sub-species variants

The overall ASV-level composition of the prasinophyte community across years, stability periods, and depths was significantly influenced by temperature and salinity (permutation test for CCA, p<0.001; Figure 5). Some prasinophyte ASVs were associated with higher temperatures, such as Class II *Micromonas* candidate species 2 ASV1156, and putative Class IX ASV2562 and ASV3858 (Figure 5). ASV-level prasinophyte community composition did not vary significantly with depth within the ML during DM (ANOSIM test statistic r= -0.08, *p*= 1); however, the DM ML prasinophyte community was statistically different from that of the SS surface mixed layer (ANOSIM test statistic r= 0.78, *p*<0.001) and SS DCM (ANOSIM test statistic r= 0.14, *p*<0.001; Supplementary table 4).

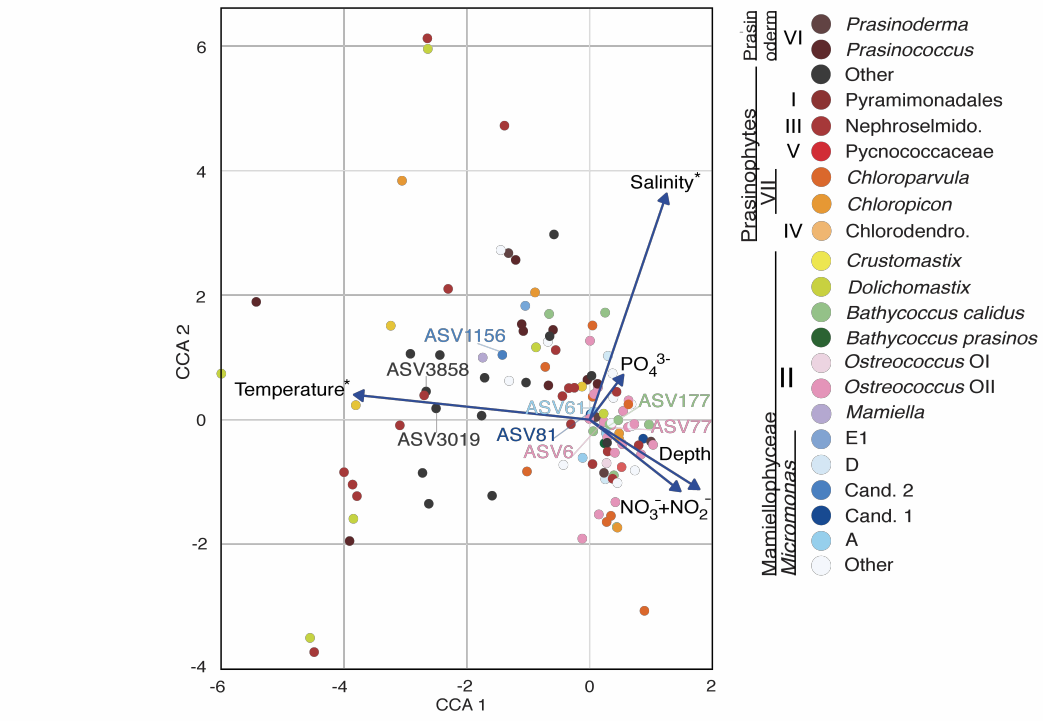

Figure 5. Relationship of prasinophyte ASVs to environmental variables. Partial canonical correspondence analysis plot of prasinophyte ASVs with water column

stability period as the conditioning variable, with vectors representing temperature (ºC), salinity, nitrate + nitrite (μmol kg^{-1}), and phosphate (μmol kg^{-1}). Vectors with an asterix indicate that variable was significantly correlated with the variation in the prasinophyte ASVs. Prasinophyte groups are indicated by color, with several important ASVs labelled by number.

Some prasinophytes demonstrated strong partitioning connected to stability periods and vertical positioning and others were persistently present (Figure 6a). Taxa considered 'persistent' included those represented at both low and high relative abundances. For example, in 2017 putative Class IX ASV3858 (on average 0.2% of plastid amplicons across all samples) was detected in all stability periods in 2017, but its largest relative contributions were in the AT, generally between 40 and 80 m (Figure 6b; Supplementary table 1). Other persistent ASVs were Class II sub-species variants that also had highest relative abundances among prasinophytes—specifically, *Ostreococcus* Clade OII ASV77 and *B. calidus* ASV177 (Figure 6a-d, see also Figure 4). *Ostreococcus* Clade OII ASV6 exhibited persistence in 2017 and was detected in three of the four stability periods in 2018 and 2019 (all but the AT). These ASVs were abundant throughout the photic zone during DM and ST and then present at the DCM during SS and AT. *M. commoda s.s.* ASV61 was detected in three stability periods at multiple depths (all but the AT) in 2017 and 2018 and persistent in 2019, similar to *Micromonas* candidate species 1 ASV81 which was generally detected in all stability periods except AT (Figure 6a-d). Some of the persistent ASVs—such as putative class IX ASV3858 and ASV1638—could be found at the surface and DCM in the SS, while others—such as ASV77, ASV81, and ASV177—are found only below the SS mixed layer, mostly at the DCM.

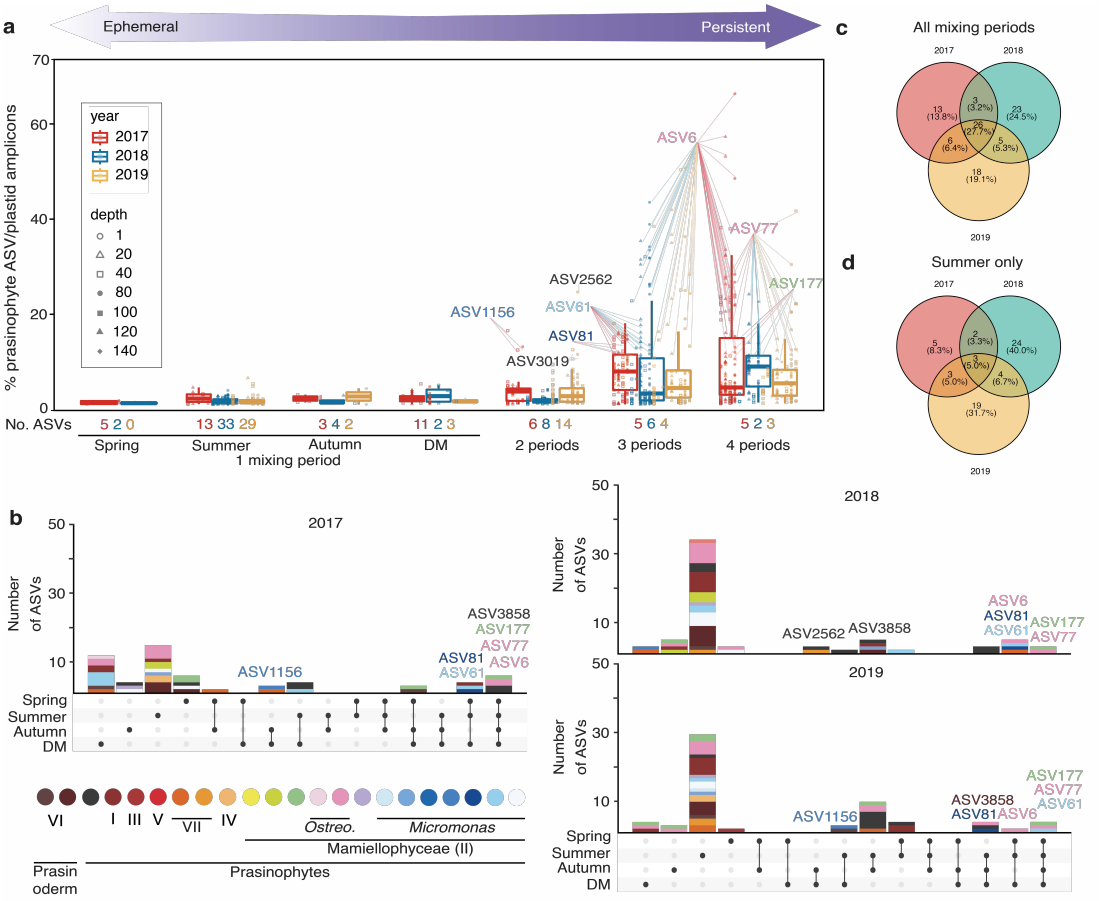

Figure 6. Ephemeral and persistent green algal sub-species variants or ecotypes. (a) Box and whisker plot of relative abundance of prasinophyte ASVs out of plastid amplicons by the number of water column stability periods these ASVs are found in, further broken out by depth (from 1 to 140 m) and year (2017-2019, as 2016 did not have samples from all four seasons). Some ASVs that make up at least 10% of plastid amplicons were labelled with the ASV number and singletons were excluded. (b) UpSet plots by year indicating prasinophyte ASV distribution by stability period (a black dot on the row indicating season means ASVs in the bar graph above detected in that period), with prasinophyte groups indicated by color. (c) Venn diagram of ASVs both unique and shared among years for all mixing periods and (d) Venn diagram of the same but only considering the summer.

The stability period with the highest number of ASVs in the photic zone (94 in total) was the SS (Figure 6). Additionally, the largest proportion of ephemeral ASVs were unique to SS periods, 78 out of 105 ephemerals in total. Three of the 78 ASVs

found only in the SS were detected across all three years: specifically, Class I ASV5929, *Ostreococcus* OII ASV33032, and Class VI *Prasinococcus* ASV17508. Among ephemeral ASVs unique to SS, the top 10 with respect to relative abundance (2-6 % of plastid amplicons) were from Class II (one undetermined *Micromonas* related to the A/B/C lineage and four *Ostreococcus* Clade OII, including ASV33032), two Class IV, and one each from Class VI *Prasinococcus* and putative Class IX. The most abundant ephemerals in spring, autumn, and winter belonged to Class II. Thus, exclusively SS ephemerals exhibited considerable interannual variation (Figure 6d).

Of the 94 prasinophyte ASVs detected during the SS (but not necessarily exclusive to the SS), 19 were detected in all three years, 10 others only in 2018 and 2019, two in 2017 and 2019, and one only in 2017 and 2018 (Figure 6a, Figure S7). Most of the 19 SS 'all years' ASVs were at the DCM (80-120 m), not the upper photic zone. Collectively, these ranged to 71% of plastid relative amplicon abundance, with *Ostreococcus* Clade OII being dominant, while *Bathycoccus calidus*, *Micromonas* Clade A, Clade E1, and candidate species 1 had lesser contributions. In the upper 5 m SS, the average plastid relative amplicon contributions of the 19 'all years' ASVs detected there was ~13%, and the dominants were *Micromonas* Clade A and putative Class IX (Figure S2b). For ephemeral summer ASVs at the surface *Micromonas* candidate species 2 ASV1156 was the dominant in 2019. At 40 m the community had shifted such that for the 'all years' set putative Class IX and Class I *Pyramimonas* dominated among prasinophytes and formed on average ~13% of plastid amplicons. Contributions from Class VI *Prasinococcus*, *Ostreococcus* Clade

OII, *M. commoda*, and *Micromonas* Clade E1 were lesser but still notable, while ephemeral ASVs from Class I, Class IV, and the *Micromonas* candidate species 2 ASV mentioned previously were detected only sporadically.

Among non-dominant sub-species variants, most did not follow the vertical distribution patterns of the more dominant ASVs of that species (Table S1). Moreover, many of the ephemeral variants appeared in depths where the dominant sub-species variant was not detected, or they reached markedly higher relative abundances whereas the 'main' one was rare. Those cases include both rare and ephemeral lineages with preference for deeper (below the DCM) and shallower (upper 40 m) layers.

DISCUSSION

There is still much to be learned about successional patterns of the subtropical phytoplankton communities that are so important to global primary production (Chavez et al., 2011). Ocean time-series studies provide the opportunity to elucidate phytoplankton dynamics and are essential for gaining environmentally contextualized baselines as well as a catalog of microbial diversity that spans annual cycles (Fuhrman et al., 2015; Giovannoni & Vergin, 2012). Importantly, there is growing recognition that understanding of ecological dynamics and evolutionary trajectories requires resolution of microbial communities at the level of species and sub-species variants (Carlson et al., 2009; VanInsberghe et al., 2020). Such studies promise connection of patterns in microbial diversity and distributions to niche differentiation

and the forces that underpin the trajectories of individual taxa. Amplicon-based studies in ongoing time-series regions such as BATS (Blanco-Bercial et al., 2022), the Hawai‘i Ocean Time-Series (HOT) (Ollison et al., 2021), and the San Pedro Ocean Time-Series (SPOT) (Yeh & Fuhrman, 2022) have addressed specific prasinophytes, particularly Mamiellophyceae (Countway & Caron, 2006; D. Y. Kim et al., 2012, 2014), although, to our knowledge, a time-series with an analytical focus on prasinophyte diversity and subspecies variants in the open ocean has not been attempted. Here we utilized 16S rRNA amplicon and ASV analyses to examine picoeukaryotes. The approach is valuable in part because plastid-derived 16S rRNA gene copy numbers are considered more constrained than 18S rRNA genes, potentially enhancing the extent to which relative amplicon abundance reflects natural abundances (Choi et al., 2020; Needham & Fuhrman, 2016). Moreover, information on eukaryotic phytoplankton can be recovered from prior bacterially focused 16S rRNA-based studies, in addition more generally having contextual information on the broader microbial community. The fact that seasonal transitions in open ocean environments result in changes in the depth of the photic zone ML, nutrient injection, and overall water column stability is well known, but how species and populations respond to these changes is unknown for picoeukaryotes. Here, we performed systematic time-resolved sampling at BATS to determine the successional patterns of prasinophyte green algae – which harbor many picoeukaryotic species – over defined stability periods.

Resolving species and rectifying misidentification of prasinophytes

The potential importance of prasinophytes in oligotrophic environments has only been recognized in the last two decades, even though the first picoeukaryotic phytoplankton species discovered more than half a century ago was what we now know to be the Class II prasinophyte *Micromonas* (Knight-Jones & Walne, 1951). The lack of recognition in open ocean seems to come from three primary issues: i.) the small size of picoeukaryotes in general makes morphological identification of individual species virtually impossible. Thus, it is with the advent of molecular approaches that regular identification has been achieved. ii.) Many open ocean surveys have only sampled the surface skin of the water column, missing regions where these cells might thrive. iii.) Issues with weather and challenges to sampling at certain times of the year have led to sampling biases for more quiescent times of the year. An additional hindrance to understanding of dynamics lies in the fact that prasinophytes are polyphyletic, comprising 9 divergent lineages, one of which (Class VI) has recently been reclassified as its own phylum, the Prasinodermophyta (L. Li et al., 2020). Another (VIII) has recently been collapsed as being a being a subgroup within Clade VII, specifically, into VII.B (Chloroparvula) (Lopes dos Santos, Pollina, et al., 2017), however in the long term it is likely these will be split again due to phylogenetic distances. Furthermore, several species cannot be delineated using commonly analysed 18S rRNA gene marker regions (Bachy, Wittmers, et al., 2022; Monier et al., 2016). For example, the 18S rRNA gene does not discriminate between *B. prasinos* and *B. calidus*, the latter having first been discriminated using

metagenomics (Vannier et al., 2016). *B. calidus* can be resolved from *B. prasinos* using 5 nt mismatches present in the 16S rRNA V1-V2 region (Simmons et al., 2016). Thus, information from genomic and metagenomic analyses alongside full-length gene phylogenetic analyses, as well as use of appropriate marker regions, are provisioning a more nuanced view of prasinophyte speciation and distributions in the oceans.

Here, our Viridiplantae 16S rRNA gene tree covered the diversity of chlorophyte and prasinophyte algae, as well as prasinodermophyte algae (Figure S4). Streptophyte algae were used as outgroup sequences. The reconstruction also included sequences from eukaryotic lineages that harbor plastids of green algal origin (Sibbald & Archibald, 2020). Sequences used for this reconstruction included the V1-V2 hypervariable region, which is absent from some GenBank sequences. Unfortunately, 16S rRNA gene sequences are not available for all cultured prasinophytes and for uncultured taxa it is difficult to connect 18S and 16S rRNA genes that come from the same organism, hindering connection between 18S rRNA-based observations, such as the more complex diversity of Dolichomastigales in nature than identified using described cultures (Monier et al., 2016) and 16S rRNA-based findings and vice versa.

A challenge in connecting uncultivated lineages herein was the 14 related sequences were discovered that we ultimately termed ‘putative Clade IX’. These ASVs all had conflicting LCA / best node placements. Six were highly identical to each other while the other 8 formed a second group with greater divergence from

each other, but still related. Further examination showed they were of low relative abundance and mostly visible in surface waters of the SS, particularly ASV2562 and ASV3019 (99% identity to each other). These were highly similar to a previously recovered uncultivated group from the edge of the North Pacific subtropical gyre (Choi et al., 2017). Using those full-length sequences identified DQ438491 (this sequence lacks the V1-V2 region as do many PR2/Phytoref sequences) which is linked in PR2 to prasinophyte Class IX 18S rRNA sequences, the basis for this linkage is unclear. We could not find a statistical link between 'putative Class IX' and 18S rRNA Class IX as assigned by PR2. This is not conclusive as relative amplicons abundances from different markers are subject to different biases. Thus, further analyses will be needed to establish the evolutionary relationships between these uncultivated algae and green algae or the broader Archaeplastida.

In the case of *Micromonas*, the species or Clades are diverse and two remain uncultured, thus few studies have clearly partitioned the 7 evolutionarily distinct lineages in environmental data. Our comparisons of 16S and 18S ASVs from the same samples allowed us to identify 16S ASVs potentially belonging to *Micromonas* candidate species 1 and 2 (Figure S5), and a similar correspondence has also recently been reported in Caribbean Sea samples (Eckmann et al., 2023). These findings propel use of the Micromonas genus as indicators of ocean conditions and climate change by increasing the amount of available data in which they can be evaluated.

Key members of subtropical picophytoplankton communities

With the prasinophyte phylogenetic reference tree developed and refined herein and data from the V1-V2 16S rRNA marker region in hand, our results expose new distributional insights. Most of the prasinophyte ASVs that reached notable relative amplicon abundances came from Mamiellophyceae taxa, whereas Class I, Class VII.A and VII.B (former Class VIII) together contributed <10% of total plastid amplicons (Figure S6). Their greatest relative contributions to were seemingly during the stability period and depths where were prasinophytes are minor among eukaryotes and cyanobacteria dominate. New patterns came first in detection og *B. calidus* across all years and stability periods, while *B. prasinos* was only detected on three occasions. These findings support the proposal that *B. calidus* is the dominant *Bathycoccus* species in warm oligotrophic environments, while *B. prasinos* appears in fact to be scarce (Bachy et al., 2021; Limardo et al., 2017). In light of these findings, the distributions of *B. prasinos* reported in the literature based on 18S rRNA gene sequencing should be revaluated. We also identified *Micromonas* candidate species 1 and 2 as having roles at BATS, alongside the more abundant *M. commoda* (Clade A). In contrast the dominant *Micromonas* species comprising the North Atlantic Bloom in subtropical influenced waters (from 40 - 51 ºN) during spring were different from BATS dominants. There, *Micromonas pusilla*, *Micromonas bravo* (Clade E1) and candidate species 1 were present (ASVs that were 100% nt identity to ASV2535 and ASV81 herein), alongside high abundance of *O. lucimarinus* (Clade OI), all of which are rare at BATS. In subtropical winter samples *M. polaris* (Clade E2) dominated

prasinophytes, and in some cases the total phytoplankton community. In the subpolar eastern North Atlantic in the Fram Strait, *M. polaris* also is dominants in terms of relative amplicon abundance (plastid-derived) in many samples (Bachy, Sudek, et al., 2022). In that environment *M. commoda*-like Clade C (sensu Šlapeta) is also present, and neither of these (Clade E2 and Clade C) were detected herein.

In the Bay of Bengal region of the Indian Ocean, the Mamiellophyceae composition was more similar to that discussed here. *M. commoda*, including an ASV that was identical to ASV61 herein, contributed consistently to plastid amplicons in the surface, especially in more southern stations of a north-south transect (Strauss, Choi, Grone et al. rev.). An identical ASV to putative candidate species 2 ASV1156 was also detected. *Ostreococcus* OII contributed greatly to plastid amplicons at the surface in more southern stations and dominated the subsurface chlorophyll maximum (SCM) throughout; two *Ostreococcus* OII ASVs were identical to ASV6 and ASV77 reported here. A novel *Ostreococcus* reported therein, *Ostreococcus bengalensis*, was found at high relative abundance in the surface in the southernmost Bay of Bengal stations where the influence of the Arabian Sea is strongest was not detected at BATS. *Bathycoccus*, including an ASV identical to ASV177, was also found at the SCM, although at lower relative abundances than *Ostreococcus* OII. Similar to the DCM at BATS, the SCM had higher nutrient concentrations compared to the surface, and little mixing between due to strong vertical salinity gradient, while there was not a discernible temperature gradient, with temperatures similar to the SS surface at BATS.

Another region with similar species was Curaçao, where *Micromonas* A, E1, and candidate species 1 and 2 were the major *Micromonas* species in mangroves, above reefs, and in the open sea (Eckmann et al. in press), all of which had ASVs that matched those found here (ASV61, ASV81, ASV1156, and ASV12724). *Ostreococcus* OII was the major *Ostreococcus* above reefs and in the open sea, with the most abundant ASV matching ASV6 and the second most abundant corresponding to ASV77. *Ostreococcus bengalensis* was a major *Ostreococcus* in mangroves, although as mentioned previously it was not detected here. *Bathycoccus* had similar distribution as *Ostreococcus* OII, although at lower relative abundances, and was likely the same *Bathycoccus calidus* detected here at in the Bay of Bengal. While temperatures were similar to those of BATS SS surface water, nutrient concentrations were higher, especially at mangroves and above reefs.

The different distributions of the Mamiellophyceae groups described above are likely linked to environmental differences and could change with warming oceans. Diversity, genomic differentiation, and modelled temperature tolerances have led *Micromonas* in particular to be proposed as sentinels of ocean change (Demory et al., 2019; Worden et al., 2009). The species and sub-species mapping accomplished herein provide a baseline against which such change can be assessed. Perhaps more importantly we see a group of relatively abundant ASVs from different species that are globally distributed in warm oceanic waters and, at least at BATS, are persistently present, albeit not per say in the surface in all seasons.

Annual cycles and the emerging importance of prasinophytes in the open ocean

Many amplicon-based studies of phytoplankton communities have focused largely on surface samples, despite known shifts connected to vertical and seasonal variability of the photic zone (DuRand et al., 2001; Giovannoni & Vergin, 2012; Lomas et al., 2009; Steinberg et al., 2001). We evaluated the community over photic zone profiles in which recurring biogeochemical and chlorophyll variations observed over annual cycles between July 2016 and December 2019 at BATS (Figure 1 and S1) were similar to those in other studies (Steinberg et al., 2001; Treusch et al., 2012) that have established the presence of strong seasonal transitions at BATS. The demonstrated patterns associated with a vigorous deep mixing period in the winter / early spring were followed by a stable stratified period in summer / early autumn.

Generally, primary production at BATS is higher within the surface 80 m of the DM and into the ST than during other parts of the annual cycle (Lomas & Bates, 2004; Steinberg et al., 2001). However decreased estimates of 0-140 m integrated primary production have been noted from 2010 to 2020 (Lomas et al., 2022), potentially indicating ecosystem-wide changes to the phytoplankton community. These findings make it important to determine which communities contribute to productivity at BATS and when.

To characterize how prasinophytes contribute to phytoplankton distributions at broad levels, we examined the relationship between Chl *a* measurements and prasinophyte distributions (Figure 1, 2, 3). We observed highest Chl *a* concentrations during DM throughout the ML and at the DCM during the rest of the annual cycle

(Figure 1c and S1c). These concentrations were positively correlated to prasinophyte contributions, which showed a similar pattern (Figure 1d). While differences in size and distribution of phytoplankton taxa underpin the total phytoplankton biomass and connect to Chl *a* fluorescence per cell, this relationship is not straightforward due to taxonomic diversity and occurrence of photoacclimation. Therefore, we also compared the Chl *a* and POC contributions which can be correlated at BATS (Lomas et al., 2010, 2022; Michaels et al., 1994). In our data higher Chl *a* concentrations were correlated with higher POC concentrations, potentially indicating higher chlorophyll values were reflective of greater phytoplankton biomass, and at least during DM unlikely to result from photoacclimation. This is supported by previous flow-cytometry-derived estimates of eukaryotic phytoplankton biomass, which found that eukaryotic phytoplankton contribute most to total phytoplankton biomass during the winter/spring (Casey et al., 2013; DuRand et al., 2001).

Successional patterns over stability periods and depth zones highlight Class II dominance of relative amplicon abundances

The temporally resolved data herein shows that particular Class II species dominate relative abundances in many of the higher chlorophyll samples (Figure 2, Figure 3). The largest share of the prasinophyte contributions to all eukaryotic phytoplankton during DM is attributed to the Class II prasinophytes *Ostreococcus* Clade OII, *M. commoda*, and *M. candidate sp.* 1 (Figure 2-4). After stratification, these taxa as well as newly recognized *B. calidus* (Bachy et al., 2021) remained important at the DCM (Figure 2 and 3). These findings align well with data from flow cytometric

enumeration showing picoeukaryote abundance is significantly correlated with periods of higher Chl *a* around the DM at BATS (Singh et al., 2015). Additionally, a study combining T-RFLP with 18S rRNA qPCR data found prasinophytes were an early contributor to the winter/spring bloom at the BATS site between 1991 and 2004, while other phytoplankton (cryptophytes, haptophytes, and pelagophytes) has their individual maxima later in the spring bloom period (Treusch et al., 2012).

Large contributions by picoprasinophytes in the photic zone have also been observed in spring phytoplankton blooms in the North Atlantic (Bolaños et al., 2020). In that study, as mentioned previously, *Micromonas* was particularly abundant in the subpolar spring, while still significant but less abundant at lower subtropical latitudes (still northwards of BATS). *Ostreococcus* Clade OII showed the opposite trend, growing in prominence moving southward. *Ostreococcus* Clade OI was a significant contributor to the North Atlantic subtropical spring community (Bolaños et al., 2020), in contrast to our results, given that it was rarely detected at BATS. This is in agreement with previous observations of *Ostreococcus* biogeography that used 18S qPCR probes and showed that *Ostreococcus* Clade OII is present throughout the ML until waters stratify, and is then found at the DCM of oligotrophic subtropical gyres such as BATS (Demir-Hilton et al., 2011; Treusch et al., 2012) and HOT station ALOHA (Limardo et al., 2017). *Ostreococcus* Clade OI has been reported in cooler mesotrophic and coastal waters and not previously at BATS (Limardo et al., 2017; Treusch et al., 2012).

The DCM is refuge and and reservoir of sub-species variants

Our results support the hypothesis put forward by (Treusch et al., 2012) that the same groups that comprise the spring bloom relocate to the DCM during the rest of the year, but with the added complexity that there is also a reservoir of novel genetic diversity in the SS stability period. The dominant prasinophytes were all Class II members, specifically *B. calidus* ASV177, *Ostreococcus* OII ASV6 and ASV77, and *Micromonas* Clade A ASV61 and candidate species 2 ASV81 were found throughout the ML during the DM periods and within and below the DCM during the SS stability period (Figure 4).

Despite the persistence of these key sub-species variants, there are significant differences in the ASV-level prasinophyte community composition when comparing the entire DM ML to that of the DCM. These differences could reflect temporal and depth partitioning within prasinophytes. While the dominant prasinophyte ASVs mentioned above, particularly ASV77 and ASV177, are regularly detected in both the DM ML and stratified DCM, it should be acknowledged that variations in other ASVs can influence these types of observations. Additionally, *Micromonas* candidate species 2 (ASV1156) was detected during the DM of all three years but was largely undetected in the DCM, although it was found throughout the ML in the AT of 2017 and at the surface during the 2019 SS period (Figure S6b). While detection limits could play a role in their not being observed during other periods or strata, the presence of *Micromonas* candidate species 2 ASV1156 and *Micromonas* Clade A ASV273 in both summer and winter could indicate a wide thermal tolerance, or

affinity for co-associated factors. Several prasinophytes, and even other Mamiellophyceae ASVs, such as ASV33032 which was found consistently during the SS, were only detected during summer, indicating adaption to those conditions.

This heterogeneity could provide a pool of genetic variants that utilize different ecological strategies than today's persistent variants and presumably are better optimized for life in a stratified warm water ocean. However, while they might therefore be considered capable of maintaining primary producer functions, the amounts of primary production, and many other factors would likely be altered, making overall ecosystem function unclear.

Annual cycles of prasinophyte taxa and importance to eukaryotic phytoplankton

Ordination analysis indicated the distribution of prasinophyte ASVs was influenced by temperature and salinity, which were variable with the stability periods (Figure 5). Categorization of sub-species variants along the spectrum from persistent across stability periods to ephemeral showed that a few ephemeral ASVs were responsible for a large fraction of phytoplankton in terms of relative abundance. It should be noted that differences in ASV distributions can be biased by sampling frequency within a stability period, e.g., herein fewer profiles were collected during AT than other periods. Classification of persistent for the key dominants identified herein may be reflected by their presence in three periods during some years and four in others, which may be impacted by sampling efforts or other factors.

The greatest diversity of prasinophytes, as reflected by overall ASVs assigned to prasinophytes, was observed in summer, but interestingly had relatively little overlap between years (Figure 6a,d). Indeed, the SS was different in terms of numbers of ephemeral ASVs, contrasting with those designated as ephemeral in other stability periods. Even when considering the upper ML and the DCM and below as distinct environments this number is still in sharp contrast to other stability periods. These SS ephemeral ASVs were generally lower in relative abundance than more persistent ASVs, and often displayed depth zonation patterns, including around the DCM where other groups, species, and sub-variants had much higher relative abundance (Figure S2b). Thus, they represent a reservoir of genetic diversity for which conditions can shift leading to episodic importance in the phytoplankton community.

There was a significant shift in prasinophyte community composition at the surface from the DM period into the stratified period (Figure 2b). The DM dominants, all being Class II, followed the trajectory of the nutricline as stratification set in and virtually disappeared from the upper 40 m (Figure 2b, 4). The SS prasinophyte community exhibited Class I Pyramimonadales and putative Class IX prasinophytes (Figure 2b) extending to ~40 m. Some of these classes had within-Class dominant ASVs, such as ASV5929 for Class I and ASV1248 for putative Class IX in the SS surface. As stratification inhibits nutrient entrainment from deeper water to the surface, primary production by these classes is presumably low, both due to their low relative abundances among eukaryotic phytoplankton, and the fact that cyanobacteria dominate here. The possibility of a predatory mixotrophic mode exists, however most

studies that have put forward this possibility have utilized gene-catalog based trophic models, and presence of genes affiliated with the phagosome, as evidence for prey consumption. However, the cell biological aspects of this assignment process and manner of projecting potential predatory mixotrophy has many complexities routed in the long-term evolution of eukaryotes that may preclude definitive pronouncements regarding predatory trophic modes. More generally, establishment of potential mixotrophy is still much debated (Wilken et al., 2019). While niche differentiation clearly is a factor underpinning the shift in dominant prasinophyte genera across stability periods and depth zones at BATS, further research is required to determine whether mixotrophy may contribute to strategic differences. Notably, an Ocean Sampling Day-based study that included BATS data from the stratified period (surface data only) identified Class I, Class VII, and Class II as the major prasinophyte groups (Tragin & Vaulot, 2018). Another TARA based study suggested that Class VII are the most important prasinophytes in the oligotrophic open ocean with average contribution to the total photosynthetic eukaryote sequences being 8% (Lopes dos Santos, Gourvil, et al., 2017). Class VII has also been reported to contribute to primary production in the South Pacific Subtropical Gyre, however the extent of its contribution is unclear as approximately half of primary production was performed by cyanobacteria and half by a picoeukaryotes community primarily containing prymnesiophytes and pelagophytes, at the sites studied (Rii et al., 2016). Differences in the approach to sequence analysis, specifically resolution in 18S rRNA V9 data (Monier et al., 2016) and use of the SWARM method make it difficult to

perform more nuanced comparisons. Here, although at BATS both Class I and VII are present in the upper 40 m during SS, they were detected only intermittently and had low relative amplicon contributions to the eukaryotic phytoplankton community (Figure S2b, S6).

We find that although pronounced distinctions between prasinophyte community composition in coastal versus open ocean regions has been described in some studies, these largely came from studies that were not contextualized with respect to seasonality or stability periods. Moreover, here we note clear oceanic dominants among Class II prasinophytes. Historically, Class II prasinophytes were proposed to be coastal, but even more than a decade ago the possibility of marked contributions to oceanic phytoplankton communities in the DCM has been reported (Demir-Hilton et al., 2011). By now several studies that incorporate seasonally and vertically defined sampling protocols have highlighted their presence in open-ocean environments (Bolaños et al., 2020; Limardo et al., 2017).

Late DM stratification dynamics may lead to export of picoprasinophytes

One of the complicating factors for understanding the fate of picophytoplankton is the fact these cells presumably do not sink on their own accord because of their small size (Richardson & Jackson, 2007). A growing body of evidence backs export of picophytoplankton through other mechanisms such as eddy-driven subduction (Omand et al., 2015) and aggregation via exopolymeric substances or fecal pellets (Richardson, 2019). Indeed, picoprasinophytes have been shown using molecular

approaches to be exported in Arctic waters and in the North Atlantic bloom through different physical mechanisms (Bachy, Sudek, et al., 2022; Bolaños et al., 2020). At BATS, *Ostreococcus, Micromonas*, and *Bathycoccus* have been reported in sediment trap material from 2008-2010 (Amacher et al., 2013). Furthermore, a microscopy-based sediment trap particle analysis from 2017-2018 reported *Bathycoccus* (which, unlike *Ostreococcus* and *Micromonas*, does have distinguishing scales), in both phytodetrital and fecal aggregates, particularly in spring (Cruz et al., 2021).

In the years sampled here, the deepest mixing observed occurred in April 2017 with the ML extending to >300 m, well beyond the photic zone (Figure 1b,c). While the 2017 DM appeared to have deeper convective mixing than the other years sampled, this observation is likely due the fact that the 2017 sampling serendipitously coincided with a deep mixing event that was not captured during the DM period of 2018-2019. This higher resolution targeted sampling of the event clearly captured the shoaling of the ML as the water column warmed and stratified, which appeared to trap prasinophytes at depth. Thus, the DM prasinophyte community — mostly comprised of *M. commoda ss* (Šlapeta et al., 2006), *Micromonas* candidate sp. 1, *B. calidus*, and *Ostreococcus* Clade OII throughout the mixed layer — not only would be subject to losses by predation or viral lysis — but additionally could be exported or, at minimum, their biomass would have become a resource for communities below the photic zone. This type of physical mixing and subsequent trapping of photoautotropic biomass phenomenon has been reported in other ocean regions

(Baetge et al., 2022; Dall'Olmo et al., 2016), and our studies indicate it serves as a mechanism for picophytoplankton export.

Conclusions and Perspectives

Open ocean gyres like BATS are seasonally dynamic and yet for eukaryotic phytoplankton our understanding of central players through transitions in water column stability is limited. Our time-series measurements allowed detailed assessment of prasinophytes that have recently emerged as potentially important primary producers in the open ocean. We observe the dominance of particular prasinophyte species and sub-species variants – as well as patterning in their distributions across the stability periods and depths of the photic zone. The results established prasinophytes as being among the most important eukaryotic phytoplankton at BATS, particularly picoplanktonic species observed during DM. Further, the prasinophyte community partitioned into taxa that represent reservoirs of genetic diversity detected largely in warm summertime waters at low relative abundances, versus key dominants. The latter tracked the nutricline as the system stratified, and thus were poised to utilize nutrient pulses associated with convective mixing, enabling strong recolonization of the entire ML during the periods when primary production is highest at BATS. Specific ASVs from the major prasinophytes (*Ostreococcus* Clade OII, *M. commoda*, and *B. calidus*) at the DM and DCM were persistent across stability periods – and across subtropical and tropical oceans, while other subspecies variants withing these genera and species, and from other entire

prasinophyte Classes were more ephemeral. These results support the hypothesis that DM dominants (sub-species variants) relocate to the DCM during the stratified period (Treusch et al., 2012). However, there are other sub-species variants that provide a reservoir of diversity associated with different stability periods, particularly warm summer waters. The latter do not appear to be entrained or involved in the same mechanisms as those that shift from a DM distribution throughout the ML into the DCM, but rather have distinct patterns or ephemeral punctuated appearances. Importantly, while mechanisms of export for picoplanktonic phytoplankton are an area of active research given their low propensity of sinking (Bachy, Sudek, et al., 2022; Bolaños et al., 2020; Omand et al., 2015; Richardson, 2019), we find that as stratification sets up, the DM/ST primary producer communities can become 'trapped' under the mixed layer depth (MLD), in a manner that could result in their vertical export from the photic zone. This mechanism suggests that picoprasinophytes at BATS contribute to biomass export to the mesopelagic. With this type of data in hand, we can begin to effectively track and develop predictive models on annual cycles, primary production and its seasonally nuanced fate in subtropical systems, as well as future transitions in these communities associated with surface ocean warming.

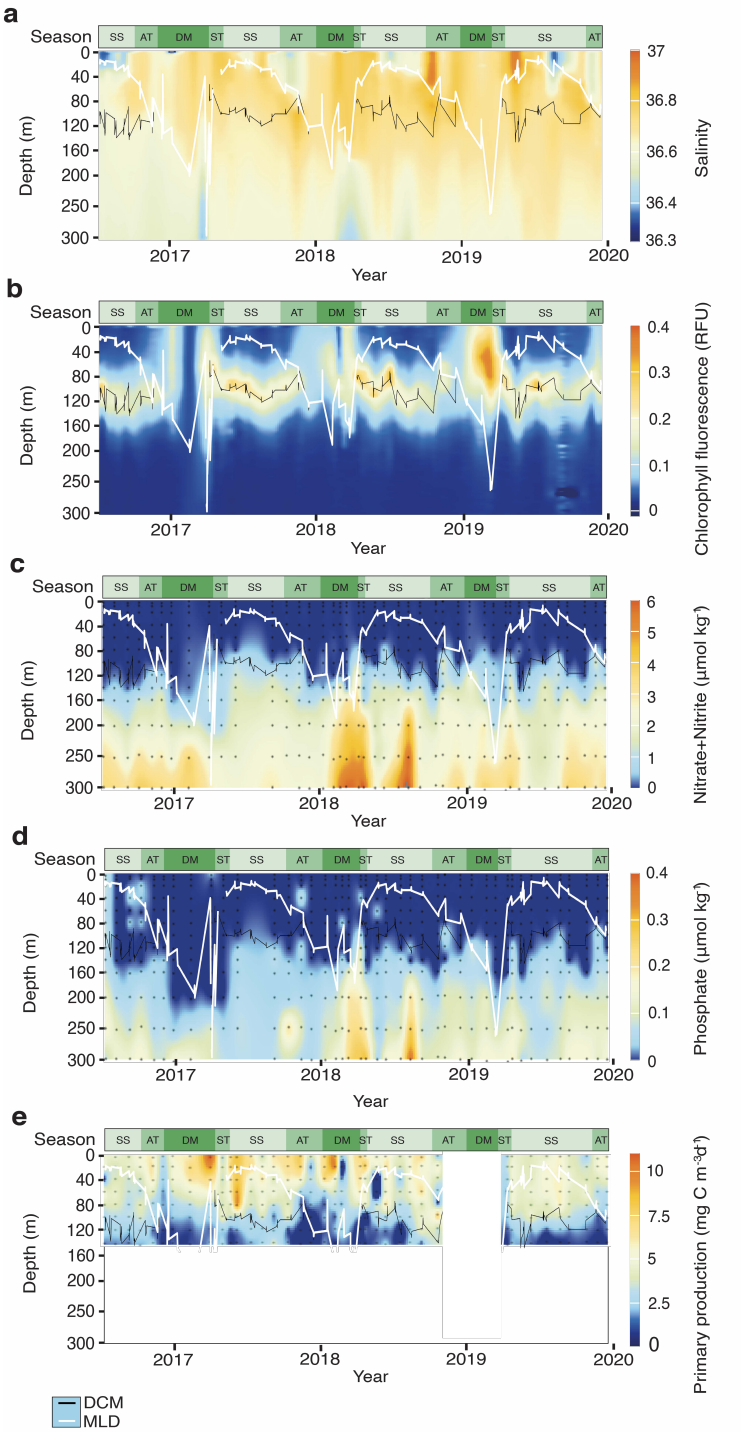

Supplementary Figure 1. Biogeochemical variability at the Bermuda Atlantic Time-Series Study (BATS) site between July 2016 and December 2019. (a) salinity, (b) CTD-sensor derived Chlorophyll fluorescence, (c) nitrate + nitrate (µmol

kg^{-1}) and (d) phosphate (µmol kg^{-1}) determined using spectrophotometric approaches and plotted based on interpolation from discrete data points (black dots corresponding to 13 depths per profile), and (e) primary production (mg C m^{-3} d^{-1}). Superimposed are lines indicating the DCM (black) and MLD (white). The stability periods (SS= stratified summer, AT= autumn transition DM= deep mixing, and ST= spring transition) are indicated by a green bar and are shown as such in other relevant figures.

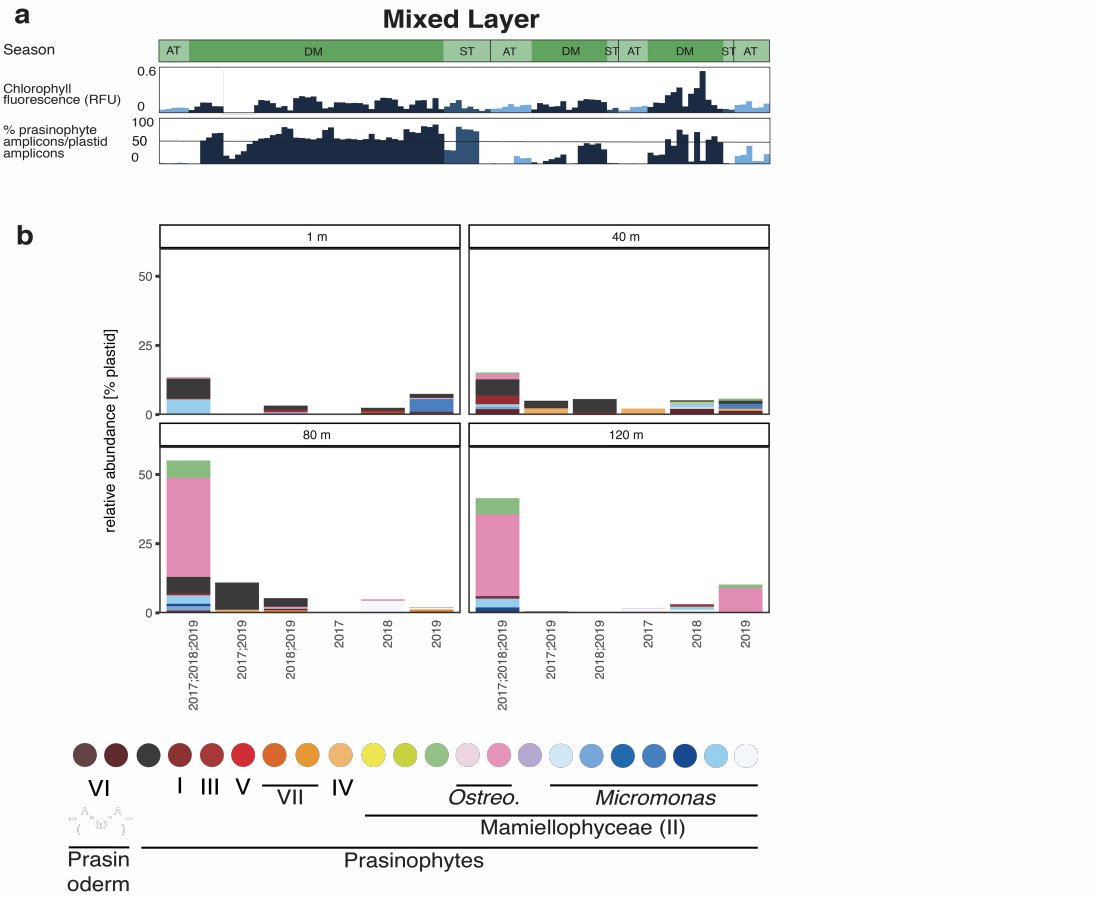

Supplementary Figure 2. Prasinophyte contributions by depth layer and season. (a) Percent prasinophyte amplicons out of plastid amplicons in the mixed layer with a line indicating the 50% contribution level. Note the X-axis represents sampling dates and is not scaled linearly according to time, due to heavier sampling during highly dynamic periods. Months with an asteria indicate where sampling did not take place at those depths. Water column stability l (SS= stratified summer, AT= autumn transition, DM= deep mixing, and ST= spring transition) are indicated by the green bar. (b) Bar plots of average relative plastid abundances of prasinophyte ASVs detected during the SS, with each quadrant a separate depth and the x-axes delineating in which years they were detected.

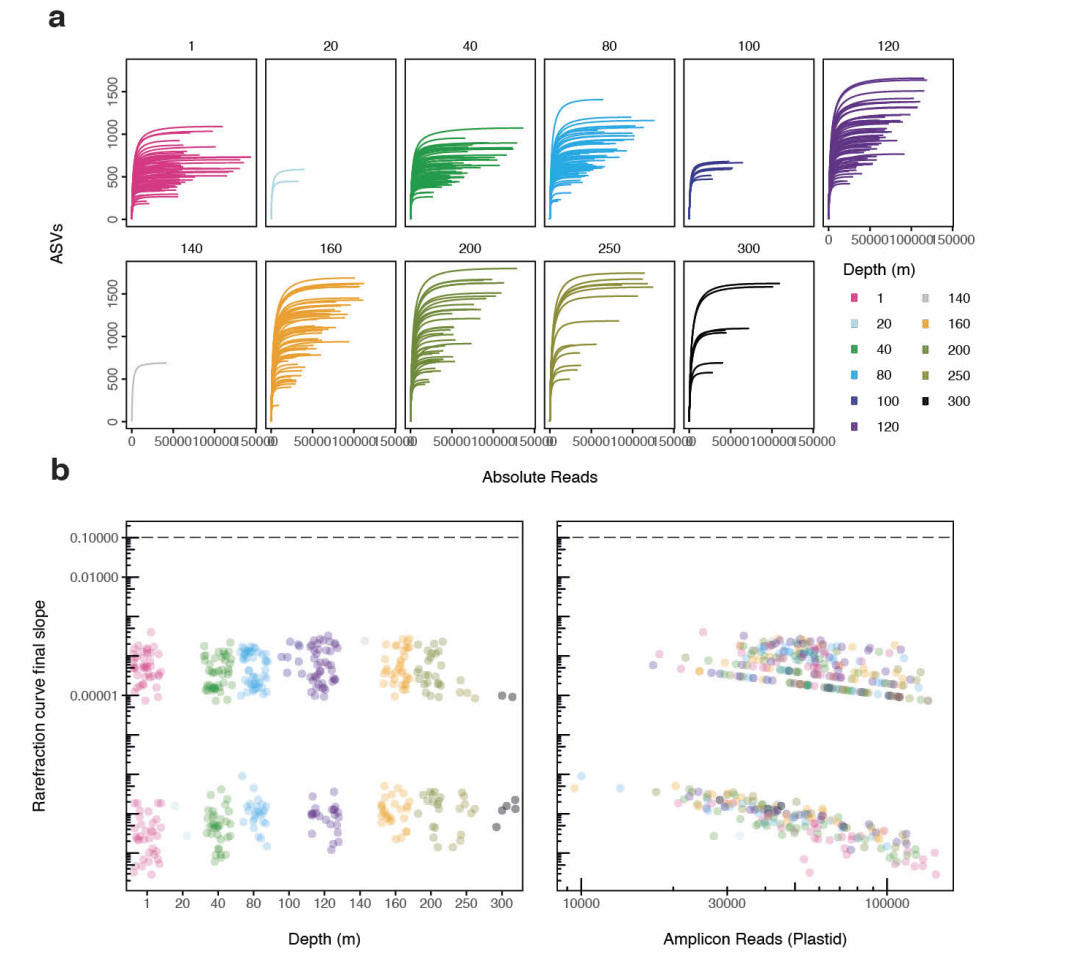

Supplementary Figure 3. Rarefaction analysis for the 435 samples used in the study (samples collected during the study period with <50 plastid amplicons were not considered) at all depths down to 300 m to determine sequencing saturation. (a) The final slope of the rarefaction curves of amplicons vs. depth and (b) number of amplicons. Final slopes of below 0.1 are plotted below the dotted line and are considered to have reached saturation. (c) Rarefaction curves; number of ASVs vs. number of absolute reads.

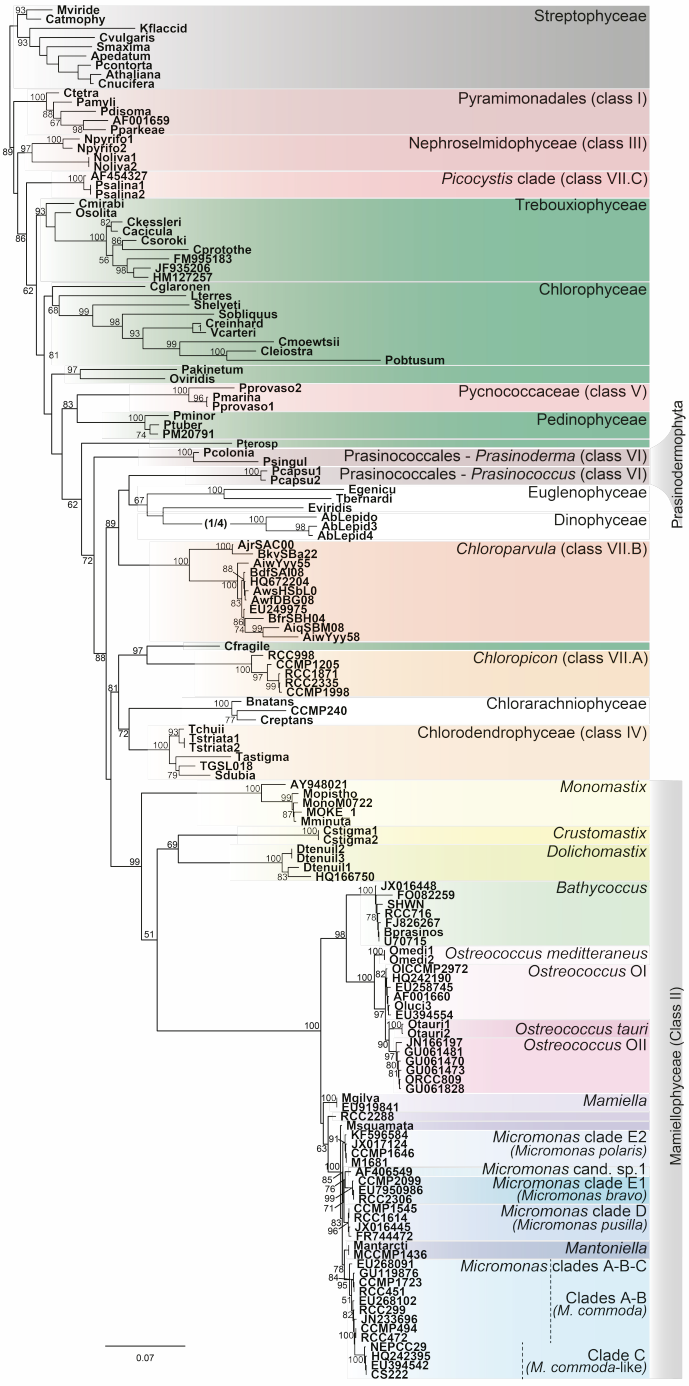

Figure S4

Supplementary Figure 4. 16S rRNA gene tree reference tree for Viridiplantae consisting of 149 sequences of near full-length sequences with nine streptophyte sequences used as outgroup. Bootstrap values are indicated by the number at the node. Prasinophyte groups (as well as Prasinodermaphyta, i.e., former prasinophyte Class VI) are designated by a variety of color gradients, with other Viridiplantae groups in dark green and non-Viridiplantae groups from secondary endosymbiosis with no color gradient.

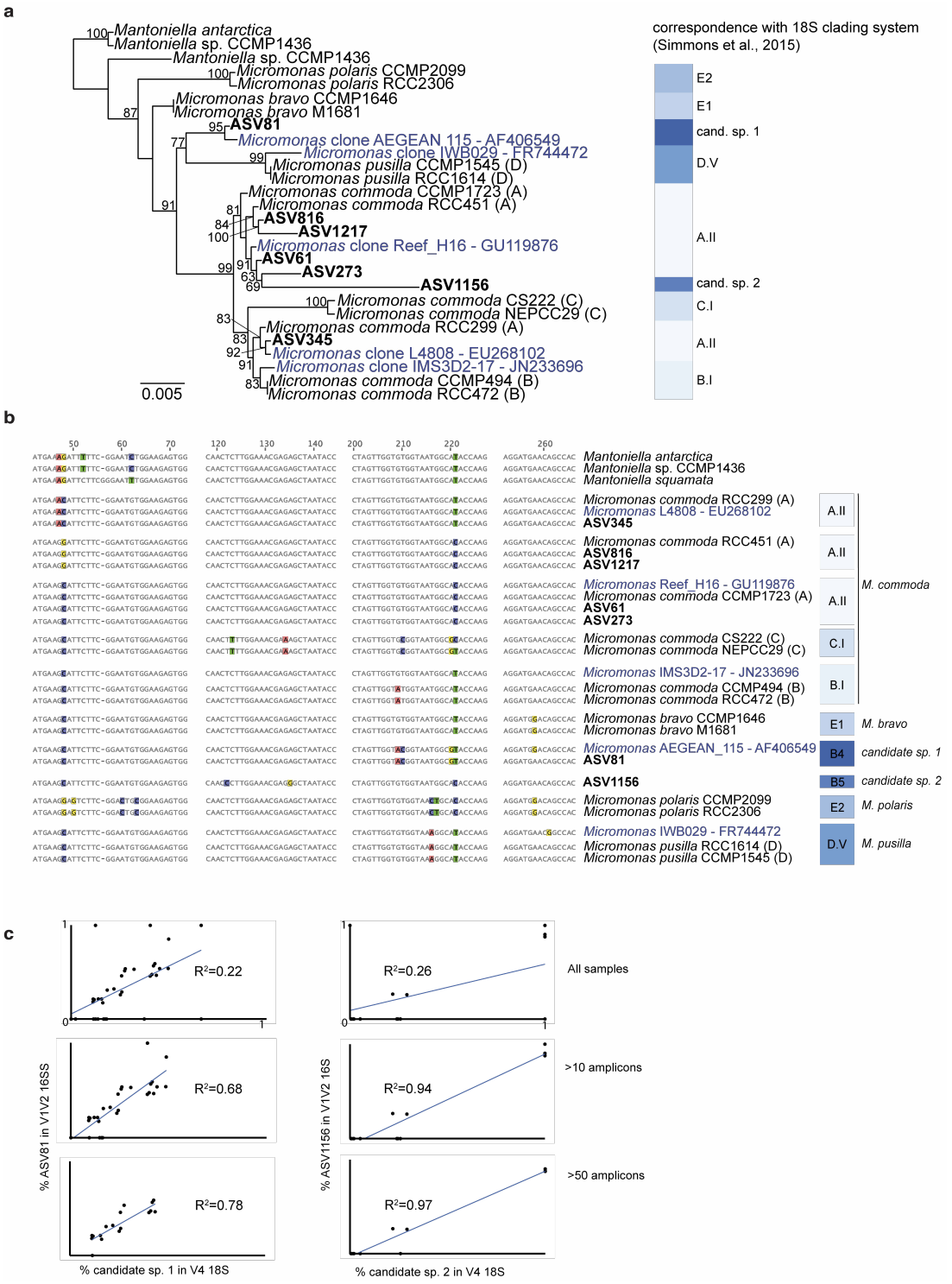

Supplementary Figure 5. Comparison of *Micromonas* ASVs from this study to known *Micromonas* sequences from culture and environmental isolates. (a) Maximum Likelihood phylogenetic tree of V1-V2 16S sequences of *Micromonas* (all sequences trimmed to V1-V2 16S amplicon size). Environmental sequence names are

in blue font, sequences from culture in black font, and *Micromonas* ASVs from this study indicated in bold black font. Corresponding groups were labelled according to naming determined with near full-length 18S rRNA sequences by [35]. (b) comparison of alignments of the 16S rRNA gene V1-V2 region of *Micromonas* sequences in the above tree. (c) linear regression comparing percent contribution of 16S ASV81 to *Micromonas* amplicons in 16S to percent contribution of *Micromonas* candidate species 1 to *Micromonas* amplicons in 18S for all samples with either assignment (n=36), then samples with greater than 10 *Micromonas* amplicons (n=28), then samples with >50 *Micromonas* amplicons (n=26). The same was done with ASV1156 and *Micromonas* candidate species 2 (n=17, 16, and 11, respectively).

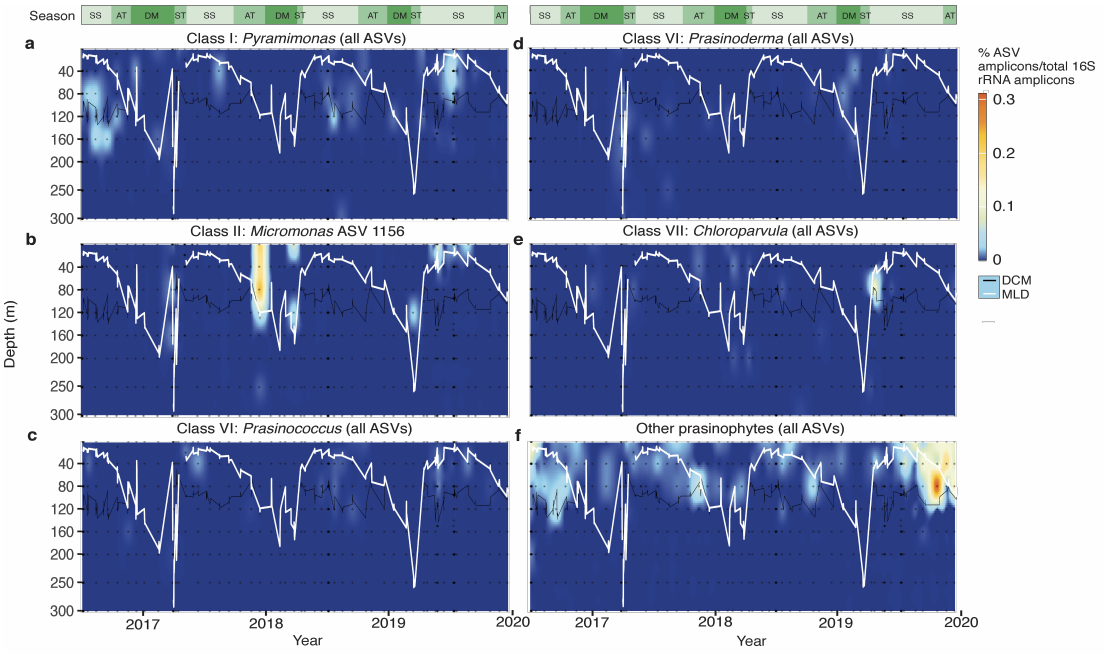

Supplementary Figure 6. Distribution of prasinophyte groups and ASVs. Distribution of (a) Class I *Pyramimonas,* (b) Class II *Micromonas* candidate species 2 ASV 1156*,* (c) Class VI *Prasinococcus*, (d) Class VI *Prasinoderma,* (e) Class VII *Chloroparvula*, and (f) other prasinophytes out of total amplicons at a range of depths from 1 m to 300 m from July 2016 to December 2019 based on interpolation from discrete data points (black dots corresponding to the 8 depths per profile). Note that all except for (b) represent a sum of all ASVs for that group. The stability periods, defined by DCM and MLD, are indicated by a green bar.

SUPPLEMENTARY TABLE LEGENDS

Supplementary Table 1. Table of collection data (data ID, program, cruise ID, cast, depth, Niskin bottle, date, time, latitude, and longitude), oceanographic context (stability period, DCM, MLD, vertical zone, sigma-t), environmental data (temperature, salinity, CTD-derived Chl fluorescence, Chl *a*, nitrate+nitrite, phosphate), and sequencing data (counts of all prasinophyte ASVs, and prasinophyte, chlorophyte, cyanobacteria, plastid, and total amplicon counts per sample for all 435 DNA samples used in the study. Please note the environmental data is synoptic and may not originate from the same casts as the DNA samples; each parameter has columns indicating collection date and sample ID that can be compared to those of the DNA samples.

Supplementary Table 2. Averages of environmental data (temperature, salinity, Chl *a*, nitrate+nitrite, phosphate, and primary production) and percent prasinophyte of plastid amplicons by depth and stability period.

Supplementary Table 3. CTD-derived fluorescence values and GFF-quantified Chl *a* values for depth profiles during the study period.

Supplementary Table 4. Summary of parameters and results of statistical tests (Kruskal-Wallis Dunn, Spearman correlations, and ANOSIM).

CHAPTER 2:
Eukaryotic algal community composition of Curaçao's aquatic environments from solar salterns to the open sea

ABSTRACT

Tropical environments with unique abiotic and biotic factors—such as salt ponds, mangroves, and coral reefs—are often in close proximity. The heterogeneity of these environments is reflected in community shifts over short distances, resulting in high biodiversity. While phytoplankton assemblages physically associated with corals, particularly their symbionts, are well studied, less is known about phytoplankton diversity across tropical aquatic environments. We assess shifts in phytoplankton community composition along inshore to offshore gradients by sequencing and analyzing 16S rRNA gene amplicons using primers targeting the V1-V2 region that capture plastids from eukaryotic phytoplankton and cyanobacteria. Microbial alpha diversity computed from 16S V1-V2 amplicon sequence variant (ASV) data from 282 samples collected in and around Curaçao, in the Southern Caribbean Sea, varied more within the dynamic salt ponds, salterns, and mangroves, compared to the seemingly stable above-reef, off-reef, and open sea environments. Among eukaryotic phytoplankton, stramenopiles exhibited the highest relative abundances in mangrove forests, above-reef, off-reef, and open sea environments, where cyanobacteria also showed high relative abundances. Within stramenopiles, diatom amplicons dominated in salt ponds and mangroves, while dictyochophytes and pelagophytes prevailed above reefs and offshore. Green algae and cryptophytes were also present, and the former exhibited transitions following the gradient from inland to offshore. Chlorophytes and prasinophyte Class IV dominated in salt ponds, while prasinophyte Class II, including *Micromonas commoda* and *Ostreococcus* Clade OII,

had the highest relative abundances of green algae in mangroves, above-reef, off-reef, and the open sea. To improve Class II prasinophyte classification, we sequenced 18S rRNA gene amplicons from the V4 region in 41 samples which were used to interrelate plastid-based results with uncultured prasinophyte species information from 18S rRNA gene-based studies. This highlighted the presence of newly described *Ostreococcus bengalensis* and two *Micromonas* candidate species. Network analyses identified co-occurrence patterns between individual phytoplankton groups, including cyanobacteria, and heterotrophic bacterial ASVs. Our study reveals multiple uncultured and novel lineages within green algae and dictyochophytes in tropical marine habitats. Collectively, the algal diversity patterns and potential co-occurrence relationships observed in connection to physicochemical and spatial influences help provide a baseline against which future change can be assessed.

INTRODUCTION

Aquatic environments in the tropics comprise areas of high biodiversity (Jablonski et al., 2006) and primary productivity (Behrenfeld et al., 2006). Large environmental gradients occur over short geographic distances, with disparate ecosystems such as salt ponds, mangrove forests, and coral reefs existing in close proximity and hosting unique biota (Hunting et al., 2008; Nagelkerken & Velde, 2002). Much of the research concerning phytoplankton in these environments concerns epiphytic and benthic diatoms, dinoflagellates, and cyanobacteria (Alvarenga et al., 2015; Desrosiers et al., 2014; Lefrançois et al., 2011; Vidal et al., 2015), whereas less is known about free-living eukaryotic phytoplankton that reside in the water column. With respect to molecular diversity surveys, reefs are the best represented of these environments, while mangrove forests (Hossain et al., 2022; Samanta & Bhadury, 2014), salt ponds (Filker et al., 2015), and comparative studies across environments (J. Bakker et al., 2019; C. C. Becker et al., 2020) are scarcer. Additionally, in many cases different methodologies have been employed making comparison difficult. More generally, recently concerns have been raised that few studies focus on different habitats within close proximity, and how habitat change in one type of aquatic environment might influence connected aquatic habitats (Qin et al., 2019).

Among the more 'coastal/inland' tropical island habitats are salt ponds and mangrove forests. Salt ponds are known for their halophilic phytoplankton, such as the green alga *Dunaliella* which has been observed in these habitats worldwide using

culturing, microscopy, and other methods (Ben-Amotz et al., 2019; Oren, 2005). Ponds with lower but still hypersaline salinity levels exhibit a greater diversity of eukaryotic phytoplankton, including cryptophytes and stramenopiles, as observed in Portugal (Filker et al., 2015). These hypersaline habitats can occur when seawater is totally or partially separated from the open sea, whether by natural mechanisms or human intervention (e.g., for salt production); in the latter case, they are also referred to as solar salterns (Benlloch et al., 2002). Due to their typically large surface to volume ratio these habitats are subject to considerable salinity fluctuations over short timescales, and the cost of osmotic compensation to these fluctuations appears to constrain the biotic community composition (Yang et al., 2016).

Mangrove forests have their own unique attributes, being prominent features of tropical and subtropical coastlines and formed by salt-tolerant trees and shrubs. They also undergo large daily fluctuations driven by tidal influences on factors such as temperature, salinity, and light availability, among others. They are considered to be among the world's most productive ecosystems while also being often nutrient-limited (Reef et al., 2010). Multiple studies of phytoplankton in mangrove forests have been conducted in India and Malaysia, especially focused on diatoms typically using microscopy but also marker gene cloning (Saifullah et al., 2016; Samanta & Bhadury, 2014). Cyanobacteria have also been reported as important to nutrient cycling in mangroves, as well as contributing to nitrogen fixation in African, Indian, Central and South American mangrove habitats (Alvarenga et al., 2015; Toledo et al., 1995). In addition to primary production that occurs in these habitats, including that

by benthic microalgae, much of the organic carbon input comes from leaf litter (Saifullah et al., 2016). In general, phytoplankton in mangrove forests are less well characterized than benthic microalgae (Saifullah et al., 2016) and their overall contributions to photosynthetic carbon fixation is considered highly variable (Kristensen et al., 2008).

As noted above, among the tropical aquatic habitats best characterized are coral reefs, which are both oligotrophic and highly productive (Fong & Paul, 2011). The main sources of organic carbon in these ecosystems are considered to be primary production by coralline red algae and the symbioses of corals with dinoflagellates of the family Symbiodiniaceae (Haas et al., 2016; LaJeunesse et al., 2018). Degradation of coral reefs due to anthropogenic influences has led to the shift from calcifying corals and algae to fleshy macroalgae, resulting in increased bacterial abundances in reefs and decreased carbon transfer to higher trophic levels based on data collected from reefs in the Caribbean Sea, Indian, and Pacific Oceans (Haas et al., 2016). While the Symbiodiniaceae-coral association is well-known, the dynamics of free-living phytoplankton in the water column above reefs are less well characterized, but likely important to understanding changes in the system and potential consequences.

Salt ponds, solar salterns, mangrove forests, and coral reefs can be found in or near the tropical island Curaçao, in the southern Caribbean Sea (~65 km north of South America). Aquatic environments around the island undergo varied influences, with the north shore exposed to the trade winds and therefore largely barren while the southern leeward coast contains salt ponds, mangrove forests, and fringing reefs (van

Duyl et al., 2002). As seen elsewhere, benthic cyanobacterial mats have been observed and reported as performing nitrogen fixation in Curaçao reefs (Brocke et al., 2018; D. M. de Bakker et al., 2017). Other research studies have focused on coral-associated microbes (Diekmann et al., 2002; Engelen et al., 2018) and coral feeding, taking into account water column phytoplankton, particularly cyanobacteria, as a food resource (Hoadley et al., 2021; Scheffers et al., 2004). In terms of eukaryotic phytoplankton, stramenopiles, green algae, cryptophytes, and haptophytes have been reported in above-reef Curaçao waters, with stramenopiles and green algae appearing to dominate these groups (Hoadley et al., 2021). To our knowledge, this study is the first multi-year sampling of phytoplankton community composition in Curaçao.

We sought to characterize phytoplankton molecular diversity and community composition from inland environments to the open sea using coherent methods, with additional focus on those groups that appeared to dominate based on amplicon relative abundances. Recently, a number of studies have indicated that the 16S rRNA gene (which is found in the chloroplast genomes of eukaryotic phytoplankton, as well as in bacterial genomes) has a more constrained copy number in eukaryotes than does the nucleus-encoded 18S rRNA gene (Choi et al., 2020; Needham & Fuhrman, 2016). This makes data from the 16S rRNA gene marker potentially closer to representing shifts in true abundance than the 18S rRNA gene marker. Here, we analyzed the V1-V2 hypervariable region of the 16S rRNA gene (16S V1-V2) from salt pond, saltern, mangrove, above-reef, and farther offshore microbial communities from samples collected annually from 2015 to 2019. In addition to examining microbial diversity

and potential co-occurrence of ASVs from different microbial (i.e., including phytoplankton) taxa, ASVs from eukaryotic phytoplankton (plastid-derived) and cyanobacteria were used to characterize the phytoplankton community. Additionally, a selection of above-reef and off-reef samples were sequenced for the V4 hypervariable region of the 18S rRNA gene (18S V4) to compare with 16S V1-V2 amplicon data and connect to literature on eukaryotic phytoplankton species that have previously been defined using 18S rRNA gene phylogenies. Collectively, our study provides insights on how phytoplankton diversity and community composition change along the tropical inland – offshore habitat gradient.

Materials and Methods

Study sites

Samples were collected in mid-to-late April and early May in the years 2015 (14-23 April), 2016 (19-29 April), 2017 (17-30 April), 2018 (11-18 April), and 2019 (26 April-4 May) at sites spanning the south coast of the island and encompassing salt ponds, salterns, mangrove forests, above-reef, off-reef, and open sea, as detailed hereafter. Salt pond samples were collected from Playa Santa Cruz (~12.307 °N, 69.144 °W) and Spanish Bay/Spaanse (~12.074 °N, 68.862 °W). Saltern samples were collected from Sint Willibrordus (~12.214 °N, 69.054 °W), Sint Michiel (~12.148 °N, 68.998 °W coastal, ~12.156 °N, 68.987 °W inland), and Jan Thiel (~12.089 °N, 68.880 °W). Mangrove samples were collected from within mangrove root systems and in mangrove lagoons (hereafter the entire habitat is referred to as

"mangrove") at Playa Santa Cruz (~12.307 °N, 69.145 °W), the Caribbean Research and Management of Biodiversity foundation (CARMABI)/Piscadera Bay (~12.136 °N, -68.969 °W), and Spanish Bay/Spaanse (~12.136 °N, 68.969 °W) using a sea kayak. More offshore environments were sampled by divers, either swimming from shore or being deposited by boat, and by deploying equipment from a boat. The reefs sampled were located at CARMABI/Piscadera Bay (~12.125 °N, 68.973 °W), Water Factory (~12.109 °N, 68.954 °W), Spanish Bay/Spaanse (~12.136 °N,68.969 °W), and East Point (~12.043 °N, 68.739 °W). Reef water was sampled at both the surface (0-0.5 m) and directly above corals (3-23 m). A shelf of fringing coral reef extends about ~70 m from the shore before sloping down into a ~1000 m deep marine trench. Off-reef samples were collected past the reef above the trench and samples that we characterized as open Caribbean Sea were from ~25 km off the east coast of Curaçao (~12.021 °N, 68.453 °W). Sites were mapped using Google Earth to determine distances relative to the coastline.

Collection of DNA, physico-chemical samples, and initial processing

The general method for collecting water for DNA sequencing varied between habitats. For salt ponds and mangroves, water was collected by submerging 1L amber bottles with care taken to avoid stirring up bottom sediments. For reefs and offshore environments, Niskin bottles or carboys were used. Biomass from ~7 to 515 mL of water (for most samples water volumes were at the upper end of this range, but for some salt ponds and salterns the high particulate load limited the volume that could

be filtered) was collected on a sterile 47 mm, 0.2 μm Supor filter (Pall, USA) using a vacuum or peristaltic pump. The filters were stored at -80 °C until DNA extraction. Between samples filtration vessels were rinsed with either reverse osmosis (RO) or 18.2 MΩ water (MilliQ) and left to dry before reuse. In 2017 and 2018, 500 ml volumes of the rinse water were also collected as controls. Also note that DNA filters collected in 2015 and 2016 were flash-frozen in liquid nitrogen before being stored at -80 °C. DNA extractions were performed using the QIAGEN DNeasy Plant kit (QIAGEN, USA) with a modified protocol including a bead-beating step (Cuvelier et al., 2010; Demir-Hilton et al., 2011).

Nutrient samples (silicate, phosphate, nitrate, and nitrite) were collected in 2017, 2018, and 2019 (n=182). For those collected in 2017 and 2018, 40 mL water was filtered through a 0.45 μm polyethersulfone syringe into separate duplicate 50 mL conical tubes and stored at -20 °C until further processing. For nutrient samples collected in 2019, 10 mL of water was collected and stored at -80 °C until further processing. Nutrient samples were measured using an AlpKem autoanalyzer according to protocols from Sakamoto et al., 1990. Salinity was measured using a hand refractometer from 2016-2019. Additionally, the sampling method used in 2019 did not allow for measurements above 100‰; therefore, for the hypersaline samples, the exact value was not measured but was considered above the range in which quantification is possible. Temperature throughout the day was measured for CARMABI/Piscadera Bay mangrove and reef in 2017 and 2019, Spanish Bay salt pond, mangrove, and reef in 2019, Sint Michiel and Sint Willibrordus salterns in

2019, and Water Factory reef in 2019 using a HOBO data logger (Onset Brands, Bourne, Massachusetts). Temperature data for open ocean sites was retrieved from global daily 5 km satellite data from the National Oceanic and Atmospheric Administration Satellite and Information Service.

16S rRNA gene amplicon sequencing, rarefaction, and diversity analyses

DNA from 282 samples coming from the salt pond, saltern, mangrove, above-reef, off-reef, and open sea environments sampled between 2015 and 2019 was PCR amplified using the primers that amplify heterotrophic bacteria, cyanobacteria, and eukaryotic plastid 16S rRNA gene amplicons, specifically the universal primers 27F (5-AGRGTTYGATYMTGGCTCAG-3) and 338R (5-GCWGCCWCCCGTAGGWGT-3) targeting the 16S V1-V2 (Daims et al., 1999; Vergin, Beszteri, et al., 2013). Paired-end library sequencing (2×300bp) was performed on PCR products and PCR negative controls using the Illumina MiSeq platform.

Raw sequencing reads were trimmed using cutadapt (v2.6; Martin, 2011) trimming with forward and reverse primers and default settings. Sequence data were trimmed (forward reads to 210 bp and reverse reads to 180 bp for 16S V1-V2), dereplicated, checked for chimeras, and assigned to amplicon sequence variants (ASVs) using the DADA2 R package, version (v1.10.0; Callahan et al., 2016). On average there were 245,708±110,167 resulting 16S V1-V2 amplicons. Note that a Water Factory above-

reef sample from 2018 only rendered 430 total amplicons and was excluded from further analyses.

Rarefaction was performed in R using the rareslope function in the vegan package (version 2.5.7) to determine sample saturation (Oksanen et al., 2020). All samples were considered to have reached saturation (final slopes of rarefaction curves less than 0.1). Alpha diversity was calculated based on 16S V1-V2 as the inverse Simpson index using the diversity function in the vegan package. The normality of the alpha diversity distributions was tested using the Shapiro test in the R stats package, and, since not all were normally distributed, the medians between sites and environments were compared using Kruskall-Wallis and Dunn tests (generating the KWDT statistic, herein KWDTS) using the R stats and rstatix packages (Kassambara, 2019). The medians and interquartile ranges of the inverse Simpson indexes were plotted by site and environment using the geom_boxplot function in ggplot2 (Wickham, 2011).

16S V1-V2 rRNA ASV taxonomic assignment

16S V1-V2 ASVs were taxonomically classified using the best node placement mode in the phylogenetic placement pipeline PhyloAssigner (Vergin et al. 2013). ASVs were first placed on a global 16S rRNA gene reference tree (Vergin, Beszteri, et al., 2013). Those assigned at the broad level to plastid or cyanobacterial best-node placements were subsequently placed on a more resolved plastid and cyanobacteria reference tree (Choi et al., 2017). Those that were placed with heterotrophic bacteria

were then further classified using the SILVA 138 pre-trained Bayesian classifier in QIIME 2 (Bolyen et al., 2019; Quast et al., 2013). Negative (PCR) controls on each plate were also run, appeared negative on gels, and rendered <100 amplicons when sequenced alongside samples. We also ran controls in which 500 ml of RO or 18.2 MΩ water from the research station (used for rinsing filter rigs) was filtered, extracted, and sequenced. One of the latter (2017) rendered amplicons that were assigned to cyanobacteria and eukaryotic algae, and it is unclear whether this derives from well cross contamination or switched samples.

ASVs assigned to the cyanobacterial region of the tree were further classified using a designated phylogeny (Sudek et al., 2015). ASVs assigned to the Viridiplantae, which includes chlorophyte and prasinophyte algae, as well as the newly designated Prasinodermophyta phylum (L. Li et al., 2020), were then placed on a Viridiplantae reference tree in a second classification step to assign the final taxonomy of these ASVs. ASVs assigned to stramenopiles in the plastid and cyanobacteria placement were re-classified in a multi-step approach using reference trees as described in Choi et al., 2020, 2017.

A subset of green algae could not be placed at terminal nodes using PhyloAssigner, and therefore were manually checked. In the case of salt pond and saltern chlorophyte ASV placements, they were used as blast queries against GenBank nr and found to be *Dunaliella*. Mangrove, salt pond, and saltern diatom ASV placements were further investigated using them as queries against GenBank nucleotide database. Amplicons from *Micromonas* clades A and B can be delineated

from Clades C, D, and E *sensu* Šlapeta et al., 2006, but phylogenetic placement of 16S V1-V2 ASVs did not resolve A/B from one another with statistical support; therefore, sequences assigned to the A/B/C lineage as a whole were manually aligned for evaluation of known single nucleotide polymorphisms in the 16S V1-V2 that distinguish them from each other.

Improving Class II classification via connecting 16S (plastid derived) and 18S rRNA gene sequences

Because little information is available connecting 16S rRNA genes and 18S rRNA genes for several uncultured prasinophyte species (which have largely been defined using the 18S rRNA gene), we sequenced the V4 hypervariable region of the 18S rRNA gene for a subset of above-reef and off-reef samples from 2019 so that correlation studies would be possible (41 in total). Here, DNA was PCR amplified using the primers TAReuk454FWD1 (5'-CCAGCASCYGCGGTAATTCC-3') and TAReukREV3 (5'-ACTTTCGTTCTTGATYRA-3') targeting the V4 (Stoeck et al., 2010). Paired-end library sequencing (2×300bp) was performed on PCR products and PCR negative controls using the Illumina MiSeq platform. Sequence data were trimmed (forward reads to 220 bp and reverse reads to 200 bp), dereplicated, checked for chimeras, and assigned to ASVs using the DADA2 R package, version (v1.10.0). Post quality control this rendered 287,092±56,468 18S V4 amplicons per sample. Rarefaction of 18S V4 amplicons was performed as for 16S rRNA gene amplicons. 18S V4 ASVs were initially classified using the sklearn trained classifier and the PR2 database (Guillou et al., 2013). The relevant prasinophyte ASVs were then used to

connect 18S rRNA gene derived clade information with the 16S rRNA gene (plastid derived) ASVs that were the focus of our study. Connections were made by comparing relative contributions of specific amplicons/ASVs to all those from the genus in both 16S V1-V2 and 18S V4 (in the same samples). For example, ASVs determined to be *O. bengalensis* in the 18S V4 were compared to those considered likely *O. bengalensis* in the 16S V1-V2 of the samples with both types of sequencing available using Pearson's correlation in the R stats package (R Core Team, 2002). Using this approach, we determined connections between the two types of marker genes for *Micromonas* candidate species 1 and 2 (again, initially described using 18S rRNA gene sequences (Simon et al., 2017; Worden, 2006) and *O. bengalensis* (described using molecular phylogenies in Strauss, Choi, Grone et al. in rev.). 16S V1-V2 ASVs were then assigned at the highest taxonomic level possible using manual comparison after initial genus placement using PhyloAssigner as above.

Relative abundances and links to environmental variables

For each sample the relative abundance of eukaryotic algal and cyanobacterial amplicons was computed relative to total phytoplankton amplicons (as the sum of cyanobacterial and plastid-derived 16S V1-V2 amplicons). The percent of each eukaryotic algal group was also computed out of total plastid amplicons in the sample, that is with cyanobacterial and heterotrophic bacterial amplicons removed, or computed at higher taxonomic resolution, for example each prasinophyte group out of all prasinophyte amplicons, or each stramenopile group out of all stramenopile

amplicons, or each ASV in the same manner. These relative abundances were plotted as pie charts using ggplot2 (Wickham et al., 2019). Each fraction of the pie represents the relative abundance of the group out of all amplicons in the larger group across the sum of all samples and years per site. The number of individual ASVs per phytoplankton group is specified adjacent to each pie fraction. We also determined the percent of cyanobacterial amplicons out of total amplicons and *Prochlorococcus*, *Synechococcus*, and "other cyanobacteria" out of all cyanobacterial amplicons. Heatmaps of relative abundance were generated using the ggplot2 geom_tile function. For the 41 samples that were also sequenced for 18S V4 amplicons, relative abundances of photosynthetic groups (excluding purely heterotrophic groups e.g., stramenopile groups Pseudofungi and Opalozoa) were computed for each sample with alveolates and deep-branching plastid lineages (DPLs) excluded.

Differences in microbial community composition were investigated at the ASV level by site and environment via non-metric multidimensional scaling (NMDS). NMDS plots were generated in R with the vegan and ggplot2 packages using Hellinger-transformed count data of all ASVs (heterotrophic bacteria, cyanobacteria, and plastid-bearing eukaryotes), which in some plots was then subset by ASV type (photosynthetic ASVs, stramenopile ASVs, and green algae ASVs). For the NMDS plot of the entire microbial community, environmental vectors (salinity, nitrate, nitrite, phosphate, and silicate; temperature was not included in this analysis due to too few data points) were superimposed on the plot; note that over the five

years nutrients and salinity were not consistently sampled (Table S1), such that in this analysis 182 out of 282 total samples were included.

The possible relationship between silicate and diatom relative abundance out of plastid amplicons was investigated via linear regression initially for all environments and then restricted to samples with salinities <40‰. The potential links between environmental parameters and ASV-level distributions of green algae and chlorarachniophytes were investigated via canonical correspondence analysis (CCA) using the R packages tidyverse, reshape2, and ggplot2 (Wickham et al., 2019). A Variance Inflation Factor (VIF) analysis was performed in order to check for multicollinearity among variables using the car package (J. Fox et al., 2022). ASV data were normalized using the Hellinger method and both data normalization and CCA were run using the vegan library. The significance of the association of environmental parameters with ASV distribution was determined using the ANOVA-like permutation test for CCA in vegan, anova.cca. Analysis of similarity (ANOSIM) tests were performed on Hellinger-transformed count data of green algal and stramenopile ASVs. This was performed in the vegan package in R to test differences in microbial community composition between environments (Dixon, 2003).

Co-occurrence analyses

In order to contextualize the major photosynthetic groups within the wider microbial community, we conducted a network co-occurrence analysis using the cooccur, igraph, and SpiecEasi packages in R (Csardi & Nepusz, 2005; Griffith et al., 2016;

Kurtz et al., 2015). The analysis was performed in two ways. The first involved ASVs that occurred in at least 25% of samples across environments and had a mean relative abundance of at least 0.05%. These cutoff criteria were used to avoid detection of "pseudo" co-occurrence, that occurs when there are a considerable number of rare ASVs found only in a handful of samples, so that those are identified as co-occurrence (although only in a handful of samples) by co-incidence. The second set of criteria, mean relative abundance of at least 0.05% across the top 5 samples in which a given ASV was most abundant, was used in order to detect formation of habitat specific networks in those habitats that made up low proportion of samples and had potentially distinct ASV communities. In both cases significant interactions between photosynthetic ASVs and other photosynthetic or heterotrophic ASVs were plotted in a co-occurrence network with each point representing an ASV and the shape of the point corresponding to the environment type in which it occurs most often.

RESULTS

Microbial diversity across tropical aquatic habitats

To characterize habitats, we evaluated a number of abiotic parameters resulting in five general categories based on local topography and connectivity to the sea: salt ponds (further dividing to salterns and natural salt ponds), mangroves, above-reef, off-reef, and open sea (Figure 1, Table S1). We then undertook amplicon sequencing for samples from each of these, generating on average 249,603±110,247 (± standard deviation (SD), n=282) 16S V1-V2 amplicons per sample which resulted in

1,554±708 ASVs per sample. By environment, there was an average of 242,637±153,030 amplicons (resulting in 765±502 ASVs) from the 16 salt pond samples, 323,768±124,987 amplicons (resulting in 1,499±810 ASVs) from the 41 saltern samples, 241,736±94,365 amplicons (1,685±766 ASVs) for 59 mangrove samples, 233,385±105,086 amplicons (1,628±657 ASVs) from 140 above-reef samples, 236,778±49,835 amplicons (1,302±164 ASVs) from 14 off-reef samples, and finally, 248,352±88,624 amplicons (1,572±598 ASVs) from 12 open Caribbean Sea samples. Rarefaction analysis indicated that saturation was reached for all samples regardless of environment (Figure S1).

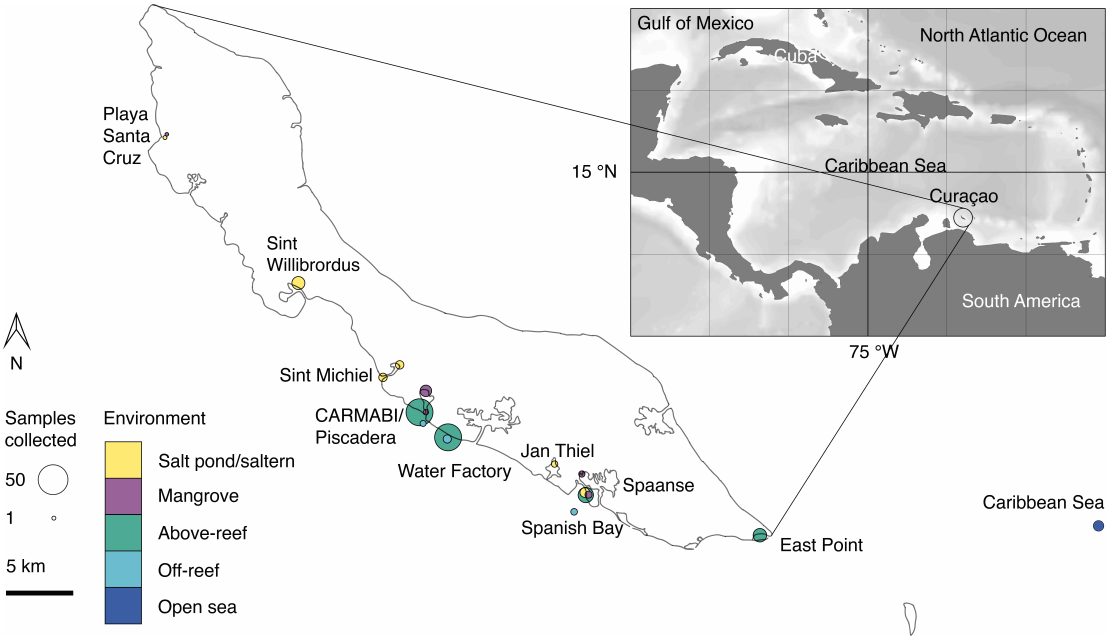

Figure 1: Overview map of sampling sites on or near Curaçao collected between 2015 and 2019. Environment type is indicated by color and circle radius size indicates the number of samples collected at the site throughout the time series. In total 282 DNA samples were collected, all of which were sequenced for 16S V1-V2 amplicons, and 41 (2019 only) of which were sequenced for 18S V4 amplicons. Inset,

location of Curaçao within the Caribbean Sea, with the closest continent being South America.

Microbial alpha diversity was examined by computing the median inverse Simpson index from the ASVs generated from each site and grouped by habitat (Table S2, Table S3). Within salt ponds and salterns, Sint Michiel coastal and Sint Willibrordus had the highest median inverse Simpson index, at 38.6±12.9 (± interquartile range) and 27.0±11.0 respectively, followed by Sint Michiel inland (21.0±5.0), Jan Thiel (7.3±1.1), Spanish Bay/Spaanse (6.0± 10.2), and Playa Santa Cruz (3.9) (Figure 2b, Table S2). Significant differences in diversity were found between Sint Willibrordus and Jan Thiel (KWDTS=3.6, p=0.04), Sint Michiel coastal and Jan Thiel (KWDTS=4.6, p<0.001), and Sint Michiel coastal and Spanish Bay/Spaanse (KWDTS=-5.9, p<0.001, Table S3). There were also significant differences in the median inverse Simpson index between Sint Michiel coastal and inshore samples (KWDTS=4.0, p=0.01). Within mangroves, Playa Santa Cruz had the highest average alpha diversity at 39.4, then CARMABI/Piscadera (30.7±13.7), then Spanish Bay/Spaanse (18.8±6.8) (Figure 2b), with significant difference between CARMABI/Piscadera and Spanish Bay/Spaanse (KWDTS=-5.0, p<0.001). There was less variation in above-reef, off-reef, and open sea samples, with no significant differences between sites in those environments (Figure 2b). There was no significant difference between the median inverse Simpson index observed in above-reef samples collected at the surface (25.5±7.1) versus samples taken at depth closer to the

corals (25.0±6.6) (KWTS=3.8, p=0.05). Considered together across sites, above-reef, off-reef, and open sea had an overall median inverse Simpson index of 21.9±7.3.

Statistical tests on the diversity indices were also used to compare between environments. These showed for example that the CARMABI/Piscadera mangroves had a significantly higher median inverse Simpson index than the Jan Thiel saltern (KWDTS =-4.2, p=0.004), the Spanish Bay/Spaanse salt pond (KWDTS =-5.9, p<0.001), inshore Sint Michiel (KWDTS =-3.6, p=0.04), and the East Point reef (KWDTS =-3.7, p=0.03). Among other significant differences the Sint Willibrordus and coastal Sint Michiel salterns had significantly higher median inverse Simpson indexes than Spanish Bay/Spaanse mangrove (KWDTS =-3.7, p=0.03 and KWDTS =-4.9, p<0.001, respectively) and likewise, CARMABI/Piscadera reefs had a higher median inverse Simpson index than the Jan Thiel saltern (KWDTS = -3.7, p=0.04), Spanish Bay/Spaanse mangrove (KWDTS = -4.1, p=0.01), and Spanish Bay/Spaanse salt pond (KWDTS = -5.2, p<0.001).

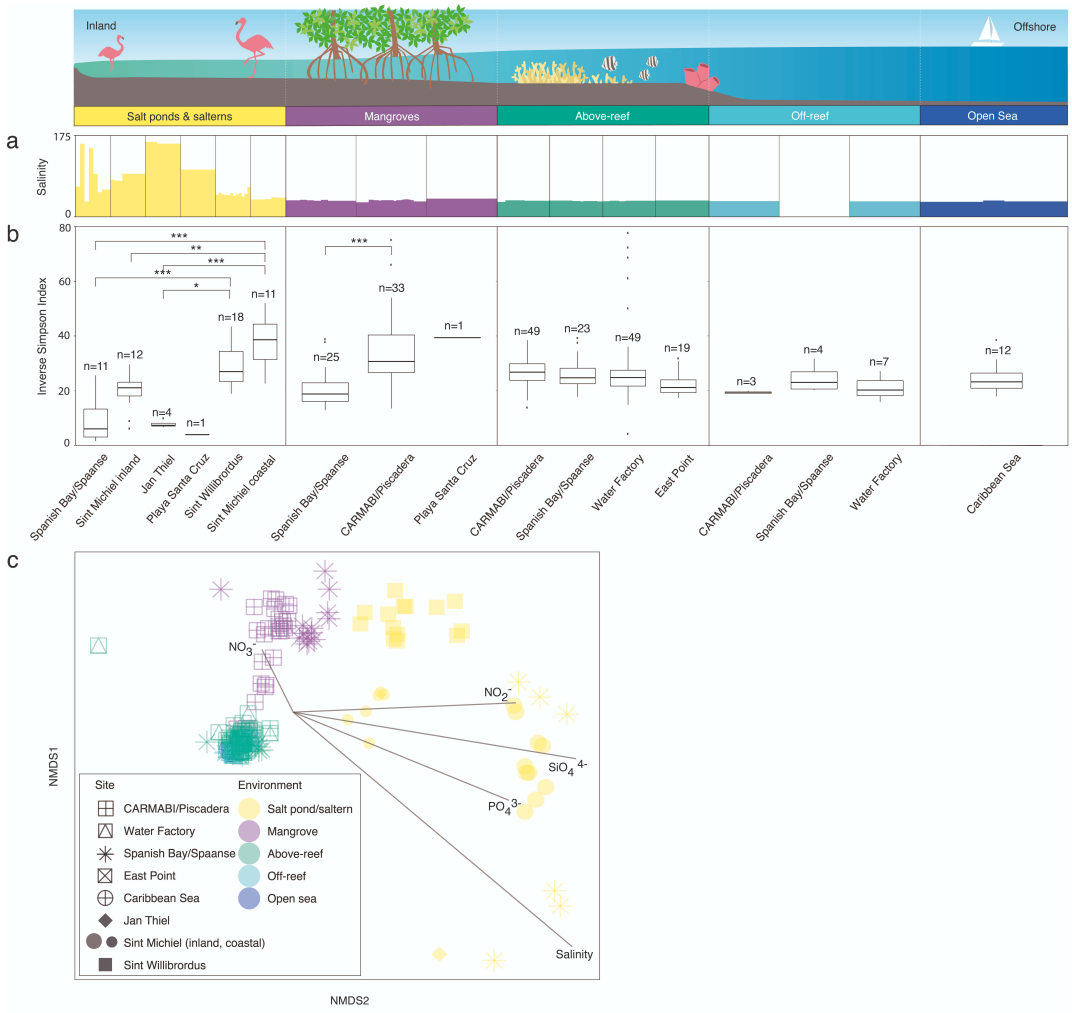

Figure 2: Microbial community diversity based on 16S rRNA gene amplicons. Variations in salinity (a) and inverse Simpson index (b) as the median and distribution from 2015 to 2019, respectively, from inland to offshore environments. Outliers are shown by individual data points. Significant differences in the median inverse Simpson index between sites are indicated by brackets and asterisks (adjusted p-value of ≤0.05, *; ≤0.01, **; ≤0.001, ***) (Table S3). Note that the Sint Michiel saltern has the highest connectivity to the sea out of the salterns and salt ponds and has one location close to the coastline and the other farther inland. Sint Willibrordus and Jan Thiel, respectively, follow in terms of connectivity to the sea, while the Spanish Bay/Spaanse and Playa Santa Cruz salt ponds have no apparent connection to the sea. (c) NMDS analysis with each point indicating an individual sample, distinguished by site (shape) and environment type (color) and overlain with vectors of environmental parameters (salinity, nitrate, nitrite, phosphate, and silicate) to visualize similarity of the total ASV-level community composition (heterotrophic bacteria, cyanobacteria, and plastid-bearing eukaryotes) among sites and environments. Symbols for open sea and off-reef samples are partially obscured

beneath above-reef samples. For off-reef and open sea samples environmental parameter data come from 2017 sampling. Note that the dotted white vertical lines on the cartoon above environments is included to make sure it is clear that the habitats were not necessarily sampled along a linear line, because organization of the natural environment does not necessarily occur in that fashion. Note also that over the five years nutrients and salinity were not consistently sampled (Table S1), such that in this analysis 182 out of 282 total samples were included.

Silicate concentrations were highest in salt ponds (ranging from 18-243 μmol kg^{-1}) and salterns (3-184 μmol kg^{-1}), with the next highest values found in mangroves (0.5-13 μmol kg^{-1}) and the lowest over reefs and farther offshore (overall, 0.2-2 μmol kg^{-1}) (Table S1 and Figure S2). Phosphate and nitrite values followed the same trend, with salt ponds ranging from 0.4-60 μmol phosphate kg^{-1} and 0.2-6 μmol nitrite kg^{-1}, salterns ranging from 0.1-14 μmol phosphate kg^{-1} and 0-3 μmol nitrite kg^{-1}, mangroves ranging from 0.1 to 1 μmol phosphate kg^{-1} and 0-0.7 μmol nitrite kg^{-1}, and reefs and offshore habitats as a whole ranging from 0-0.3 μmol phosphate kg^{-1} and 0-0.2 μmol nitrite kg^{-1}. Nitrate values were highest above reefs (0.1-6 μmol kg^{-1}) and mangroves (0-3 μmol kg^{-1}) and next highest in salt ponds (0-2 μmol kg^{-1}) and salterns (0-1 μmol kg^{-1}) compared to off-reef and open sea (0-0.1 μmol kg^{-1}) (Table S1 and Figure S2). Salinities ranged from >170‰ at salt ponds to more standard open ocean salinities (e.g., 36‰; Table S1). Water temperatures reached their highest value out of all environments in salterns (ranging from 25.4- 36.8 °C), next highest in salt ponds (26.9- 31.4 °C), then mangroves (27.0-31.3 °C), and above reefs (24.5- 31.1 °C); farther offshore sites do not have temperature data measured in this study, but satellite data indicates temperatures of 26.6-27.2 °C at the time of sampling.

To interrelate microbial ASV diversity to environmental parameters, we performed NMDS analyses that incorporated all samples with available nutrient (nitrite, nitrate, silicate, and phosphate) and salinity data (Table S1). Overall, the environmental vectors in the NMDS plot indicated salterns and salt ponds were associated with higher nitrite, silicate, phosphate, and salinity, while higher nitrate was associated with mangroves and above-reef samples (temperature was not included in this analysis due to too few data points; Figure 2c). Significant differences in microbial community composition were observed among the different environments (Figure 2c; ANOSIM test statistic $r=0.72$, $p<0.001$). Microbial communities in above-reef, off-reef, and open sea samples grouped together in an NMDS plot and did not appear significantly different (ANOSIM test statistic $r=-0.18$, $p=0.8$, Figure 2c). Additionally, microbial communities from surface and deeper above-reef samples did not exhibit significant differences (ANOSIM test statistic $r=0.02$, $p=0.07$; not shown in plot). Mangrove samples also generally grouped together more tightly in the NMDS, with more separation based on location, and exhibited some overlap with above-reef samples (Figure 2c). Within salterns and salt ponds, Sint Willibrordus samples grouped together, Sint Michiel inland and coastal formed two separate groups, and Spanish Bay/Spaanse samples were more varied (Figure 2c). The more coastal saltern samples (Sint Willibrordus and Sint Michiel coastal) grouped closer to other environments than to samples from the inland Sint Michiel, Spanish Bay/Spaanse, and Jan Thiel salt pond/saltern sites (Figure 2c).

Eukaryotic phytoplankton community composition along environmental gradients

To compare the primary producer communities across these habitats, we parsed the photosynthetic component of the microbial community from non-pigmented bacteria and performed taxonomic assignment using previously established phylogenetic approaches (Table S4). Out of all 16S V1-V2 amplicons from photosynthetic taxa (cyanobacterial and plastid-derived amplicons), relative contributions of eukaryotic phytoplankton were variable, ranging from the lowest being above-reef (8±6%) (Mean ± SD), off-reef (4±2%), and in the open sea (7±7%). Higher contributions were observed in mangroves (33±17%), salt ponds (51±42%), and salterns (44±32%). Stramenopiles exhibited highest relative abundances of eukaryotic algal groups except in salt ponds, making up 5±8% of photosynthetic eukaryotic amplicons in salt ponds, 34±23% in salterns, 47±19% in mangroves, 61±16% above-reef, 71±6% off-reef, and 63±20% in the open sea (Figure 3c). Green algae exhibited the next highest relative abundances across environments, comprising 72±39% of photosynthetic eukaryotic amplicons in salt ponds, 31±28% in salterns, 32±15% in mangroves, 31±15% above-reef, 30±17% off-reef, and 24±17% in the open sea (Figure 3c). Several other major phytoplankton groups exhibited punctuated appearances. For example, cryptophytes had the highest relative abundances among photosynthetic eukaryotes in Sint Willibrordus saltern (43±25%) and had high relative abundances in Spanish Bay/Spaanse mangroves (24±14%) (Figure 3). Likewise, chlorarachniophytes (which contain a green-algal derived plastid) were the major

photosynthetic group in some Spanish Bay/Spaanse and Sint Michiel salt pond/saltern samples. Haptophytes and alveolates were also detected, with haptophytes reaching their highest relative abundances above-reef (5±3%), off-reef (10±2%), and in the open sea (7±4%; Figure 3c). Comparison of broad taxonomic distributions for 41 samples in which both 16S V1-V2 and 18S V4 were sequenced indicated similar proportions of photosynthetic groups (Table S5, Table S6). Finally, we observed sequences from glaucophytes, rhodophytes, and recently described eukaryotes from the DPLs identified in Choi et al., 2017. These groups had low overall relative abundances (Figure 3c, grouped under "other eukaryotes"). Given the dominance of stramenopiles and green algae over the sampled habitats, and the fact that these groups harbor extensive diversity, we then analyzed them at higher taxonomic resolution.

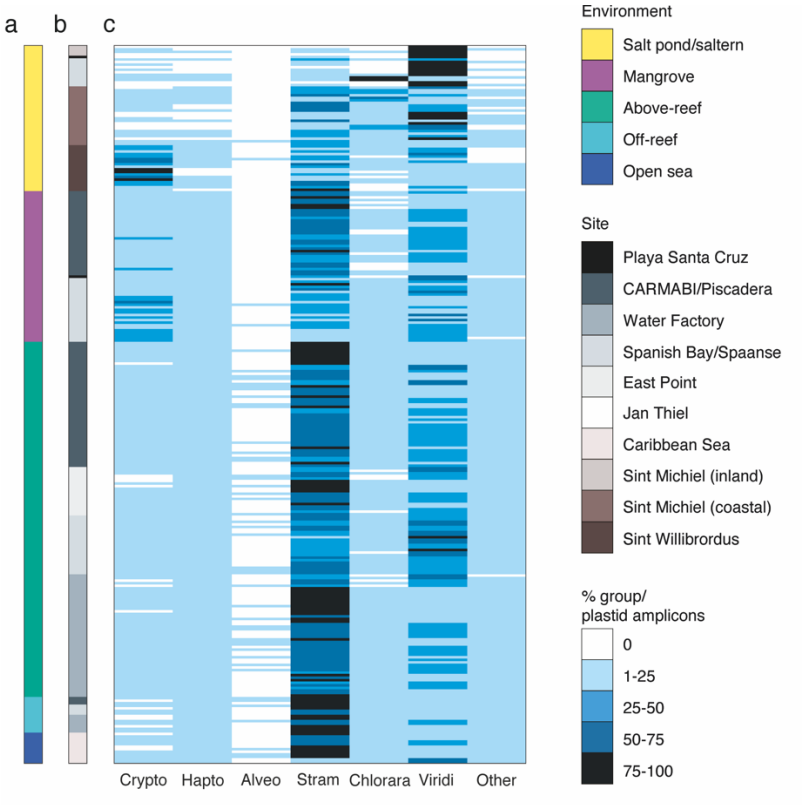

Figure 3: Major phytoplankton groups associated to different Curaçao aquatic environments. Relative abundance of 16S V1-V2 ASVs assigned to major eukaryotic phytoplankton groups by (a) environment and (b) sampling site. The relative percent abundance of each major photosynthetic eukaryotic group is computed out of all plastid amplicons and is indicated by the heatmap in (c), with each row indicating an individual sample (n=282). Low relative abundance of dinoflagellates may reflect primer biases. Abbreviations are as follows: Crypto, cryptophytes; Hapto, haptophytes; Alveo, alveolates, specifically photosynthetic dinoflagellates; Stram, stramenopiles; Chlorara, chlorarachniophytes; Viridi, Viridiplantae green algae (prasinophytes, chlorophytes and prasinodermophytes); Other, the sum of glaucophytes, rhodophytes, and members of the deep-branching plastid lineages (DPL), averaged 1±2% of plastid-derived sequences and are therefore collapsed for figure simplicity.

Variations in Stramenopile and Green Algal Diversity

Stramenopiles and green algae represented the two major eukaryotic phytoplankton groups in the ASV data across the habitats (Figure 3c). Each displayed distinct

community composition among environments when just considering these two major groups independently (ANOSIM test statistic $r=0.64$, $p<0.001$ for each). When analyzing the stramenopile community, those in mangrove habitats, particularly in Spanish Bay/Spaanse, grouped closer to salterns located at Sint Willibrordus than seen for either the whole community NDMS analysis or that for the photosynthetic community (Figure S3). In contrast, above-reef, off-reef, and open sea communities mostly grouped closely, similar to the other NMDS plots (Figure S3). Differences between coastal and inland Sint Michiel samples were observable, but less pronounced than in the NMDS plots with all ASVs (Figure S3a and c).

We next characterized the global averages of different stramenopile groups by averaging the relative amplicon abundances (as percent of total stramenopile amplicons) from each site, using all data collected over the five years regardless of available metadata (e.g., nutrients, etc.). We also determined the total number of ASVs found for each group in those five years.

In salt ponds, the dominant stramenopiles comprised several diatom lineages, but because diatoms were not present in all samples their average contribution across the samples was highly variable (41±44% relative abundance of all stramenopile amplicons). The most abundant stramenopile ASV (ASV7549) was closest to the pennate diatom *Synedra hyperborea* (98.6% nucleotide (nt) identity). The exception to the overall dominance of diatoms occurred in the Spanish Bay/Spaanse salt pond, which had relatively high but variable contribution of eustigmatophytes (maximum 91%, with an average of 26±40% at this site) (Figure 4a). Salterns were similarly

mostly composed of diatoms (84±18%), with ASV308 being the most relatively abundant and closest to the benthic diatom *Navicula phyllepta* (98.9% nt identity). Stramenopile amplicons in mangroves were also dominated by diatoms (82±13%), with ASV97 being the most abundant and closest to members of the Thalassiosirales order (100% nt identity to several species: *Thalassiosira profunda*, *Skeletonema tropicum*, *Skeletonema costatum,* and *Skeletonema marinoi*). However, moving offshore, diatom contributions declined in terms of relative abundance above-reef (47±17% of stramenopile amplicons), off-reef (27±8%), and in the open sea (40±13%; Figure 4c-d). ASV32, corresponding most closely to *Chaetoceros* (100% nt identity to *C. simplex* and *C. tenuissimus*) was the most relatively abundant diatom ASV across above-reef samples, while in off-reef and open sea samples ASV87 (99.3% nt identity to *Tryblionella apiculata*) had the highest relative abundances. Above-reef and mangrove diatom taxa overlapped the most, followed by salterns and mangroves (Figure S4a). Just three diatom ASVs were found across all five environment types: ASV32 and ASV87, as above, and ASV620, which corresponds to *Rhizosolenia imbricata* (100% nt identity). Diatom relative abundance within total plastid amplicons decreased with decreasing silicate concentrations ($R=0.55$, $p<0.001$) when saline habitats >40‰ were excluded.

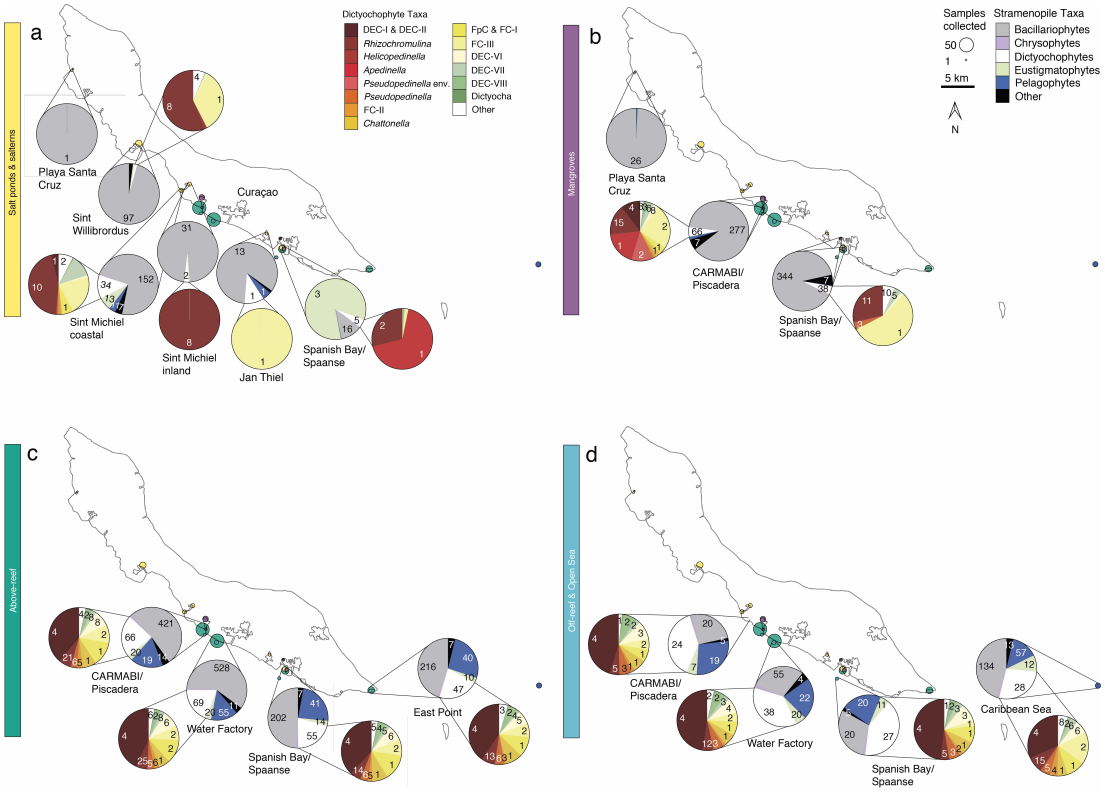

Figure 4: Stramenopile algae and dictyochophytes from salterns to the open sea. Composition of the photosynthetic stramenopile community based on 16S V1-V2 amplicons out of all stramenopiles and a second, separate and more refined breakdown of dictyochophytes (where present) out of all dictyochophyte amplicons for (a) salt ponds and salterns, (b) mangroves, (c) above-reef, and (d) off-reef and open sea habitats averaged over 2015-2019. Coloring of groups is as indicated in the on-figure color legend. Each pie fraction reflects the relative abundance of the specific group out of all stramenopile amplicons, across the sum of all samples (and all years) from that site; the number given reflects the number of ASVs (not the average) in all samples at that site.

Dictyochophytes and pelagophytes had higher relative abundances in more offshore environments than the other habitats sampled (Figure 4c-d).

Dictyochophytes averaged 23±12% of stramenopile amplicon relative abundances above-reef, 40±9% off-reef, and 30±9% in the open sea, and pelagophytes had

slightly lower relative abundances among stramenopiles, with relative abundances of 20±9% above-reef, 22±5% off-reef, and 16±8% in the open sea. The major pelagophyte groups across sites and environments based on relative abundances were *Pelagomonas calceolata* (most relatively abundant ASVs being ASV165 and ASV279) and pelagophyte environmental clade VIII (PEC-VIII, particularly ASV650), apart from Playa Santa Cruz mangroves, which had a majority of pelagophyte environmental clade VI (PEC-VI, especially ASV12487).

Dictyochophytes had higher levels of diversity and distinction among environments than pelagophytes based on phylogenetic analyses. Because of their diversity, and how little is known about dictyochophytes in tropical ecosystems, we analyzed these protists at a higher taxonomic resolution (Figure 4, Figure S4b). Salt ponds and salterns had highly variable dictyochophyte contributions (Figure 4a). Considering only samples that exhibited dictyochophyte amplicons, in Sint Willibrordus and Sint Michiel (n= 28), *Rhizochromulina* (55±38%) and *Florenciella* clade (FC) FC-III (22±31%) dominated the dictyochophyte amplicons (Figure 4a), and Sint Michiel coastal samples (n= 10) additionally harbored dictyochophyte environmental clade (DEC) DEC-VII (10±7%) and two environmental (uncultured) clades DEC-I and DEC-II (0.6±0.7%). The most relatively abundant dictyochophytes in Spanish Bay/Spaanse salt pond samples were *Rhizochromulina* (74±42%) and *Apedinella* (22±43%), and only *Florenciella* clade FC-III was detected at one Jan Thiel sample (Figure 4a). Mangroves showed lower relative abundances of dictyochophytes. CARMABI/Piscadera mangroves (n=33) comprised primarily DEC-

I and DEC-II (5±11%), *Rhizochromulina* (21±12%), *Apedinella* (20±18%), *Pseudopedinella* environmental clade (15±11%), and *Florenciella* clade FC-III (27±13%). Spanish Bay mangroves were mostly FC-III (46±21%) and *Rhizochromulina* (30±22%). In above-reef, off-reef, and open sea samples (n=165) the highest relative abundance belonged to DEC-I/DEC-II, which together formed relative abundances of 40±10% out of dictyochophyte amplicons (note these two clades were not resolved from each other), with lesser but consistent contributions from other dictyochophyte groups (Figure 4c-d). Similar to diatoms, above-above-reef sites had the greatest number of dictyochophyte ASVs that appeared to be unique to that habitat, followed by mangroves and salterns (Figure S4b). Only one dictyochophyte ASV (ASV419) was shared among all environments; however, when salt ponds were excluded this number increased to 19 ASVs (Figure S4b).

The other major supergroup in our study was the Archaeplastida and in particular the Viridiplantae, which in our analyses encompassed three green algal groups, the chlorophytes, prasinophytes, and the prasinodermophytes (Bachy, Wittmers, et al., 2022). NMDS analysis incorporating only green algal ASVs exposed significant differences between above-reef and off-reef samples compared to the open sea (ANOSIM test statistic r= 0.24, p=0.01, and ANOSIM test statistic r= 0.13, p=0.02) (Figure S3d), differing from NMDS results for the total microbial community (Figures 2b and S3a). There was some overlap between mangrove and Sint Willibrordus saltern samples, but not as much as for stramenopiles (Figure S3c).

Finally, differences in the more coastal and farther inland Sint Michiel samples were also evident in green algal NMDS analysis (Figure S3d).

The composition of the green algal community also varied across sites and environments. Prasinophyte Class IV (Chlorodendrophyceae) was the only green algal taxon detected at Playa Santa Cruz and also formed a large but variable portion of green algal amplicon abundances in the Sint Michiel inland saltern (35±36%), Spanish Bay/Spaanse salt pond (34±44%), and Sint Willibrordus saltern (48±36%) (Figure 5). The most abundant ASV (ASV27) within this class was phylogenetically placed with *Tetraselmis*. Chlorophyceae (mostly *Dunaliella*) reached their highest relative abundance in Spanish Bay/Spaanse salt pond (35±48%) and Jan Thiel saltern (97±6%) (Figure 5). In mangroves, the green algal community shifted almost entirely to Class II prasinophytes (Mamiellophyceae), particularly *Ostreococcus* and *Micromonas*, as seen at CARMABI/Piscadera and Spanish Bay/Spaanse (Figure 5b). The major *Ostreococcus* groups were *Ostreococcus* Clade OII and an *Ostreococcus* identical in the 16S V1-V2 to *Ostreococcus bengalensis* (Strauss, Choi, Grone et al. in rev.; Figures 5b and S5). Here, because this is a newly defined species that has not been cultured, we utilized the 18S V4 ASV data (Table S5) and found that the 18S V4 was also identical to that of *O. bengalensis*. Major *Micromonas* groups included *Micromonas bravo* (Clade E1), *Micromonas commoda* (Clade A, sensu Simmons et al. 2015), and candidate species 1 and 2 (Simon et al., 2017; Worden, 2006; Figure 5b). The 16S V1-V2 sequence for *Micromonas* candidate species 1 and 2 were identified based on comparison between 18S V4 amplicons and 16S V1-V2

amplicons analyzed in this paper (Figure S5). In the CARMABI/Piscadera mangroves, 3 out of 28 *Micromonas* ASVs (3±2% of green algal relative amplicon abundances) could not be assigned at the species or clade level. In the singular Playa Santa Cruz mangrove sample, chlorophytes, specifically members of the class Trebouxiophyceae, including relatives of the halotolerant *Picochlorum soloecismus* and *Chlorella desiccate*, as well as an unidentified chlorophyte (phylogenetically closest to the Marsupiomonadales), were the most abundant among green algal amplicons (Figure 5b).

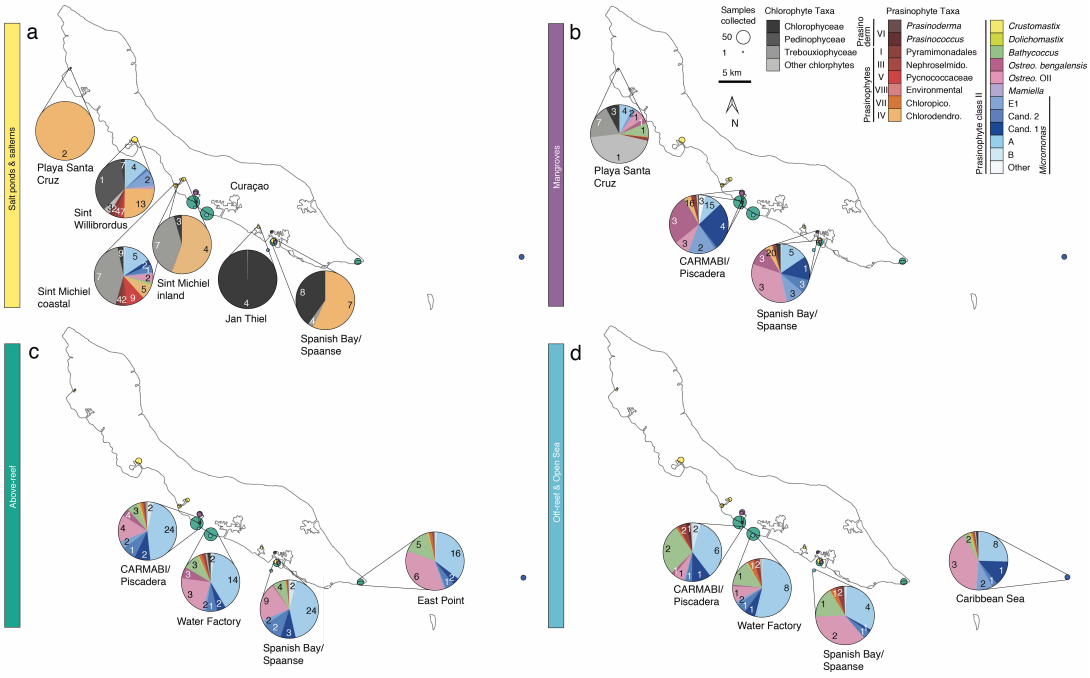

Figure 5: Green algae from salterns to the open sea. Green algae from salterns to the open sea. Composition of the green algal community by environment and sampling site based on 16S V1-V2 amplicons for (a) salt ponds and salterns, (b) mangroves, (c) above-reef, and (d) off-reef and open sea habitats spanning from 2015 to 2019. Each pie chart represents relative contributions of the individual taxa within chlorophyte, prasinodermophyte (recently elevated to a separate phylum from prasinophytes), and prasinophyte groups to green algal amplicons, as indicated by

colors. The total summed number of ASVs found within each taxonomic group across the 5 sampling years is specified for each pie fraction.

Prasinophytes in above-reef, off-reef, and open sea samples were also dominated by Class II, particularly *Micromonas*, *Bathycoccus*, and *Ostreococcus*. *Ostreococcus* OII increased in relative importance above reefs and farther offshore compared to mangroves where *O. bengalensis* rivaled it. *Micromonas* groups included Clade E1, Clade A, and candidate species 1 and 2, with relatively more Clade A compared to mangrove samples. In above-reef samples two of 33 *Micromonas* ASVs could not be assigned to a species or clade (<2% of green algal relative amplicon abundances). These two unassigned ASVs were similar to each other (1 nt difference) and otherwise most closely related to members of the *Micromonas* A/B/C lineage.

A CCA was used to compare green algal distribution and environmental parameters. The VIF analysis showed no multicollinearity among the environmental variables. The CCA showed ASVs from Class II grouped more closely to the nitrate vector in a CCA analysis of green algal ASVs, while other prasinophyte such as Class VII *Picocystis*, Class V Pycnococcaceae, and Class IV Chlorodendrophyceae grouped closer to the other nutrients and salinity vectors, as did Trebouxiophyceae, Chlorophyceae, and other chlorophyte ASVs (Figure S6). As shown by the permutation test, the CCA ordination was significant (p-value < 0.001) and the environmental variables salinity, phosphate, nitrite, and silicate were significant (p-value < 0.001), explaining most variance.

Green algae and dictyochophytes across habitats

To further tease apart potential differences that might connect to factors not quantified herein, samples were sorted by their proximity to the coast using only the years for which we had the most comprehensive environmental data (2017-2019). This subset of samples exhibited the trends in salinity and nutrients akin to those over the entire sample set. For example, Spanish Bay/Spaanse salt pond (average salinity 71±20‰; 187±80 µmol silicate kg^{-1}) and Sint Michiel inland (96±8‰; 61±27 µmol kg^{-1}) had both higher salinity and silicate than those of Sint Willibrordus (52±3‰; 17±12 µmol kg^{-1}), and Sint Michiel coastal (42±2‰; 4±1 µmol kg^{-1}) (Figure 6a, 6b, Table S1). Salinities of other environments were less variable, and silicate declined to 4±3 µmol kg^{-1} in mangroves and was lower above-reef, off-reef, and in the open sea (averaging 0.8±0.3 µmol kg^{-1}; Figure 6b). The highest phosphate concentrations were found in inland salt pond and saltern samples, reaching 3 µmol kg^{-1} in Spanish Bay/Spaanse and Sint Michiel inland, followed by CARMABI/Piscadera mangroves (reaching 1 µmol kg^{-1}), then declining to <0.3 µmol kg^{-1} in coastal salterns and other environments (Figure 6c). Nitrate reached a maximum of 3 µmol kg^{-1} (CARMABI/Piscadera mangroves), followed by 2 µmol kg^{-1} maximally above-reefs and otherwise <1 µmol kg^{-1} (Figure 6a-d). Environmental gradients in salinity, silicate, phosphate, and nitrate (Figure 6a-d) corresponded to shifts in the green algal classes present. Specifically, in inland salt ponds (Spanish Bay/Spaanse and inland Sint Michiel) fewer green algal taxa were detected compared to the coastal, sea-

connected Sint Michiel saltern, which had more consistent representation of Class II prasinophytes (Figure 6e). *O. bengalensis* had high relative abundances among green algae in CARMABI/Piscadera mangroves in 2019. *Micromonas* candidate species 1 dominated green algae relative abundances in 2018 CARMABI/Piscadera and in 2019 Spanish Bay/Spaanse. *Micromonas* Clade A (*sensu* Simmons et al. 2015) showed highest relative abundances among green algae in above-reef, off-reef, and open sea environments, across all years and sites, with *Ostreococcus* OII having similar relative abundances in some samples. Dictyochophytes displayed similar patterns to green algae in that there were fewer dictyochophyte taxa in inland salt pond and saltern samples compared to the coastal Sint Michiel saltern (Figure 6f). Similar to *Micromonas* Clade A for green algae, DEC-I & DEC-II had the highest relative abundances among dictyochophytes in above-reef, off-reef, and open sea environments.

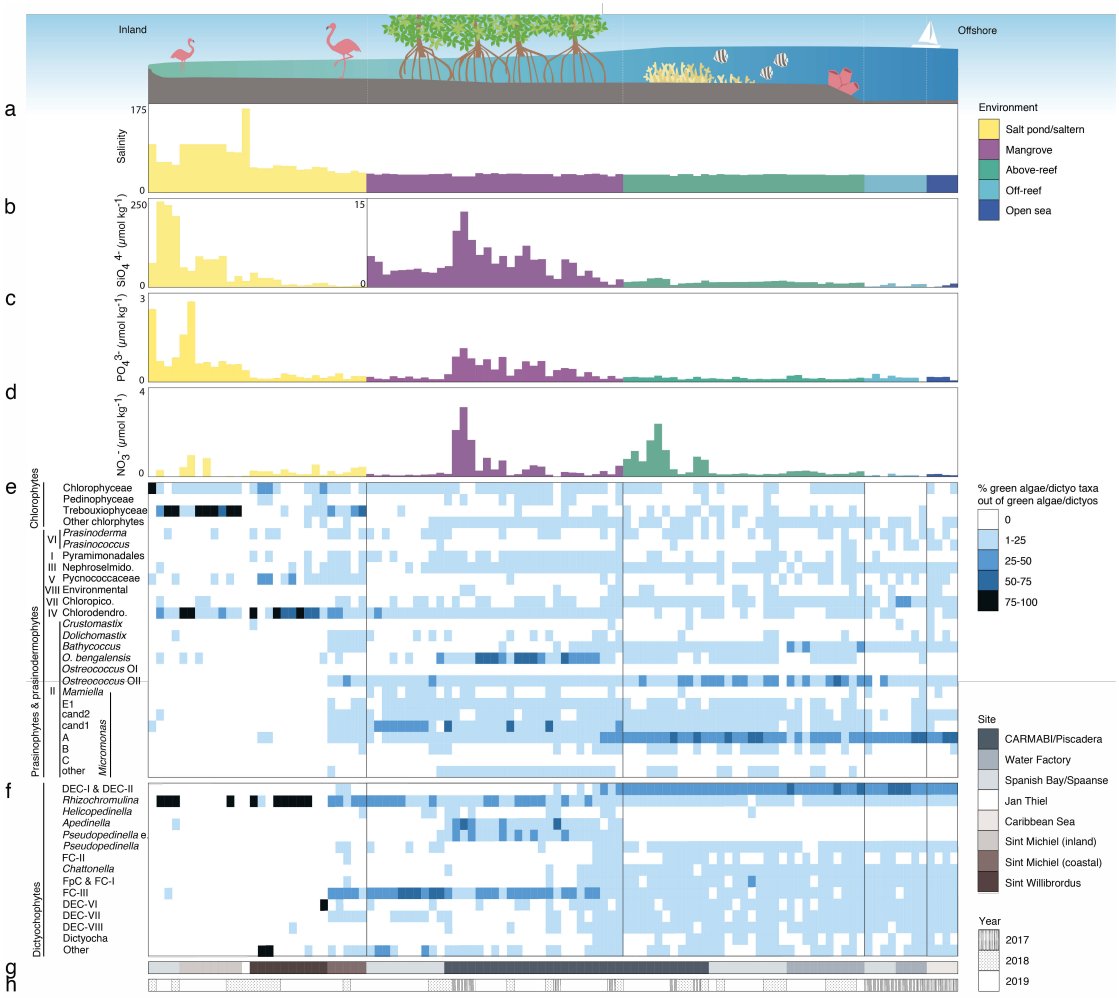

Figure 6: Green algal and dictyochophyte community composition aligned along a gradient from farthest inland to farthest offshore study sites from 2017 to 2019 (previous years did not have all requisite environmental data). Here relative abundances of ASVs within each group on the Y-axis have been collapsed. Sites were arranged from most inland to most offshore, as determined using the collection site coordinates in Google Earth. Due to the large number of samples ranging over depths above the reef, here only the most surficial samples (0-0.5 m) have been plotted. Salinity (a), silicate (b, note the change in Y-axis scale), phosphate (c), and nitrate (d) are indicated by bar graphs colored according to environment with each bar indicating a single sample. Note that salinity measurements were not available for 2017 off-reef and open sea samples; therefore, average values from 2016 or 2019 were used. In (e) the percent of each green algal group out of all green algal sequences is shown with heat, and in (f) the percent of each dictyochophyte out of all dictyochophyte sequences is shown with heat. The site (g) and year (h) where each sample was collected is also indicated. Dotted vertical white lines on cartoon are as in Figure 2.

Non-eukaryotic phytoplankton community members

Cyanobacteria had higher relative abundances (out of total 16S V1-V2 amplicons including heterotrophic bacteria) above-reef (39±6%), off-reef (41±4%), and in open sea (36±7%) than in mangroves (15±9%) and salt ponds and salterns (11±17%). For salt pond and saltern samples, there were differences by site; groups other than *Synechococcus* and *Prochlorococcus* showed highest relative abundances among cyanobacterial amplicons at Jan Thiel, Playa Santa Cruz, Spanish Bay/Spaanse, and the inland Sint Michiel samples. These "other" cyanobacterial amplicons were likely diazotrophic halophiles, with ASV18 having highest nucleotide identity (100-98%) to *Cyanothece* and *Dactylococcopsis salina*. Coastal Sint Michiel samples and Sint Willibrordus had higher relative abundances of *Synechococcus* (70±25%; Figure S7). Mangroves also had *Synechococcus* as the dominant cyanobacterial group, with average relative abundance of 84±19% out of all cyanobacterial amplicons. In contrast, *Prochlorococcus* showed the highest relative abundances among cyanobacterial groups in most above-reef (86±13%), off-reef (93±3%), and open sea samples (75±33%; Figure S7).

Co-associations among bacterial and photosynthetic eukaryotic microbial community members

Co-occurrences were assessed between individual phytoplankton taxa (16S V1-V2 ASVs) and within individual habitats when considering the entire microbial community sequenced (Figure 7). At first, analyses were designed to identify co-

occurrences that span multiple habitats. Among phytoplankton, cyanobacterial ASVs had the greatest number of network connections, mostly to each other and to heterotrophic bacteria, such as SAR11 and SAR406 (Table S7). The ASV with the overall highest number of connections in this network analysis was *Prochlorococcus* high light II (HLII) ecotype ASV103, which had 21 connections. Among co-occurrences involving eukaryotes, we found nine diatoms that had significant co-occurrences with other taxa (Figure 7a). For example, *Chaetoceros* ASV32 was associated with another diatom (ASV245), *Synechococcus* (ASV73 and ASV186), and various heterotrophic ASVs including Gammaproteobacteria, Alphaproteobacteria (mostly SAR11), and Flavobacteria (NS9 marine group). Diatom *Tryblionella apiculata*-like ASV87 was likewise associated with Alphaproteobacteria, including SAR86 and SAR11, as well as a *Micromonas* Clade A ASV126, and pelagophyte ASV165. Pelagophyte *P. calceolata* ASV165 was additionally associated with *Prochlorococcus* ASV9, SAR86 ASV48, a Flavobacterium ASV344, *Bathycoccus* ASV270, and diatom ASV267. Another *P. calceolata* ASV, ASV279, groups closely with ASV165 and is associated with the same *Bathycoccus* ASV as above, as well as two alphaproteobacterial ASVs (SAR11 ASV343 and SAR406 ASV320). There were also two dictyochophyte ASVs (DEC-I/DEC-II ASV198 and *Florenciella* ASV376) that both had significant co-occurrences with diatom ASV267 and planctomycete ASV355. Dichtyochophyte ASV198 was also associated with *Prochlorococcus* (ASV192), 2 SAR11 ASVs (ASV178 and ASV336) and SAR406 (ASV198). In addition, a number of ASVs from heterotrophic bacteria exhibited co-

occurrences, largely from the classes Alphaproteobacteria (particularly clades SAR11, SAR406, and SAR116) and Bacteroidota (particularly the order Flavobacteriales) (Table S7).

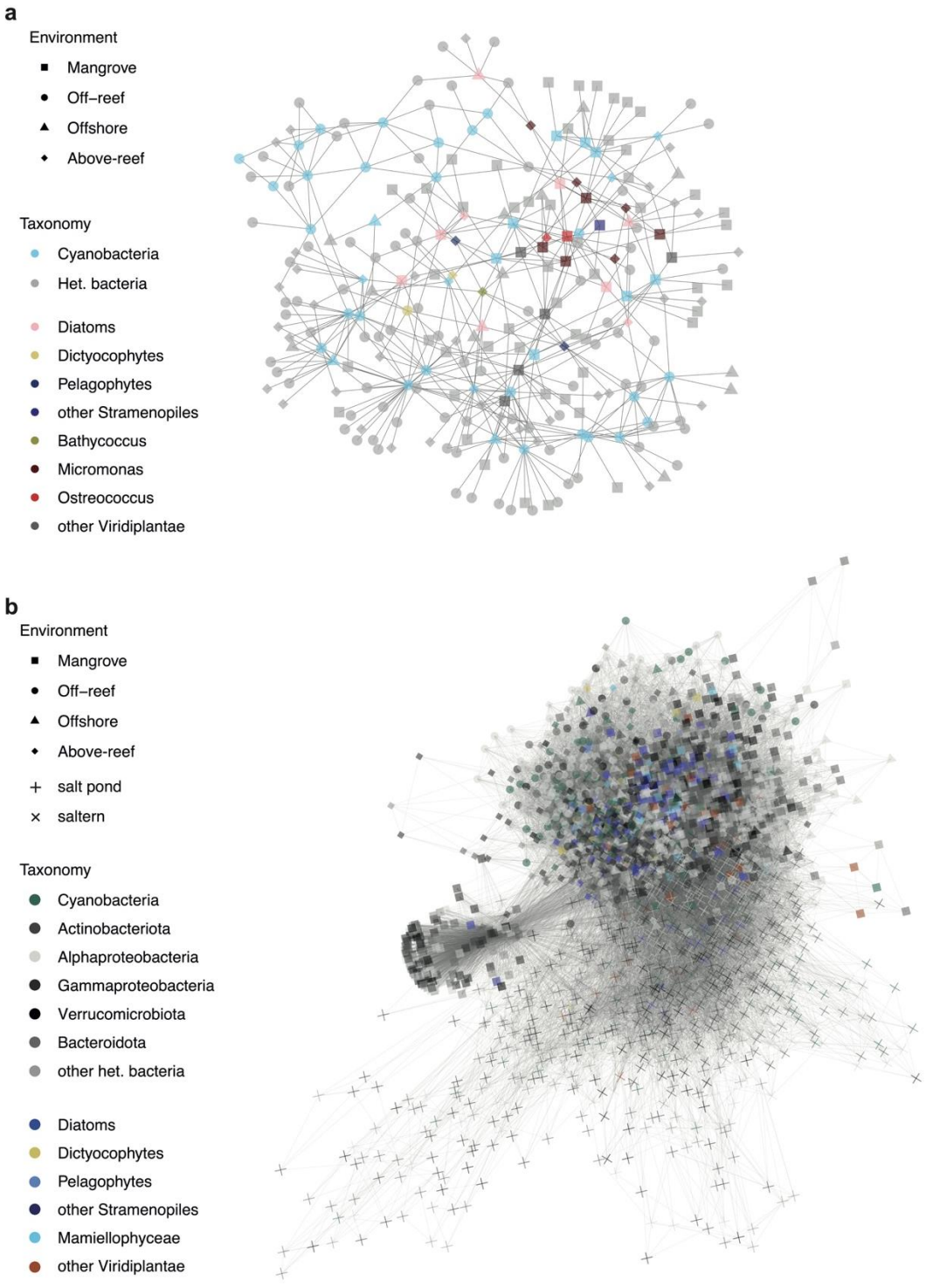

Figure 7: Significant co-occurrences observed in taxa frequent across habitats and habitat specific community members. (a) Network co-occurrence analysis on ASVs that occurred in at least 25% of samples across environments and a had a mean

relative abundance of at least 0.05% and (b) Network co-occurrence analysis on ASVs with a mean relative abundance of at least 0.05% across the top 5 samples in which a given ASV was most abundant. For both networks, significant interactions between photosynthetic ASVs and other photosynthetic or heterotrophic ASVs are shown with each point representing an ASV and the shape of the point corresponding to the environment type in which it occurs most often.

Green algae tended to group together in the network and had various interconnections (Figure 7a, Table S7). *Micromonas* Clade A ASV126, mentioned previously, was associated with other Mamiellophyceae: *Ostreococcus* OII (ASV133) and *Micromonas* candidate species 2 (ASV235). *Micromonas* candidate species 1 ASV129 was associated with a cryptophyte (ASV164), *Micromonas* Clade E1 (ASV187), *Micromonas* candidate species 2 (ASV235), a diatom (ASV204), *Synechococcus* (ASV106), SAR116 (ASV105), Flavobacteriales (ASV69), and a gammaproteobacterium (ASV316). *Micromonas* candidate species 2 ASV235 was also associated with a cryptophyte (ASV164) and two *Micromonas* clade A, ASV228 and ASV480. *Micromonas* Clade E1 ASV187 was additionally associated with SAR406 (ASV320), *Synechococcus* (ASV414 and ASV73), two cryptophytes (ASV164 and ASV524), a diatom (ASV204), *Micromonas* Clade A (ASV228), *Micromonas* candidate species 1 (ASV441), and *O. bengalensis* (ASV144). *O. bengalensis* ASV144 was itself associated with SAR11 (ASV94, ASV251, ASV172, and ASV199), diatoms (ASV204, ASV207, and ASV245), and *Micromonas* candidate species 1 (ASV441).

The second analysis has lower stringency for inclusion in that the ASVs did not have to occur in at least 25% of the samples, and thus it grouped the more extreme habitats with lower sampling effort to a great extent. Salt pond and saltern

ASVs largely grouped separately from the other environments and had a large proportion of heterotrophic bacteria (Figure 7b). While some mangrove samples grouped with above-reef and farther offshore samples, a subset of mangrove samples, mostly consisting of heterotrophic bacteria including those from the phyla Actinobacteriota and Bacteroidota, formed their own section of the network. Mangroves had the greatest number of photosynthetic eukaryote-heterotrophic bacterial interactions with 2101, followed by above-reef (1027), salterns (702), off-reef (232), open sea (225), and salt ponds (69). Off-reef samples had the greatest number of cyanobacterial-heterotrophic bacterial interactions with 774, followed by above-reef (620), salterns (461), mangroves (438), salt ponds (124), and open sea (121). Of photosynthetic groups, cyanobacteria had the most connections with heterotrophic bacteria with 6512, followed by diatoms (6101), Mamiellophyceae (1678), other Viridiplantae (1665), other stramenopiles (883), and dictyochophytes (854).

Discussion

Our study sites spanned a range of distinct tropical island aquatic habitats. In general, these types of environments are under marked anthropogenic influences, both local (van der Schoot & Hoeksema, 2022) and climatic (Bove et al., 2022), and hence it is important to establish coherent relatable data sets for different regions within tropical ecosystems for benchmarking potential downstream changes. There were differences in the level of connectivity to the sea and/or human impact between sites

within the same habitat type. For example, among mangroves, those at Playa Santa Cruz were the most remote, while Spanish Bay/Spaanse had more nearby human development, and CARMABI/Piscadera Bay was near the most developed part of the island (Brocke et al., 2015). We sampled above the shelf of fringing reef corals, which extend about 70 m from the shore, at CARMABI and the Water Factory located toward the midpoint of the island perimeter (again in a more anthropogenically forced area) as well as East Point, which is less impacted. A study of the impact of eutrophication on coral reef fauna around Curaçao found that sewage run-off was high around CARMABI/Piscadera, Water Factory, and Spanish Bay, while Sint Michiel and sites farther north from that had lower sewage output, as determined using $\delta^{15}N$ isotope data (van der Schoot & Hoeksema, 2022). Off-reef samples were collected just past the reef above the 1000 m trench, while the open sea samples were from ~25 km away from shore (Figure 1), both presumably being less impacted by human activities. We also delineated two types of salt ponds based on the level of anthropogenic modification, the first being salterns (Sint Willibrordus, Sint Michiel inland and coastal, and Jan Thiel) which have undergone construction of retaining walls to isolate areas for evaporative salt harvesting – but with the former two sites having inflow of fresh salt water in order to replenish the system. The second type was natural salt ponds (Playa Santa Cruz and Spanish Bay/Spaanse).

In general, our results indicated a number of differences in environmental parameters, with salinity perhaps being the most predictable (Figure 2, Figure 6, and Figure S2). Water temperatures around Curacao remain fairly constant, between ~26–

29 °C (Brocke et al., 2015), although they were sometimes much higher in the inland environments we sampled (Table S1). Trend-wise, silicate and phosphate concentrations were higher in salt ponds, salterns, and mangroves compared to above-reef, off-reef, and in the open sea. Nitrate concentrations were highest in mangroves and above reefs, particularly those at CARMABI/Piscadera. However, deconvoluting these results further to degree of impactedness was not within reach without more comprehensive sampling. Data from similar habitats sampled at St. John (also Caribbean) also reported higher phosphate and silicate in mangrove samples than on nearby reefs (C. C. Becker et al., 2020). However, in their samples, mangroves had higher nitrite+nitrate concentrations compared to reefs, and hence may not be highly analogous to our study region. Given the upfront differences in organic matter apparent in our samples (not measured, but higher in mangroves and inland settings, as also reflected in filtration rates, than e.g., open sea), our goal was to determine if there were systematic differences in microbial diversity and phytoplankton communities between the sampled sites and habitats. We demonstrated pronounced site-specific divergence in diversity and specific network connections. Moreover, comprehensive evaluation of the phytoplankton communities, with particular attention to the molecular diversity of eukaryotic groups that exhibited the highest relative abundances and/or the broadest distributions, exposed unique aspects of communities residing in each of the sampled habitats.

Microbial diversity across Caribbean Sea – Island tropical aquatic habitats

In terms of microbial community, that is heterotrophic bacteria, cyanobacteria, and eukaryotic phytoplankton (all 16S V1-V2 ASVs, Figure 2), the highest diversity levels were found at the Sint Michiel coastal and Sint Willibrordus salterns and the CARMABI/Piscadera and Playa Santa Cruz mangroves (Figure 2b). A considerable amount of this diversity was likely contributed by bacterial taxa. Perhaps counterintuitively, the human-made salterns exhibited higher diversity than natural salt ponds, likely due to differences in seawater replenishment and delivery and mixing in of 'external' communities via channels from the sea. A relationship between overall salinity levels and diversity was also observed, akin to a 18S V4 rDNA-based study of protists and fungi in Portuguese salt ponds where diversity decreased as salinity increased (Filker et al., 2015). Here, the higher salinity salt pond and saltern samples, specifically Spanish Bay/Spaanse and inland Sint Michiel, had lower diversity than the lower salinity Sint Willibrordus and coastal Sint Michiel salterns (Figures 2a and 6a). Note that higher water volumes (~500 mL) were filtered for mangrove, above-reef, off-reef, and open sea samples, as compared to some salt pond and saltern samples where low volumes were obtained due to high biomass and particulates in the water. This could have influenced diversity indices. However, we found that all salt pond and saltern samples did saturate in rarefaction analysis (Figure S1).

With respect to mangroves, the highest microbial diversity was found in the CARMABI/Piscadera mangroves. It is unexpected, given that these mangroves are

closer to a heavily populated location than other areas and our results show that they are exposed to higher nutrient levels (Figure 6b-d; Brocke et al., 2015). As for above-reef sites, those at CARMABI and the Water Factory are similarly located toward the midpoint of the island in a more anthropogenically impacted area, while the East Point reef is farther from human activity (Brocke et al., 2015). However, here statistical differences were not observed in microbial alpha diversity between CARMABI/Piscadera and Water Factory reefs and the less human-impacted reefs at East Point (Figure 2b). There were also no significant differences in median inverse Simpson index or microbial community composition with depth in above-reef samples.

Broad transitions in primary producer groups across habitats

Explicit analyses of the primary producer communities were used to move beyond single group or single environment studies to try to understand the complete community that contributes to tropical primary production across habitats. Prior studies have shown phytoplankton are important primary producers in the tropics (Kristensen et al., 2008); diatoms can be prey for zooplankton (S. Hu et al., 2020), and picophytoplankton, including cyanobacteria and small eukaryotes, can be consumed by sponges (McMurray et al., 2016) and corals (Hoadley et al., 2021), but again there is much to be learned to overall contributions taking a more agnostic approach. While tentative at best, we found that eukaryotic phytoplankton community as determined by 16S V1-V2 exhibited similar proportions of major groups as seen in

18S V4 analyses in the 41 above-reef and off-reef samples that were sequenced for both markers (Table S6). Note that for this analysis DPLs (Choi et al., 2017) were excluded because their 18S rRNA gene sequence is not known, and alveolates were excluded due to issues with partitioning photosynthetic from heterotrophic lineages using 18S rRNA genes sequences arising from their diversity and complicated evolutionary history (Leander & Keeling, 2003; Moreira & López-García, 2002). Putative under representation of haptophytes by the 16S V1-V2 primers did not appear to significantly bias the general patterns herein given that higher relative percentages were detected in 16S V1-V2 than 18S V4 (Table S6). The inflation of stramenopiles in 18S V4 data may be due to inclusion of heterotrophic members that are closely related to photosynthetic taxa, and therefore included with them. Sequencing of 18S V4 was designed for and most valuable when it came to refining knowledge of uncultured lineages for which pairing between 18S V4 and 16S V1-V2 could be constrained using statistical analyses of presence absence patterns as shown in results.

We found that stramenopiles, but not those within the diatoms, had high relative abundances in nearly all open sea samples and some above-reef samples. Stramenopile presence in salt ponds and salterns was more sporadic and also varied in mangroves, in all of which diatoms were the more relatively abundant stramenopiles (apart from Spanish Bay/Spaanse where eustigmatophytes took this role). Diatom contributions diminished above-reef and were proportionally less than those of dictyochophytes in the off-reef and open sea environments, where pelagophytes also

gained in relative abundance values. The dictyochophytes exhibited significant contributions from uncultured environmental clades that are thought to be mixotrophic (Choi et al., 2020) and from multiple *Florenciella* ASVs, with *Florenciella* also having recently been shown to be mixotrophic (Q. Li et al., 2021). In contrast, in the more coastal and inland sample sites *Rhizochromulina* exhibited high relative abundances.

Cryptophytes had punctuated bursts in 16S V1-V2 amplicon relative abundance, specifically at Spanish Bay/Spaanse mangroves and the Sint Willibrordus saltern (Figure 3). In mangroves along the East coast of India near the border to Bangladesh, *rbc*L gene clone libraries indicated cryptophytes were the most abundant chromophytic phytoplankton (a subset of phytoplankton characterized by a particular form of RuBisCO derived from the red algal lineage) after diatoms (Samanta & Bhadury, 2014). They have been observed in Portuguese salt ponds, where they were relatively more abundant in lower salinity than higher salinity ponds (Filker et al., 2015). Here, the punctuated appearances with higher relative abundances in our study did not correspond to salinity level; Sint Michiel coastal samples were similar in salinity to Sint Willibrordus, but cryptophytes did not play a major role. Moreover, all mangrove samples had similar salinities and yet again the distributions varied considerably. These findings indicate that more complex environmental variables or community interactions underpin changes in cryptophyte relative abundances. Chlorophytes (particularly *Dunaliella*) and Trebouxiophyceae were the most relatively abundant green algae in several salt ponds, whereas in others prasinophyte

Class IV dominated (Figure 5a), indicating the heterogeneity of these environments. The observed chlorophyte taxa are relatively well known for high salinity environments, with *Dunaliella* perhaps being the most common (Larson & Belovsky, 2013; Oren, 2005). For Class IV, *Tetraselmis* had the most relatively abundant ASVs, a genus that is known to have many euryhaline species (Fon-Sing and Borowitzka, 2016), but has not been well studied in the tropics (Arora et al., 2013). The most relatively abundant Trebouxiophyceae ASVs were related to *Picochlorum soloecismus* and *Chlorella desiccata*, also known to be halotolerant, but not previously reported from tropical environments (Borovsky et al., 2020; Gonzalez-Esquer et al., 2019).

In habitats other than the salterns and salt ponds, Class II prasinophytes dominated relative abundances of green algae, and in some cases exhibited relative abundances akin to stramenopiles (Figure 3, Figure 5b-d). Surprisingly however, Class II prasinophytes were also observed in the high salinity habitats. Apart from the results herein to our knowledge just one other study has shown Class II members in salt ponds (in Portugal), where they represented more than half of the green algal 18S V4 amplicons in a salt pond with 40 ‰ salinity (Filker et al., 2015). However, it is not straightforward to compare our molecular data with the latter study as it is based on 18S V4 amplicons and reads obtained by pyrosequencing were clustered, potentially resulting in loss of diversity data. Class II prasinophytes reached their highest relative abundances in lower salinity Sint Michiel coastal and/or Sint Willibrordus salterns whereas *Dunaliella*'s relative abundance was highest in the high

salinity Spanish Bay/Spaanse salt pond (Figures 3 and 6e). The amplified importance of Class II in the salterns may well reflect renewal of these communities by incoming coastal waters.

With respect to cyanobacteria, *Prochlorococcus* typically had highest relative abundances above-reefs, off-reef, and in the open sea (Figure S7). This is in agreement with a recent study of waters above CARMABI reefs using flow cytometry and 16S V1-V2 amplicon sequencing to demonstrate that *Prochlorococcus* was mostly composed of the HLII ecotype, and *Synechococcus* was largely made up of clade II with notable contributions from clades III, IX, and XVI (Hoadley et al., 2021). Similarly, a study using flow cytometry in St. John reported a higher number of *Prochlorococcus* cells found over reefs than in mangroves, while distribution patterns were less clear for *Synechococcus* (C. C. Becker et al., 2020). Surveys of other Caribbean reefs found higher abundances of *Prochlorococcus* in offshore sites compared to reefs based on flow cytometry (Weber et al., 2020). With respect to mangroves, similar to our study, *Synechococcus* has also been reported in Brazilian (Rigonato et al., 2013; Silva et al., 2014) and Indian (Bhadury & Singh, 2020; Ganesan et al., 2012) mangroves, although typically without clade specific taxonomy. Likewise, the coastal Sint Michiel and Sint Willibrordus salterns were more similar to mangrove samples than to the other salt ponds, with *Synechococcus* as the major cyanobacterial group (Figure S7). Finally, we found that the more inland salt ponds mostly comprised an ASV most closely related to *Cyanothece* and *Dactylococcopsis salina*, both of which have been reported in hypersaline environments (Muir &

Perissinotto, 2011; Walsby et al., 1983). These results provide a relatable database for comparison of cyanobacterial groups both across habitats and to other marine locations.

Cultured stramenopile phytoplankton species in relation to prior tropical studies

As previously mentioned, the stramenopile community in most salt ponds contained a large fraction of diatoms, although their absence in some ponds led to high overall variation (Figure 4). The most abundant diatom ASV in salt ponds was closest to estuarine pennate diatom *Synedra hyperborea*. In salterns the most abundant ASV was closest to another estuarine benthic pennate diatom, *Navicula phyllepta.* As observed herein (Figure 4) and in Portuguese salt ponds (Filker et al., 2015), contribution of diatoms increases with decreasing salinity of the ponds. Moreover, in that study most sequences found were from the Naviculaceae and Bacillariaceae families, and, as far as taxonomic assignments can be consistently overlain from different methodologies, we also found generally high representation from a member of the Naviculaceae, specifically the *N. phyllepta* ASV mentioned above.

Diatoms have been extensively studied in mangroves, particularly in the Indian/Bangladeshi Sundarbans and Malaysia (Saifullah et al., 2016), with a focus on epibenthic taxa (Bhattacharjee et al., 2013). Planktonic communities and their stability in mangroves are less well understood and only a few studies have addressed them (e.g. in mangroves of Bangladesh (Aziz, 2011)). We postulate that high relative abundances of planktonic diatoms in the Curaçao mangroves are connected to the

dampened tidal range they experience, which leaves them permanently inundated with water. The influence of variations in tidal levels has previously been implicated as a driver for differences in juvenile fish communities and numbers in Caribbean mangrove species compared to other mangrove systems (Igulu et al., 2014). Here, the overall most relatively abundant diatom ASV across mangroves was a member of the Thalassiosirales order, possibly *Thalassiosira profunda*, *Skeletonema tropicum*, *Skeletonema costatum,* or *Skeletonema marinoi,* all of which are planktonic species for at least part of their life stage (Arsenieff et al., 2020; Gao et al., 2000; Sakshaug et al., 1989). Clear delineation between planktonic and benthic diatom cells is challenging because they can have life stages that delineate along these lines and benthic taxa can be uplifted from the sediment into the water column through physical forcing (Godhe & Härnström, 2010). Nevertheless, because the mangroves we studied are permanently inundated with water and were sampled during calm conditions, we take the taxa identified herein as having resided in the water column at this time of year.

In the reef and offshore sites, several groups were important in terms of stramenopile relative abundances. An ASV closest to *Chaetoceros* was the most relatively abundant diatom ASV among stramenopile amplicons across above-reef samples, while off-reef and in the open sea an ASV closest to *Tryblionella apiculata* took this position (Table S4). *Chaetoceros* is common in many oceanic environments while *T. apiculata* has been reported in Hungarian rivers and coastal South Korea (Kókai et al., 2015; Pandey et al., 2018). The pelagophytes we observed were those

from oligotrophic and some mesotrophic environments, instead of well-known coastal species like *Aureococcus*. For example, *Pelagomonas* is the key taxon that has been reported in mesotrophic waters and the subtropical open ocean. Indeed, it has been reported to be among the most relatively abundant eukaryotic phytoplankton and/or pelagophytes in the subtropical North Atlantic gyre deep chlorophyll maximum (DCM), eastern North Pacific (Choi et al., 2020), and subtropical Pacific (Dupont et al., 2015) at least during specifical seasonal conditions. We also found that pelagophyte environmental clade VIII (PEC-VIII) has high relative abundances among pelagophytes with a similar distribution to *P. calceolata*. These two pelagophyte groups exhibited import contributions both above and off reefs, as well as in the open sea samples, while pelagophyte contributions in other habitats were minimal (Table S4).

Distributions of novel uncultured phytoplankton and key groups that are commonly taxonomically misassigned

The above-reef, off-reef, and open sea samples had increasing relative abundances of dictyochophytes. Many dictyochophyte groups observed in oceanic environments are uncultured; for instance, environmental clades DEC-I and DEC-VI dominate dictyochophyte relative abundances in stratified surface waters of the North Atlantic subtropical gyre (Choi et al., 2020). Those with cultured representatives that had high relative abundances, including *Florenciella* and *Rhizochromulina*, are demonstrated phagotrophic phytoplankton (mixotrophs) shown to feed on *Prochlorococcus* (Q. Li et al., 2021, 2022). Mixotrophic feeding by eukaryotic phytoplankton is considered

advantageous in oligotrophic conditions, where nutrients are scarce (Mitra et al., 2014; Wilken et al., 2019). This is consistent with distributions observed herein; however, the most abundant dictyochophyte group belonged to uncultured environmental clades I and II (DEC-I and DEC-II, which are unable to be resolved in 16S V1-V2), making their trophic modes still unclear. Dictyochophyte diversity in tropical coastal habitats, such as salt ponds and mangroves, to our knowledge, has not yet been investigated in detail. Here we show that while dictyochophytes are more common and diverse in offshore habitats, they are present in salterns and mangroves and their composition here is distinct at the ASV level (Figure 4). Notably, the dictyochophytes observed in some salt ponds and some mangroves, where nutrient concentrations were higher than in the offshore environments, were largely *Rhizochromulina*, *Apedinella*, and *Florenciella*-related clade FC-III. While much research remains to be done, including basic demonstration of mixotrophic capabilities in uncultivated clades, it is possible that differences in feeding along the mixotrophy gradient could influence the dictyochophyte species distributions along habitats with different nutrient availability.

Because there are few reports of the widespread and well-studied prasinophyte class Mamiellophyceae (Bachy, Wittmers, et al., 2022) from repeat sampling of tropical island and reef habitats, and because of high relative abundances at some sites herein, we examined taxonomically resolved data from the different habitats. One of the major Mamiellophyceae groups here was *Ostreococcus* (Figure 4b) but the taxa detected here were not *O. tauri* or *O. lucimarinus*, but rather the more open

ocean Clade OII (also known as Clade B; (Limardo et al., 2017)) and the newly described *O. bengalensis* (Strauss, Choi, Grone et al. rev.). The former was previously thought to be deep-adapted, but here is prominent in surface waters especially above- and off-reefs, and is also seen in well-mixed oligotrophic waters (Rodríguez et al., 2005; Treusch et al., 2012). Indeed, *Ostreococcus* OII has been found to be important in the subtropical North Atlantic in well mixed waters during the winter and spring bloom in addition to being present at the DCM in stratified summertime waters (Bolaños et al., 2020; Demir-Hilton et al., 2011; Treusch et al., 2012). *Ostreococcus* OII has also been detected in tropical regions previously. For example, it has been reported in anthropogenically-impacted bays in the Philippines, where an uncultivated clade, now known to be *O. bengalensis* (previously Clade E) dominates *Ostreococcus* variants based on 18S V4 amplicon relative abundances (de la Peña et al., 2021). Here, we found *O. bengalensis* to have its highest relative importance in mangroves and it was the dominant *Ostreococcus* species at CARMABI/Piscadera (Figure 5b). Our cursory reevaluation of a study at a coral atoll in the Indian Ocean, which reported *Ostreococcus tauri* (Jeffries et al., 2015) suggests these are likely more related to *Ostreococcus* OII and were mislabeled as *O. tauri*. These results emphasize the importance of phylogenetic approaches to amplicon analyses as well as continued pursuit of uncultured lineages.

A second genus of Class II prasinophytes was also prevalent, specifically *Micromonas*, with several clades having notable relative abundances in our study. To our knowledge our results provide the first evidence of *Micromonas* in mangroves.

The different clades overlapped to some extent, but with different dominants. For example, in mangroves *M. commoda* Clade A (*sensu* Simmons et al. 2015), *Micromonas* candidate species 1 and 2, and *Micromonas* Clade E1 (named *M. bravo* in Simon et al. 2017) had highest relative abundances (Figure 4b). *Micromonas* candidate species 1, which was overall second in relative abundance after *M. commoda* Clade A, was first reported in the Pacific Ocean and Mediterranean Sea (Worden, 2006). It has since been found in the Florida Keys (Laas et al., 2021), and herein was especially well-represented in mangroves (Figure 5). *Micromonas* candidate species 2, here detected across all environments (Figure 5), was first reported in Wu et al., 2014 and then described in Simon et al., 2017 and has been reported in tropical coastal waters (Chénard et al., 2019; de la Peña et al., 2021). *Micromonas* Clade E1, here found across all habitats except salt ponds, and especially well-represented in mangroves, has been reported in the Florida Keys (Laas et al., 2021) in addition to the eastern North Pacific Ocean and its original site of isolation in the Mediterranean (Worden, 2006) and other temperate coastal waters (Tragin & Vaulot, 2019).

M. commoda Clade A (*sensu* Simmons et al. 2015) was detected in all but salt ponds, with highest relative abundances at above-reef and off-reef sites (Figure 5c,d) and is considered ubiquitous in tropical and subtropical regions (J. Bakker et al., 2019; Laas et al., 2021; Simmons et al., 2015; Tragin & Vaulot, 2019). Some mangrove and above-reef samples had unknown *Micromonas* ASVs that were closest to *Micromonas* A/B/C clades, yet still distinct enough that they could represent novel

diversity within these clades. *Micromonas* Clade C was not detected in this study, supporting emerging information on distributions that indicate this lineage is adapted to colder environments (i.e., being more abundant in waters <20 °C) (Bachy, Sudek, et al., 2022; Simon et al., 2017). A two-year time series of coral reefs in a subtropical site with greater seasonality near Okinawa based on 16S V1-V2 amplicons reported *M. commoda* Clade A in proportions between 5-20% of picophytoplankton, with *Bathycoccus* in similar proportions in fall, winter, and spring (Nuryadi et al., 2018). Here, *Bathycoccus* was most relatively abundant above reefs and farther offshore, similarly to *M. commoda* Clade A, although generally not as high in relative abundance as the latter (Figure 5c-d). While we did not resolve seasonality here, such marked seasonally related shifts do not occur near Curaçao.

Developing understanding of potential community member interconnectedness

As the co-occurrence based on relative abundance data is not simple to interpret, here we looked at amplicon data as indicating presence or 'absence' of a taxon. Absence in amplicon data could imply lack of detection instead of true absence, but in the case of our fully rarefied data seemed a reasonable proxy to use. *Prochlorococcus* overall had the greatest number of connections to other ASVs, including SAR11, which are both highly abundant in the marine environment and can have a commensal relationship (J. W. Becker et al., 2019). The singular diatom ASV620 found across all environment types corresponded most closely to *R. imbricata*, which has been reported in the temperate North Atlantic (Edwards et al., 2022), the North Sea (Buaya et al., 2017),

the East China Sea (Ishizaka et al., 2006), the Arabian Sea, Red Sea (Devassy et al., 2019), and South Pacific (Lindao & Ruiz, 2022) – hence exhibiting an exceptionally broad distribution. Despite its ubiquitous distribution, we were not able to reveal co-occurrences for this diatom. *Chaetoceros* ASV32 and *T. apiculata*-like ASV87 were found to have significant associations with members of the SAR11 clade, possibly indicating overlapping niches or interactions (Figure 7). A *P. calceolata* ASV was found to be associated with a *Prochlorococcus* ASV (Figure 7), which could imply a trophic relationship or niche overlap. There are also associations between *Synechococcus* and SAR11 and picoplanktonic Mamiellophyceae; however, it is unlikely they can feed on these bacteria, so there is probably not a trophic nature to that association (Wilken et al., 2019).

CONCLUSIONS

Molecular diversity and community composition data exposed different phytoplanktonic communities and dominant primary producer taxa (based on relative abundances) among the distinct but often interconnected environments investigated here. The types and distributions of diatoms are in agreement with previous work in similar environments in other tropical regions, while also suggesting presence of a suite of planktonic diatoms in mangroves. While microscopy has contributed to the tremendous knowledge on diatoms in these environments, until now little data has been available on green algae, apart from those in tropical salt ponds, or dictyochophytes. The dynamics of green algae revealed here provide extensive new

information on species distributions that reveal key habitats for several clades, including novel uncultivated lineages. Additionally, our findings on the relative importance of dictyochophytes, again especially for uncultivated lineages, provide insights that have been lacking for tropical environments. Comprehensive studies on phytoplanktonic composition in coastal island environments are important as these areas are subject to sea rise level, more so than many other environments. These habitats are also important regions for spawning and juvenile fish, hence comprehension of the phytoplankton that underpin primary production in these regions will facilitate future modelling studies. Given the paucity of phytoplankton studies that encompass multiple tropical saline habitats (J. Bakker et al., 2019; C. C. Becker et al., 2020), the time series here provides a valuable point of references for future work on similar environments globally, as well as for this particular island and nearby waters in the Caribbean.

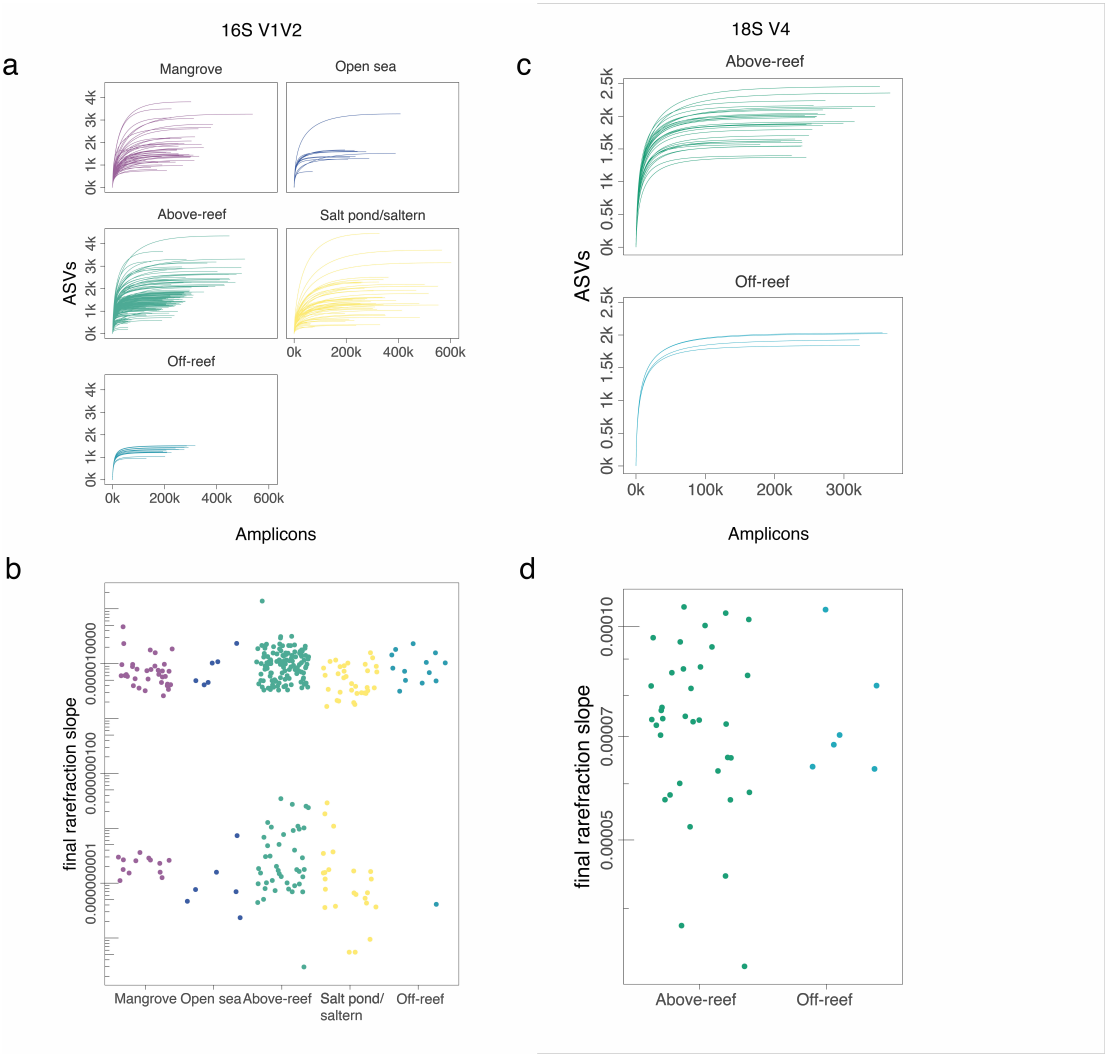

Supplementary Figure 1: Sequencing depth by environments for (a-b) 16S V1-V2 amplicons and (c-d) 18S V4 amplicons. Rarefaction curves (number of ASVs vs. number of amplicons per sample) for (a) 16S V1-V2 and (c) 18S V4 and rarefaction curve final slopes for (b) 16S V1-V2 and (d) 18S V4.

Supplementary Figure 2: Environmental parameters for all samples. Salinity (a), silicate (d, note the change in Y-axis scale), phosphate (e), nitrate (f), and nitrite (g) are plotted for all samples with each bar indicating a single sample. For salinity, bar (b) indicates the site and bar (c) the year; for the nutrients, bar (h) indicates the site and bar (i) the year. Note that 2019 values for highest salinity environments were compromised because methodological issues did not allow quantification of values >100‰.

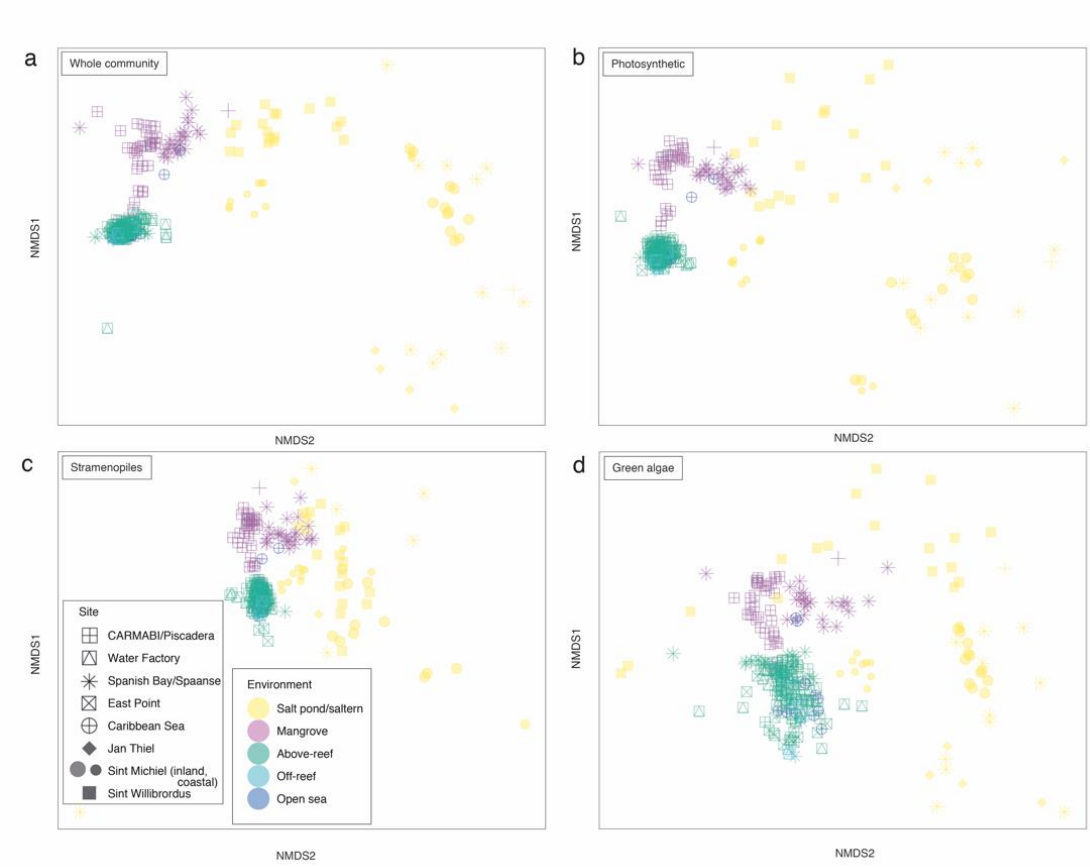

Supplementary Figure 3: NMDS plot of all samples for (a) all 16S V1-V2 ASVs, (b) 16S V1-V2 ASVs classified as being from cyanobacteria or eukaryotic plastids, (c) stramenopile 16S V1-V2 ASVs, and (d) green algae and Chlorarachniophyceae 16S V1-V2 ASVs with each point indicating an individual sample, by site (shape) and environment type (color).

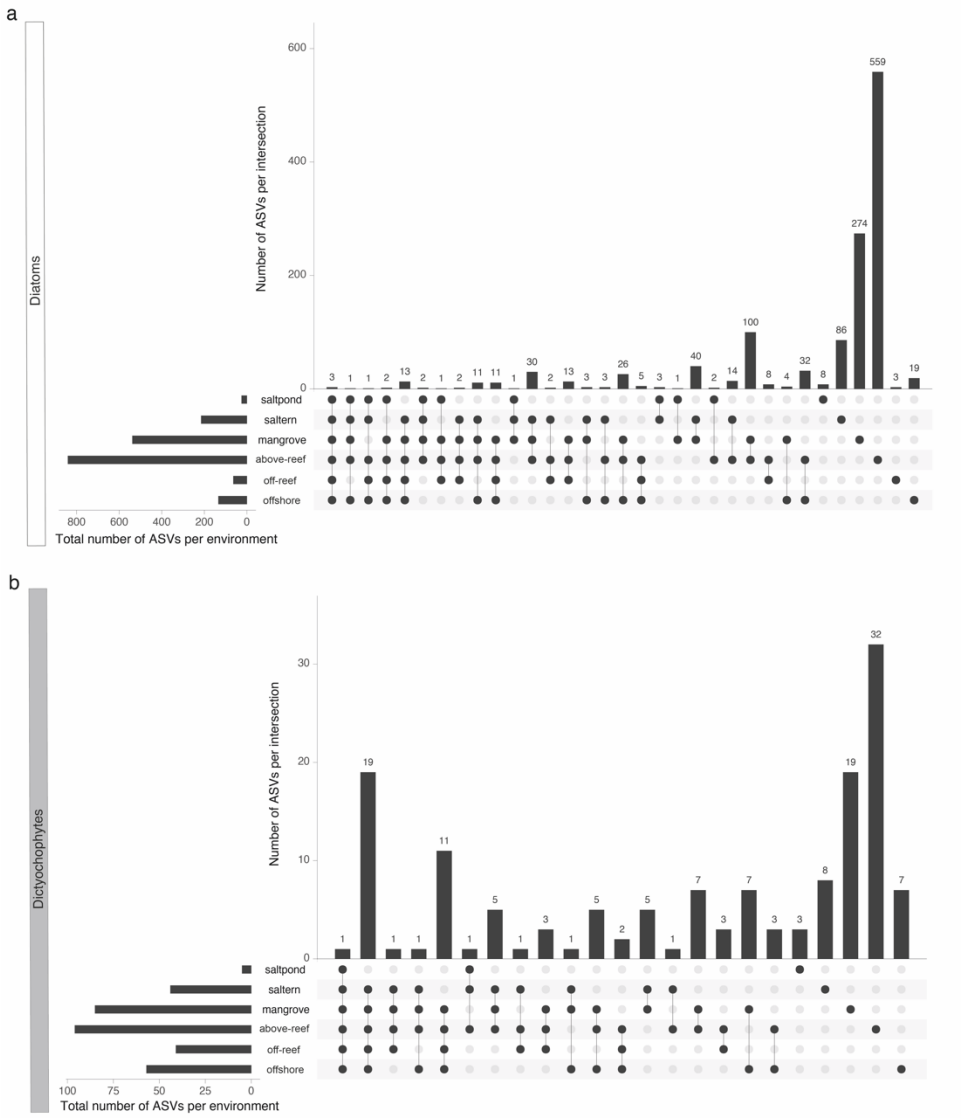

Supplementary Figure 4: UpSet plots of (a) diatom and (b) dictyochophyte 16S V1-V2 ASVs. Intersection size indicates the number of 16S V1-V2 ASVs in the category, and set size is overall number of ASVs in that group per environment. For example, in (b), there are 5 dictyochophyte ASVs found in both salterns and mangroves that are not detected in any other environment.

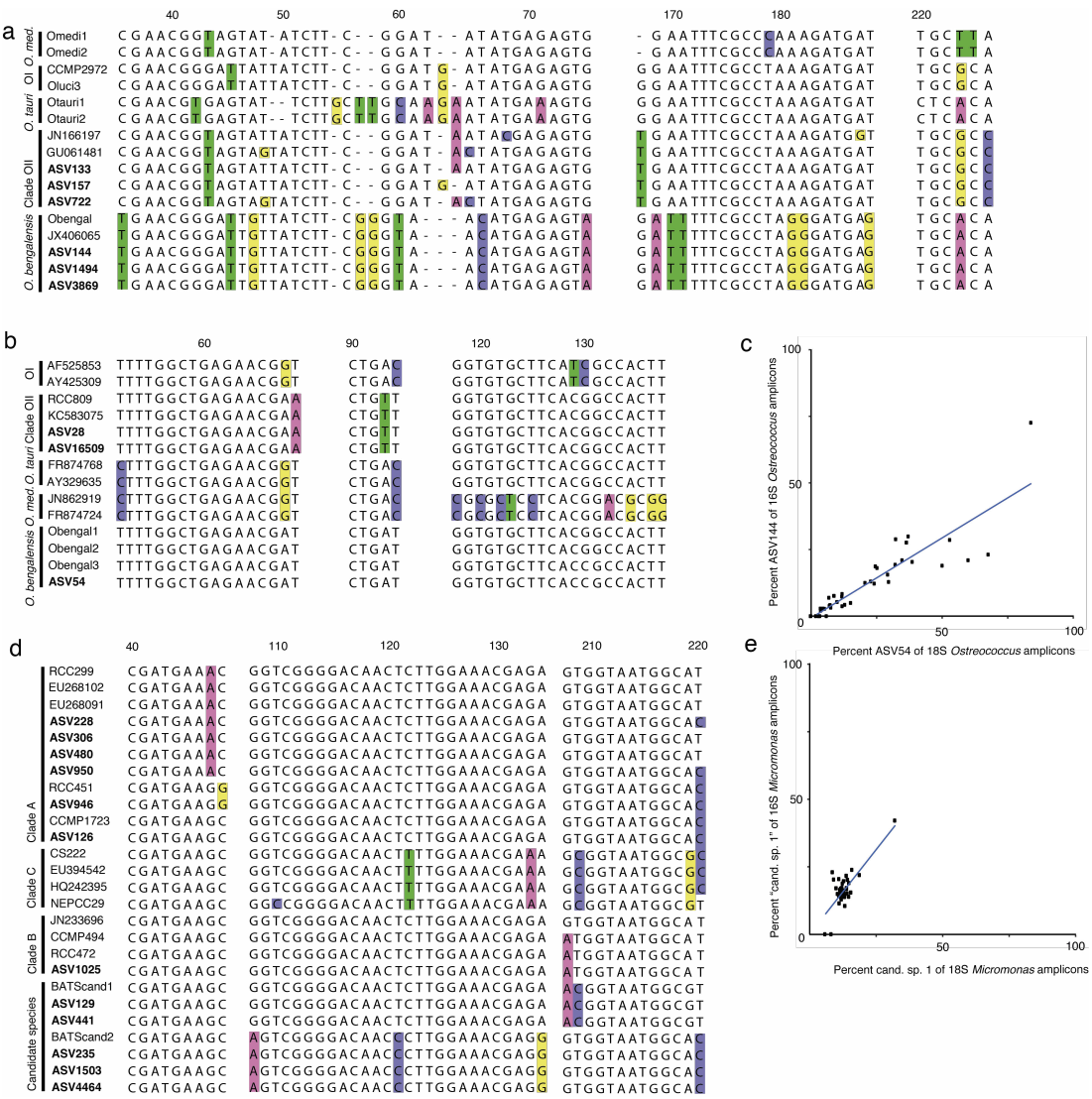

Supplementary Figure 5: Comparisons of *Ostreococcus* and *Micromonas* ASVs to amplicons from other studies for purposes of identification – using both 16S and 18S rRNA gene information. (a) Alignment of *Ostreococcus* 16S V1-V2 ASVs from this study with 16S V1-V2 ASVs from Strauss, Choi, Grone et al. in rev. (b) Alignment of *Ostreococcus* 18S V4 ASVs from this study with 18S V4 rRNA ASVs from Strauss, Choi, Grone et al. rev. (c) Plot of ASV54 (corresponding to *O. bengalensis* in the 18S V4) percent contribution to all *Ostreococcus* ASVs in the 18S V4 data versus ASV144 (the ASV corresponding to *O. bengalensis* in the 16S V1-V2) percent contribution to all *Ostreococcus* ASVs in the 16S V1-V2. (d) Alignment of *Micromonas* Clades A, B, and C and candidate species 1 and 2 with ASVs from this study (except for Clade C, which was not detected herein). (e) Plot of ASVs assigned to *Micromonas* candidate species 1 in the 18S V4 percent contribution to all *Micromonas* ASVs in the 18S V4 versus ASVs assigned to *Micromonas* candidate species 1 in the 16S V1-V2 percent contribution to all *Micromonas* ASVs in the 16S V1-V2.

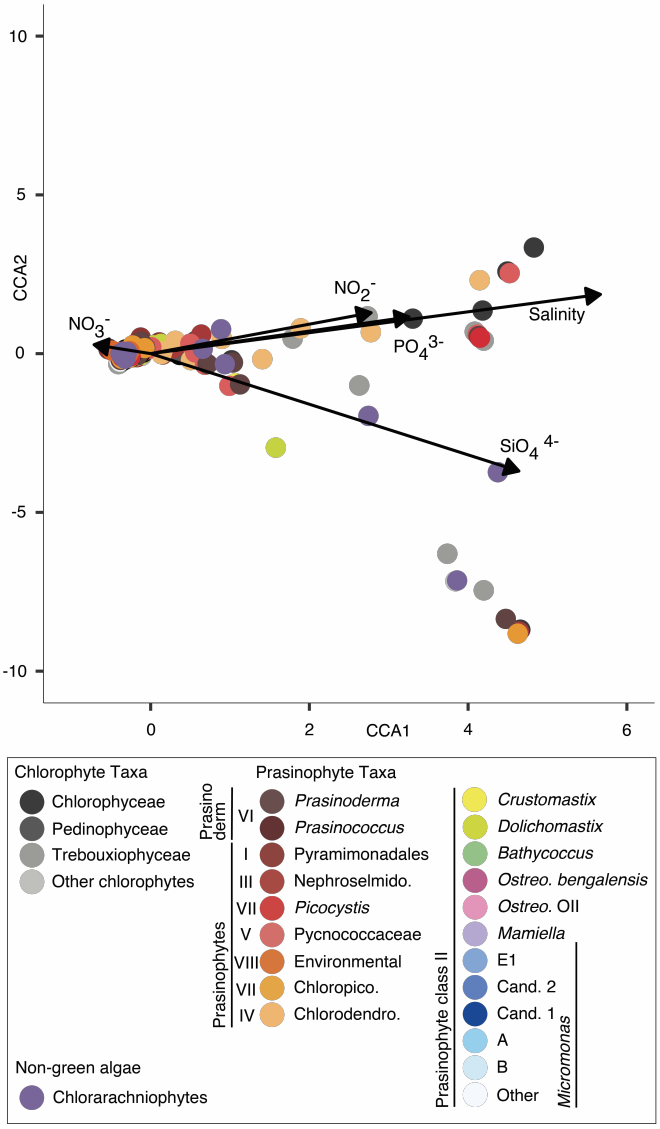

Supplementary Figure 6: **A CCA plot of distribution of green algal and Chlorarachniophyceae** (which have plastids derived from green algae) ASVs along with environmental parameters (salinity, nitrate, nitrite, phosphate, and silicate).

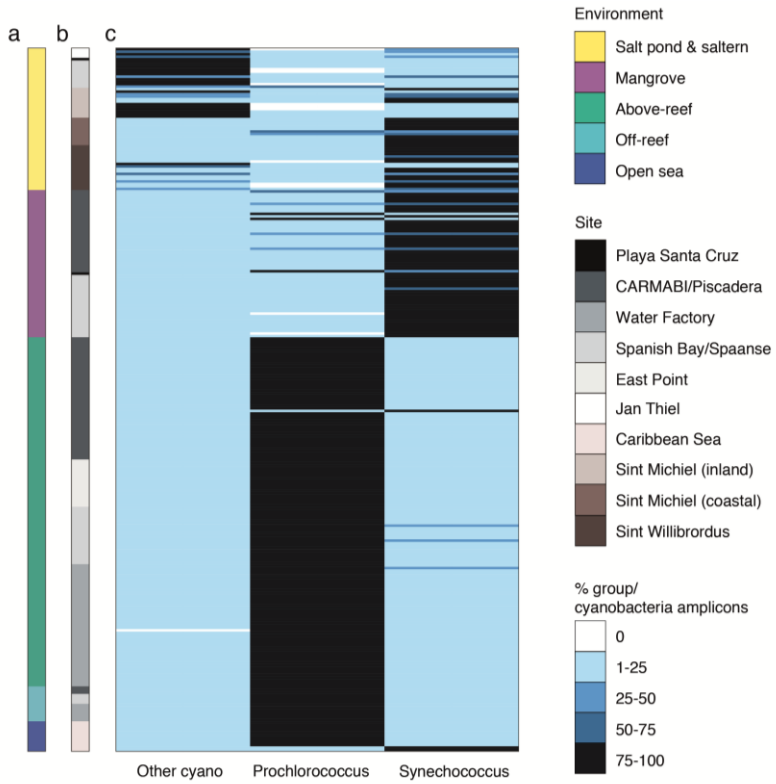

Supplementary Figure 7: Relative abundances of major cyanobacterial phytoplankton groups by (a) environment and (b) sampling site. The percent of the cyanobacterial group of total cyanobacterial amplicons is indicated by the heatmap in (c), with each row indicating an individual sample.

SUPPLEMENTARY TABLE LEGENDS

Supplementary Table 1: Collection data for all samples, including collection date, sampling site, environment type, depth, salinity, water temperature, silicate, phosphate, nitrate, and nitrite concentrations (all in μmol kg^{-1}), latitude, longitude, and the number of 16S V1-V2 amplicons generated. NA indicates not available or not collected; *, indicates that the latitude and longitude are by prior estimate from sites regularly sampled. Note that 2019 values for highest salinity environments were compromised because methodological issues did not allow quantification of values >100‰. Also note that open sea temperature values are derived from satellite measurements, while all others were measured in this study.

Supplementary Table 2: Summary of inverse Simpson indexes generated from 16S V1-V2 amplicons from all samples, including sample size, minimum, maximum, median, and interquartile range. NA indicates not available due to lack of replication.

Supplementary Table 3: Summary of Kruskall-Wallis and Dunn test results comparing the inverse Simpson indexes for all samples, based on 16S V1-V2 amplicons. Significance levels are indicated for adjusted p-values <0.05, *; ≤0.01, **; ≤0.001, ***; ns, not significant.

Supplementary Table 4: Feature table and taxonomy for the photosynthetic community, including cyanobacteria and eukaryotic plastid 16S V1-V2 ASVs. PhyloAssigner taxonomy contains taxonomy based on all consecutive PhyloAssigner reference database classifications. All columns starting from 'C1-1-16' contain amplicon read counts per sample. NA indicates that the method was not used and therefore result "not available."

Supplementary Table 5: Amplicon counts and taxonomic assignments (based on PR2) for all 18S V4 rRNA samples (41 in total). Bold text indicates ASVs that are from prasinophyte clades/species discussed in detail herein.

Supplementary Table 6: Comparison of 16S V1-V2 and 18S V4 ASV taxonomic assignments. Shown are the average relative abundances for each eukaryotic taxonomic group (cryptophytes, haptophytes, stramenopiles, chlorarachiophytes, green algae, and “others”, i.e., glaucophytes and rhodophytes) out of all eukaryotic ASVs with alveolates removed. Averaging was performed across the 35 above-reef samples and the 6 off-reef samples for which both markers were sequenced. Assignments are based on PhyloAssigner values for 16S V1-V2 and from PR2 for 18S V4. Note that for this analysis deep branching plastid lineages (DPL) (Choi et al., 2017) were excluded because their 18S rRNA gene sequence is not known and alveolates were excluded due to problems partitioning photosynthetic from heterotrophic lineages. Moreover, stramenopile 18S V4 values could be inflated due to inclusion of some heterotrophic members that are closely related to photosynthetic taxa, and therefore were lumped with them; purely heterotrophic stramenopile groups (e.g., Pseudofungi and Opalozoa) were excluded.

Supplementary Table 7: List of significant interactions between ASVs in co-association networks with corresponding taxonomy for both connected nodes of each interaction. Phytoplankton taxonomy was by PhyloAssigner as detailed in methods and bacterial taxonomy is by SILVA 138. NA, method not used (and therefore assignment not available).

CHAPTER 3:
Effects of limiting environmental conditions on the cell quotas of pico-prasinophytes

ABSTRACT

The life and death of phytoplankton shape carbon and nutrient cycles in the ocean. A better understanding of their elemental composition and how they change under differing environmental regimes is useful in understanding the roles of individual phytoplankton species in these processes and could be useful to parameterize models of future ocean change. In this chapter, cultured strains of the Mamiellophyceae genera *Ostreococcus* and *Micromonas* were grown under different nutrient and CO_2 concentrations. Both semi-continuous batch cultures and photo-bioreactors were used for culturing experiments. Cell numbers, a proxy for cell size, and chlorophyll per cell were measured via flow cytometry. The cellular quotas of carbon, nitrogen, and phosphorus were quantified by filtering cultures through combusted glass microfiber filters which were then measured for particulate carbon (C), nitrogen (N), and phosphorus (P). The cell quotas under replete, near maximal light conditions differed between species, but were within similar ranges. Under phosphate starvation the cell sizes, CNP content, and chlorophyll fluorescence of *M. commoda* RCC 299 and *O. lucimarinus* CCMP 2972 increased. Similar results were found when *M. commoda* was subjected to phosphate limitation. Under nitrate limitation, chlorophyll fluorescence decreased, although patterns in cell size were less straightforward, with evidence *M. commoda* RCC 299 decreased in size and CNP content, while *M. polaris* CCMP 2099 increased in these parameters. Recommendations for best practices in performing these experiments and measurements are also discussed. Understanding and quantifying these cellular

characteristics under various environmental changes provides information that can be used to refine carbon estimates of different phytoplankton groups in the oceans, as well as serving as constraints for modelling efforts.

INTRODUCTION

Phytoplankton live, replicate, and die at much shorter timescales than their land plant counterparts. The turnover rates and cellular characteristics with respect to nutrient and carbon quotas are important because they shape biogeochemical cycling of carbon, nitrogen and phosphorous (Litchman et al., 2015). Phytoplankton fixation of inorganic carbon (C), phosphorus (P), and nitrogen (N) via primary production makes them major players in global nutrient cycles (Chavez et al., 2011). The C:N:P ratios of phytoplankton have classically been characterized as the Redfield ratio of 106:16:1; the ratios of these elements in seawater are determined by the biochemical requirements of the phytoplankton that take up these elements in that specific ratio and then release them in that ratio upon their decomposition (Redfield, 1958). While there is some contention about the degree to which the biotic processes shape the abiotic composition of the ocean, the Redfield ratio has been a useful way to account for phytoplankton in ecological models. However, when models adopt Redfield ratios as the universal C:N:P ratio in all phytoplankton they could underestimate ocean carbon uptake (Klausmeier et al., 2008; Kwiatkowski et al., 2018).

In fact, the C:N:P ratio stoichiometry in phytoplankton is variable even within the same species under different conditions (Fábregas et al., 2002; Glibert et al., 2013; Harrison et al., 1990). Cell stoichiometry is determined by the relative and absolute amounts of different macromolecules within the cell; most of the cellular nitrogen is found in proteins and nucleic acids, while most of the phosphorus is found

in nucleic acids and phospholipids (Geider & La Roche, 2002). Changes in environmental conditions can prompt phytoplankton to change the ratios of these macromolecules, thus changing their stoichiometric ratios. These environmental parameters include light availability (Thompson et al., 1991), nutrient availability (Rhee & Gotham, 1981), temperature (Stawiarski et al., 2016), CO_2 (Verschoor et al., 2013), micronutrient availability (Twining et al., 2004), and circadian cycle (Fábregas et al., 2002).

Environmental parameters such as these are considered major ecological axes relevant to modelling phytoplankton using trait-based models (Litchman & Klausmeier, 2008). Trait-based models, which rely on the could address the problems of over-generalization and model ocean ecology in a more robust and comprehensive way by taking stoichiometric plasticity into account (Bonachela et al., 2016; Finkel et al., 2010; Lindemann et al., 2017). The interplay of environmental conditions and tradeoffs in traits determines which phytoplankton are likely to thrive in certain conditions, and increased knowledge of these interactions will allow for better predictions of future phytoplankton dynamics under projected climate changes (P. W. Boyd et al., 2010).

This chapter seeks to contribute to the knowledge of stoichiometry of picophytoplankton within the class Mamiellophyceae. Picophytoplankton (plankton with $\leq$2 μm cell diameter) contribute significantly to the primary production in the low-nutrient oligotrophic subtropical oceans (Li, 1994; Worden et al., 2004). The Mamiellophyceae clade in particular is ubiquitous; this group was initially considered

important primarily in coastal areas (Lovejoy et al., 2007; Tragin & Vaulot, 2018), but members have also been from the oligotrophic subtropical North Pacific Gyre (Limardo et al., 2017), to the seasonally oligotrophic subtropical BATS (as demonstrated in chapter 1). Decreased nutrients in surface waters and increasing ocean acidity related to anthropogenic climate forcing could favor certain picoplanktonic prasinophytes (Agawin et al., 2000; W. K. W. Li et al., 2009; Meakin & Wyman, 2011), and there is evidence that oligotrophic areas of the ocean are expanding (Bopp et al., 2013). Projected changes in the distributions of *Micromonas* species could serve as a proxy for diversity changes of the wider phytoplankton community (Demory et al., 2019).

Environmentally relevant representatives of the Mamiellophyceae genera *Ostreococcus* and *Micromonas* were grown under different light and nutrient regimes to investigate associated changes in cell quotas and growth parameters. *Ostreococcus* is a non-flagellated naked prasinophyte that is around 0.8 to 1.1 µm in cell diameter, while *Micromonas* is a flagellated naked prasinophyte that is between 1.4 and 1.8 µm in diameter depending on the species (Chrétiennot-Dinet et al., 1995; Simon et al., 2017; Worden et al., 2004). The species investigated are among those detected in environmental samples in the previous two chapters and were isolated from various oceanic and coastal regions. *Micromonas* Clade A (*M. commoda sensu stricto*) isolate RCC 299 (van Baren et al., 2016) was isolated from the south Pacific Ocean and is identical in the 16S V1-V2 to amplicons found at BATS in Chapter 1 (ASV345) and in Curaçao in Chapter 2 (ASV306). *Micromonas* Clade D (*Micromonas pusilla*)

isolate CCMP 1545 was isolated from the temperate English Channel, see (Worden et al., 2009). It is found at high cellular abundances in the English Channel (Not et al., 2004) and Norwegian Sea (Not et al., 2005) and seen in the eastern North Pacific (Simmons et al., 2016), North Atlantic, North Sea, and Mediterranean Sea (Simon et al., 2017) and is also identical in the 16S V1-V2 to a rare amplicon from BATS (ASV2535). The final *Micromonas* species, *Micromonas* Clade E2 (*Micromonas polaris*) strain CCMP 2099, was isolated from the polar Baffin Sea (Lovejoy et al., 2007). As this thesis is concerned with tropical and temperate regions, this species is not included in the previous two chapters, but serves as an interesting point of comparison to the other *Micomonas* cultures; the various species with unique temperature/geographic ranges are an aspect of the genus that can make it important in climate research (Demory et al., 2019; Worden et al., 2009). In terms of *Ostreococcus*, *Ostreococcus* OI (*Ostreococcus lucimarinus*) strain CCMP 2972 has 99% nt identity to an *Ostreococcus* OI amplicon from BATS, while *Ostreococcus tauri* CA OTH 95 was isolated from a Mediterranean lagoon (Chrétiennot-Dinet et al., 1995). *O. tauri* is not observed frequently in coastal or open ocean environments, and rather appears more affiliated to brackish estuaries and lagoons (Demir-Hilton et al., 2011), however it is currently being used as a model organism and hence was used as a comparator (Blanc-Mathieu et al., 2013; Derelle et al., 2006). The information presented in this chapter could contribute to trait-based phytoplankton models seeking to elucidate the role of eukaryotic picophytoplankton the changing oceans.

Materials and Methods

Semi-continuous batch cultures:

Replete conditions: Axenic *M. commoda* RCC 299, *O. lucimarinus* CCMP 2972, *O. tauri* CA OTH 95, and *M. pusilla* CCMP 1545 were grown in bio-quadruplicate or bio-triplicate semi-continuous batch culture. Cultures were acclimated to and grown exponentially for at least 10 generations at 110-120 μE m^{-2} s^{-1} photosynthetically active radiation (PAR) or 210 -220 PAR at 21.5 °C and a 14:10 light:dark cycle. PAR was measured with a Walz Universal Light Meter-500. Cultures were grown in L1 media (National Center for Marine Algae and Microbiota) prepared with natural seawater from CalCOFI (California Cooperative Ocean Fisheries Investigations) Line 67 station 135 (33.953 °N, 128.048 °W), an oligotrophic region in the North Pacific Ocean. Media had a salinity of 35‰ and a pH ranging from 8.2-8.3. For *O. lucimarinus* CCMP 2972, the media was amended with an additional 0.01 μM H_2SeO_3. Please note that a summary of culturing conditions for all experiments can be found in Supplementary table 1. Cell densities were maintained at 15 million cells mL^{-1} or lower to keep the cultures optically clear and prevent self-shading. Periodically, an aliquot of culture was added to bacterial test media (artificial seawater with yeast and peptone extracts) to ensure the cultures were still axenic. Samples were taken daily at approximately the same time of day to monitor growth rate (see *Flow cytometry* section for details).

Phosphate starvation RCC 299: Axenic *M. commoda* RCC 299 was grown in bio-quadruplicate semi-continuous batch culture at 150 μE m^{-2} s^{-1} PAR and 21.5 °C

with a 14:10 light:dark cycle. Cultures were grown in L1 media with natural seawater from CalCOFI line 67 station 135 with a salinity of 35‰ and a pH of 8.2-8.3. Cultures were transferred to fresh media at the frequency needed to maintain exponential growth for 10 days, cultures were concentrated by centrifugation, washed with phosphate-deplete media (L1 with no added NaH_2PO_4, pH = 8.18, salinity = 35‰), and re-suspended in a small volume of phosphate-deplete media. Re-suspended cells were combined and aliquoted into quadruplicate 800 mL flasks containing either nutrient replete (standard L1 media) or phosphate-deplete media, at a starting density of ~7 x 10^5 cells mL^{-1} (the precise density was measured for each replicate). Samples were taken daily to monitor growth rates. Sampling was done after the low-phosphate treatment had consistent negative growth rates for two days, which was nine days after resuspension. Both control cultures and low-phosphate cultures were diluted with fresh media before harvest to ensure cultures did not become limited by other nutrients.

Phosphate starvation CCMP 2972: Axenic *O. lucimarinus* CCMP 2972 was grown in bio-quadruplicate semi-continuous batch culture at 110 µE m^{-2} s^{-1} PAR and 18 °C with a 14:10 light:dark cycle. Cultures were grown in L1 media with natural seawater from CalCOFI line 67 station 135 with a salinity of 35‰ and a pH of 8.27. After growing exponentially for 7 days, cultures were concentrated by centrifugation, washed with phosphate-deplete media (L1 with no added NaH_2PO_4, 0.2 uM PO_4, pH = 8.28, salinity = 35‰), and re-suspended in a small volume phosphate-deplete media. Re-suspended cells were combined and aliquoted into triplicate flasks

containing either nutrient replete (L1 media with standard 36.2 μM NaH_2PO_4) or phosphate-deplete media, at a starting density of ~7 x 10^5 cells mL^{-1}. All flasks were allowed to grow for two days (no more dilutions) before sampling. Samples were taken daily to monitor growth rate.

Photo-bioreactors:

Phosphate limitation RCC 299: Axenic RCC 299 was grown in semi-continuous batch culture at 150 μE m^{-2} s^{-1} PAR and 21 °C with a 14:10 light:dark cycle. Cultures were grown in L1 media (36.2 μM NaH_2PO_4). After growing exponentially for 10 days, cultures were concentrated by centrifugation, washed with phosphate-deplete media (L1 with no added NaH_2PO_4), and used to inoculate 3 photo-bioreactors (bio-triplicate). All photo-bioreactor experiments were conducted in custom-built photo-bioreactors as described in (Guo et al., 2018). Cultures were grown at the same temperature and light conditions as they were in batch culture. After eight days in this low-phosphate media (1 μM), the concentration of phosphates was increased to 3 μM due to variable near-zero growth rates under the initial low-phosphate conditions (see Guo et al 2018 for more detailed methods). Herein, four timepoints experiment were used, corresponding to replete, transitional, phosphate-limited, phosphate refed, and the return to complete conditions.

Nitrate limitation and CO_2 changes RCC 299: Axenic RCC 299 was grown in 4 photo-bioreactors (bio-quadruplicate) at 250 μE m^{-2} s^{-1} PAR peak irradiance and 24 °C in L1 medium made with artificial seawater under both NO_3^- replete and limited

conditions (80 µM and 0.4 µM NO_3^-) in both high and ambient CO_2 (1000 µatm CO_2 and 400 µatm). For this paper, the timepoints 15, 37, 56, and 68 days were used, corresponding to replete NO_3^- high CO_2, limited NO_3^- ambient CO_2, limited NO_3^- high CO_2, and replete NO_3^- and ambient CO_2.

Nitrate limitation and CO_2 changes CCMP 2099: M. polaris CCMP 2099 was grown in 4 photo-bioreactors (bio-quadruplicate) under both NO_3-replete and limited conditions (150 µM and 10 µM NO_3) in both high and ambient CO_2 (400 µatm and 1000 µatm CO_2). For this paper, the timepoints 1, 20, 54, and 71/73 days were used, corresponding to replete NO_3 high CO_2, limited NO_3 ambient CO_2, limited NO_3 high CO_2, and replete NO_3 and ambient CO_2.

Flow cytometry:

Measurements of cell density were conducted daily using the Accuri C6 flow cytometer (BD Biosciences, San Jose, California) on unfixed culture samples diluted with artificial seawater. Cell populations were gated using cytograms of forward angle light scatter (FALS) and chlorophyll fluorescence (692 / 40 nm filter). Size measurements were standardized by dividing the forward scatter value of the cell population by the forward scatter value of the 2 µm red fluorescent bead population. Chlorophyll fluorescence measurements were standardized by dividing the fluorescence value of the cell population by value of the 0.75 µm yellow-green fluorescent beads.

For several experiments, culture samples were fixed with glutaraldehyde, incubated in the dark for 15-30 minutes, then flash-frozen in liquid nitrogen before being stored at -80 °C for later analysis of cell density and cell size on the more precise Influx flow cytometer (BD Biosciences). 0.5 µm green beads and 0.75 µm yellow-green beads were used for standardization. To standardize cell counts between flow cytometers, Accuri-based flow cytometry counts were converted to better match Influx-based counts by dividing by 1.5, a conversion factor determined by measuring samples from the same cultures on both instruments and comparing.

Growth rates for semi-continous batch culture were calculated by taking the natural logarithm of the density difference between two time points, divided by the time between measurements:

$$\mu = \frac{\ln(\frac{N_2}{N_1})}{t_2 - t_1}$$

where µ is growth rate, N_1 is the cell density at time 1 (t_1), and N_2 is the cell density at time 2 (t_2).

Growth rates for continuous culture were calculated the same way, with the addition of D_1, the dilution rate at time t_1:

$$\mu = D_1 + \frac{\ln(\frac{N_2}{N_1})}{t_2 - t_1}$$

where D_1 is dilution rate at time t_1, and N_1 is the cell density at time 1 (t_1) and N_2 is the cell density at time 2 (t_2).

Cell quota measurements:

Particulate C and N samples were collected by filtering 10-50 mL of culture or media sample using vacuum filtration (<10 kPa) through a 25 mm glass microfiber (GFF) filter that had been previously combusted for 3-4 hours at 450 °C. The filters were either placed in a well of a sterile 12-well plate and stored at -20 °C or folded in half and wrapped in a combusted aluminium foil sleeve and stored at -80 °C until processing (note: for CA OTH 95 *O. tauri* the filters were not folded before being wrapped, which likely resulted in an underestimation of POC and PON). Samples were processed for PON and POC simultaneously, either on an CE-440 Elemental Analyzer from Exeter International Inc. using the procedure recommended by the company at either the Horn Point Analytical Laboratory at the University of Maryland Center for Environmental Science or the SOEXT Laboratory for Analytical Biogeochemistry at the University of Hawai'i at Mānoa.

For POP, the samples were collected and stored the same way except for when 0.2 µm pore-size Sterilitech PC filters or 0.65 µm pore-size Durapore Membrane (DVPP) filters were used in place of GFF filters. The filter was subjected to high temperature ashing and quantified on a Seal Analytical AA3 HR Nutrient Autoanalyzer, also at the SOEXT Laboratory. POP samples were combusted in a muffle furnace at 550 °C for 90 minutes and then extracted in 1N HCl for a minimum of 24 hours before being analyzed on the Technicon AutoAnalyzer II, also at the Horn Point Laboratory.

Directly following the collection of the POP onto a filter, the flow-through was collected in an acid-cleaned 50 mL Falcon tube and stored at -20 °C. Samples were processed for SRP using an established colorimetric procedure (Murphy & Riley, 1962) or an automated version of that procedure at the Horn Point Laboratory using a Technicon AutoAnalyzer II or at SOEXT Laboratory using the SEAL Analytical AA3.

For chlorophyll, 20 mL of culture was filtered through a GFF filter, the filter was then folded in half, wrapped in aluminum foil, and stored at -80 °C until ready for processing. Chlorophyll was then extracted from the filter using 90% acetone, and the resulting solution incubated at -20 °C for 24 hours to allow the acetone to extract the chlorophyll from the filters. After 24 hours, the samples were removed from the freezer and allowed to warm to room temperature in the dark before being processed. Samples were measured on a Turner fluorometer then 5% HCl was added to convert chlorophyll in the sample into phaeophytin and a second reading was taken. Chlorophyll concentration was calculated using the following formula:

$$Chl\ a\ (\mu g\ L^{-1}) = F \times V_e \times \frac{F_o - F_a}{V_f}$$

Where F = fluorometer calibration factor, F_o = total fluorescence, F_a = fluorescence after HCl addition, V_e = extract volume after acid, and V_f = filtration volume (volume culture filtered in liters).

For the phosphate starvation RCC 299 experiment, cell volumes were measured using a Coulter counter (Beckman Coulter Life Sciences), that was not available for most other experiments.

For the phosphate limitation RCC 299 photo-bioreactor experiment, lipids were also measured. Phospholipids were measured according to (Zink et al., 2003), glycolipids were measured according to (Schubotz et al., 2013), aminolipids measured according to (Brandsma et al., 2012; Furlong & Caulfield, 1986; López-Lara et al., 2005), sulfolipids according to (Brandsma et al., 2012), and neutral lipids according to (Blachnio-Zabielska et al., 2013; M. Li et al., 2014). Lipid content was normalized to cell number as determined by flow cytometry.

Calculations and statistics:

Data was generally returned as μG or μmol per filter or mg per liter, both for culture samples and for fresh media samples. For the semi-continuous-batch-culture-based replete conditions and P-limitation experiments, the average N and C values for the fresh media, both nutrient replete and P-limited (n=2-3 for each), were initially subtracted from the values from the nutrient replete and P-limited culture samples, respectively. Using the volume and cell density of the culture filtered, the μG of N and C per cell was calculated based on these media-blank-corrected values. However, this approach generated negative values for P content per cell, likely due to a known phenomenon (Bertilsson et al., 2003) wherein available phosphate is retained by the filter. For some replete conditions experiments, the culture was spun down in a

centrifuge and the resulting supernatant was filtered and used for particulate CNP and SRP analysis. However, since this was only done for a subset of the experiments considered here, this was not used for blanking purposes. Therefore, only combusted filters were used as blanks to maintain standardization across experiments.

The mass per cell of an element was divided by the molar mass of that element to yield the moles of that element per cell. These numbers were then used to compare elemental ratios. Example:

$$C{:}N = \frac{\frac{fg\ C\ cell^{-1}}{12.0107}}{\frac{fg\ N\ cell^{-1}}{14.0067}}$$

The normality of the distributions of cell growth and quota parameters was tested via Shapiro test using the R stats package. If the distribution was normal, differences between groups were tested using one-way ANOVA and Tukey's honestly significant difference (HSD) test. If the data were normally distributed, the groups were compared using the Kruskal-Wallis and Dunn tests using the R stats and rstatix packages (Kassambara, 2019). The correlations between variables were tested using Spearman's rank correlation.

RESULTS

To serve as a comparison for nutrient and CO_2 manipulation studies, *M. commoda* RCC 299, *M. polaris* CCMP 2099, *M. pusilla* CCMP 1545, *O. tauri* CA OTH 95, and *O. lucimarinus* CCMP 2972 were grown under sufficient light (200 PAR or 100 PAR in the case of *O. tauri*) and nutrient conditions (L1 media) in semi-continuous batch

culture (Supplementary table 1). Growth rates from three days prior to the day of collection or, in the case of *M. polaris* CCMP 2099 from the day of harvest, were recorded. *M. commoda* RCC 299 had an average growth rate of 0.66±0.05 day^{-1}, for *M. polaris* CCMP 2099 average growth rate was 0.44±0.13 day^{-1}, *M. pusilla* CCMP 1545 was 0.63±0.22 day^{-1}, *O. tauri* CA OTH 95 was 1.25±0.25 day^{-1}, and *O. lucimarinus* strain CCMP 2972 had an average growth rate of 0.53±0.12 day^{-1} (Figures 1a, supplementary 2a, and supplementary table 2). Average bead normalized flow-cytometry-derived chlorophyll fluorescence per cell was 0.115±0.002 for *M. commoda* RCC 299, 0.108±0.003 for *M. polaris* CCMP 2099, 0.121±0.003 for *M. pusilla* CCMP 1545, 0.060±0.002 for *O. tauri*, and 0.041±0.003 for *O. lucimarinus* strain CCMP 2972. Average chlorophyll *a* in fg per cell from Turner fluorometry was 12±1 for *M. commoda* RCC 299, 12±1 for *M. pusilla* CCMP 1545, 10±1 for *O. tauri*, and 5±0 for *O. lucimarinus* CCMP 2972. Chlorophyll *a* per cell from Turner fluorometry was not measured for *M. polaris* CCMP 2099. Turner chlorophyll and flow-cytometry-derived chlorophyll fluorescence were found to be significantly correlated (Spearman rho=0.74, p>0001; supplementary figure 2). The average cell quotas in fg $cell^{-1}$ were 747±52 C, 137±15 N, and 39±11 P for *M. commoda* RCC 299; 822±40 C, 156±1 N, and 22±1 P for *M. polaris* CCMP 2099; 804±88 C, 123±12 N, and 21±5 P for *M. pusilla* CCMP 1545; 319±93 C, 76±19 N, and 13±1 P *O. tauri*; and 390±20 C, 87±5 N, and 15±1 P for *O. lucimarinus* CCMP 2972 (Figures 1b and supplementary 2b).

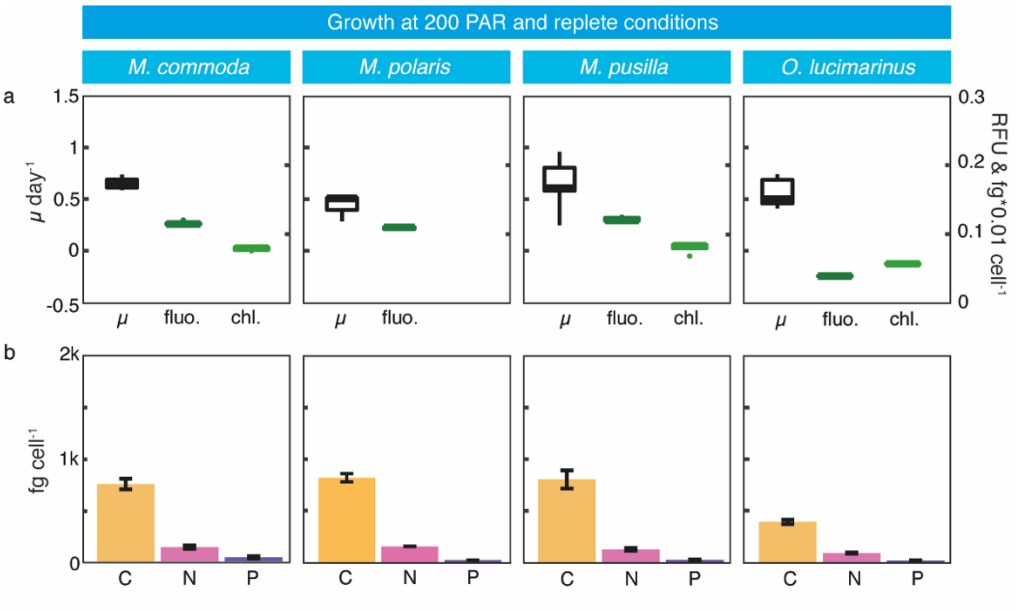

Figure 1. Cell quotas of carbon, nitrogen, and phosphorus for *Micromonas* and *Ostreococcus* strains in replete conditions at ~200 PAR. (a) Box and whisker plots of growth rate (day^{-1}), chlorophyll fluorescence per cell (Relative Fluorescence Units, RFU), and chlorophyll *a* content (fg *0.01 cell^{-1}). (b) Bar plots of average C, N, and P (fg cell^{-1}) with error bars reflecting the standard deviation of three to four measurements.

Representatives from both genera, *M. commoda* RCC 299 and *O. lucimarinus* CCMP 2972, were grown in semi-continuous batch culture with in both replete and phosphorus-starved conditions under sufficient light conditions (Supplementary table 1). In the replete controls, *M. commoda* RCC 299 had an average growth rate of 0.59±0.14 day^{-1} and *O. lucimarinus* CCMP 2972 0.61±0.24 day^{-1} (Figure 2a and supplementary table 2). Under P starvation, that dropped to -0.09±0.16 day^{-1} and -0.02±0.03 day^{-1}, respectively, on the day of harvest, which was significantly lower than the control for both (one-way ANOVA, $p<0.001$) (Supplementary table 3). Average chlorophyll fluorescence under replete conditions was 0.115±0.003 for *M. commoda* RCC 299 and 0.022±0.002 for *O. lucimarinus* CCMP 2972, this increased

to 0.190±0.003 and 0.028±0.001 in P starved conditions, respectively, which was significantly higher than the control for both (one-way ANOVA, $p<0.001$ and $p=0.003$, respectively). The average cell quotas in fg cell^{-1} were 422±50 C, 87±7 N, and 39±2 P for *M. commoda* RCC 299 and 290±6 C, 94±7 N, and 48±3 P for *O. lucimarinus* CCMP 2972 in replete conditions, and 1499±196 / 524±11 C, 167±23 / 160±10 N, and 5±0 / 10±1 P in P starved conditions, respectively, all of which were significantly different between treatments (Figure 2b and supplementary table 3). For the *M. commoda* RCC 299 experiment, cell volume was also measured, and was 2.52±0.06 μm^3 cell^{-1} for replete and 4.17±0.09 μm^3 cell^{-1} for phosphate starved, with control being significantly higher (one-way ANOVA, $p<0.001$).

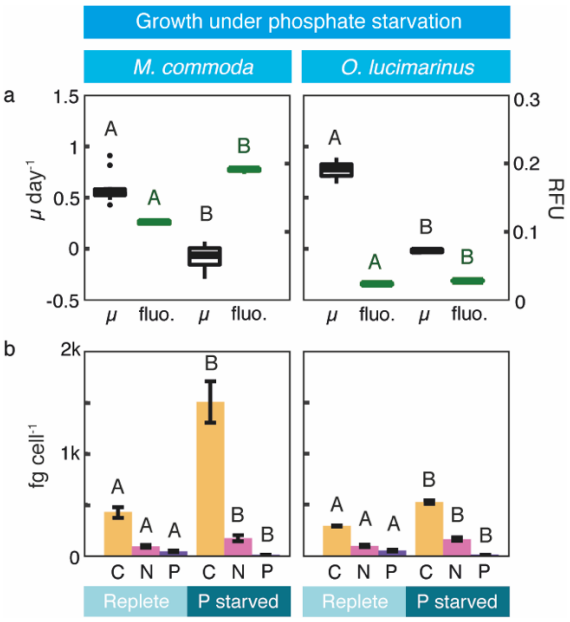

Figure 2. Cell quotas of carbon, nitrogen, and phosphorus of *Micromonas* and *Ostreococcus* strains under replete conditions and PO_4 starvation. (a) Box and whisker plots of growth rate (day^{-1}) and chlorophyll fluorescence (RFU). (b) Bar plots of average C, N, and P (fg cell^{-1}) with error bars for standard deviation. The same

letter designates statistically indiscernible differences, while different letters designate significant differences, with comparisons only made within each experiment.

Changes in cell parameters in response to more gradual changes in phosphate availability were measured via a photo-bioreactor-based experiment. The culture started out in replete conditions (36 μM phosphate), then the phosphate content was lowered to 1 μM in the transitional phase, before raising to 3 μM for the limited phase, then increasing to beginning values for the re-fed phase and returning to replete again (Figure 3a and supplementary table 1). Average growth rate started at 0.61±0.00 day^{-1} during replete conditions before lowering to 0.15±0.07 day^{-1} in transitional when phosphate values were lowest and staying low at 0.21±0.02 day^{-1} in limited before increasing to 0.57±0.05 day^{-1} in refed and 0.64±0.04 day^{-1} in the ending replete conditions. The two lowest were statistically not shown to be different from each other, as were the three highest, but the low and high values were significantly different (Supplementary table 3). Average chlorophyll fluorescence started at 0.152±0.004 during replete conditions stayed similar at 0.152±0.009 in transitional and increased to 0.167±0.011 in limited before decreasing to 0.136±0.002 in refed and 0.129±0.002 in the ending replete conditions. The chlorophyll fluorescence values for the first replete, transitional, and limited were all significantly higher than the second replete (Supplementary table 3). The average P in fg $cell^{-1}$ was highest at the first replete 18±0, next highest but significantly lower at the second replete 8±0 and refed 9±1, which were statistically not differentiated, and lowest for the transitional 5±1 and limited 5±0, which were also statistically not

found to be different from each other (Figure 3b and supplementary table 3). A significant correlation was found between growth rate and P cell^{-1} (Spearman rho=0.71, p=0.003) (Figure 3b).

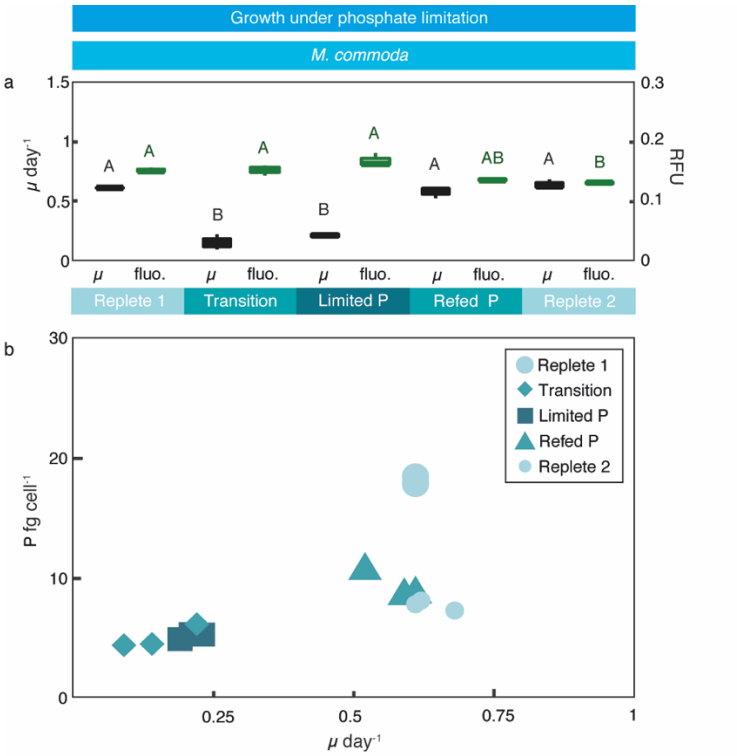

Figure 3. Cell quotas of phosphorus for *Micromonas commoda* with changes in PO_4 availability. (a) Box and whisker plots of growth rate (day^{-1}) and chlorophyll fluorescence (RFU). Phosphate availability conditions are indicated by the bar; note first replete was in semi-continuous batch culture, while other timepoints are from photo-bioreactor. (b) Scatterplot of P (fg cell^{-1}) vs. growth rate (day^{-1}), with points colored according to the phosphate availability conditions. The same letter designates statistically indiscernible differences, while different letters designate significant differences, with comparisons only made within each experiment.

Photobioreactors were also used to investigate the combined effects of nitrate limitation and differences in partial pressure of CO_2 for *M. commoda* RCC 299 and *M. polaris* CCMP 2099. For each experiment, cell quota samples were taken at four different conditions: high CO_2 (1000 µatm) and replete nitrate (80 µM) abbreviated

HCRN, ambient CO_2 (400 µatm) and limited nitrate (<1 µM NO_3) abbreviated ACLN, high CO_2 and limited nitrate (HCLN), and ambient CO_2 and replete nitrate (ACRN) (Figure 4a and supplementary table 1).

For *M. commoda* RCC 299, average growth rate started at 0.58±0.10 at HCRN before lowering to 0.25±0.05 in ACLN and 0.26±0.10 HCLN when nitrate values were lowest before increasing to 0.70±0.09 in ACRN, with growth rate at ACLN and HCLN significantly lower than ACRN (Figure 4a and supplementary table 3). Average chlorophyll fluorescence started at 0.17±0.01 at HCRN before lowering to 0.06±0.00 in ACLN and 0.05±0.00 in HCLN when nitrate values were lowest before increasing to 0.15±0.00 in ACRN, with growth rate at ACLN and HCLN significantly lower than HCRN and ACRN (Supplementary table 3). In terms of cell quotas, the ACLN N in fg $cell^{-1}$ was 100±16 and was significantly lower than that of ACRN which was 169±11 (Tukey HSD test, $p>0.001$). The ACLN C in fg $cell^{-1}$ (636±52) was also significantly lower than that of the ACRN (888±61; Tukey HSD test, $p>0.001$), and P per cell was not measured (Supplementary table 3).

For *M. polaris* CCMP 2099, average growth rate started at 0.28±0.02 at HCRN before lowering to 0.11±0.06 in ACLN and 0.20±0.03 at HCLN when nitrate values were lowest before increasing to 0.32±0.01 in ACRN, with growth rate at ACLN and HCLN significantly lower than HCNR and ACRN (Figure 4a and supplementary table 3). For *M. polaris* CCMP 2099, average chlorophyll fluorescence started at 0.20±0.01 at HCRN before lowering to 0.11±0.01 in ACLN

and 0.11±0.01 in HCLN when nitrate values were lowest before increasing to 0.20±0.01 in ACRN, with growth rate at ACLN and HCLN significantly lower than HCRN and ACRN (Supplementary table 3). In terms of CNP quota, the ACLN C quota (1830±167 cell^{-1}) was significantly higher than ACRN (851±168 cell^{-1}) and HCRN (709±160 cell^{-1}), and the ACLN P quota (41±10 cell^{-1}) was significantly higher than ACRN (24±2 cell^{-1}; figure 4c and supplementary table 3). There were no significant differences in the N quotas (Supplementary table 3).

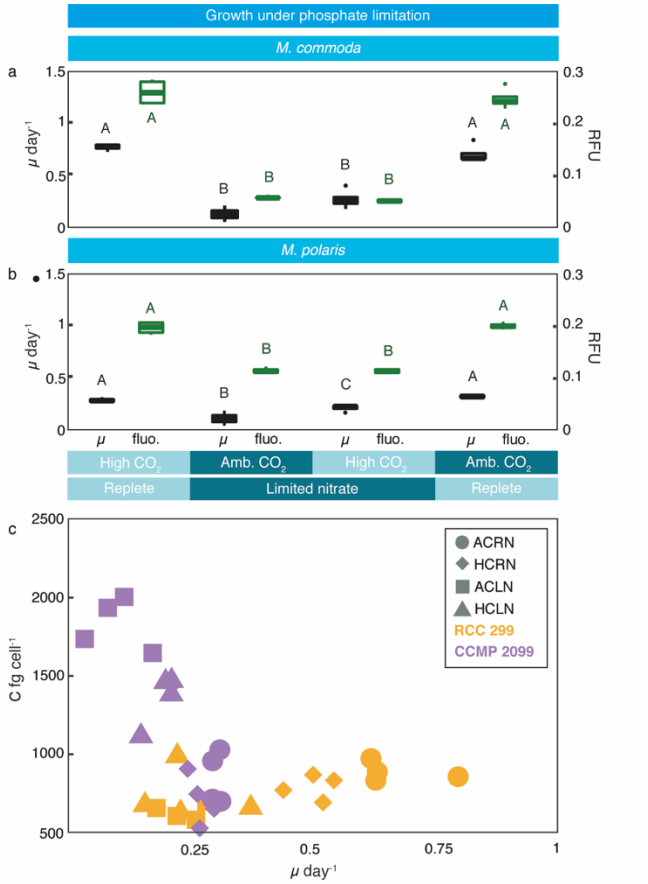

Figure 4. Cell quotas of carbon for *Micromonas commoda* with changes in NO_3 availability and pCO_2. Box and whisker plots of growth rate (day^{-1}) and chlorophyll fluorescence (RFU) for (a) *M. commoda* and (b) *M. polaris*. Nitrate availability and pCO_2 conditions are indicated by the bar. (c) Scatterplot of C (fg cell^{-1}) vs. growth rate (day^{-1}), with points shaped according to the treatment and colored according to

strain. The same letter designates statistically indiscernible differences, while different letters designate significant differences, with comparisons only made within each experiment.

To investigate the similarity of cell quotas under similar replete light and nutrient conditions across experiments, we compared the baseline *M. commoda* RCC 299 cell quota to those of the *M. commoda* RCC 299 replete controls used in the phosphate starvation batch culture, phosphate limitation photo-bioreactor, and nitrate limitation photo-bioreactor studies (Supplementary figure 3). There were significant differences in C and N quotas among all studies, although values were more similar between the baseline study and N-limited photo-bioreactor than between either one and the P-starvation study (Supplementary table 3; note P quotas were not compared due to insufficient data across experiments).

Discussion

A better understanding of how phytoplankton respond to replete and limiting conditions is important for understanding field-based observations and for development of models of potential distributions. In this chapter, *Micromonas* and *Ostreococcus* cultures were grown under various conditions to characterize baseline cell quotas at sufficient conditions and measure how they change in limiting or starvation scenarios. In the baseline study under replete conditions, growth rates of the three *Micromonas* and one *Ostreococcus* species were around 0.5 day^{-1} or higher, indicating cells were actively dividing (Figure 1a). The chlorophyll and CNP $cell^{-1}$ was high for the *Micromonas* species, as expected given their cell sizes (Guillou et

al., 2004; Simon et al., 2017) compared to *Ostreococcus* (Chrétiennot-Dinet et al., 1995; Subirana et al., 2013). The chlorophyll and flow-cytometry-measured chlorophyll fluorescence were significantly positively correlated across all replete cultures, implying the latter is a good proxy for the former in culturing studies (Supplementary figure 1).

When *M. commoda* RCC 299 and *O. lucimarinus* CCMP 2972 were subjected to phosphate limitation or starvation, they demonstrated similar responses of decreased growth rate, increased chlorophyll fluorescence, and increased cell size, as demonstrated by increase in cell CN quotas and, in the case of *M. commoda* RCC 299, cell volume (Figures 2 and 3). Only P was lower in the phosphate-starved or limited cells, as expected. There was a significant positive correlation between growth rate and P content per cell in the phosphate limitation study with *M. commoda* RCC 299, indicating cells were actively dividing and incorporating P in the re-fed and replete conditions (Figure 3b). These results were in partial contrast to a photo-bioreactor study of phosphate limitation in *M. pusilla*, which found the replete control to have higher C, N, and P content than the P-limited experimental conditions (Maat et al., 2014).

M. commoda RCC 299 demonstrated a different physiological response to nitrate limitation as compared to P limitation, in which cells had less C and N in the limited nitrate as compared to the replete conditions, both under ambient levels of CO_2. Additionally, nitrate limited cells under both ambient and high CO_2 levels had lower growth rates and chlorophyll fluorescence (Figure 4a). Another photo-

bioreactor-based study also using *M. commoda* RCC 299 found that N-limited cells had less N per cell, as was found here, but no discernible change in C per cell, with cell volume decreased in N-limited (Halsey et al., 2014).

When *M. polaris* was subjected to the same changes in nitrate and CO_2 availability, it exhibited lower growth rates and chlorophyll fluorescence, similar to responses seen for *M. commoda.* The fact that *M. polaris* has overall much lower growth rates, at least based on culturing studies, is known for replete cultures (Lovejoy et al., 2007). However, unlike *M. commoda*, the C content of *M. polaris* cells increased under nitrate deplete conditions. A semi-continuous batch culture-based study on *M. polaris* CCMP 2099 found N replete cells had less C than N starved (in which the cells had ceased growing), which agrees with the results presented here, and also that replete cells had more N and P per cell than N-starved cells, which was not found here (Liefer et al., 2019).

The differing responses in cell quotas to P and N limitation could reflect different strategies of dealing with nitrate and phosphate limitation. Increased CNP and chlorophyll in nutrient limited or starved cells could indicate cells were readying for division but unable to complete the process, and this has been previously reported for *M. commoda* (Guo et al., 2018).

While the changes in cell quotas shown in limitation and starvation experiments are unlikely to be the result of imprecise measurement, the differences in cell quotas among replete conditions across experiments are less easily explained. These differences could demonstrate the sensitivity of the cells to even minute

environmental changes, as these experiments had variations in light level despite all light levels used previously demonstrated to be sufficient and not photo-inhibitory (Cuvelier et al., 2017). Interestingly, in the comparison of replete *M. commoda* RCC 299 cultures across experiments, one semi-continuous batch culture study had more similar CNP values to a photo-bioreactor study than to the other semi-continuous batch culture study (Supplementary figure 3). Another factor to consider in overall quotas is the process for blanks. Here, combusted filters were used as blanks as performed in other studies using these methods, such as (DuRand et al., 2002). Some other studies have used filters through which fresh media had been passed (Zimmerman et al., 2014), and others the filtrate of spent media filtered again to catch any missed particulates in the leftover media – but also noted that this approach could artificially inflate blank levels (Bertilsson et al., 2003; Halsey et al., 2014). Indeed, this issue is so well-recognized that recently (after the completion of the experiments conducted herein) a publication addressing the topic was published (Y.-Y. Hu et al., 2022). For the phosphate-starvation experiment herein, it was found that using fresh media as a blank could result in an overestimation in particulate P outside of the cells. In the approach used here all values (all species) were standardized to combusted filter blanks for comparison across experiments but spent media controls should also be evaluated for future studies. There is still likely much natural variability even under sufficient conditions (Garcia et al., 2018), and models should incorporate a range of likely values from different scenarios obtained from the literature of culture-based studies.

In addition to measures of overall CNP cellular quotas, quantification of how they are allocated within the cell, i.e., macromolecular content, is an important complement to studies such as these. Overall protein content per cell was quantified for the N-limitation photobioreactor study, and a detailed breakdown of lipid content was generated for the P-limitation photobioreactor study, both using *M. commoda* RCC 299, discussed herein. There is evidence of P-limitation affecting the lipid ratios of *M. pusilla* (Maat et al., 2016), so, although out of the scope of this chapter, it will be useful to compare the responses to those of *M. commoda*. Another potential avenue of research would be to expand the scope from Mamiellophyceae to the other prasinophyte classes represented in culture. Work has already been done to compare Mamiellophyceae and Class VII cell quotas under N starved and replete conditions (Ebenezer et al., 2022), and it would be interesting to see how other classes compare; the large morphogenic variation within and among prasinophyte classes will likely be reflected in their cell quotas. Comparisons within the pico-phytoplankton, e.g., to cyanobacteria *Prochlorococcus* and *Synechococcus* (Mouginot et al., 2015), provides helpful comparisons within this size class; despite their genetic and morphological differences, they share size-related constraints and advantages in terms of nutrient uptake and assimilation (Finkel et al., 2010; Marañón et al., 2013). Better characterizations of cell quota changes, including overall CNP and macromolecular content, use of photo-bioreactor experiments to carefully maintain limiting nutrient concentrations, and comparisons within phylogenetic and size-based groupings will

make studies such as those included in this chapter more accurate and useful for understanding the physiology of phytoplankton and for feeding into models.

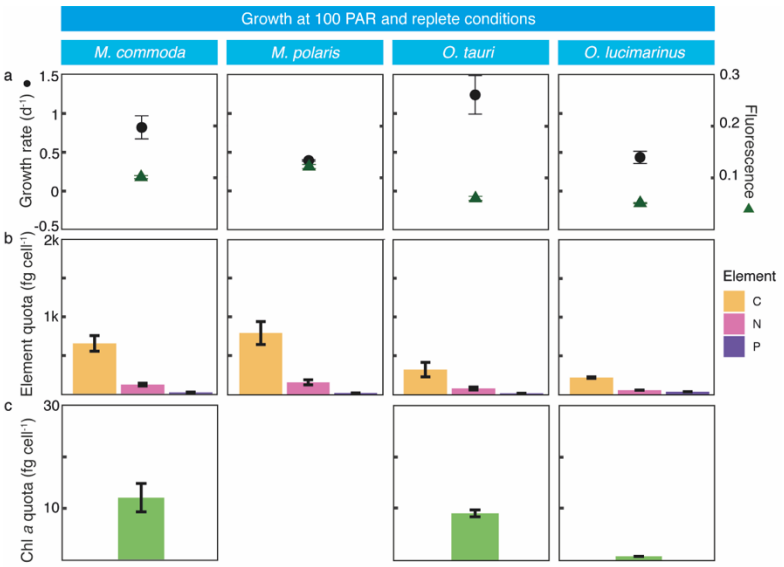

Supplementary figure 1. Cell quotas of carbon, nitrogen, and phosphorus for *Micromonas* and *Ostreococcus* strains in replete conditions at ~100 PAR. (a) Plots of growth rate and chlorophyll fluorescence per cell (Relative Fluorescence Units, RFU) with standard deviation bars. (b) Bar plots of average C, N, and P (fg cell^{-1}) and (c) chlorophyll *a* with error bars reflecting the standard deviation of three to four measurements.

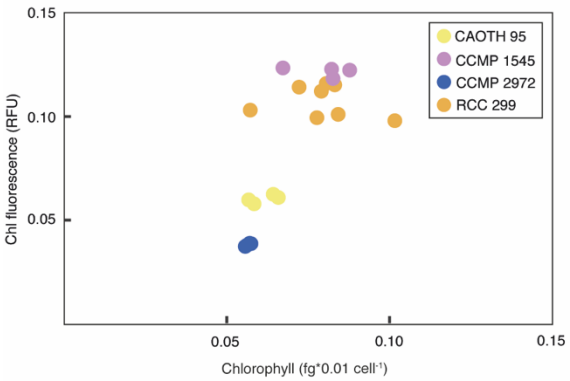

Supplementary figure 2. Comparison of Turner chlorophyll and flow cytometry-derived chlorophyll fluorescence. Scatterplot of Turner chlorophyll (fg *0.01 cell^{-1}) vs. flow cytometry-derived chlorophyll fluorescence (Relative Fluorescence Units, RFU) for *Micromonas* and *Ostreococcus* strains, indicated by point color, under sufficient conditions.

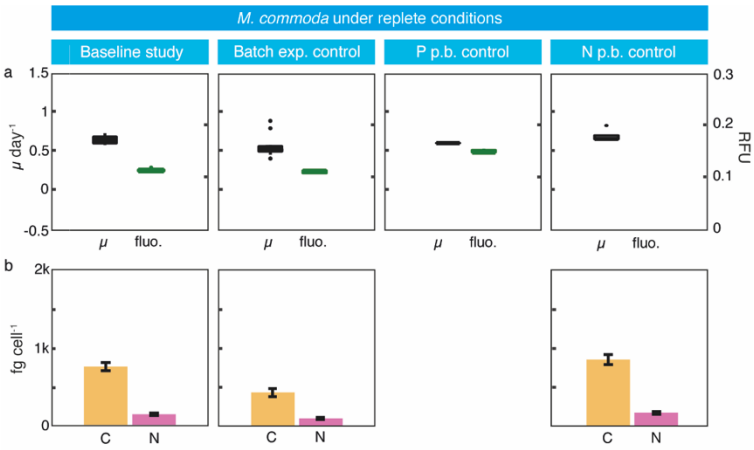

Supplementary figure 3. Cell quotas of carbon, nitrogen, and phosphorus for *Micromonas* RCC 299 in replete conditions and sufficient light. (a) Box and whisker plots of growth rate (day^{-1}) and chlorophyll fluorescence per cell (Relative Fluorescence Units, RFU). (b) Bar plots of average C, N, and P ($fg\ cell^{-1}$) with error bars reflecting the standard deviation of three to four measurements. The bars at the top indicate which experiment results are from (from left to right: baseline study semi-continuous batch culture, P-starvation semi-continuous batch culture, P-limitation photo-bioreactor, and N-limitation and CO_2 changes photo-bioreactor.

SUPPLEMENTARY TABLE LEGENDS

Supplementary Table 1: Summary of culturing conditions for all experiments.

Supplementary Table 2: Summary of growth rates, chlorophyll fluorescence, and cell quotas of CNP for all experiments.

Supplementary Table 3: Summary of statistics for all experiments.

Conclusions and Perspectives

Phytoplankton distributions across seasonal and geographic scales have important implications for primary production (W. K. W. Li, 1994), nutrient cycling (Franz et al., 2012), and carbon sequestration (Pinckney et al., 2015). These distributions are driven by different environmental preferences, which can be interrogated at the level of single strains to larger functional groupings. A detailed understanding of phytoplankton distributions and the drivers behind them not only allows us a better understanding of the current state of marine environments, especially subtropical gyres that account for large amounts of the PP that supports most life in the ocean (Behrenfeld et al., 2006; Chavez et al., 2011), but also serves as a baseline to which to compare future changes and to tailor models to better predict these changes.

In the first two chapters of this dissertation, phytoplankton communities are examined across years using 16S and 18S rRNA gene sequencing. Chapter one concerns the northwest Sargasso Sea, which experiences strong seasonal variations in abiotic factors such as temperature and salinity (Steinberg et al., 2001). Prasinophytes (mostly Class II Mamiellophyceae) contribute greatly to the phytoplankton community here during periods with high Chl *a* and elevated nutrients, comprising approximately half the eukaryotic phytoplankton amplicons during the winter/spring deep mixing. Timing of sampling in 2017 allowed for a high resolution look at the deep mixing period of that year, when prasinophytes were detected at high relative abundance down to 300 m. The mixed layer then shoaled quickly, which could render

these phytoplankton trapped at depth, thus sequestering that carbon away from the surface ocean. A prasinophyte community similar to the deep mixing community but statistically significantly distinct at the ASV level was observed in the DCM across years. This could imply differences in environmental niches of prasinophytes at the ASV level and a potential reservoir of genetic diversity that could allow for adaptation to different environmental conditions. The surface prasinophyte community shifted from Mamiellophyceae at the deep mixing period to other prasinophyte groups such as Classes I and III and putative class IX; some members of Class I have been demonstrated to supplement photosynthesis with phagotrophy, potentially explaining their persistence in the low-nutrient surface water. Overall changes in the prasinophyte community were significantly correlated to temperature and salinity, which could serve as a proxy for nutrient concentrations, which were often below detection limit, as the nutrient-deplete summer surface waters were warmer and fresher. The Sargasso Sea is an important area of study as the summer stratification could serve as a proxy for widespread ocean changes associated with anthropogenically-linked climate change. This research will hopefully be useful for the development of predictive models for annual cycles, primary production, and future transitions in subtropical phytoplankton communities.

The second chapter similarly strives to serve as a phytoplankton community baseline, moving from the subtropics to the tropics and expanding in taxonomic scope to encompass all eukaryotic phytoplankton. Tropical island habitats are vulnerable to anthropogenic influence, and this chapter covers a range of environments on and

around the island of Curaçao, some more impacted than others. The abiotic parameters of these environments varied greatly, with strong nutrient gradients in temperature, salinity, and nutrient concentrations, with inland salt ponds and salterns having higher values compared to more offshore environments. Green algae were most relatively abundant out of eukaryotic algae in salt ponds and solar salterns, with differences in the green algae community depending on the connectivity of the salterns to the sea. The more inland salt ponds had a higher share of chlorophytes, while sea-influenced salterns had a higher proportion of Mamiellophyceae, which were the dominant green algae group in mangroves, above reefs, and farther offshore, where green algae overall were less relatively abundant and stramenopiles were the major eukaryotic group. Within stramenopiles, diatoms were the most abundant group in mangroves and above reefs and were also one of the major stramenopile groups off-reef and farther offshore. Dictyochophytes, another stramenopile group, became increasingly important in more offshore environments, where they were mostly made up of uncultured environmental clades. This chapter addresses the dearth of research on green algae and dictyochophytes in tropical environments, as well as provides novel insights into other taxonomic groups, such as the importance of planktonic diatoms to Curaçao's mangrove forests. Like chapter 1, this chapter strives to be a detailed baseline of phytoplankton distributions around Curaçao and the Caribbean at large.

The importance of time-series to the understanding of phytoplankton dynamics was underscored in the first two chapters. At BATS, sampling both at high

frequency at the timescale of days during the DM and at monthly intervals across years was useful in both catching rapidly changing conditions and determining which groups persisted throughout. At Curaçao, yearly sampling demonstrated that even in the comparatively stable environments, there were between-year changes in certain groups. These approaches have demonstrated repeated sampling at the same location can detect changes that could be missed in point sampling. However, there is simply not the resources not infrastructure to have ongoing time-series studies at all oceanographically interesting areas. To achieve a more detailed understanding of biogeography of *Micromonas*, *Ostreococcus*, and other important prasinophyte groups, and phytoplankton in general, data drawn from cruises and other temporally limited sampling efforts is also important. For instance, I participated in a research cruise during January-March 2023 (6 weeks) that followed filaments of cold, nutrient-rich water from the upwelling region at the Namibian coast across the continental shelf as eddies propelled the filaments offshore until the signal dissipated. This region experiences perennial upwelling, unlike the seasonal mixing of the BATS DM or the relatively stable conditions around Curaçao (Heymans & Baird, 2000). This constant influx of nutrients at the coast supports a fishing economy that, despite still recovering from foreign exploitation, is a major source of income for the country (Belhabib et al., 2016). It will be interesting to track the phytoplankton communities throughout this process, which could lead to an influx of carbon in the form of phytoplankton and zooplankton into areas outside the upwelling zone. To my knowledge, information on prasinophyte distributions – as well as information on the

broader microbial community in general - in this area is limited. It will be important to discover which groups can be found there, and how they change over the lifespan of the filament.

The first two chapters addressed the first objective put forth in the introduction of determining the seasonal and geographical patterns in phytoplankton distributions at various taxonomic levels. These chapters also identified environmental factors linked to these patterns, thereby also addressing the second objective. Comparing the prasinophyte communities in these environments, some insights into prasinophyte sub-species distribution patterns might emerge, particularly Mamiellophyceae which appear to be among the most relatively abundant. For instance, major ASVs in terms of amplicon relative abundances were shared across these environments (i.e., *Ostreococcus* OII ASV6 at BATS was a 100% nt match to top Curaçao ASV133, and likewise for *M. commoda* ASV61 and ASV126). This could imply the relatively warm water systems in the subtropics and tropics share dominant sub-species of these groups. However, there are limitations to the amplicon-based approach used in these chapters. The 16S V1-V2 amplicons are relatively short, and, while useful for detecting a wide range of phytoplankton (i.e., both eukaryotic and prokaryotic), they are not long enough to definitively delineate some phylogenies. Through comparisons between 16S and 18S rRNA amplicons, both chapters sought to link 16S sequences to groups characterized in 18S phylogenies such as the *Micromonas* candidate species and *O. bengalensis*; however, to make definitive linkages, longer sequences are needed. The retrieval of full-length 16S and

18S sequences from BATS DM and Curaçao reefs even for just a subset of samples would be instrumental in building more refined phylogenies. Additionally, as recently identified groups such as the *Micromonas* candidate species remain uncultured, isolating and culturing these groups could allow for an understanding of their morphology and physiology. There is a concern that sequencing-only approaches to ecology ignore important information only obtained by studying the whole organism, not just its genetic material.

The third chapter concerns Mamiellophyceae species that already exist in culture and particularly species that were present in the studies conducted herein, or in other ecosystems I sampled during my PhD, but not included herein (e.g., the eastern North Pacific where *Ostreococcus* Clade OI (*O. lucimarinus*) thrives. The effects of light, nutrient concentration, and pCO_2 on the cell quotas of several *Micromonas* and *Ostreococcus* species is examined, thereby addressing the third and final objective of this thesis. This chapter provides a baseline of cell quotas under replete, sufficient light conditions. The differences in some cell quotas even under nearly identical conditions in different experiments could indicate natural variation in physiology even in sufficient conditions or could be due to limitations of the methods. Recommendations for best practices, such as using spent media as a blank to account for leftover nutrients in the media, are put forward. This chapter additionally highlights differing responses to limitation of nitrogen vs. phosphate, which could be useful information for modelling studies – for example providing constraints in the DARWIN multi-phytoplankton model (Lévy et al., 2015). Culturing studies allow for

predictions of how species could react to changing ocean conditions. There is a balance to be made between controlling for factors to ensure the signal is from the parameter(s) under study and maintaining as naturalistic a setup as possible to best simulate real-world conditions. The use of constant-flow photo-bioreactors as opposed to semi-continuous batch culturing in flasks allows for conditions to be changed more slowly, as they would be in response to gradual environmental changes such as warming and acidification of ocean water, and maintained at limiting levels though continuous supply of low concentrations of nutrients (Huisman et al., 2002). Experiments such as these provide important information that supplements field research and could generate quantitative information to feed into models.

This thesis integrated both environmental and lab-based studies to contribute to knowledge of eukaryotic algae, particularly prasinophytes, in subtropical and tropical environments. The distributions of these groups could impact the movement of nutrients and carbon in marine environments. The high-resolution phylogeny of Mamiellophyceae in particular underscored the ubiquity of some groups and the potential specialization of others. There is still much to learn about these groups through future sequencing and culturing-based studies. As mentioned previously, supplementing amplicon abundance studies with full-length 16S and 18S sequencing to resolve fine-scale phylogeny would improve studies of phytoplankton distribution. Additionally, amplicon relative abundances paired with flow cytometry counts would address the issue of gene copy number differences skewing abundance estimates. Tailoring the depths of sample collection, especially in open ocean areas such as

BATS, to properties such as chlorophyll fluorescence signal and oxygen content, as measured by CTD, could better characterize the oceanographically interesting depths of the water column. While this thesis has focused on water column sampling, a holistic approach to understanding the microbial underpinnings of ocean processes encompasses studies of the microbiomes of organisms and benthic substrates in additional to those of the water. Although not within the scope of this thesis, during my graduate studies I contributed to collection and processing of benthic invertebrate and sediment samples over the course of seven research cruises in the eastern North Pacific gyre. These studies will provide insights into the phytoplankton from the surface ocean to the seafloor, with potential implications for better understanding nutrient cycling and carbon sequestration from the light to dark ocean regions. As demonstrated in the Curaçao chapter, employing the same methods to investigate distinct environments allows for robust comparisons and insight into the connections among them. As mentioned in the introduction, there is still much to learn about phytoplankton physiology and distribution. This thesis sought to expand the scope of our knowledge of algae in subtropical and tropical environments and will hopefully serve as a basis for exciting future research from myself and others in these areas.

References

Acevedo-Trejos, E., Marañón, E., & Merico, A. (2018). Phytoplankton size diversity and ecosystem function relationships across oceanic regions. *Proceedings of the Royal Society B: Biological Sciences*, *285*(1879), 20180621. https://doi.org/10.1098/rspb.2018.0621

Adl, S. M., Simpson, A. G. B., Lane, C. E., Lukeš, J., Bass, D., Bowser, S. S., Brown, M. W., Burki, F., Dunthorn, M., Hampl, V., Heiss, A., Hoppenrath, M., Lara, E., le Gall, L., Lynn, D. H., McManus, H., Mitchell, E. A. D., Mozley-Stanridge, S. E., Parfrey, L. W., … Spiegel, F. W. (2012). The Revised Classification of Eukaryotes. *Journal of Eukaryotic Microbiology*, *59*(5), 429–514. https://doi.org/10.1111/j.1550-7408.2012.00644.x

Agawin, N. S. R., Duarte, C. M., & Agustí, S. (2000). Nutrient and temperature control of the contribution of picoplankton to phytoplankton biomass and production. *Limnology and Oceanography*, *45*(3), 591–600. https://doi.org/10.4319/lo.2000.45.3.0591

Alvarenga, D. O., Rigonato, J., Branco, L. H. Z., & Fiore, M. F. (2015). Cyanobacteria in mangrove ecosystems. *Biodiversity and Conservation*, *24*(4), 799–817. https://doi.org/10.1007/s10531-015-0871-2

Amacher, J., Neuer, S., & Lomas, M. (2013). DNA-based molecular fingerprinting of eukaryotic protists and cyanobacteria contributing to sinking particle flux at the Bermuda Atlantic time-series study. *Deep Sea Research Part II: Topical Studies in Oceanography*, *93*, 71–83. https://doi.org/10.1016/j.dsr2.2013.01.001

Archibald, J. M. (2012). Chapter Three—The Evolution of Algae by Secondary and Tertiary Endosymbiosis. In G. Piganeau (Ed.), *Advances in Botanical Research* (Vol. 64, pp. 87–118). Academic Press. https://doi.org/10.1016/B978-0-12-391499-6.00003-7

Arora, M., Anil, A. C., Leliaert, F., Delany, J., & Mesbahi, E. (2013). Tetraselmis indica (Chlorodendrophyceae, Chlorophyta), a new species isolated from salt pans in Goa, India. *European Journal of Phycology*, *48*(1), 61–78. https://doi.org/10.1080/09670262.2013.768357

Arsenieff, L., Le Gall, F., Rigaut-Jalabert, F., Mahé, F., Sarno, D., Gouhier, L., Baudoux, A.-C., & Simon, N. (2020). Diversity and dynamics of relevant

nanoplanktonic diatoms in the Western English Channel. *The ISME Journal*, *14*(8), Article 8. https://doi.org/10.1038/s41396-020-0659-6

Aziz, A. (2011). New record of planktonic diatoms from the Sundarban Mangrove Forests, Bangladesh. *Bangladesh Journal of Botany*, *40*(2), Article 2. https://doi.org/10.3329/bjb.v40i2.9772

Bachy, C., Hehenberger, E., Ling, Y.-C., Needham, D. M., Strauss, J., Wilken, S., & Worden, A. Z. (2022). Marine Protists: A Hitchhiker's Guide to their Role in the Marine Microbiome. In L. J. Stal & M. S. Cretoiu (Eds.), *The Marine Microbiome* (pp. 159–241). Springer International Publishing. https://doi.org/10.1007/978-3-030-90383-1_4

Bachy, C., Sudek, L., Choi, C. J., Eckmann, C. A., Nöthig, E.-M., Metfies, K., & Worden, A. Z. (2022). Phytoplankton surveys in the Arctic Fram Strait demonstrate the tiny eukaryotic alga *Micromonas* and other picoprasinophytes contribute to deep sea export. *Microorganisms*, *10*(5), Article 5. https://doi.org/10.3390/microorganisms10050961

Bachy, C., Wittmers, F., Muschiol, J., Hamilton, M., Henrissat, B., & Worden, A. Z. (2022). The land-sea connection: Insights into the plant lineage from a green algal perspective. *Annual Review of Plant Biology*, *73*, 585–616. https://doi.org/10.1146/annurev-arplant-071921-100530

Bachy, C., Yung, C. C. M., Needham, D. M., Gazitúa, M. C., Roux, S., Limardo, A. J., Choi, C. J., Jorgens, D. M., Sullivan, M. B., & Worden, A. Z. (2021). Viruses infecting a warm water picoeukaryote shed light on spatial co-occurrence dynamics of marine viruses and their hosts. *The ISME Journal*, *15*(11), Article 11. https://doi.org/10.1038/s41396-021-00989-9

Baetge, N., Bolaños, L. M., Penna, A. D., Gaube, P., Liu, S., Opalk, K., Graff, J. R., Giovannoni, S. J., Behrenfeld, M. J., & Carlson, C. A. (2022). Bacterioplankton response to physical stratification following deep convection. *Elementa: Science of the Anthropocene*, *10*(1), 00078. https://doi.org/10.1525/elementa.2021.00078

Bakker, J., Wangensteen, O. S., Baillie, C., Buddo, D., Chapman, D. D., Gallagher, A. J., Guttridge, T. L., Hertler, H., & Mariani, S. (2019). Biodiversity assessment of tropical shelf eukaryotic communities via pelagic eDNA metabarcoding. *Ecology and Evolution*, *9*(24), 14341–14355. https://doi.org/10.1002/ece3.5871

Bates, N. R. (2007). Interannual variability of the oceanic CO2 sink in the subtropical gyre of the North Atlantic Ocean over the last 2 decades. *Journal of*

Geophysical Research: Oceans, *112*(C9). https://doi.org/10.1029/2006JC003759

Becker, C. C., Weber, L., Suca, J. J., Llopiz, J. K., Mooney, T. A., & Apprill, A. (2020). Microbial and nutrient dynamics in mangrove, reef, and seagrass waters over tidal and diurnal time scales. *Aquatic Microbial Ecology*, *85*, 101–119. https://doi.org/10.3354/ame01944

Becker, J. W., Hogle, S. L., Rosendo, K., & Chisholm, S. W. (2019). Co-culture and biogeography of Prochlorococcus and SAR11. *The ISME Journal*, *13*(6), Article 6. https://doi.org/10.1038/s41396-019-0365-4

Behrenfeld, M. J., O'Malley, R. T., Siegel, D. A., McClain, C. R., Sarmiento, J. L., Feldman, G. C., Milligan, A. J., Falkowski, P. G., Letelier, R. M., & Boss, E. S. (2006). Climate-driven trends in contemporary ocean productivity. *Nature*, *444*(7120), 752–755. https://doi.org/10.1038/nature05317

Belhabib, D., Mendy, A., Subah, Y., Broh, N. T., Jueseah, A. S., Nipey, N., Boeh, W. W., Willemse, N., Zeller, D., & Pauly, D. (2016). Fisheries catch under-reporting in The Gambia, Liberia and Namibia and the three large marine ecosystems which they represent. *Environmental Development*, *17*, 157–174. https://doi.org/10.1016/j.envdev.2015.08.004

Bell, E. M., & Laybourn-Parry, J. (2003). Mixotrophy in the Antarctic phytoflagellate *Pyramimonas gelidicola* (chlorophyta: Prasinophyceae). *Journal of Phycology*, *39*(4), 644–649. https://doi.org/10.1046/j.1529-8817.2003.02152.x

Ben-Amotz, A., Polle, J. E. W., & Rao, D. V. S. (2019). *The Alga Dunaliella*. CRC Press.

Benlloch, S., López-López, A., Casamayor, E. O., Øvreås, L., Goddard, V., Daae, F. L., Smerdon, G., Massana, R., Joint, I., Thingstad, F., Pedrós-Alió, C., & Rodríguez-Valera, F. (2002). Prokaryotic genetic diversity throughout the salinity gradient of a coastal solar saltern. *Environmental Microbiology*, *4*(6), 349–360. https://doi.org/10.1046/j.1462-2920.2002.00306.x

Bertilsson, S., Berglund, O., Karl, D. M., & Chisholm, S. W. (2003). Elemental composition of marine Prochlorococcus and Synechococcus: Implications for the ecological stoichiometry of the sea. *Limnology and Oceanography*, *48*(5), 1721–1731. https://doi.org/10.4319/lo.2003.48.5.1721

Berube, P. M., Coe, A., Roggensack, S. E., & Chisholm, S. W. (2016). Temporal dynamics of *Prochlorococcus* cells with the potential for nitrate assimilation in the subtropical Atlantic and Pacific oceans. *Limnology and Oceanography*, *61*(2), 482–495. https://doi.org/10.1002/lno.10226

Bhadury, P., & Singh, T. (2020). Analysis of Marine Planktonic Cyanobacterial Assemblages From Mooriganga Estuary, Indian Sundarbans Using Molecular Approaches. *Frontiers in Marine Science*, *7*. https://doi.org/10.3389/fmars.2020.00222

Bhattacharjee, D., Samanta, B., Danda, A. A., & Bhadury, P. (2013). Temporal Succession of Phytoplankton Assemblages in a Tidal Creek System of the Sundarbans Mangroves: An Integrated Approach. *International Journal of Biodiversity*, *2013*, 1–15. https://doi.org/10.1155/2013/824543

Blachnio-Zabielska, A. U., Zabielski, P., & Jensen, M. D. (2013). Intramyocellular diacylglycerol concentrations and [U-13C]palmitate isotopic enrichment measured by LC/MS/MS. *Journal of Lipid Research*, *54*(6), 1705–1711. https://doi.org/10.1194/jlr.D035006

Blanc-Mathieu, R., Sanchez-Ferandin, S., Eyre-Walker, A., & Piganeau, G. (2013). Organellar Inheritance in the Green Lineage: Insights from Ostreococcus tauri. *Genome Biology and Evolution*, *5*(8), 1503–1511. https://doi.org/10.1093/gbe/evt106

Blanco-Bercial, L., Parsons, R., Bolaños, L. M., Johnson, R., Giovannoni, S. J., & Curry, R. (2022). The protist community traces seasonality and mesoscale hydrographic features in the oligotrophic Sargasso Sea. *Frontiers in Marine Science*, *9*. https://www.frontiersin.org/articles/10.3389/fmars.2022.897140

Bock, N. A., Charvet, S., Burns, J., Gyaltshen, Y., Rozenberg, A., Duhamel, S., & Kim, E. (2021). Experimental identification and in silico prediction of bacterivory in green algae. *The ISME Journal*, 1–14. https://doi.org/10.1038/s41396-021-00899-w

Bolaños, L. M., Karp-Boss, L., Choi, C. J., Worden, A. Z., Graff, J. R., Haëntjens, N., Chase, A. P., Della Penna, A., Gaube, P., Morison, F., Menden-Deuer, S., Westberry, T. K., O'Malley, R. T., Boss, E., Behrenfeld, M. J., & Giovannoni, S. J. (2020). Small phytoplankton dominate western North Atlantic biomass. *The ISME Journal*, *14*, 1663–1674. https://doi.org/10.1038/s41396-020-0636-0

Bolyen, E., Rideout, J. R., Dillon, M. R., Bokulich, N. A., Abnet, C. C., Al-Ghalith, G. A., Alexander, H., Alm, E. J., Arumugam, M., Asnicar, F., Bai, Y., Bisanz, J. E., Bittinger, K., Brejnrod, A., Brislawn, C. J., Brown, C. T., Callahan, B. J., Caraballo-Rodríguez, A. M., Chase, J., … Caporaso, J. G. (2019). Reproducible, interactive, scalable and extensible microbiome data science using QIIME 2. *Nature Biotechnology*, *37*(8), Article 8. https://doi.org/10.1038/s41587-019-0209-9

Bonachela, J. A., Klausmeier, C. A., Edwards, K. F., Litchman, E., & Levin, S. A. (2016). The role of phytoplankton diversity in the emergent oceanic stoichiometry. *Journal of Plankton Research*, *38*(4), 1021–1035. https://doi.org/10.1093/plankt/fbv087

Bopp, L., Resplandy, L., Orr, J. C., Doney, S. C., Dunne, J. P., Gehlen, M., Halloran, P., Heinze, C., Ilyina, T., Séférian, R., Tjiputra, J., & Vichi, M. (2013). Multiple stressors of ocean ecosystems in the 21st century: Projections with CMIP5 models. *Biogeosciences*, *10*, 6225–6245. https://doi.org/10.5194/bg-10-6225-2013

Borovsky, D., Nauwelaers, S., & Shatters, R. (2020). Biochemical and Molecular Characterization of Pichia pastoris Cells Expressing Multiple TMOF Genes (tmfA) for Mosquito Larval Control. *Frontiers in Physiology*, *11*. https://www.frontiersin.org/articles/10.3389/fphys.2020.00527

Bove, C. B., Mudge, L., & Bruno, J. F. (2022). A century of warming on Caribbean reefs. *PLOS Climate*, *1*(3), e0000002. https://doi.org/10.1371/journal.pclm.0000002

Boyd, C. M., & Johnson, G. W. (1995). Precision of size determination of resistive electronic particle counters. *Journal of Plankton Research*, *17*(1), 41–58. https://doi.org/10.1093/plankt/17.1.41

Boyd, P. W., Strzepek, R., Fu, F., & Hutchins, D. A. (2010). Environmental control of open-ocean phytoplankton groups: Now and in the future. *Limnology and Oceanography*, *55*(3), 1353–1376. https://doi.org/10.4319/lo.2010.55.3.1353

Brandsma, J., Hopmans, E. C., Philippart, C. J. M., Veldhuis, M. J. W., Schouten, S., & Sinninghe Damsté, J. S. (2012). Low temporal variation in the intact polar lipid composition of North Sea coastal marine water reveals limited chemotaxonomic value. *Biogeosciences*, *9*(3), 1073–1084. https://doi.org/10.5194/bg-9-1073-2012

Brock, T. D. (1978). Use of fluorescence microscopy for quantifying phytoplankton, especially filamentous blue-green algae 1. *Limnology and Oceanography*, *23*(1), 158–160. https://doi.org/10.4319/lo.1978.23.1.0158

Brocke, H. J., Piltz, B., Herz, N., Abed, R. M. M., Palinska, K. A., John, U., Haan, J. den, de Beer, D., & Nugues, M. M. (2018). Nitrogen fixation and diversity of benthic cyanobacterial mats on coral reefs in Curaçao. *Coral Reefs*, *37*(3), 861–874. https://doi.org/10.1007/s00338-018-1713-y

Buaya, A. T., Ploch, S., Hanic, L., Nam, B., Nigrelli, L., Kraberg, A., & Thines, M. (2017). Phylogeny of Miracula helgolandica gen. Et sp. Nov. And Olpidiopsis

drebesii sp. Nov., two basal oomycete parasitoids of marine diatoms, with notes on the taxonomy of Ectrogella-like species. *Mycological Progress*, *16*(11), 1041–1050. https://doi.org/10.1007/s11557-017-1345-6

Burki, F., Roger, A. J., Brown, M. W., & Simpson, A. G. B. (2020). The New Tree of Eukaryotes. *Trends in Ecology & Evolution*, *35*(1), 43–55. https://doi.org/10.1016/j.tree.2019.08.008

Burki, F., Sandin, M. M., & Jamy, M. (2021). Diversity and ecology of protists revealed by metabarcoding. *Current Biology*, *31*(19), R1267–R1280. https://doi.org/10.1016/j.cub.2021.07.066

Callahan, B. J., McMurdie, P. J., Rosen, M. J., Han, A. W., Johnson, A. J. A., & Holmes, S. P. (2016). DADA2: High-resolution sample inference from Illumina amplicon data. *Nature Methods*, *13*(7), Article 7. https://doi.org/10.1038/nmeth.3869

Campbell, L., Liu, H., Nolla, H., & Vaulot, D. (1997). Annual variability of phytoplankton and bacteria in the subtropical North Pacific Ocean at Station ALOHA during the 1991-1994 ENSO event. *Deep Sea Research Part I: Oceanographic Research Papers*, *44*, 167–192. https://doi.org/10.1016/S0967-0637(96)00102-1

Carlson, C. A., Morris, R., Parsons, R., Treusch, A. H., Giovannoni, S. J., & Vergin, K. (2009). Seasonal dynamics of SAR11 populations in the euphotic and mesopelagic zones of the northwestern Sargasso Sea. *The ISME Journal*, *3*(3), 283–295. https://doi.org/10.1038/ismej.2008.117

Casey, J. R., Aucan, J. P., Goldberg, S. R., & Lomas, M. W. (2013). Changes in partitioning of carbon amongst photosynthetic pico- and nano-plankton groups in the Sargasso Sea in response to changes in the North Atlantic Oscillation. *Deep Sea Research Part II: Topical Studies in Oceanography*, *93*, 58–70. https://doi.org/10.1016/j.dsr2.2013.02.002

Chavez, F. P., Messié, M., & Pennington, J. T. (2011). Marine primary production in relation to climate variability and change. *Annual Review of Marine Science*, *3*(1), 227–260. https://doi.org/10.1146/annurev.marine.010908.163917

Chénard, C., Wijaya, W., Vaulot, D., Lopes dos Santos, A., Martin, P., Kaur, A., & Lauro, F. M. (2019). Temporal and spatial dynamics of Bacteria, Archaea and protists in equatorial coastal waters. *Scientific Reports*, *9*(1), Article 1. https://doi.org/10.1038/s41598-019-52648-x

Choi, C. J., Bachy, C., Jaeger, G. S., Poirier, C., Sudek, L., Sarma, V. V. S. S., Mahadevan, A., Giovannoni, S. J., & Worden, A. Z. (2017). Newly

discovered deep-branching marine plastid lineages are numerically rare but globally distributed. *Current Biology*, *27*(1), R15–R16. https://doi.org/10.1016/j.cub.2016.11.032

Choi, C. J., Jimenez, V., Needham, D. M., Poirier, C., Bachy, C., Alexander, H., Wilken, S., Chavez, F. P., Sudek, S., Giovannoni, S. J., & Worden, A. Z. (2020). Seasonal and geographical transitions in eukaryotic phytoplankton community structure in the Atlantic and Pacific Oceans. *Frontiers in Microbiology*, *11*. https://doi.org/10.3389/fmicb.2020.542372

Chrétiennot-Dinet, M.-J., Courties, C., Vaquer, A., Neveux, J., Claustre, H., Lautier, J., & Machado, M. C. (1995). A new marine picoeucaryote: Ostreococcus tauri gen. et sp. nov. (Chlorophyta, Prasinophyceae). *Phycologia*, *34*(4), 285–292. https://doi.org/10.2216/i0031-8884-34-4-285.1

Clayton, S., Lin, Y.-C., Follows, M. J., & Worden, A. Z. (2017). Co-existence of distinct Ostreococcus ecotypes at an oceanic front. *Limnology and Oceanography*, *62*(1), 75–88. https://doi.org/10.1002/lno.10373

Coelho, S. M., Simon, N., Ahmed, S., Cock, J. M., & Partensky, F. (2013). Ecological and evolutionary genomics of marine photosynthetic organisms. *Molecular Ecology*, *22*(3), 867–907. https://doi.org/10.1111/mec.12000

Conway, J. R., Lex, A., & Gehlenborg, N. (2017). UpSetR: An R package for the visualization of intersecting sets and their properties. *Bioinformatics*, *33*(18), 2938–2940. https://doi.org/10.1093/bioinformatics/btx364

Countway, P. D., & Caron, D. A. (2006). Abundance and Distribution of Ostreococcus sp. In the San Pedro Channel, California, as Revealed by Quantitative PCR. *Applied and Environmental Microbiology*, *72*(4), 2496–2506. https://doi.org/10.1128/AEM.72.4.2496-2506.2006

Cruz, B. N., Brozak, S., & Neuer, S. (2021). Microscopy and DNA-based characterization of sinking particles at the Bermuda Atlantic Time-series Study station point to zooplankton mediation of particle flux. *Limnology and Oceanography*, *n/a*(n/a). https://doi.org/10.1002/lno.11910

Csardi, G., & Nepusz, T. (2005). The Igraph Software Package for Complex Network Research. *InterJournal Complex Systems*, *1695*, 1–9.

Cunningham, A., & Buonnacorsi, G. A. (1992). Narrow-angle forward light scattering from individual algal cells: Implications for size and shape discrimination in flow cytometry. *Journal of Plankton Research*, *14*(2), 223–234. https://doi.org/10.1093/plankt/14.2.223

Cuvelier, M. L., Allen, A. E., Monier, A., McCrow, J. P., Messie, M., Tringe, S. G., Woyke, T., Welsh, R. M., Ishoey, T., Lee, J.-H., Binder, B. J., DuPont, C. L., Latasa, M., Guigand, C., Buck, K. R., Hilton, J., Thiagarajan, M., Caler, E., Read, B., … Worden, A. Z. (2010). Targeted metagenomics and ecology of globally important uncultured eukaryotic phytoplankton. *Proceedings of the National Academy of Sciences*, *107*(33), 14679–14684. https://doi.org/10.1073/pnas.1001665107

Cuvelier, M. L., Guo, J., Ortiz, A. C., Baren, M. J. van, Tariq, M. A., Partensky, F., & Worden, A. Z. (2017). Responses of the picoprasinophyte Micromonas commoda to light and ultraviolet stress. *PLOS ONE*, *12*(3), e0172135. https://doi.org/10.1371/journal.pone.0172135

Daims, H., Brühl, A., Amann, R., Schleifer, K.-H., & Wagner, M. (1999). The domain-specific probe EUB338 is insufficient for the detection of all bacteria: Development and evaluation of a more comprehensive probe set. *Systematic and Applied Microbiology*, *22*(3), 434–444. https://doi.org/10.1016/S0723-2020(99)80053-8

Dall'Olmo, G., Dingle, J., Polimene, L., Brewin, R. J. W., & Claustre, H. (2016). Substantial energy input to the mesopelagic ecosystem from the seasonal mixed-layer pump. *Nature Geoscience*, *9*(11), Article 11. https://doi.org/10.1038/ngeo2818

de Bakker, D. M., van Duyl, F. C., Bak, R. P. M., Nugues, M. M., Nieuwland, G., & Meesters, E. H. (2017). 40 Years of benthic community change on the Caribbean reefs of Curaçao and Bonaire: The rise of slimy cyanobacterial mats. *Coral Reefs*, *36*(2), 355–367. https://doi.org/10.1007/s00338-016-1534-9

de la Peña, L. B. R., Tejada, A. J., Quijano, J. B., Alonzo, K., Gernato, E. G., Caril, A., Cruz, M., & Onda, D. F. (2021). Diversity of Marine Eukaryotic Picophytoplankton Communities with Emphasis on Mamiellophyceae in Northwestern Philippines. *Philippine Journal of Science*, *150*, 27–42.

Demir-Hilton, E., Sudek, S., Cuvelier, M. L., Gentemann, C. L., Zehr, J. P., & Worden, A. Z. (2011). Global distribution patterns of distinct clades of the photosynthetic picoeukaryote *Ostreococcus*. *The ISME Journal*, *5*(7), 1095–1107. https://doi.org/10.1038/ismej.2010.209

Demory, D., Baudoux, A.-C., Monier, A., Simon, N., Six, C., Ge, P., Rigaut-Jalabert, F., Marie, D., Sciandra, A., Bernard, O., & Rabouille, S. (2019). Picoeukaryotes of the *Micromonas* genus: Sentinels of a warming ocean. *The ISME Journal*, *13*(1), 132–146. https://doi.org/10.1038/s41396-018-0248-0

Derelle, E., Ferraz, C., Rombauts, S., Rouzé, P., Worden, A. Z., Robbens, S., Partensky, F., Degroeve, S., Echeynié, S., Cooke, R., Saeys, Y., Wuyts, J., Jabbari, K., Bowler, C., Panaud, O., Piégu, B., Ball, S. G., Ral, J.-P., Bouget, F.-Y., … Moreau, H. (2006). Genome analysis of the smallest free-living eukaryote Ostreococcus tauri unveils many unique features. *Proceedings of the National Academy of Sciences of the United States of America*, *103*(31), 11647–11652. https://doi.org/10.1073/pnas.0604795103

Desrosiers, C., Witkowski, A., Riaux-Gobin, C., Zgłobicka, I., Kurzydłowski, K. J., Eulin, A., Leflaive, J., & Ten-Hage, L. (2014). Madinithidium gen. Nov. (Bacillariophyceae), a new monoraphid diatom genus from the tropical marine coastal zone. *Phycologia*, *53*(6), 583–592. https://doi.org/10.2216/14-21R2

Devassy, R. P., El-Sherbiny, M. M., Al-Sofyani, A. A., Crosby, M. P., & Al-Aidaroos, A. M. (2019). Seasonality and latitudinal variability in the diatom-cyanobacteria symbiotic relationships in the coastal waters of the Red Sea, Saudi Arabia. *Symbiosis*, *78*(3), 215–227. https://doi.org/10.1007/s13199-019-00610-w

Diekmann, O. E., Bak, R. P. M., Tonk, L., Stam, W. T., & Olsen, J. L. (2002). No habitat correlation of zooxanthellae in the coral genus Madracis on a Curaçao reef. *Marine Ecology Progress Series*, *227*, 221–232.

Dixon, P. (2003). VEGAN, a package of R functions for community ecology. *Journal of Vegetation Science*, *14*(6), 927–930. https://doi.org/10.1111/j.1654-1103.2003.tb02228.x

Dupont, C. L., McCrow, J. P., Valas, R., Moustafa, A., Walworth, N., Goodenough, U., Roth, R., Hogle, S. L., Bai, J., Johnson, Z. I., Mann, E., Palenik, B., Barbeau, K. A., Craig Venter, J., & Allen, A. E. (2015). Genomes and gene expression across light and productivity gradients in eastern subtropical Pacific microbial communities. *The ISME Journal*, *9*(5), Article 5. https://doi.org/10.1038/ismej.2014.198

DuRand, M. D., Green, R. E., Sosik, H. M., & Olson, R. J. (2002). Diel Variations in Optical Properties of Micromonas Pusilla (prasinophyceae). *Journal of Phycology*, *38*(6), 1132–1142. https://doi.org/10.1046/j.1529-8817.2002.02008.x

DuRand, M. D., Olson, R. J., & Chisholm, S. W. (2001). Phytoplankton population dynamics at the Bermuda Atlantic Time-series station in the Sargasso Sea. *Deep Sea Research Part II: Topical Studies in Oceanography*, *48*(8), 1983–2003. https://doi.org/10.1016/S0967-0645(00)00166-1

Ebenezer, V., Hu, Y., Carnicer, O., Irwin, A. J., Follows, M. J., & Finkel, Z. V. (2022). Elemental and macromolecular composition of the marine Chloropicophyceae, a major group of oceanic photosynthetic picoeukaryotes. *Limnology and Oceanography*, *67*(3), 540–551. https://doi.org/10.1002/lno.12013

Eckmann, C., Eberle, J., Wittmers, F., Wilken, S., Bergauer, K., Poirier, C., Blum, M., Makareviciute-Fichter, K., Jimenez, V., Bachy, C., Vermeij, M., & Worden, A. Z. (2023). Eukaryotic algal community composition of tropical environments from solar salterns to the open sea. *Submitted*, *10*. https://doi.org/10.3389/fmars.2023.1131351

Edwards, M., Beaugrand, G., Kléparski, L., Hélaouët, P., & Reid, P. C. (2022). Climate variability and multi-decadal diatom abundance in the Northeast Atlantic. *Communications Earth & Environment*, *3*(1), Article 1. https://doi.org/10.1038/s43247-022-00492-9

Eikrem, W. (1990). The ultrastructure of Bathycoccus gen. Nov. And B. prasinos sp. Nov., a non-motile picoplanktonic alga (Chlorophyta, Prasinophyceae) from the Mediterranean and Atlantic. *Phycologia*, *29*(3), 344–350. https://doi.org/10.2216/i0031-8884-29-3-344.1

Engelen, A. H., Aires, T., Vermeij, M. J. A., Herndl, G. J., Serrão, E. A., & Frade, P. R. (2018). Host Differentiation and Compartmentalization of Microbial Communities in the Azooxanthellate Cupcorals Tubastrea coccinea and Rhizopsammia goesi in the Caribbean. *Frontiers in Marine Science*, *5*. https://doi.org/10.3389/fmars.2018.00391

Eppley, R. W., Holmes, R. W., & Strickland, J. D. H. (1967). Sinking rates of marine phytoplankton measured with a fluorometer. *Journal of Experimental Marine Biology and Ecology*, *1*(2), 191–208. https://doi.org/10.1016/0022-0981(67)90014-7

Evenson, K. (2016, May 21). Natural Beauty. *Beehive*. https://www.masshist.org/beehiveblog/2016/05/natural-beauty/

Fábregas, J., Maseda, A., Domınguez, A., Ferreira, M., & Otero, A. (2002). Changes in the cell composition of the marine microalga, Nannochloropsis gaditana, during a light:dark cycle. *Biotechnology Letters*, *24*, 5.

Fawley, M. W. (1992). Photosynthetic Pigments of Pseudoscourfieldia Marina and Select Green Flagellates and Coccoid Ultraphytoplankton: Implications for the Systematics of the Micromonadophyceae (chlorophyta)1. *Journal of Phycology*, *28*(1), 26–31. https://doi.org/10.1111/j.0022-3646.1992.00026.x

Fawley, M. W., Qin, M., & Yun, Y. (1999). THE RELATIONSHIP BETWEEN PSEUDOSCOURFIELDIA MARINA AND PYCNOCOCCUS PROVASOLII (PRASINOPHYCEAE, CHLOROPHYTA): EVIDENCE FROM 18S rDNA SEQUENCE DATA. *Journal of Phycology*, *35*(4), 838–843. https://doi.org/10.1046/j.1529-8817.1999.3540838.x

Fawley, M. W., Yun, Y., & Qin, M. (2000). Phylogenetic analyses of 18s rdna sequences reveal a new coccoid lineage of the prasinophyceae (Chlorophyta). *Journal of Phycology*, *36*(2), 387–393. https://doi.org/10.1046/j.1529-8817.2000.99105.x

Field, C. B. (1998). Primary Production of the Biosphere: Integrating Terrestrial and Oceanic Components. *Science*, *281*(5374), 237–240. https://doi.org/10.1126/science.281.5374.237

Filker, S., Gimmler, A., Dunthorn, M., Mahé, F., & Stoeck, T. (2015). Deep sequencing uncovers protistan plankton diversity in the Portuguese Ria Formosa solar saltern ponds. *Extremophiles*, *19*(2), 283–295. https://doi.org/10.1007/s00792-014-0713-2

Finkel, Z. V., Beardall, J., Flynn, K. J., Quigg, A., Rees, T. A. V., & Raven, J. A. (2010). Phytoplankton in a changing world: Cell size and elemental stoichiometry. *Journal of Plankton Research*, *32*(1), 119–137. https://doi.org/10.1093/plankt/fbp098

Finley, A. O., Banerjee, S., Hjelle, øyvind, & Bivand, R. (2017). *Package 'MBA': Multilevel B-Spline Approximation*.

Fogg, G. E. (1986). Review Lecture—Picoplankton. *Proceedings of the Royal Society of London. Series B. Biological Sciences*, *228*(1250), 1–30. https://doi.org/10.1098/rspb.1986.0037

Fong, P., & Paul, V. J. (2011). Coral Reef Algae. In Z. Dubinsky & N. Stambler (Eds.), *Coral Reefs: An Ecosystem in Transition* (pp. 241–272). Springer Netherlands. https://doi.org/10.1007/978-94-007-0114-4_17

Fon-Sing, S., & Borowitzka, M. A. (2016). Isolation and screening of euryhaline Tetraselmis spp. Suitable for large-scale outdoor culture in hypersaline media for biofuels. *Journal of Applied Phycology*, *28*(1), 1–14. https://doi.org/10.1007/s10811-015-0560-2

Foulon, E., Not, F., Jalabert, F., Cariou, T., Massana, R., & Simon, N. (2008). Ecological niche partitioning in the picoplanktonic green alga Micromonas pusilla: Evidence from environmental surveys using phylogenetic probes.

Environmental Microbiology, *10*(9), 2433–2443. https://doi.org/10.1111/j.1462-2920.2008.01673.x

Fox, G. E., Pechman, K. R., & Woese, C. R. (1977). Comparative Cataloging of 16S Ribosomal Ribonucleic Acid: Molecular Approach to Procaryotic Systematics. *International Journal of Systematic and Evolutionary Microbiology, 27*(1), 44–57. https://doi.org/10.1099/00207713-27-1-44

Fox, J., Weisberg, S., & Price, B. (2022). *Package 'car'* (3.1-1). https://cran.r-project.org/web/packages/car/index.html

Franz, J., Krahmann, G., Lavik, G., Grasse, P., Dittmar, T., & Riebesell, U. (2012). Dynamics and stoichiometry of nutrients and phytoplankton in waters influenced by the oxygen minimum zone in the eastern tropical Pacific. *Deep Sea Research Part I: Oceanographic Research Papers*, *62*, 20–31. https://doi.org/10.1016/j.dsr.2011.12.004

Fučíková, K., Leliaert, F., Cooper, E. D., Škaloud, P., D'hondt, S., De Clerck, O., Gurgel, C. F. D., Lewis, L. A., Lewis, P. O., Lopez-Bautista, J. M., Delwiche, C. F., & Verbruggen, H. (2014). New phylogenetic hypotheses for the core Chlorophyta based on chloroplast sequence data. *FRONTIERS IN ECOLOGY AND EVOLUTION*, *2*. https://doi.org/10.3389/fevo.2014.00063

Fuhrman, J. A., Cram, J. A., & Needham, D. M. (2015). Marine microbial community dynamics and their ecological interpretation. *Nature Reviews Microbiology*, *13*(3), 133–146. https://doi.org/10.1038/nrmicro3417

Furlong, S. T., & Caulfield, J. P. (1986). CHARACTERIZATION OF LIPID SYNTHESIZED BY CULTURED SCHISTOSOMULA, SCHISTOSOMA-MANSONI. *FEDERATION PROCEEDINGS*, *45*(3).

Ganesan, S., Ramanathan, & Kandasamy, K. (2012). Diversity of Marine Cyanobacteria from Three Mangrove Environment in Tamil Nadu Coast, South East Coast of India. *Current Research Journal of Biological Sciences*, *4*, 235–238.

Gao, Y., Smith, G. J., & Alberte, R. S. (2000). Temperature dependence of nitrate reductase activity in marine phytoplankton: Biochemical analysis and ecological implications. *Journal of Phycology*, *36*(2), 304–313. https://doi.org/10.1046/j.1529-8817.2000.99195.x

Garcia, N. S., Sexton, J., Riggins, T., Brown, J., Lomas, M. W., & Martiny, A. C. (2018). High Variability in Cellular Stoichiometry of Carbon, Nitrogen, and Phosphorus Within Classes of Marine Eukaryotic Phytoplankton Under

Sufficient Nutrient Conditions. *Frontiers in Microbiology*, *9*. https://doi.org/10.3389/fmicb.2018.00543

Geider, R., & La Roche, J. (2002). Redfield revisited: Variability of C:N:P in marine microalgae and its biochemical basis. *European Journal of Phycology*, *37*(1), 1–17. https://doi.org/10.1017/S0967026201003456

Giovannoni, S. J., DeLong, E. F., Schmidt, T. M., & Pace, N. R. (1990). Tangential flow filtration and preliminary phylogenetic analysis of marine picoplankton. *Applied and Environmental Microbiology*, *56*(8), 2572–2575. https://doi.org/10.1128/aem.56.8.2572-2575.1990

Giovannoni, S. J., & Vergin, K. L. (2012). Seasonality in Ocean Microbial Communities. *Science*, *335*(6069), 671–676. https://doi.org/10.1126/science.1198078

Glibert, P. M., Kana, T. M., & Brown, K. (2013). From limitation to excess: The consequences of substrate excess and stoichiometry for phytoplankton physiology, trophodynamics and biogeochemistry, and the implications for modeling. *Journal of Marine Systems*, *125*, 14–28. https://doi.org/10.1016/j.jmarsys.2012.10.004

Godhe, A., & Härnström, K. (2010). Linking the planktonic and benthic habitat: Genetic structure of the marine diatom Skeletonema marinoi. *Molecular Ecology*, *19*(20), 4478–4490. https://doi.org/10.1111/j.1365-294X.2010.04841.x

Gonzalez-Esquer, C. R., Wright, K. T., Sudasinghe, N., Carr, C. K., Sanders, C. K., Turmo, A., Kerfeld, C. A., Twary, S., & Dale, T. (2019). Demonstration of the potential of Picochlorum soloecismus as a microalgal platform for the production of renewable fuels. *Algal Research*, *43*, 101658. https://doi.org/10.1016/j.algal.2019.101658

Griffin, N. J., & Aken, M. E. (1990). Interactions between the prasinophycean tidal pool flagellates Pyramimonas parkeae and Tetraselmis apiculata in batch culture. *South African Journal of Botany*, *56*(6), 593–598. https://doi.org/10.1016/S0254-6299(16)30996-6

Griffith, D. M., Veech, J. A., & Marsh, C. J. (2016). cooccur: Probabilistic Species Co-Occurrence Analysis in R. *Journal of Statistical Software*, *69*, 1–17. https://doi.org/10.18637/jss.v069.c02

Grolemund, G., & Wickham, H. (2011). Dates and times made easy with lubridate. *Journal of Statistical Software*, *40*, 1–25. https://doi.org/10.18637/jss.v040.i03

Guillou, L., Bachar, D., Audic, S., Bass, D., Berney, C., Bittner, L., Boutte, C., Burgaud, G., de Vargas, C., Decelle, J., del Campo, J., Dolan, J. R., Dunthorn, M., Edvardsen, B., Holzmann, M., Kooistra, W. H. C. F., Lara, E., Le Bescot, N., Logares, R., … Christen, R. (2013). The Protist Ribosomal Reference database (PR2): A catalog of unicellular eukaryote Small Sub-Unit rRNA sequences with curated taxonomy. *Nucleic Acids Research*, *41*(D1), D597–D604. https://doi.org/10.1093/nar/gks1160

Guillou, L., Eikrem, W., Chrétiennot-Dinet, M.-J., Le Gall, F., Massana, R., Romari, K., Pedrós-Alió, C., & Vaulot, D. (2004). Diversity of picoplanktonic prasinophytes assessed by direct nuclear SSU rDNA sequencing of environmental samples and novel isolates retrieved from oceanic and coastal marine ecosystems. *Protist*, *155*(2), 193–214. https://doi.org/10.1078/143446104774199592

Guindon, S., Dufayard, J.-F., Lefort, V., Anisimova, M., Hordijk, W., & Gascuel, O. (2010). New algorithms and methods to estimate maximum-likelihood phylogenies: Assessing the performance of PhyML 3.0. *Systematic Biology*, *59*(3), 307–321. https://doi.org/10.1093/sysbio/syq010

Guo, J., Wilken, S., Jimenez, V., Choi, C. J., Ansong, C., Dannebaum, R., Sudek, L., Milner, D. S., Bachy, C., Reistetter, E. N., Elrod, V. A., Klimov, D., Purvine, S. O., Wei, C.-L., Kunde-Ramamoorthy, G., Richards, T. A., Goodenough, U., Smith, R. D., Callister, S. J., & Worden, A. Z. (2018). Specialized proteomic responses and an ancient photoprotection mechanism sustain marine green algal growth during phosphate limitation. *Nature Microbiology*, *3*(7), 781–790. https://doi.org/10.1038/s41564-018-0178-7

Haas, A. F., Fairoz, M. F. M., Kelly, L. W., Nelson, C. E., Dinsdale, E. A., Edwards, R. A., Giles, S., Hatay, M., Hisakawa, N., Knowles, B., Lim, Y. W., Maughan, H., Pantos, O., Roach, T. N. F., Sanchez, S. E., Silveira, C. B., Sandin, S., Smith, J. E., & Rohwer, F. (2016). Global microbialization of coral reefs. *Nature Microbiology*, *1*(6), Article 6. https://doi.org/10.1038/nmicrobiol.2016.42

Halsey, K. H., Milligan, A. J., & Behrenfeld, M. J. (2014). Contrasting Strategies of Photosynthetic Energy Utilization Drive Lifestyle Strategies in Ecologically Important Picoeukaryotes. *Metabolites*, *4*(2), 260–280. https://doi.org/10.3390/metabo4020260

Harrison, P. J., Thompson, P. A., & Calderwood, G. S. (1990). Effects of nutrient and light limitation on the biochemical composition of phytoplankton. *Journal of Applied Phycology*, *2*(1), 45–56. https://doi.org/10.1007/BF02179768

Helmke, P., Neuer, S., Lomas, M. W., Conte, M., & Freudenthal, T. (2010). Cross-basin differences in particulate organic carbon export and flux attenuation in the subtropical North Atlantic gyre. *Deep Sea Research Part I: Oceanographic Research Papers*, *57*(2), 213–227. https://doi.org/10.1016/j.dsr.2009.11.001

Heymans, J. J., & Baird, D. (2000). A carbon flow model and network analysis of the northern Benguela upwelling system, Namibia. *Ecological Modelling*, *126*(1), 9–32. https://doi.org/10.1016/S0304-3800(99)00192-1

Hoadley, K. D., Hamilton, M., Poirier, C. L., Choi, C. J., Yung, C.-M., & Worden, A. Z. (2021). Selective Uptake of Pelagic Microbial Community Members by Caribbean Reef Corals. *Applied and Environmental Microbiology*, *87*(9), e03175-20. https://doi.org/10.1128/AEM.03175-20

Hossain, M. M. M., Mojumdar, S., Farjana, N., Islam, M. S., Raihan, M. A., Rahman, M. A., & Rahman, M. A. (2022). 16S rRNA genes developed a baseline of the microbial community associated with soil, water, fish and shellfishes in the sundarbans of Bangladesh. *Journal of Biological Studies*, *5*(3 (Special Issue)), Article 3 (Special Issue).

Hu, S., Li, T., Liu, S., & Huang, H. (2020). Dietary separation between co-occurring copepods in a food-limited tropical coral reef of the Sanya Bay. *Acta Oceanologica Sinica*, *39*(4), 65–72. https://doi.org/10.1007/s13131-020-1583-3

Hu, Y.-Y., Irwin, A. J., & Finkel, Z. V. (2022). Improving quantification of particulate phosphorus. *Limnology and Oceanography: Methods*, *20*(11), 729–740. https://doi.org/10.1002/lom3.10517

Huisman, J., Matthijs, H. C. P., Visser, P. M., Balke, H., Sigon, C. A. M., Passarge, J., Weissing, F. J., & Mur, L. R. (2002). Principles of the light-limited chemostat: Theory and ecological applications. *Antonie van Leeuwenhoek*, *81*(1), 117–133. https://doi.org/10.1023/A:1020537928216

Hunting, E. R., Soest, R. W. M. van, Geest, H. G. van der, Vos, A., & Debrot, A. O. (2008). Diversity and spatial heterogeneity of mangrove associated sponges of Curaçao and Aruba. *Contributions to Zoology*, *77*(4), 205–215. https://doi.org/10.1163/18759866-07704001

Igulu, M. M., Nagelkerken, I., Dorenbosch, M., Grol, M. G. G., Harborne, A. R., Kimirei, I. A., Mumby, P. J., Olds, A. D., & Mgaya, Y. D. (2014). Mangrove Habitat Use by Juvenile Reef Fish: Meta-Analysis Reveals that Tidal Regime Matters More than Biogeographic Region. *PLOS ONE*, *9*(12), e114715. https://doi.org/10.1371/journal.pone.0114715

Ishizaka, J., Kitaura, Y., Touke, Y., Sasaki, H., Tanaka, A., Murakami, H., Suzuki, T., Matsuoka, K., & Nakata, H. (2006). Satellite detection of red tide in Ariake Sound, 1998–2001. *Journal of Oceanography*, *62*(1), 37–45. https://doi.org/10.1007/s10872-006-0030-1

Jablonski, D., Roy, K., & Valentine, J. W. (2006). Out of the Tropics: Evolutionary Dynamics of the Latitudinal Diversity Gradient. *Science*, *314*(5796), 102–106. https://doi.org/10.1126/science.1130880

Jeffries, T. C., Ostrowski, M., Williams, R. B., Xie, C., Jensen, R. M., Grzymski, J. J., Senstius, S. J., Givskov, M., Hoeke, R., Philip, G. K., Neches, R. Y., Drautz-Moses, D. I., Chénard, C., Paulsen, I. T., & Lauro, F. M. (2015). Spatially extensive microbial biogeography of the Indian Ocean provides insights into the unique community structure of a pristine coral atoll. *Scientific Reports*, *5*(1), Article 1. https://doi.org/10.1038/srep15383

Johnson, Z., Zinser, E., Coe, A., Mcnulty, N., Woodward, E., & Chisholm, S. (2006). Niche partitioning among *Prochlorococcus* ecotypes along ocean-scale environmental gradients. *Science (New York, N.Y.)*, *311*, 1737–1740. https://doi.org/10.1126/science.1118052

Karl, D. M., Bidigare, R., & Letelier, R. (2001). Long-term changes in plankton community structure and productivity in the North Pacific Subtropical Gyre: The domain shift hypothesis. *Deep Sea Research Part II: Topical Studies in Oceanography*, *48*, 1449–1470. https://doi.org/10.1016/S0967-0645(00)00149-1

Kassambara, A. (2019). *Practical statistics in R II - comparing groups: Numerical variables* (1st ed.). Datanovia.

Katoh, K., & Standley, D. M. (2013). MAFFT Multiple Sequence Alignment Software Version 7: Improvements in performance and usability. *Molecular Biology and Evolution*, *30*(4), 772–780. https://doi.org/10.1093/molbev/mst010

Keeling, P. J., Burki, F., Wilcox, H. M., Allam, B., Allen, E. E., Amaral-Zettler, L. A., Armbrust, E. V., Archibald, J. M., Bharti, A. K., Bell, C. J., Beszteri, B., Bidle, K. D., Cameron, C. T., Campbell, L., Caron, D. A., Cattolico, R. A., Collier, J. L., Coyne, K., Davy, S. K., … Worden, A. Z. (2014). The Marine Microbial Eukaryote Transcriptome Sequencing Project (MMETSP): Illuminating the functional diversity of eukaryotic life in the oceans through transcriptome sequencing. *PLOS Biology*, *12*(6), e1001889. https://doi.org/10.1371/journal.pbio.1001889

Kim, D. Y., Countway, P. D., Jones, A. C., Schnetzer, A., Yamashita, W., Tung, C., & Caron, D. A. (2014). Monthly to interannual variability of microbial eukaryote assemblages at four depths in the eastern North Pacific. *The ISME Journal*, *8*(3), Article 3. https://doi.org/10.1038/ismej.2013.173

Kim, D. Y., Countway, P. D., Yamashita, W., & Caron, D. A. (2012). A combined sequence-based and fragment-based characterization of microbial eukaryote assemblages provides taxonomic context for the Terminal Restriction Fragment Length Polymorphism (T-RFLP) method. *Journal of Microbiological Methods*, *91*(3), 527–536. https://doi.org/10.1016/j.mimet.2012.09.026

Kim, E., Harrison, J. W., Sudek, S., Jones, M. D. M., Wilcox, H. M., Richards, T. A., Worden, A. Z., & Archibald, J. M. (2011). Newly identified and diverse plastid-bearing branch on the eukaryotic tree of life. *Proceedings of the National Academy of Sciences*, *108*(4), 1496–1500. https://doi.org/10.1073/pnas.1013337108

Klausmeier, C. A., Litchman, E., Daufresne, T., & Levin, S. A. (2008). Phytoplankton stoichiometry. *Ecological Research*, *23*(3), 479–485. https://doi.org/10.1007/s11284-008-0470-8

Knight-Jones, E. W., & Walne, P. R. (1951). *Chromulina pusilla* Butcher, a dominant member of the ultraplankton. *Nature*, *167*(4246), Article 4246. https://doi.org/10.1038/167445a0

Kókai, Z., Bácsi, I., Török, P., Buczkó, K., T-Krasznai, E., Balogh, C., Tóthmérész, B., & B-Béres, V. (2015). Halophilic diatom taxa are sensitive indicators of even short term changes in lowland lotic systems. *Acta Botanica Croatica*, *74*(2), 287–302. https://doi.org/10.1515/botcro-2015-0025

Kristensen, E., Bouillon, S., Dittmar, T., & Marchand, C. (2008). Organic carbon dynamics in mangrove ecosystems: A review. *Aquatic Botany*, *89*(2), 201–219. https://doi.org/10.1016/j.aquabot.2007.12.005

Kurtz, Z. D., Müller, C. L., Miraldi, E. R., Littman, D. R., Blaser, M. J., & Bonneau, R. A. (2015). Sparse and Compositionally Robust Inference of Microbial Ecological Networks. *PLOS Computational Biology*, *11*(5), e1004226. https://doi.org/10.1371/journal.pcbi.1004226

Kwiatkowski, L., Aumont, O., Bopp, L., & Ciais, P. (2018). The Impact of Variable Phytoplankton Stoichiometry on Projections of Primary Production, Food Quality, and Carbon Uptake in the Global Ocean. *Global Biogeochemical Cycles*, *32*(4), 516–528. https://doi.org/10.1002/2017GB005799

Laas, P., Ugarelli, K., Absten, M., Boyer, B., Briceño, H., & Stingl, U. (2021). Composition of Prokaryotic and Eukaryotic Microbial Communities in Waters around the Florida Reef Tract. *Microorganisms*, *9*(6), 1120. https://doi.org/10.3390/microorganisms9061120

LaJeunesse, T. C., Parkinson, J. E., Gabrielson, P. W., Jeong, H. J., Reimer, J. D., Voolstra, C. R., & Santos, S. R. (2018). Systematic Revision of Symbiodiniaceae Highlights the Antiquity and Diversity of Coral Endosymbionts. *Current Biology*, *28*(16), 2570-2580.e6. https://doi.org/10.1016/j.cub.2018.07.008

Larson, C. A., & Belovsky, G. E. (2013). Salinity and nutrients influence species richness and evenness of phytoplankton communities in microcosm experiments from Great Salt Lake, Utah, USA. *Journal of Plankton Research*, *35*(5), 1154–1166. https://doi.org/10.1093/plankt/fbt053

Leander, B. S., & Keeling, P. J. (2003). Morphostasis in alveolate evolution. *Trends in Ecology & Evolution*, *18*(8), 395–402. https://doi.org/10.1016/S0169-5347(03)00152-6

Lefrançois, E., Coat, S., Lepoint, G., Vachiéry, N., Gros, O., & Monti, D. (2011). Epilithic biofilm as a key factor for small-scale river fisheries on Caribbean islands. *Fisheries Management and Ecology*, *18*(3), 211–220. https://doi.org/10.1111/j.1365-2400.2010.00767.x

Leliaert, F., Smith, D. R., Moreau, H., Herron, M. D., Verbruggen, H., Delwiche, C. F., & Clerck, O. D. (2012). Phylogeny and Molecular Evolution of the Green Algae. *Critical Reviews in Plant Sciences*, *31*(1), 1–46. https://doi.org/10.1080/07352689.2011.615705

Lévy, M., Jahn, O., Dutkiewicz, S., Follows, M. J., & d'Ovidio, F. (2015). The dynamical landscape of marine phytoplankton diversity. *Journal of The Royal Society Interface*, *12*(111), 20150481. https://doi.org/10.1098/rsif.2015.0481

Li, L., Wang, S., Wang, H., Sahu, S. K., Marin, B., Li, H., Xu, Y., Liang, H., Li, Z., Cheng, S., Reder, T., Çebi, Z., Wittek, S., Petersen, M., Melkonian, B., Du, H., Yang, H., Wang, J., Wong, G. K.-S., … Liu, H. (2020). The genome of Prasinoderma coloniale unveils the existence of a third phylum within green plants. *Nature Ecology & Evolution*, *4*(9), Article 9. https://doi.org/10.1038/s41559-020-1221-7

Li, M., Baughman, E., Roth, M. R., Han, X., Welti, R., & Wang, X. (2014). Quantitative profiling and pattern analysis of triacylglycerol species in Arabidopsis seeds by electrospray ionization mass spectrometry. *The Plant Journal*, *77*(1), 160–172. https://doi.org/10.1111/tpj.12365

Li, Q., Edwards, K. F., Schvarcz, C. R., Selph, K. E., & Steward, G. F. (2021). Plasticity in the grazing ecophysiology of Florenciella (Dichtyochophyceae), a mixotrophic nanoflagellate that consumes Prochlorococcus and other bacteria. *Limnology and Oceanography*, *66*(1), 47–60. https://doi.org/10.1002/lno.11585

Li, Q., Edwards, K. F., Schvarcz, C. R., & Steward, G. F. (2022). Broad phylogenetic and functional diversity among mixotrophic consumers of Prochlorococcus. *The ISME Journal*, *16*(6), Article 6. https://doi.org/10.1038/s41396-022-01204-z

Li, W. K. W. (1994). Primary production of prochlorophytes, cyanobacteria, and eucaryotic ultraphytoplankton: Measurements from flow cytometric sorting. *Limnology and Oceanography*, *39*(1), 169–175. https://doi.org/10.4319/lo.1994.39.1.0169

Li, W. K. W., McLaughlin, F. A., Lovejoy, C., & Carmack, E. C. (2009). Smallest Algae Thrive As the Arctic Ocean Freshens. *Science*, *326*(5952), 539–539. https://doi.org/10.1126/science.1179798

Liefer, J. D., Garg, A., Fyfe, M. H., Irwin, A. J., Benner, I., Brown, C. M., Follows, M. J., Omta, A. W., & Finkel, Z. V. (2019). The Macromolecular Basis of Phytoplankton C:N:P Under Nitrogen Starvation. *Frontiers in Microbiology*, *10*. https://doi.org/10.3389/fmicb.2019.00763

Limardo, A. J., Sudek, S., Choi, C. J., Poirier, C., Rii, Y. M., Blum, M., Roth, R., Goodenough, U., Church, M. J., & Worden, A. Z. (2017). Quantitative biogeography of picoprasinophytes establishes ecotype distributions and significant contributions to marine phytoplankton. *Environmental Microbiology*, *19*(8), 3219–3234. https://doi.org/10.1111/1462-2920.13812

Lindao, M. R., & Ruiz, C. A. (2022). Phytoplankton distribution in marine-coastal waters in three sectors of Santa Elena Peninsula. *Revista Acta Oceanográfica Del Pacífico*, *4*(1), Article 1. https://doi.org/10.54140/raop.v4i1.51

Lindemann, C., Aksnes, D. L., Flynn, K. J., & Menden-Deuer, S. (2017). Editorial: Modeling the Plankton–Enhancing the Integration of Biological Knowledge and Mechanistic Understanding. *Frontiers in Marine Science*, *4*. https://doi.org/10.3389/fmars.2017.00358

Litchman, E., & Klausmeier, C. A. (2008). Trait-Based Community Ecology of Phytoplankton. *Annual Review of Ecology, Evolution, and Systematics*, *39*, 615–639. JSTOR.

Litchman, E., Pinto, P. de T., Edwards, K. F., Klausmeier, C. A., Kremer, C. T., & Thomas, M. K. (2015). Global biogeochemical impacts of phytoplankton: A trait-based perspective. *Journal of Ecology*, *103*(6), 1384–1396. https://doi.org/10.1111/1365-2745.12438

Lomas, M. W., & Bates, N. R. (2004). Potential controls on interannual partitioning of organic carbon during the winter/spring phytoplankton bloom at the Bermuda Atlantic time-series study (BATS) site. *Deep Sea Research Part I: Oceanographic Research Papers*, *51*(11), 1619–1636. https://doi.org/10.1016/j.dsr.2004.06.007

Lomas, M. W., Bates, N. R., Johnson, R. J., Knap, A. H., Steinberg, D. K., & Carlson, C. A. (2013). Two decades and counting: 24-years of sustained open ocean biogeochemical measurements in the Sargasso Sea. *Deep Sea Research Part II: Topical Studies in Oceanography*, *93*, 16–32. https://doi.org/10.1016/j.dsr2.2013.01.008

Lomas, M. W., Bates, N. R., Johnson, R. J., Steinberg, D. K., & Tanioka, T. (2022). Adaptive carbon export response to warming in the Sargasso Sea. *Nature Communications*, *13*(1), Article 1. https://doi.org/10.1038/s41467-022-28842-3

Lomas, M. W., Roberts, N., Lipschultz, F., Krause, J. W., Nelson, D. M., & Bates, N. R. (2009). Biogeochemical responses to late-winter storms in the Sargasso Sea. IV. Rapid succession of major phytoplankton groups. *Deep Sea Research Part I: Oceanographic Research Papers*, *56*(6), 892–908. https://doi.org/10.1016/j.dsr.2009.03.004

Lomas, M. W., Steinberg, D. K., Dickey, T., Carlson, C. A., Nelson, N. B., Condon, R. H., & Bates, N. R. (2010). Increased ocean carbon export in the Sargasso Sea linked to climate variability is countered by its enhanced mesopelagic attenuation. *BIOGEOSCIENCES*, *7*(1), 57–70. https://doi.org/ https://doi.org/10.5194/bg-7-57-2010

Lopes dos Santos, A., Gourvil, P., Tragin, M., Noël, M.-H., Decelle, J., Romac, S., & Vaulot, D. (2017). Diversity and oceanic distribution of prasinophytes clade VII, the dominant group of green algae in oceanic waters. *The ISME Journal*, *11*(2), 512–528. https://doi.org/10.1038/ismej.2016.120

Lopes dos Santos, A., Pollina, T., Gourvil, P., Corre, E., Marie, D., Garrido, J. L., Rodríguez, F., Noël, M.-H., Vaulot, D., & Eikrem, W. (2017). Chloropicophyceae, a new class of picophytoplanktonic prasinophytes. *Scientific Reports*, *7*. https://doi.org/10.1038/s41598-017-12412-5

López-Lara, I. M., Gao, J.-L., Soto, M. J., Solares-Pérez, A., Weissenmayer, B., Sohlenkamp, C., Verroios, G. P., Thomas-Oates, J., & Geiger, O. (2005). Phosphorus-Free Membrane Lipids of Sinorhizobium meliloti Are Not Required for the Symbiosis with Alfalfa but Contribute to Increased Cell Yields Under Phosphorus-Limiting Conditions of Growth. *Molecular Plant-Microbe Interactions®*, *18*(9), 973–982. https://doi.org/10.1094/MPMI-18-0973

Lovejoy, C., Vincent, W. F., Bonilla, S., Roy, S., Martineau, M.-J., Terrado, R., Potvin, M., Massana, R., & Pedrós-Alió, C. (2007). Distribution, Phylogeny, and Growth of Cold-Adapted Picoprasinophytes in Arctic Seas. *Journal of Phycology*, *43*(1), 78–89. https://doi.org/10.1111/j.1529-8817.2006.00310.x

Lu, L., Wang, J., Yang, G., Zhu, B., & Pan, K. (2017). Biomass and nutrient productivities of Tetraselmis chuii under mixotrophic culture conditions with various C:N ratios. *Chinese Journal of Oceanology and Limnology*, *35*(2), 303–312. https://doi.org/10.1007/s00343-016-5299-3

Lubiana, K. M. F., Gianesella, S. M. F., Saldanha-Corrêa, F. M. P., & Oliveira, M. C. (2017). Nephroselmis viridis (Nephroselmidophyceae, Chlorophyta), a new record for the Atlantic Ocean based on molecular phylogeny and ultrastructure. *Marine Biodiversity Records*, *10*(1), 5. https://doi.org/10.1186/s41200-017-0107-0

Maat, D. S., Bale, N. J., Hopmans, E. C., Sinninghe Damsté, J. S., Schouten, S., & Brussaard, C. P. D. (2016). Increasing P limitation and viral infection impact lipid remodeling of the picophytoplankter *Micromonas pusilla*. *Biogeosciences*, *13*(5), 1667–1676. https://doi.org/10.5194/bg-13-1667-2016

Maat, D. S., Crawfurd, K. J., Timmermans, K. R., & Brussaard, C. P. D. (2014). Elevated CO2 and Phosphate Limitation Favor Micromonas pusilla through Stimulated Growth and Reduced Viral Impact. *Applied and Environmental Microbiology*, *80*(10), 3119–3127. https://doi.org/10.1128/AEM.03639-13

Malmstrom, R. R., Coe, A., Kettler, G. C., Martiny, A. C., Frias-Lopez, J., Zinser, E. R., & Chisholm, S. W. (2010). Temporal dynamics of *Prochlorococcus* ecotypes in the Atlantic and Pacific oceans. *The ISME Journal*, *4*(10), Article 10. https://doi.org/10.1038/ismej.2010.60

Marañón, E., Cermeño, P., López-Sandoval, D. C., Rodríguez-Ramos, T., Sobrino, C., Huete-Ortega, M., Blanco, J. M., & Rodríguez, J. (2013). Unimodal size scaling of phytoplankton growth and the size dependence of nutrient uptake and use. *Ecology Letters*, *16*(3), 371–379. https://doi.org/10.1111/ele.12052

Martin, M. (2011). Cutadapt removes adapter sequences from high-throughput sequencing reads. *EMBnet.Journal*, *17*(1), Article 1. https://doi.org/10.14806/ej.17.1.200

Massjuk, & Lilitska, Г. Г. (2006). *Chlorodendrophyceae class. Nov. (Chlorophyta, Viridiplantae) у флорі України. II. Рід Tetraselmis F. Stein*. http://dspace.nbuv.gov.ua/xmlui/handle/123456789/3597

McMurray, S. E., Johnson, Z. I., Hunt, D. E., Pawlik, J. R., & Finelli, C. M. (2016). Selective feeding by the giant barrel sponge enhances foraging efficiency. *Limnology and Oceanography*, *61*(4), 1271–1286. https://doi.org/10.1002/lno.10287

Meakin, N. G., & Wyman, M. (2011). Rapid shifts in picoeukaryote community structure in response to ocean acidification. *The ISME Journal*, *5*(9), 1397–1405. https://doi.org/10.1038/ismej.2011.18

Michaels, A., Knap, A., Dow, R., Gundersen, K., Johnson, R., Sorensen, J., Close, A., Knauer, G., Lohrenz, S., Asper, V., Tuel, M., & Bidigare, R. (1994). Seasonal patterns of ocean biogeochemistry at the U.S. JGOFS Bermuda Atlantic time-series study site. *Deep Sea Research Part I: Oceanographic Research Papers*, *41*(7), 1013–1038. https://doi.org/10.1016/0967-0637(94)90016-7

Mitra, A., Flynn, K. J., Burkholder, J. M., Berge, T., Calbet, A., Raven, J. A., Granéli, E., Glibert, P. M., Hansen, P. J., Stoecker, D. K., Thingstad, F., Tillmann, U., Våge, S., Wilken, S., & Zubkov, M. V. (2014). The role of mixotrophic protists in the biological carbon pump. *Biogeosciences*, *11*(4), 995–1005. https://doi.org/10.5194/bg-11-995-2014

Moestrup, Ø., Hori, T., & Kristiansen, A. (1987). Fine structure of Pyramimonas octopus sp. Nov., an octoflagellated benthic species of Pyramimonas (Prasinophyceae), with some observations on its ecology. *Nordic Journal of Botany*, *7*(3), 339–352. https://doi.org/10.1111/j.1756-1051.1987.tb00950.x

Moestrup, Ø., Inouye, I., & Hori, T. (2003). Ultrastructural studies on Cymbomonas tetramitiformis (Prasinophyceae). I. General structure, scale microstructure, and ontogeny. *Canadian Journal of Botany*, *81*(7), 657–671. https://doi.org/10.1139/b03-055

Moestrup, Ø., & Throndsen, J. (1988). Light and electron microscopical studies on Pseudoscourfieldia marina, a primitive scaly green flagellate (Prasinophyceae) with posterior flagella. *Canadian Journal of Botany*, *66*(7), 1415–1434. https://doi.org/10.1139/b88-197

Monier, A., Worden, A. Z., & Richards, T. A. (2016). Phylogenetic diversity and biogeography of the Mamiellophyceae lineage of eukaryotic phytoplankton across the oceans. *Environmental Microbiology Reports*, *8*(4), 461–469. https://doi.org/10.1111/1758-2229.12390

Moreira, D., & López-García, P. (2002). The molecular ecology of microbial eukaryotes unveils a hidden world. *Trends in Microbiology*, *10*(1), 31–38. https://doi.org/10.1016/S0966-842X(01)02257-0

Mouginot, C., Zimmerman, A. E., Bonachela, J. A., Fredricks, H., Allison, S. D., Mooy, B. A. S. V., & Martiny, A. C. (2015). Resource allocation by the marine cyanobacterium Synechococcus WH8102 in response to different nutrient supply ratios. *Limnology and Oceanography*, *60*(5), 1634–1641. https://doi.org/10.1002/lno.10123

Muir, D. G., & Perissinotto, R. (2011). Persistent Phytoplankton Bloom in Lake St. Lucia (iSimangaliso Wetland Park, South Africa) Caused by a Cyanobacterium Closely Associated with the Genus Cyanothece (Synechococcaceae, Chroococcales). *Applied and Environmental Microbiology*, *77*(17), 5888–5896. https://doi.org/10.1128/AEM.00460-11

Munk, W., & Riley, G. A. (1952). *Absorption of nutrients by aquatic plants*. /paper/Absorption-of-nutrients-by-aquatic-plants-Munk-Riley/125174b77d94b5e7d46e70ccb387dbb9cc1e951b

Murphy, J., & Riley, J. P. (1962). A modified single solution method for the determination of phosphate in natural waters. *Analytica Chimica Acta*, *27*, 31–36. https://doi.org/10.1016/S0003-2670(00)88444-5

Nagelkerken, I., & Velde, G. van der. (2002). Do non-estuarine mangroves harbour higher densities of juvenile fish than adjacent shallow-water and coral reef habitats in Curaçao (Netherlands Antilles)? *Marine Ecology Progress Series*, *245*, 191–204. https://doi.org/10.3354/meps245191

Nakayama, T., Marin, B., Kranz, H. D., Surek, B., Huss, V. A. R., Inouye, I., & Melkonian, M. (1998). The Basal Position of Scaly Green Flagellates among the Green Algae (Chlorophyta) is Revealed by Analyses of Nuclear-Encoded SSU rRNA Sequences. *Protist*, *149*(4), 367–380. https://doi.org/10.1016/S1434-4610(98)70043-4

Nakayama, T., Suda, S., Kawachi, M., & Inouye, I. (2007). Phylogeny and ultrastructure of Nephroselmis and Pseudoscourfieldia (Chlorophyta), including the description of Nephroselmis anterostigmatica sp. Nov. And a proposal for the Nephroselmidales ord. Nov. *Phycologia*, *46*(6), 680–697. https://doi.org/10.2216/04-25.1

Needham, D. M., & Fuhrman, J. A. (2016). Pronounced daily succession of phytoplankton, archaea and bacteria following a spring bloom. *Nature Microbiology*, *1*(4), 1–7. https://doi.org/10.1038/nmicrobiol.2016.5

Neuer, S., Davenport, R., Freudenthal, T., Wefer, G., Llinás, O., Rueda, M.-J., Steinberg, D. K., & Karl, D. M. (2002). Differences in the biological carbon pump at three subtropical ocean sites. *Geophysical Research Letters*, *29*(18), 32-1-32–34. https://doi.org/10.1029/2002GL015393

Nguyen, T. T. H., Zakem, E. J., Ebrahimi, A., Schwartzman, J., Caglar, T., Amarnath, K., Alcolombri, U., Peaudecerf, F. J., Hwa, T., Stocker, R., Cordero, O. X., & Levine, N. M. (2022). Microbes contribute to setting the ocean carbon flux by altering the fate of sinking particulates. *Nature Communications*, *13*(1), Article 1. https://doi.org/10.1038/s41467-022-29297-2

Not, F., Latasa, M., Marie, D., Cariou, T., Vaulot, D., & Simon, N. (2004). A Single Species, Micromonas pusilla (Prasinophyceae), Dominates the Eukaryotic Picoplankton in the Western English Channel. *Applied and Environmental Microbiology*, *70*(7), 4064–4072. https://doi.org/10.1128/AEM.70.7.4064-4072.2004

Not, F., Massana, R., Latasa, M., Marie, D., Colson, C., Eikrem, W., Pedrós-Alió, C., Vaulot, D., & Simon, N. (2005). Late summer community composition and abundance of photosynthetic picoeukaryotes in Norwegian and Barents Seas. *Limnology and Oceanography*, *50*(5), 1677–1686. https://doi.org/10.4319/lo.2005.50.5.1677

Nuryadi, H., Nguyen, T. T. M., Ito, M., Okada, N., Wakaoji, S., Maruyama, T., Nakano, Y., Fujimura, H., Takeyama, H., & Suda, S. (2018). A metabarcoding survey for seasonal picophytoplankton composition in two coral reefs around Sesoko Island, Okinawa, Japan. *Journal of Applied Phycology*, *30*(6), 3179–3186. https://doi.org/10.1007/s10811-018-1544-9

Ohtsuka, S., Suzaki, T., Horiguchi, T., Suzuki, N., & Not, F. (2015). *Marine protists: Diversity and dynamics*. Springer Japan. https://doi.org/10.1007/978-4-431-55130-0

Oksanen, J., Blanchet, F. G., Friendly, M., Kindt, R., Legendre, P., & McGlinn, D. (2020). *Vegan: Community Ecology Package. R package version 2.5-7* (2.5-7). https://CRAN.R-project.org/package=vegan

Oksanen, J., Blanchet, F. G., Kindt, R., Legendre, P., Minchin, P., O'Hara, B., Simpson, G., Solymos, P., Stevens, H., & Wagner, H. (2015). Vegan: Community Ecology Package. *R Package Version 2.2-1*, *2*, 1–2.

Ollison, G. A., Hu, S. K., Mesrop, L. Y., DeLong, E. F., & Caron, D. A. (2021). Come rain or shine: Depth not season shapes the active protistan community at station ALOHA in the North Pacific Subtropical Gyre. *Deep Sea Research Part I: Oceanographic Research Papers*, *170*, 103494. https://doi.org/10.1016/j.dsr.2021.103494

Omand, M. M., D'Asaro, E. A., Lee, C. M., Perry, M. J., Briggs, N., Cetinić, I., & Mahadevan, A. (2015). Eddy-driven subduction exports particulate organic carbon from the spring bloom. *Science*, *348*(6231), 222–225. https://doi.org/10.1126/science.1260062

Oren, A. (2005). A hundred years of Dunaliella research: 1905–2005. *Saline Systems*, *1*(1), 2. https://doi.org/10.1186/1746-1448-1-2

Pandey, L. K., Sharma, Y. C., Park, J., Choi, S., Lee, H., Lyu, J., & Han, T. (2018). Evaluating features of periphytic diatom communities as biomonitoring tools in fresh, brackish and marine waters. *Aquatic Toxicology*, *194*, 67–77. https://doi.org/10.1016/j.aquatox.2017.11.003

Philippe, H. (1993). MUST, a computer package of Management Utilities for Sequences and Trees. *Nucleic Acids Research*, *21*(22), 5264–5272. https://doi.org/10.1093/nar/21.22.5264

Pinckney, J. L., Benitez-Nelson, C. R., Thunell, R. C., Muller-Karger, F., Lorenzoni, L., Troccoli, L., & Varela, R. (2015). Phytoplankton community structure and depth distribution changes in the Cariaco Basin between 1996 and 2010. *Deep Sea Research Part I: Oceanographic Research Papers*, *101*, 27–37. https://doi.org/10.1016/j.dsr.2015.03.004

Polovina, J. J., Howell, E. A., & Abecassis, M. (2008). Ocean's least productive waters are expanding. *Geophysical Research Letters*, *35*(3). https://doi.org/10.1029/2007GL031745

Posada, D. (2008). jModelTest: Phylogenetic model averaging. *Molecular Biology and Evolution*, *25*(7), 1253–1256. https://doi.org/10.1093/molbev/msn083

Potter, D., Lajeunesse, T. C., Saunders, G. W., & Anderson, R. A. (1997). Convergent evolution masks extensive biodiversity among marine coccoid picoplankton. *Biodiversity & Conservation*, *6*(1), 99–107. https://doi.org/10.1023/A:1018379716868

Pusceddu, A., & Fabiano, M. (1996). Changes in the Biochemical Composition of Tetraselmis Suecia and Isochrysis Galbana During Growth and Decay. *Chemistry and Ecology*, *12*(3), 199–212. https://doi.org/10.1080/02757549608039082

Qin, C., Zhu, W., Ma, H., Duan, D., Zuo, T., Xi, S., & Pan, W. (2019). Are habitat changes driving protist community shifts? A case study in Daya Bay, China. *Estuarine, Coastal and Shelf Science*, *227*, 106356. https://doi.org/10.1016/j.ecss.2019.106356

Quast, C., Pruesse, E., Yilmaz, P., Gerken, J., Schweer, T., Yarza, P., Peplies, J., & Glöckner, F. O. (2013). The SILVA ribosomal RNA gene database project: Improved data processing and web-based tools. *Nucleic Acids Research*, *41*(D1), D590–D596. https://doi.org/10.1093/nar/gks1219

R Core Team. (2002). *The R stats package* (R version 2.2).

REDFIELD, A. C. (1958). THE BIOLOGICAL CONTROL OF CHEMICAL FACTORS IN THE ENVIRONMENT. *American Scientist*, *46*(3), 230A – 221. JSTOR.

Reef, R., Feller, I. C., & Lovelock, C. E. (2010). Nutrition of mangroves. *Tree Physiology*, *30*(9), 1148–1160. https://doi.org/10.1093/treephys/tpq048

Rengefors, K., Kremp, A., Reusch, T. B. H., & Wood, A. M. (2017). Genetic diversity and evolution in eukaryotic phytoplankton: Revelations from population genetic studies. *Journal of Plankton Research*, *39*(2), 165–179. https://doi.org/10.1093/plankt/fbw098

Richardson, T. L. (2019). Mechanisms and Pathways of Small-Phytoplankton Export from the Surface Ocean. *Annual Review of Marine Science*, *11*(1), 57–74. https://doi.org/10.1146/annurev-marine-121916-063627

Richardson, T. L., & Jackson, G. A. (2007). Small Phytoplankton and Carbon Export from the Surface Ocean. *Science*, *315*(5813), 838–840. https://doi.org/10.1126/science.1133471

Rigonato, J., Kent, A. D., Alvarenga, D. O., Andreote, F. D., Beirigo, R. M., Vidal-Torrado, P., & Fiore, M. F. (2013). Drivers of cyanobacterial diversity and community composition in mangrove soils in south-east Brazil. *Environmental Microbiology*, *15*(4), 1103–1114. https://doi.org/10.1111/j.1462-2920.2012.02830.x

Rii, Y. M., Duhamel, S., Bidigare, R., Karl, D., Repeta, D., & Church, M. (2016). *Diversity and productivity of photosynthetic picoeukaryotes in biogeochemically distinct regions of the South East Pacific Ocean*. https://doi.org/10.1002/LNO.10255

Rodríguez, F., Derelle, E., Guillou, L., Gall, F. L., Vaulot, D., & Moreau, H. (2005). Ecotype diversity in the marine picoeukaryote Ostreococcus (Chlorophyta,

Prasinophyceae). *Environmental Microbiology*, *7*(6), 853–859. https://doi.org/10.1111/j.1462-2920.2005.00758.x

Saifullah, A. S. M., Kamal, A. H. M., Idris, M. H., Rajaee, A. H., & Bhuiyan, Md. K. A. (2016). Phytoplankton in tropical mangrove estuaries: Role and interdependency. *Forest Science and Technology*, *12*(2), 104–113. https://doi.org/10.1080/21580103.2015.1077479

Sakamoto, C. M., Friederich, G. E., & Codispoti, L. A. (1990). MBARI procedures for automated nutrient analyses using a modified Alpkem Series 300 Rapid Flow Analyzer. *Http://Aquaticcommons.Org/Id/Eprint/1971*. https://aquadocs.org/handle/1834/19792

Sakshaug, E., Andresen, K., & Kiefer, D. A. (1989). A steady state description ofgrowth and light absorption in the marine planktonic diatom Skeletonema costatum. *Limnology and Oceanography*, *34*(1), 198–205. https://doi.org/10.4319/lo.1989.34.1.0198

Samanta, B., & Bhadury, P. (2014). Analysis of diversity of chromophytic phytoplankton in a mangrove ecosystem using rbcL gene sequencing. *Journal of Phycology*, *50*(2), 328–340. https://doi.org/10.1111/jpy.12163

Scheffers, S. R., Nieuwland, G., Bak, R. P. M., & van Duyl, F. C. (2004). Removal of bacteria and nutrient dynamics within the coral reef framework of Curaçao (Netherlands Antilles). *Coral Reefs*, *23*(3), 413–422. https://doi.org/10.1007/s00338-004-0400-3

Schubotz, F., Meyer-Dombard, D. R., Bradley, A. S., Fredricks, H. F., Hinrichs, K.-U., Shock, E. L., & Summons, R. E. (2013). Spatial and temporal variability of biomarkers and microbial diversity reveal metabolic and community flexibility in Streamer Biofilm Communities in the Lower Geyser Basin, Yellowstone National Park. *Geobiology*, *11*(6), 549–569. https://doi.org/10.1111/gbi.12051

Sheldon, R. W., & Parsons, T. R. (1967). A Continuous Size Spectrum for Particulate Matter in the Sea. *Journal of the Fisheries Research Board of Canada*, *24*(5), 909–915. https://doi.org/10.1139/f67-081

Sherr, E., & Sherr, B. (1988). Role of microbes in pelagic food webs: A revised concept. *Limnology and Oceanography*, *33*(5), 1225–1227. https://doi.org/10.4319/lo.1988.33.5.1225

Shi, X. L., Lepère, C., Scanlan, D. J., & Vaulot, D. (2011). Plastid 16S rRNA Gene Diversity among Eukaryotic Picophytoplankton Sorted by Flow Cytometry

from the South Pacific Ocean. *PLoS ONE*, *6*(4). https://doi.org/10.1371/journal.pone.0018979

Sibbald, S. J., & Archibald, J. M. (2020). Genomic insights into plastid evolution. *Genome Biology and Evolution*, *12*(7), 978–990. https://doi.org/10.1093/gbe/evaa096

Sieburth, J. McN., Smetacek, V., & Lenz, J. (1978). Pelagic ecosystem structure: Heterotrophic compartments of the plankton and their relationship to plankton size fractions 1. *Limnology and Oceanography*, *23*(6), 1256–1263. https://doi.org/10.4319/lo.1978.23.6.1256

Silva, C. S. P., Genuário, D. B., Vaz, M. G. M. V., & Fiore, M. F. (2014). Phylogeny of culturable cyanobacteria from Brazilian mangroves. *Systematic and Applied Microbiology*, *37*(2), 100–112. https://doi.org/10.1016/j.syapm.2013.12.003

Simmons, M. P., Bachy, C., Sudek, S., van Baren, M. J., Sudek, L., Ares, M., & Worden, A. Z. (2015). Intron invasions trace algal speciation and reveal nearly identical Arctic and Antarctic *Micromonas* populations. *Molecular Biology and Evolution*, *32*(9), 2219–2235. https://doi.org/10.1093/molbev/msv122

Simmons, M. P., Sudek, S., Monier, A., Limardo, A. J., Jimenez, V., Perle, C. R., Elrod, V. A., Pennington, J. T., & Worden, A. Z. (2016). Abundance and biogeography of picoprasinophyte ecotypes and other phytoplankton in the Eastern North Pacific Ocean. *Applied and Environmental Microbiology*, *82*(6), 1693–1705. https://doi.org/10.1128/AEM.02730-15

Simon, N., Foulon, E., Grulois, D., Six, C., Desdevises, Y., Latimier, M., Le Gall, F., Tragin, M., Houdan, A., Derelle, E., Jouenne, F., Marie, D., Le Panse, S., Vaulot, D., & Marin, B. (2017). Revision of the genus *Micromonas* Manton et Parke (Chlorophyta, Mamiellophyceae), of the type species *M. pusilla* (Butcher) Manton & Parke and of the species *M. commoda* van Baren, Bachy and Worden and description of two new species based on the genetic and phenotypic characterization of cultured isolates. *Protist*, *168*(5), 612–635. https://doi.org/10.1016/j.protis.2017.09.002

Singh, A., Baer, S. E., Riebesell, U., Martiny, A. C., & Lomas, M. W. (2015). C: N : P stoichiometry at the Bermuda Atlantic Time-series Study station in the North Atlantic Ocean. *Biogeosciences*, *12*(21), 6389–6403. https://doi.org/10.5194/bg-12-6389-2015

Šlapeta, J., López-García, P., & Moreira, D. (2006). Global dispersal and ancient cryptic species in the smallest marine eukaryotes. *Molecular Biology and Evolution*, *23*(1), 23–29. https://doi.org/10.1093/molbev/msj001

Stawiarski, B., Buitenhuis, E. T., & Le Quéré, C. (2016). The Physiological Response of Picophytoplankton to Temperature and Its Model Representation. *Frontiers in Marine Science*, *3*. https://doi.org/10.3389/fmars.2016.00164

Steinberg, D. K., Carlson, C. A., Bates, N. R., Johnson, R. J., Michaels, A. F., & Knap, A. H. (2001). Overview of the US JGOFS Bermuda Atlantic Time-series Study (BATS): A decade-scale look at ocean biology and biogeochemistry. *Deep Sea Research Part II: Topical Studies in Oceanography*, *48*(8), 1405–1447. https://doi.org/10.1016/S0967-0645(00)00148-X

Stoeck, T., Bass, D., Nebel, M., Christen, R., Jones, M. D. M., Breiner, H.-W., & Richards, T. A. (2010). Multiple marker parallel tag environmental DNA sequencing reveals a highly complex eukaryotic community in marine anoxic water. *Molecular Ecology*, *19*(s1), 21–31. https://doi.org/10.1111/j.1365-294X.2009.04480.x

Subirana, L., Péquin, B., Michely, S., Escande, M.-L., Meilland, J., Derelle, E., Marin, B., Piganeau, G., Desdevises, Y., Moreau, H., & Grimsley, N. (2013). Morphology, Genome Plasticity, and Phylogeny in the Genus Ostreococcus Reveal a Cryptic Species, O. mediterraneus sp nov (Mamiellales, Mamiellophyceae). *Protist*, *164*, 643–659. https://doi.org/10.1016/j.protis.2013.06.002

Suda, S., Watanabe, M. M., & Inouye, I. (2004). Electron microscopy of sexual reproduction in Nephroselmis olivacea (Prasinophyceae, Chlorophyta). *Phycological Research*, *52*(3), 273–283. https://doi.org/10.1111/j.1440-183.2004.00346.x

Sudek, S., Everroad, R. C., Gehman, A.-L. M., Smith, J. M., Poirier, C. L., Chavez, F. P., & Worden, A. Z. (2015). Cyanobacterial distributions along a physico-chemical gradient in the Northeastern Pacific Ocean. *Environmental Microbiology*, *17*(10), 3692–3707. https://doi.org/10.1111/1462-2920.12742

Thompson, P. A., Harrison, P. J., & Parslow, J. S. (1991). Influence of Irradiance on Cell Volume and Carbon Quota for Ten Species of Marine Phytoplankton. *Journal of Phycology*, *27*(3), 351–360. https://doi.org/10.1111/j.0022-3646.1991.00351.x

Toledo, G., Bashan, Y., & Soeldner, A. (1995). Cyanobacteria and black mangroves in Northwestern Mexico: Colonization, and diurnal and seasonal nitrogen

fixation on aerial roots. *Canadian Journal of Microbiology*, *41*(11), 999–1011. https://doi.org/10.1139/m95-139

Tragin, M., Santos, A. L. dos, Christen, R., & Vaulot, D. (2016). *Diversity and ecology of green microalgae in marine systems: An overview based on 18 S rRNA gene sequences*.

Tragin, M., & Vaulot, D. (2018). Green microalgae in marine coastal waters: The Ocean Sampling Day (OSD) dataset. *Scientific Reports*, *8*. https://doi.org/10.1038/s41598-018-32338-w

Tragin, M., & Vaulot, D. (2019). Novel diversity within marine Mamiellophyceae (Chlorophyta) unveiled by metabarcoding. *Scientific Reports*, *9*(1), 1–14. https://doi.org/10.1038/s41598-019-41680-6

Treusch, A. H., Demir-Hilton, E., Vergin, K. L., Worden, A. Z., Carlson, C. A., Donatz, M. G., Burton, R. M., & Giovannoni, S. J. (2012). Phytoplankton distribution patterns in the northwestern Sargasso Sea revealed by small subunit rRNA genes from plastids. *The ISME Journal*, *6*(3), 481–492. https://doi.org/10.1038/ismej.2011.117

Turmel, M., Gagnon, M.-C., O'Kelly, C. J., Otis, C., & Lemieux, C. (2009). The chloroplast genomes of the green algae Pyramimonas, Monomastix, and Pycnococcus shed new light on the evolutionary history of prasinophytes and the origin of the secondary chloroplasts of euglenids. *Molecular Biology and Evolution*, *26*(3), 631–648. https://doi.org/10.1093/molbev/msn285

Twining, B. S., Baines, S. B., & Fisher, N. S. (2004). Element stoichiometries of individual plankton cells collected during the Southern Ocean Iron Experiment (SOFeX). *Limnology and Oceanography*, *49*(6), 2115–2128. https://doi.org/10.4319/lo.2004.49.6.2115

van Baren, M. J., Bachy, C., Reistetter, E. N., Purvine, S. O., Grimwood, J., Sudek, S., Yu, H., Poirier, C., Deerinck, T. J., Kuo, A., Grigoriev, I. V., Wong, C.-H., Smith, R. D., Callister, S. J., Wei, C.-L., Schmutz, J., & Worden, A. Z. (2016). Evidence-based green algal genomics reveals marine diversity and ancestral characteristics of land plants. *BMC Genomics*, *17*(1), 267. https://doi.org/10.1186/s12864-016-2585-6

van de Poll, W. H., Kulk, G., Rozema, P. D., Brussaard, C. P. D., Visser, R. J. W., & Buma, A. G. J. (2018). Contrasting glacial meltwater effects on post-bloom phytoplankton on temporal and spatial scales in Kongsfjorden, Spitsbergen. *Elementa: Science of the Anthropocene*, *6*, 50. https://doi.org/10.1525/elementa.307

van der Schoot, R. J., & Hoeksema, B. W. (2022). Abundance of coral-associated fauna in relation to depth and eutrophication along the leeward side of Curaçao, southern Caribbean. *Marine Environmental Research*, *181*, 105738. https://doi.org/10.1016/j.marenvres.2022.105738

van Duyl, F., Gast, G., Steinhoff, W., Kloff, S., Veldhuis, M., & Bak, R. (2002). Factors influencing the short-term variation in phytoplankton composition and biomass in coral reef waters. *Coral Reefs*, *21*(3), 293–306. https://doi.org/10.1007/s00338-002-0248-3

VanInsberghe, D., Arevalo, P., Chien, D., & Polz, M. F. (2020). How can microbial population genomics inform community ecology? *Philosophical Transactions of the Royal Society B: Biological Sciences*, *375*(1798), 20190253. https://doi.org/10.1098/rstb.2019.0253

Vannier, T., Leconte, J., Seeleuthner, Y., Mondy, S., Pelletier, E., Aury, J.-M., de Vargas, C., Sieracki, M., Iudicone, D., Vaulot, D., Wincker, P., & Jaillon, O. (2016). Survey of the green picoalga Bathycoccus genomes in the global ocean. *Scientific Reports*, *6*(1), Article 1. https://doi.org/10.1038/srep37900

Vargas, C. de, Audic, S., Henry, N., Decelle, J., Mahé, F., Logares, R., Lara, E., Berney, C., Bescot, N. L., Probert, I., Carmichael, M., Poulain, J., Romac, S., Colin, S., Aury, J.-M., Bittner, L., Chaffron, S., Dunthorn, M., Engelen, S., … Karsenti, E. (2015). Eukaryotic plankton diversity in the sunlit ocean. *Science*, *348*(6237). https://doi.org/10.1126/science.1261605

Vaulot, D., Eikrem, W., Viprey, M., & Moreau, H. (2008). The diversity of small eukaryotic phytoplankton (≤3 μm) in marine ecosystems. *FEMS Microbiology Reviews*, *32*(5), 795–820. https://doi.org/10.1111/j.1574-6976.2008.00121.x

Vergin, K. L., Beszteri, B., Monier, A., Cameron Thrash, J., Temperton, B., Treusch, A. H., Kilpert, F., Worden, A. Z., & Giovannoni, S. J. (2013). High-resolution SAR11 ecotype dynamics at the Bermuda Atlantic Time-series Study site by phylogenetic placement of pyrosequences. *The ISME Journal*, *7*(7), 1322–1332. https://doi.org/10.1038/ismej.2013.32

Vergin, K. L., Done, B., Carlson, C. A., & Giovannoni, S. J. (2013). Spatiotemporal distributions of rare bacterioplankton populations indicate adaptive strategies in the oligotrophic ocean. *Aquatic Microbial Ecology*, *71*(1), 1–13. https://doi.org/10.3354/ame01661

Verschoor, A. M., Dijk, M. a. V., Huisman, J., & Donk, E. V. (2013). Elevated CO2 concentrations affect the elemental stoichiometry and species composition of an experimental phytoplankton community. *Freshwater Biology*, *58*(3), 597–611. https://doi.org/10.1111/j.1365-2427.2012.02833.x

Vidal, L. A., Quiroga, S., & Urueña, R. G. (2015). First record of the diatom Chrysanthemodiscus floriatus Mann 1925, (Chrysanthemodiscaceae) in the Caribbean coast of Colombia. *Intropica: Revista del Instituto de Investigaciones Tropicales*, *10*(1), 100–102.

Walsby, A. E., Van Rijn, J., Cohen, Y., & Fogg, G. E. (1983). The biology of a new gas-vacuolate cyanobacterium, Dactylococcopsis salina sp. Nov., in Solar Lake. *Proceedings of the Royal Society of London. Series B. Biological Sciences*, *217*(1209), 417–447. https://doi.org/10.1098/rspb.1983.0019

Warnes, Gregory, Bolker, Ben, Bonebakker, Lodewijk, Gentleman, R., Huber, W., Liaw, A., Lumley, Thomas, Maechler, M., Magnusson, A., Moeller, S., Schwartz, M., & Venables, B. (2013). *License GPL-2 repository CRAN*.

Weber, L., González-Díaz, P., Armenteros, M., Ferrer, V. M., Bretos, F., Bartels, E., Santoro, A. E., & Apprill, A. (2020). Microbial signatures of protected and impacted Northern Caribbean reefs: Changes from Cuba to the Florida Keys. *Environmental Microbiology*, *22*(1), 499–519. https://doi.org/10.1111/1462-2920.14870

Wickham, H. (2011). Ggplot2. *WIREs Computational Statistics*, *3*(2), 180–185. https://doi.org/10.1002/wics.147

Wickham, H., Averick, M., Bryan, J., Chang, W., McGowan, L. D., François, R., Grolemund, G., Hayes, A., Henry, L., Hester, J., Kuhn, M., Pedersen, T. L., Miller, E., Bache, S. M., Müller, K., Ooms, J., Robinson, D., Seidel, D. P., Spinu, V., … Yutani, H. (2019). Welcome to the Tidyverse. *Journal of Open Source Software*, *4*(43), 1686. https://doi.org/10.21105/joss.01686

Wilken, S., Yung, C. C. M., Hamilton, M., Hoadley, K., Nzongo, J., Eckmann, C., Corrochano-Luque, M., Poirier, C., & Worden, A. Z. (2019). The need to account for cell biology in characterizing predatory mixotrophs in aquatic environments. *Philosophical Transactions of the Royal Society B: Biological Sciences*, *374*(1786), 20190090. https://doi.org/10.1098/rstb.2019.0090

Worden, A. Z. (2006). Picoeukaryote diversity in coastal waters of the Pacific Ocean. *Aquatic Microbial Ecology*, *43*(2), 165–175. https://doi.org/10.3354/ame043165

Worden, A. Z., Follows, M. J., Giovannoni, S. J., Wilken, S., Zimmerman, A. E., & Keeling, P. J. (2015). Rethinking the marine carbon cycle: Factoring in the multifarious lifestyles of microbes. *Science*, *347*(6223). https://doi.org/10.1126/science.1257594

Worden, A. Z., Lee, J.-H., Mock, T., Rouzé, P., Simmons, M. P., Aerts, A. L., Allen, A. E., Cuvelier, M. L., Derelle, E., Everett, M. V., Foulon, E., Grimwood, J., Gundlach, H., Henrissat, B., Napoli, C., McDonald, S. M., Parker, M. S., Rombauts, S., Salamov, A., … Grigoriev, I. V. (2009). Green evolution and dynamic adaptations revealed by genomes of the marine picoeukaryotes *Micromonas*. *Science*, *324*(5924), 268–272. https://doi.org/10.1126/science.1167222

Worden, A. Z., Nolan, J. K., & Palenik, B. (2004). Assessing the dynamics and ecology of marine picophytoplankton: The importance of the eukaryotic component. *Limnology and Oceanography*, *49*(1), 168–179. https://doi.org/10.4319/lo.2004.49.1.0168

Wu, W., Huang, B., & Zhong, C. (2014). Photosynthetic picoeukaryote assemblages in the South China Sea from the Pearl River Estuary to the SEATS station. *Aquatic Microbial Ecology*, *71*, 271–284. https://doi.org/10.3354/ame01681

Yamaguchi, H., Suda, S., Nakayama, T., Pienaar, R. N., Chihara, M., & Inouye, I. (2011). Taxonomy of Nephroselmis viridis sp. Nov. (Nephroselmidophyceae, Chlorophyta), a sister marine species to freshwater N. olivacea. *Journal of Plant Research*, *124*(1), 49–62. https://doi.org/10.1007/s10265-010-0349-y

Yang, J., Ma, L., Jiang, H., Wu, G., & Dong, H. (2016). Salinity shapes microbial diversity and community structure in surface sediments of the Qinghai-Tibetan Lakes. *Scientific Reports*, *6*(1), Article 1. https://doi.org/10.1038/srep25078

Yeh, Y.-C., & Fuhrman, J. A. (2022). Contrasting diversity patterns of prokaryotes and protists over time and depth at the San-Pedro Ocean Time series. *ISME Communications*, *2*(1), Article 1. https://doi.org/10.1038/s43705-022-00121-8

Zakryś, B., Milanowski, R., & Karnkowska, A. (2017). Evolutionary Origin of Euglena. In S. D. Schwartzbach & S. Shigeoka (Eds.), *Euglena: Biochemistry, Cell and Molecular Biology* (pp. 3–17). Springer International Publishing. https://doi.org/10.1007/978-3-319-54910-1_1

Zimmerman, A. E., Allison, S. D., & Martiny, A. C. (2014). Phylogenetic constraints on elemental stoichiometry and resource allocation in heterotrophic marine bacteria. *Environmental Microbiology*, *16*(5), 1398–1410. https://doi.org/10.1111/1462-2920.12329

Zink, K.-G., Wilkes, H., Disko, U., Elvert, M., & Horsfield, B. (2003). Intact phospholipids—Microbial "life markers" in marine deep subsurface sediments. *Organic Geochemistry*, *34*(6), 755–769. https://doi.org/10.1016/S0146-6380(03)00041-X